NESTED SOFT-COLLINEAR SUBTRACTIONS

INTEGRATED SUBTRACTION TERMS AND QCD-ELECTROWEAK CORRECTIONS TO ON-SHELL VECTOR BOSON PRODUCTION AT THE LHC

Zur Erlangung des akademischen Grades eines

DOKTORS DER NATURWISSENSCHAFTEN (Dr. rer. nat)

von der KIT-Fakultät für Physik

des Karlsruher Instituts für Technologie (KIT)

genehmigte

DISSERTATION

von

M.SC. CARL LUDWIG MAXIMILIAN DELTO

Tag der mündlichen Prüfung:	23.07.2021
Referent:	Prof. Dr. Kirill Melnikov
Korreferent:	Prof. Dr. Matthias Steinhauser

ABSTRACT

In the forthcoming years, precise measurements at the LHC and its high-luminosity upgrade will scrutinise the inner workings of the Standard Model of particle physics to an unprecedented level. Among the most ambitious goals of this physics program is the determination of the W-boson mass with the astounding precision of $\mathcal{O}(0.01\%)$. Such a precision would match the precision achieved in electroweak fits and will allow for a powerful test of the SM at the quantum level.

The recent shift of focus from direct searches for New Physics to precision studies at the LHC is the consequence of the fact that clear evidence of physics beyond the Standard Model is so far absent. We note, however, that precision studies at the LHC are made possible by a remarkable progress on the theory side, culminating in the fully-differential description of a vast number of phenomenologically relevant processes with NNLO QCD accuracy. Two main obstacles in such computations that need to be addressed are the complicated structure of two-loop multi-scale scattering amplitudes and the appearance of infrared singularities.

This thesis consists of two parts. In the first part, we discuss the recently proposed nested soft-collinear subtraction scheme [1] which allows for a modular, analytic and local way of handling infrared singularities at NNLO [2–4]. We analytically compute a number of single- and double-unresolved integrated subtraction terms that arise in the process of regulating real-emission contributions. More specifically, we compute integrated triple-collinear subtraction terms for all possible partonic splittings, both initial- and final-state [5]. We also obtain integrated double-soft subtraction terms that arise in the context of colour-singlet decays to massive partons [6]. These results improve the efficiency and numerical stability of practical computations and contribute towards establishing a NNLO QCD subtraction formula for arbitrary hard scattering processes at hadron colliders.

In the second part of this thesis, we make use of the nested soft-collinear subtraction scheme to describe mixed QCD-EW corrections to on-shell vector-boson production at the LHC at a fully-differential level. We first obtain mixed QCD-QED corrections to on-shell Z-boson production by abelianising the corresponding NNLO QCD calculation [7]. We then extend these results by including mixed QCD-weak corrections into theoretical description of this process [8]. In the case of W-boson production [9], we focus on simplifications that arise in the regularisation of double-real contributions. We study phenomenological impact of these corrections for a number of observables studied in Z- and W-boson production processes and specifically discuss their implications for the W-boson mass measurement at the LHC [10].

CONTENTS

LIST OF FIGURES

LIST OF TABLES

ACRONYMS

BSM beyond the Standard Model

DEQ differential equation

DY Drell-Yan

EW electroweak

GPL Goncharov polylogarithm

HPL harmonic polylogarithm

IBP integration-by-parts

IR infrared

LI Lorentz invariance

LHC Large Hadron Collider

LO leading order

MI master integral

NLO next-to-leading order

NNLO next-to-next-to-leading order

N3LO next-to-next-to-next-to-leading order

NSS nested soft-collinear subtraction scheme

PDF parton distribution function

QCD Quantum Chromodynamics

QED Quantum Electrodynamics

SM Standard Model

UV ultraviolet

XS cross section

1 INTRODUCTION

The discovery of the Higgs boson in 2012 [11, 12] at the Large Hadron Collider (LHC) formally completed the experimental confirmation of the Standard Model (SM) of particle physics [13–24], a quantum field theory that encodes our current understanding of Nature at the most fundamental level. While the SM successfully describes many observables and phenomena, it fails to provide an explanation of several observations outside collider physics such as *dark matter*, *dark energy* and *matter-antimatter asymmetry*.

In recent years, focus of the physics program at the LHC has shifted to precision studies of various SM processes. In the absence of direct detection of new particles at the LHC, such studies can be used for improved extraction of many important SM parameters including particle masses, coupling constants, and parton distribution functions (PDFs). Furthermore, comparing precise measurements to precise predictions might lead either to hints towards New Physics or to refined exclusion limits on BSM models.

The prime example of a precision measurement at the LHC is the experimentally challenging determination of the W-boson mass: only recently has the ATLAS collaboration published the result of the first-ever LHC measurement $M_W = 80370 \pm 19$ MeV [25].[1] It is expected that the uncertainty of the W-boson mass measurement at the LHC can be reduced to $\mathcal{O}(10)$ MeV [28]. If this uncertainty goal is met in a direct measurement, it would match the precision of electroweak fits where the most recent result is $M_W = 80358 \pm 8$ MeV [29, 30]. It would therefore provide a strong consistency check of the SM or, in case of a discrepancy, hint towards possible contributions of BSM physics.

Strengthening the precision physics research program at the LHC requires not only an impeccable understanding of experimental systematics, but also reliable theoretical description of physical observables. It is well-known that perturbative description of hadronic cross sections at large momentum transfer is possible within the collinear factorisation framework [31, 32]

$$\mathrm{d}\sigma^{\mathrm{had}}_{pp\to X} = \sum_{i,j} \int_0^1 \mathrm{d}x_i\,\mathrm{d}x_j\, f_i(x_i) f_j(x_j)\,\mathrm{d}\sigma_{ij}\,\left[1 + \mathcal{O}\left((\Lambda_{\mathrm{QCD}}/Q)^n\right)\right]\,. \tag{1.1}$$

In Eq. (1.1), x_i (x_j) denotes the fraction of a proton momentum carried by a parton i (j), $f_{i,j}$ are corresponding PDFs, and $\mathrm{d}\sigma_{ij}$ is the partonic cross section of the hard process $i\,j \to X$. The partonic cross section depends on the (large) momentum transfer Q and on the factorisation and renormalization scales $\mu_{F,R}$. Whereas partonic cross-sections are well-defined perturbative objects, PDFs cannot be calculated *ab initio* and have to be

1 LEP and Tevatron determined M_W with an uncertainty of 33 MeV [26] and 16 MeV [27], respectively.

determined experimentally. Non-perturbative effects in Eq. (1.1) are power suppressed[2] and small, since $\Lambda_{\text{QCD}}/Q \sim 0.3\,\text{GeV}/30\,\text{GeV} \sim \mathcal{O}(1\%)$.[3] Hadronic cross sections with small momenta transfers are studied in the context of resummations and parton showers.

Reliable fixed-order predictions for LHC physics require both a good understanding of PDFs and a precise description of hard, short-range physics; the latter is accomplished using perturbation theory. Calculations of perturbative expansions of partonic cross sections $d\sigma_{ij}$ require two distinct contributions:

- *virtual* corrections to (multi-scale) amplitudes, which have intricate analytic properties. Appearing loop integrals exhibit two types of singularities: ultraviolet (UV) singularities, which are re-absorbed into physical parameters by renormalization, and infrared (IR) singularities;

- *real-emission* corrections, which feature IR singularities in unresolved regions of the phase space where emitted parton(s) become soft and/or collinear to other partons.

The appearance of IR divergences in real and virtual contributions, as well as their cancellation in infrared-safe observables, is a well-studied subject [33–35]. [4]

STRUCTURE OF THIS THESIS

The first part (I) of this thesis is dedicated to the nested soft-collinear subtraction scheme [1–4], and, in particular, to the analytic computation of some of its most intricate building blocks. We begin by discussing the reason for the appearance of infrared singularities and their treatment within the nested soft-collinear subtraction scheme (NSS) in Chapter 2. During the regularisation procedure, various subtraction terms emerge. In Chapter 3, we outline methods for the analytic computation of these subtraction terms. We begin by computing integrated single-unresolved subtraction terms by means of direct integration. Then, we present computations of integrated double-unresolved subtraction terms. Computational methods discussed in Chapter 3 have been originally developed to compute integrated massless double-soft subtraction contribution [36, 37]. Here, we extend these methods and present computation of *massive* double-soft subtraction terms [6] and the *complete* set of initial- and final-state integrated triple-collinear [5] subtraction terms.

In the second part (II) of this thesis, we present *initial-state* mixed QCD-EW corrections to the production of single on-shell vector bosons at the LHC at a fully-differential level. In particular, we describe:

2 The precise value of the exponent n in Eq. (1.1) depends on the specific processes under consideration.
3 The value of Q for a specific event is, for example, set by the transverse momentum of QCD jets.
4 Additional collinear divergences in initial-state radiation are re-absorbed into the renormalization of PDFs.

– computation of mixed QCD-QED corrections to on-shell Z-boson production at the LHC [7], which can be obtained by applying an abelianization procedure [38] to the existing implementation of NNLO QCD corrections to this process [2]. Furthermore, we compute mixed QCD-EW corrections to the same process [8], by additionally including one-loop *weak* and two-loop QCD-*weak* corrections;

– computation of mixed QCD-EW corrections to on-shell W-boson production at the LHC [9]. Here, we discuss how to build a subtraction scheme for all double-real contributions, whose IR structure is simpler than the one in the NNLO QCD case. In the course of the regularisation procedure we make use of the integrated subtraction terms that were obtained in Chapter 2. We also present spinor-helicity expressions for double-real matrix elements and several master integrals required for the two-loop QCD-EW on-shell W-boson form factor.

We use these fully-differential results to study the impact of QCD-EW corrections to various observables relevant for Z- and W-boson production at the LHC. Finally, we provide an estimate of the impact of these corrections on the W-boson mass measurement at the LHC [10].

Part I

THE NESTED SOFT-COLLINEAR SUBTRACTION SCHEME

The first part of this thesis is devoted to the nested soft-collinear subtraction scheme and its building blocks. We begin with a description of the regularisation procedure in Chapter 2. We compute various integrated subtraction terms in Chapter 3. While NLO-like subtraction terms are obtained by straightforward parametric integration, genuine NNLO-like subtraction terms that arise in the double-soft and in the triple-collinear limits, are considerably more involved. We explain how to compute these phase-space integrals using *reverse unitarity* [39] as a starting point.

2 NESTED SOFT-COLLINEAR SUBTRACTIONS

In this Chapter, we discuss how IR singularities appear in fixed-order computations, why they present an important technical challenge, and, finally, how they are regularised in the nested soft-collinear subtraction scheme (NSS) [1–4]. We begin by considering generic partonic cross section $\mathrm{d}\sigma_{ij}$ in Eq. (1.1) in a perturbative expansion in the strong coupling constant α_s and write

$$\mathrm{d}\sigma_{ij} = \mathrm{d}\sigma_{ij}^{\mathrm{lo}} + \alpha_s\, \mathrm{d}\sigma_{ij}^{\mathrm{nlo}} + \alpha_s^2\, \mathrm{d}\sigma_{ij}^{\mathrm{nnlo}} + \mathcal{O}\left(\alpha_s^3\right) . \tag{2.1}$$

Here, labels "lo", "nlo" and "nnlo" denote leading order (LO), next-to-leading order (NLO) and next-to-next-to-leading order (NNLO) in Quantum Chromodynamics perturbation theory.

LEADING ORDER For ease of notation, we assume a process $i\,j \to X$ whose LO contribution starts at tree-level and does not involve powers of α_s. In such a case, the LO partonic cross section can be written as

$$\mathrm{d}\sigma_{ij}^{\mathrm{lo}} = \frac{1}{2s} \int \mathrm{d}\Phi_X\, (2\pi)^4\, \delta\left(p_i + p_j - p_X\right) \overline{\left|\mathcal{A}^{\mathrm{tree}}\left(i, j; X\right)\right|^2} \mathcal{F}(p_X)\,, \tag{2.2}$$

where $\overline{\left|\mathcal{A}^{\mathrm{tree}}\left(i, j; X\right)\right|^2}$ is the squared tree-level amplitude of the process $i\,j \to X$, summed and averaged over spins and colors. In Eq. (2.2), $\mathrm{d}\sigma_{ij}^{\mathrm{lo}}$ is fully-differential in the sense that integration over final-state phase space $\mathrm{d}\Phi_X$ is constrained by the measurement function $\mathcal{F}(p_X)$, which refers to an IR-safe but otherwise *arbitrary* observable. The integral in Eq. (2.2) is regular across the whole phase space and can be readily computed numerically.

HIGHER-ORDER CORRECTIONS We write higher-order corrections in Eq. (2.1) as

$$\mathrm{d}\sigma_{ij}^{\mathrm{nlo}} = \mathrm{d}\sigma^{V} + \mathrm{d}\sigma^{R} + \mathrm{d}\sigma^{\mathrm{pdf,nlo}}\,, \tag{2.3}$$
$$\mathrm{d}\sigma_{ij}^{\mathrm{nnlo}} = \mathrm{d}\sigma^{VV} + \mathrm{d}\sigma^{VR} + \mathrm{d}\sigma^{RR} + \mathrm{d}\sigma^{\mathrm{pdf,nnlo}}\,, \tag{2.4}$$

where $\mathrm{d}\sigma^V$ denotes UV-renormalized virtual (loop) corrections, $\mathrm{d}\sigma^R$ refers to real corrections and σ^{pdf} are contributions that arise from collinear renormalisation of PDFs. As already discussed in the Introduction, virtual and real contributions to cross sections are *not* infrared-finite separately. In fact, IR singularities on the r. h. s. of Eq. (2.3) and Eq. (2.4) cancel *only* upon combining both types of corrections [33–35].

However, they appear in a very different way in real and virtual contributions. When loop integrals are computed in $d = 4 - 2\epsilon$ dimensions in dimensional regularisation [40–42], IR singularities manifest themselves as *explicit* and *universal* $1/\epsilon$ poles [43–46]. For example, one-loop QCD corrections to the scattering amplitude of n massless partons can be written as[1]

$$\mathcal{A}_n^{1l} = \frac{e^{\epsilon\gamma_E}}{2\,\Gamma\,(1-\epsilon)} \sum_{i,j\neq i}^{n} \left[\frac{1}{\epsilon^2} + \frac{\gamma_i}{\boldsymbol{T}_i^2\epsilon}\right] \boldsymbol{T}_i\boldsymbol{T}_j \left(\frac{\mu^2 e^{-\mathrm{i}\lambda_{ij}\pi}}{2(p_i\cdot p_j)}\right)^{\epsilon} \mathcal{A}_n^{\text{tree}} + \mathcal{A}_n^{1l,\text{fin}}\,. \tag{2.5}$$

We observe that the $1/\epsilon^2$ and $1/\epsilon$ poles of $\mathcal{A}_n^{1l}$ in Eq. (2.5) are proportional to the tree-level amplitude $\mathcal{A}^{\text{tree}}$, while $\mathcal{A}_n^{1l,\text{fin}}$ is finite.

In real corrections, on the other hand, IR singularities are *implicit*: they only arise upon integration over unresolved regions of the phase space of final-state particles. As an illustration, consider a diagram where a gluon with momentum k is emitted by a massless particle with momentum $p + k$. The amplitude reads

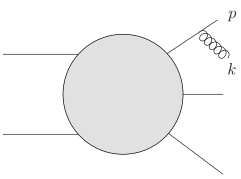

$$\sim \frac{1}{(p+k)^2} \sim \frac{1}{(p\cdot k)} \sim \frac{1}{E_p E_k(1-\cos\theta_{pk})}\,.$$

This contribution is finite for generic values of the gluon energy E_k and the angle θ_{pk} between three-momenta $\boldsymbol{p}$ and $\boldsymbol{k}$, but it becomes singular when either E_k or θ_{pk} vanishes. Divergence of the first type is called "soft", divergence of the second type is called "collinear".

INFRARED REGULARISATION The goal of any regularisation scheme for real-emission contributions is to extract and regulate all IR singularities in a fully-differential cross sections *without* integrating over resolved regions of final-state phase spaces. This is only possible since *i)* unresolved emissions have no impact on IR-safe observables and *ii)* real-emission matrix elements factorize into universal functions and lower-multiplicity matrix elements that do not depend on unresolved momenta in the soft and collinear limits.

Regularization schemes are prescriptions that allow one to re-arrange unresolved contributions to real-emission cross sections in such a way that processes with a certain number of resolved partons become separately IR finite. Then, one can write the cross sections in Eq. (2.3) and Eq. (2.4) as

$$\mathrm{d}\sigma_{ij}^{\text{nlo}} = \mathrm{d}\sigma_{X}^{\text{nlo}} + \mathrm{d}\sigma_{X+1}^{\text{nlo}}\,, \tag{2.6}$$
$$\mathrm{d}\sigma_{ij}^{\text{nnlo}} = \mathrm{d}\sigma_{X}^{\text{nnlo}} + \mathrm{d}\sigma_{X+1}^{\text{nnlo}} + \mathrm{d}\sigma_{X+2}^{\text{nnlo}}\,, \tag{2.7}$$

1 Here, $\boldsymbol{T}_i$ are color generators and the phase λ_{ij} depends on whether partons i and j are incoming or outgoing, see Ref. [45].

where contributions $X+m$ ($m=0,1,2$) have exactly m *resolved* partons in the final state and are individually finite. IR regularisation methods employ either *slicing* [47] or *subtraction* [48] techniques, that we review in what follows.

SLICING METHODS Slicing methods regulate divergences *globally* at the level of phase-space integrals. One divides the radiative phase space into resolved and unresolved regions by introducing a slicing variable $\tau \in [0,1]$ and splitting the cross section into resolved $\tau \in [\delta,1]$ and unresolved $\tau \in [0,\delta]$ regions, where δ is taken to be small. In the resolved region the computation at a certain perturbative order in QCD requires corrections of one order lower to the $X+$jet process. Matrix elements in unresolved regions factorize so that phase-space integration can be performed and IR singularities can be exposed as $1/\epsilon$ poles and logarithms of δ. While the former cancel when virtual and PDF renormalisation contributions are included, logarithms of δ cancel against the integrated resolved contribution. As a toy example, consider the parametric integral

$$\mathcal{I}_{\text{ex}} = \int_0^1 \mathrm{d}x\, x^{-1+n\epsilon} f(x)\,, \tag{2.8}$$

where $f(x)$ is a function that is regular in the entire integration domain. We note that the integral in Eq. (2.8) is singular at the endpoint $x \to 0$. To regularise it, we split the integration region and write

$$\mathcal{I}_{\text{ex}} = \int_0^\delta \mathrm{d}x\, x^{-1+n\epsilon} f(x) + \int_\delta^1 \mathrm{d}x\, x^{-1+n\epsilon} f(x)\,. \tag{2.9}$$

The first integral can be expanded in $\delta \ll 1$, whereas the second integral is regular. We find

$$\mathcal{I}_{\text{ex}} = \left(\frac{1}{n\epsilon} + \ln(\delta)\right) f(0) + \int_\delta^1 \frac{\mathrm{d}x}{x} f(x) + \mathcal{O}(\delta,\epsilon)\ . \tag{2.10}$$

We note that we have extracted the $1/\epsilon$ singularity, which is independent of δ, and that the logarithmic dependence on δ cancels in the final result, i. e. after the integration over x in the second term in Eq. (2.10) is performed. Moreover, this cancellation involves numerical integration over the resolved region that may lead to numerical problems in realistic applications [49, 50].

SUBTRACTION METHODS Subtraction methods regulate divergences *locally*, at the level of real-emission integrands, by subtracting and adding back a suitable approximant of the matrix element squared. This procedure yields regulated contributions and subtraction terms with lower final-state multiplicity. Regulated contributions can be evaluated numerically in $d=4$ dimensions. Subtraction terms, on the other hand, give rise to $1/\epsilon$ poles, which cancel against $1/\epsilon$ poles in virtual contributions and in PDF renormalisation.

We consider the toy example in Eq. (2.8) to illustrate these points. To compute $\mathcal{I}_{\rm ex}$, we subtract the behaviour of the integrand at the endpoint $x \to 0$ and write

$$\mathcal{I}_{\rm ex} = \int_0^1 \frac{{\rm d}x}{x^{1-n\epsilon}} \left[f(x) - f(0) + f(0)\right] = \int_0^1 {\rm d}x \, \frac{f(x)-f(0)}{x} + \frac{f(0)}{n\epsilon} + \mathcal{O}(\epsilon) \; . \quad (2.11)$$

By construction, the first term on the r. h. s. of Eq. (2.11) is finite and could be Taylor-expanded in ϵ *before* integrating over x. The second term, on the other hand, could be integrated independently of the function f, yielding an explicit $1/\epsilon$ pole.

STATE OF THE ART IR singularities in NLO calculations can be handled with various subtraction schemes, including Frixione-Kunszt-Signer [51, 52], Catani-Seymour [53, 54], and Nagy-Soper [55–59] ones.[2] This understanding, combined with advances in one-loop computations [60–62], enabled automation of NLO computations for arbitrary processes [63–68].

NNLO QCD calculations can be performed using q_T- [69–76] and N-jettiness [77–80] slicing. Furthermore, subtraction schemes such as antenna subtraction [81–93], geometric subtraction [94], the STRIPPER framework [95–100], local analytic sector subtraction [101–103], and the CoLoRFull method [104–115] have been proposed. Another useful approach is the projection-to-Born method [116–118].[3] These developments, together with advances in two-loop computations, have resulted in an impressive number of predictions at NNLO QCD, see Ref. [120] for a recent review.

TOWARDS AN OPTIMAL SUBTRACTION SCHEME In spite of the fact that a large number of subtraction schemes has been developed and the impressive number of predictions that these schemes enabled, it is fair to say, that an optimal subtraction scheme is yet to be found. While the implementation of slicing schemes might be relatively straightforward, they suffer from large numerical cancellations between "resolved" and "unresolved" contributions [49, 50]. Subtraction methods, on the other hand, regulate divergences point-wise in phase space and for this reason are more stable numerically.

Nevertheless, subtraction schemes are complex constructions that could benefit from further optimization. In fact, we believe that an "optimal" subtraction scheme should fulfill the following criteria:

- in order to ensure a numerically efficient scheme, the regularisation should be *local* and *minimal*;
- integrated subtraction terms should be known *analytically*;
- cancellation of poles should be demonstrated analytically for an arbitrary hard processes;

2 For earlier computations of NLO QCD corrections using slicing, see for example Refs. [43, 48].
3 Very recently, this method was used to obtain fully-differential predictions at N3LO [119].

- the scheme should be *modular*, to allow for the implementation of new processes with minimal effort;
- the scheme schould be *physically transparent*.

It is fair to say that none of the schemes that were proposed so far meets all these requirements, which means that further work on improving subtraction schemes is necessary.

In the following, we introduce the recently proposed nested soft-collinear subtraction scheme [1–4], an extension of the original sector-improved residue subtraction-scheme [95, 96], which attempts to fulfill the criteria listed above. The scheme is based on the observation that QCD color coherence ensures that soft and collinear singularities are not entangled at the level of gauge-invariant matrix elements. This allows for a *minimal* and *iterative* subtraction starting from soft singularities and followed by collinear subtraction, which is applied to soft-subtracted cross sections.

In what follows, we will only discuss double-real corrections, since they represent the most involved case. The discussion of single-real corrections and virtual contributions can be found in Refs. [1–4].

LAYOUT OF THE CHAPTER The remainder of this Chapter is organized as follows. After establishing notations in Sec. 2.1, we explain how to regulate soft singularities that arise when computing NNLO QCD corrections within the NSS in Sec. 2.2. There, we also point out simplifications that arise when mixed NNLO QCD-EW corrections are considered. The simplified construction will be used in Part II of this thesis to describe mixed QCD-EW corrections to W-boson hadroproduction at a fully-differential level. In Sec. 2.3, we consider soft-regulated contributions and explain how to regulate their collinear singularities. Again, we discuss simplifications that arise when mixed QCD-EW corrections are computed. In Sec. 2.4, we consider the process $q\bar{q} \to Zgg$ and provide an overview of the subtraction procedure. We conclude the Chapter by discussing the most intricate, double-soft and triple-collinear subtraction terms in Sec. 2.5 and Sec. 2.6, respectively.

2.1 NOTATIONS

In order to introduce the nested soft-collinear subtraction scheme, we consider production of a final state X in collisions of two partons with momenta p_1 and p_2. We study double-real corrections that appear due to the partonic process $f_1(p_1) + f_2(p_2) \to X + f_4(k_4) + f_5(k_5)$, where $f_{1,2}$ are the incoming partons and $f_{4,5}$ are the massless partons that can become unresolved.[4] We write the contribution of the double-real emission process to the differential cross section as

$$
\begin{aligned}
2s \cdot \mathrm{d}\sigma^{RR}_{X+f_4+f_5} &= \int [\mathrm{d}k_4][\mathrm{d}k_5]\; F_{\mathrm{LM}}(1_{f_1}, 2_{f_2}, X; 4_{f_4}, 5_{f_5}) \\
&= \left\langle [\mathrm{d}k_4][\mathrm{d}k_5]\; F_{\mathrm{LM}}(1_{f_1}, 2_{f_2}, X; 4_{f_4}, 5_{f_5}) \right\rangle ,
\end{aligned}
\tag{2.12}
$$

where $s = s_{12}$ denotes the partonic center-of-mass energy squared. Throughout this thesis, we denote kinematic invariants for massless particles with the symbol s_{ij}. Then,

$$
s_{ij} = 2(q_i \cdot q_j) = 2E_iE_j(1 - \boldsymbol{n}_i\boldsymbol{n}_j) = 2E_iE_j(1 - \cos\theta_{ij}) = 2E_iE_j\rho_{ij} = 4E_iE_j\eta_{ij} , \tag{2.13}
$$

where $q \in \{p, k\}$ and θ_{ij} is the relative angle between partons i and j. The quantity F_{LM} that was introduced in Eq. (2.12), is defined as follows

$$
\begin{aligned}
F_{\mathrm{LM}}(1_{f_1}, 2_{f_2}, X; 4_{f_4}, 5_{f_5}) &= \mathcal{N} \sum_{\mathrm{col,pol}} |\mathcal{A}^{\mathrm{tree}}(p_1, p_2, p_X; k_4, k_5)|^2 \mathcal{F}(p_X, k_4, k_5) \\
\times\, (2\pi)^d\, \delta^d(p_1 + p_2 - p_X - k_4 - k_5) &\frac{\mathrm{d}^{d-1}\boldsymbol{p}_X}{(2\pi)^{d-1}2E_X} .
\end{aligned}
\tag{2.14}
$$

Note that the function F_{LM} includes the matrix element squared, the energy-momentum conserving δ-function, the phase-space factor of final state X and the measurement function $\mathcal{F}$ of an arbitrary IR-safe observable. It also includes all required ($d-$dimensional) initial-state color- and helicity-averaging factors and final-state symmetry factors, denoted by $\mathcal{N}$. However, it does *not* contain the phase-space volume elements for the potentially unresolved partons f_4 and f_5. These phase-space volumes appear explicitly in Eq. (2.12); they read

$$
[\mathrm{d}k_i] = \frac{\mathrm{d}^{d-1}\boldsymbol{k}_i}{(2\pi)^{d-1}2E_i}\, \theta(E_{\max} - E_i) , \quad i = 4, 5 . \tag{2.15}
$$

We note that we introduced an energy cut-off $E_{\max}$ in Eq. (2.15), which should be chosen large enough so that it does not alter the value of the integral in Eq. (2.12).[5] The need for this cut-off parameter will become clear later when the double-soft limit of Eq. (2.12) is discussed. For now, we note that this cut-off is not Lorentz-invariant but it does leave rotational invariance intact.

DOUBLE-REAL SUBTRACTION PROCEDURE Below, we will explain how to re-arrange the double-real cross section in Eq. (2.12) in order to arrive at the following form

$$
\mathrm{d}\sigma^{RR} = \mathrm{d}\sigma^{RR}_{X+2} + \mathrm{d}\sigma^{RR}_{X+1}(\epsilon) + \mathrm{d}\sigma^{RR}_{X}(\epsilon) . \tag{2.16}
$$

4 We use the term “parton” to describe gluons, quarks, *and* photons in order to incorporate both NNLO QCD and mixed NNLO QCD-EW real-emission corrections.

5 More precisely, $E_{\max}$ should be greater then or equal to the maximal energy that partons $f_{4,5}$ can have according to energy-momentum conservation.

Quantities $\mathrm{d}\sigma^{RR}_{X+h}$ in Eq. (2.16) denote contributions with $h = 0, 1, 2$ resolved partons in addition to the final state X. The first term, $\mathrm{d}\sigma^{RR}_{X+2}$ comprises *fully-regulated* contributions that can be integrated numerically in $d = 4$. The second and third terms, $\mathrm{d}\sigma^{RR}_{X+1}$ and $\mathrm{d}\sigma^{RR}_{X}$, denote *single-* and *double-unresolved* subtraction terms, respectively. Integration of these contributions over the unresolved phase space of one or two partons is *independent* of the measurement function $\mathcal{F}$ and yields explicit poles in ϵ. The poles of subtraction terms[6] cancel, once real, virtual, and PDF renormalisation contributions to the IR finite cross section in Eq. (2.7) are combined. We aim at computing integrated subtraction terms analytically, since doing so has two advantages. First, analytic cancellation of poles establishes confidence in the subtraction procedure. Second, it makes numerical evaluation of the finite remainder more efficient.

The desired representation of the double-real cross section, displayed in Eq. (2.16), can be found by introducing appropriate subtraction terms for the unresolved kinematic configurations, associated with the integration over $[\mathrm{d}k_4][\mathrm{d}k_5]$ in Eq. (2.12). The precise singularity structure depends on the partonic configuration $f_1 + f_2 \to X + f_4 + f_5$. In general, singularities can arise when radiated partons $f_{4,5}$ become soft and/or collinear to other partons. Explicitly, particles $f_{4,5}$ can become collinear to each other, to partons $f_{1,2}$ or to particles appearing in the unspecified final state X. Moreover, these limits can be approached in several ways, rendering the construction of the subtraction procedure a rather non-trivial task.

Within the NSS, soft and collinear singularities are subtracted *iteratively* and *independently* of each other. We stress that subtractions in the NSS are defined at the level of gauge-invariant on-shell scattering amplitudes F_{LM} (cf. Eq. (2.14)). For these quantities, QCD color coherence ensures that soft and collinear singularities are not entangled [121]. We shortly discuss the absence of soft-collinear limits in Appendix B.4. We note that factorization of tree-level matrix elements squared in double-unresolved limits has been understood a long time [122, 123]. In Sec. 2.2 and Sec. 2.3, we discuss the regularisation of soft and collinear singularities, respectively.

To write subtraction terms in a transparent way, we will work under the assumption that final-state particles which can become unresolved are always labeled as $f_{4,5}$. In what follows, we will shortly explain how to distinguish the potentially unresolved partons $f_{4,5}$ from partons in the "hard " final state X.

DAMPING FACTORS So far, we have assumed that we can clearly separate the "resolved" final state X from partons $f_{4,5}$, which can become unresolved. This is for example the case for NNLO QCD corrections to color-singlet production, where X denotes all color-neutral particles.[7] However, there are many processes for which this distinction becomes

6 We note that single-unresolved terms $\mathrm{d}\sigma^{RR}_{X+1}$ contribute to the pole structure starting from $1/\epsilon^2$, while double-unresolved Born-like terms $\mathrm{d}\sigma^{RR}_{X}$ start at $1/\epsilon^4$.

7 Here, the final state $X \in \{Z, W, H, ZZ, WW, \gamma\gamma, \dots\}$ does not contain any particles that are indistinguishable from the quarks and gluons that are emitted in real-emission contributions.

more complicated. For example, this is the case in double-real corrections to hadronic Higgs-boson decays that were discussed in the context of the NSS in Ref. [3]. To explain how the separation can be achieved, we consider the partonic channel $H \to gggg$ and write [3]

$$2m_H^2 \cdot \mathrm{d}\Gamma^{RR}_{H\to gggg} = \left\langle [\mathrm{d}k_4][\mathrm{d}k_5]\ F_{\mathrm{LM}}(1_g, 2_g, H; 4_g, 5_g) \right\rangle . \tag{2.17}$$

Here, m_H denotes the mass of the Higgs boson. We introduce a partion of unity, and write

$$1 = \frac{(k_1 + k_2 + k_4 + k_5)^2}{m_H^2} = \frac{1}{m_H^2} \sum_{i \neq j = 1}^{4} s_{ij} , \tag{2.18}$$

where k_i is the four-momentum of gluon i and $s_{ij} = 2(k_i \cdot k_j)$,cf. Eq. (2.13). We insert the relation Eq. (2.18) into Eq. (2.17) and find

$$\begin{aligned} &\left\langle [\mathrm{d}k_4][\mathrm{d}k_5]\ F_{\mathrm{LM}}(1_g, 2_g, H; 4_g, 5_g) \right\rangle \\ &= 12 \times \left\langle [\mathrm{d}k_4][\mathrm{d}k_5] \frac{s_{12}}{m_H^2}\ F_{\mathrm{LM}}(1_g, 2_g, H; 4_g, 5_g) \right\rangle , \end{aligned} \tag{2.19}$$

where the combinatorial factor 12 arises from exploiting the symmetry of the matrix element squared and the phase space under gluon re-labeling. The damping factor s_{12}/m_H^2 in Eq. (2.19) ensures that no singularities arise when gluons $g(k_1)$, $g(k_2)$ become soft and/or collinear to each other. This means that these gluons can be identified as part of the hard final-state X, while gluons $g(k_4)$, $g(k_5)$ are the ones that can become unresolved. We note that damping factors only influence the phase-space of hard particles X and we will not explicitly display them in subtraction formulas below. However, they will become important in the computation of subtraction terms that arise in the triple-collinear emission off external particles in the final-state.

2.2 SOFT REGULARISATION

Soft singularities in double-real corrections $f_1 + f_2 \to X + f_4 + f_5$ arise whenever the energy of a photon, a gluon, or a quark-antiquark pair vanishes. *Single-soft* singularities arise in processes with at least one gluon (photon) with vanishing energy $E_g \to 0$ ($E_\gamma \to 0$). Processes in which the emitted partons are a gluon-gluon, a quark-antiquark or a gluon-photon pair, i. e. $\{f_4, f_5\} \in \{gg, q\bar{q}, g\gamma\}$, exhibit a *double-soft* singularity. In the case of soft gg or $q\bar{q}$ emission, the double-soft singularity arises in a *correlated* fashion when the energies of these partons vanish at a comparable rate, $E_4 \sim E_5 \to 0$.[8] The case of emission of a soft gluon-photon pair, on the other hand, is somewhat simpler. Here,

8 Here, "correlated" means that singularities arise from terms in matrix elements that behave as $\sim 1/(E_4 + E_5)$ in the $E_4 \to 0$, $E_5 \to 0$ limit.

the *uncorrelated* double-soft singularity arises in the limit $E_\gamma \to 0, E_g \to 0$.[9] Furthermore, these partonic channels exhibit an (additional) single-soft singularity whenever the energy of a gluon or a photon vanishes. We discuss each of these cases in Sec. 2.2.1 and Sec. 2.2.2, respectively. Then, in Sec. 2.2.3, we discuss soft regularisation of partonic channels that *only* feature single-soft singularities.

2.2.1 *Correlated double-soft singularities*

In case of correlated singularities of soft emissions of gg or $q\bar{q}$ pairs it is convenient to introduce energy ordering $E_5 < E_4$.[10] We define a modified phase space

$$\widetilde{[\mathrm{d}k_4][\mathrm{d}k_5]} = [\mathrm{d}k_4][\mathrm{d}k_5]\,\theta(E_4 - E_5)\;, \tag{2.20}$$

and a symmetrized matrix element

$$\begin{aligned}&\overleftrightarrow{F_{\mathrm{LM}}}(1_{f_1}, 2_{f_2}, X; 4_{f_4}, 5_{f_5})\\ &= F_{\mathrm{LM}}(1_{f_1}, 2_{f_2}, X; 4_{f_4}, 5_{f_5}) + F_{\mathrm{LM}}(1_{f_1}, 2_{f_2}, X; 4_{f_5}, 5_{f_4})\;,\end{aligned} \tag{2.21}$$

and find

$$\left\langle [\mathrm{d}k_4][\mathrm{d}k_5]\; F_{\mathrm{LM}}(1_{f_1}, 2_{f_2}, X; 4_{f_4}, 5_{f_5}) \right\rangle = \left\langle \widetilde{[\mathrm{d}k_4][\mathrm{d}k_5]}\; \overleftrightarrow{F_{\mathrm{LM}}}(\ldots; 4_{f_4}, 5_{f_5}) \right\rangle . \tag{2.22}$$

We denote the (correlated) double-soft limit by an operator $\mathbb{S}$, insert the identity $1 = (I - \mathbb{S}) + \mathbb{S}$ into Eq. (2.12), and obtain

$$\begin{aligned}&\left\langle \widetilde{[\mathrm{d}k_4][\mathrm{d}k_5]}\; \overleftrightarrow{F_{\mathrm{LM}}}(1_{f_1}, 2_{f_2}, X; 4_{f_4}, 5_{f_5}) \right\rangle\\ &= \left\langle \widetilde{[\mathrm{d}k_4][\mathrm{d}k_5]}\; (I - \mathbb{S})\, \overleftrightarrow{F_{\mathrm{LM}}}(\ldots; 4_{f_4}, 5_{f_5}) \right\rangle + \left\langle \widetilde{[\mathrm{d}k_4][\mathrm{d}k_5]}\; \mathbb{S}\, \overleftrightarrow{F_{\mathrm{LM}}}(\ldots; 4_{f_4}, 5_{f_5}) \right\rangle .\end{aligned} \tag{2.23}$$

The first term on the r. h. s. of Eq. (2.23) is regular in the double-soft limit; we discuss how remaining singularities can be extracted from this term right after Eq. (2.30). The second term in Eq. (2.23) is the so-called double-soft subtraction term. It enters the double-real cross section in Eq. (2.16) through the double-unresolved, Born-like contribution $\mathrm{d}\sigma_X^{RR}(\epsilon)$. We defer a detailed discussion of the double-soft subtraction term to Sec. 2.5.

We now define the double-soft operator $\mathbb{S}$ that appears in Eq. (2.23). The double-soft limit removes momenta $k_{4,5}$ from the momentum-conserving δ-function and the measurement function $\mathcal{F}$ so that

$$\begin{aligned}&\mathbb{S}\; F_{\mathrm{LM}}(1_{f_1}, 2_{f_2}, X; 4_{f_4}, 5_{f_5}) = \mathcal{N} \sum_{\mathrm{col,pol}} \mathbb{S} |\mathcal{A}^{\mathrm{tree}}(p_1, p_2, p_X; k_4, k_5)|^2\\ &\times \mathcal{F}(p_X)\,(2\pi)^d\, \delta^d(p_1 + p_2 - p_X)\, \frac{\mathrm{d}^{d-1}\boldsymbol{p}_X}{(2\pi)^{d-1} 2E_X} .\end{aligned} \tag{2.24}$$

9 We note that we use the term "uncorrelated", since in this case the singularities behave as $\sim 1/E_g/E_\gamma$.
10 The energy ordering will simplify the single-soft regularisation, see Eq. (2.30).

We *define* action of the operator $\mathbb{S}$ on the matrix element squared in such a way that it extracts the most singular behaviour of the matrix element in the double-soft limit. To this end, we consider the scaling $E_4 \sim E_5 \sim \lambda$ and define

$$\mathbb{S}|\mathcal{A}^{\text{tree}}(\{p\};k_4,k_5)|^2 = \lim_{\lambda\to 0} \lambda^4 |\mathcal{A}^{\text{tree}}(\{p\};\lambda k_4,\lambda k_5)|^2 \,. \tag{2.25}$$

In the following, we will discuss the emission of a soft gluon pair and the emission of a soft quark-antiquark pair separately.

Gluon-pair emission

The double-soft function that describes emission of two gluons with momenta k_4 and k_5 for an amplitude with n hard emitters reads [123]

$$\begin{aligned}\mathbb{S}|\mathcal{A}^{\text{tree}}_{gg}(\{p\};k_4,k_5)|^2 = g_{s,b}^4 \Bigg\{ \frac{1}{2} \sum_{i,j,k,l=1}^{n} \mathcal{S}_{ij}(k_4)\mathcal{S}_{kl}(k_5)|\mathcal{A}^{\{(ij),(kl)\}}(\{p\})|^2 \\ - C_A \sum_{i,j=1}^{n} \mathcal{S}_{ij}(k_4,k_5)|\mathcal{A}^{(ij)}(\{p\})|^2 \Bigg\} \,.\end{aligned} \tag{2.26}$$

Here the set $\{p\}$ denotes the momenta of the emitters and $g_{s,b}$ is the bare strong coupling. Colour correlations in Eq. (2.26) are encoded in the Born-like matrix elements $\mathcal{A}^{\{(ij),(kl)\}}(\{p\})$ and $\mathcal{A}^{(ij)}(\{p\})$, see Eq. (B.12) for details. The first term on the right-hand side of Eq. (2.26) is the *abelian* contribution. It is simply a product of single-eikonal factors, given by

$$\mathcal{S}_{ij}(k) = \frac{(p_i \cdot p_j)}{(p_i \cdot k)(p_j \cdot k)} \,. \tag{2.27}$$

The second, *non-abelian* contribution is proportional to the colour factor C_A. It is given by the function $\mathcal{S}_{ij}(k_4,k_5)$, which reads [96, 123]

$$\mathcal{S}_{ij}(k_4,k_5) = \mathcal{S}^0_{ij}(k_4,k_5) + \left[m_i^2 \mathcal{S}^m_{ij}(k_4,k_5) + m_j^2 \mathcal{S}^m_{ji}(k_4,k_5) \right] \,. \tag{2.28}$$

In Eq. (2.28) both functions $\mathcal{S}^0_{ij}(k_1,k_2)$ and $\mathcal{S}^m_{ij}(k_1,k_2)$ implicitly depend on the masses of the emitters, $m_{i,j}$. These functions can be found in Eqs. (B.13)-(B.14).

Quark-antiquark pair emission

The double-soft limit of the matrix element squared that describes the emission of a quark-antiquark pair reads

$$\mathbb{S}|\mathcal{A}^{\text{tree}}_{q\bar{q}}(\{p\};k_4,k_5)|^2 = g_{s,b}^4\, T_F \sum_{i,j=1}^{n} \mathcal{I}_{ij}(k_4,k_5)|\mathcal{A}^{(ij)}(\{p\})|^2 \,, \tag{2.29}$$

where $T_F = 1/2$ and the function $\mathcal{I}_{ij}(k_1,k_2)$ is given in Appendix B.2.

Remaining single-soft divergence

To complete the soft regularisation, we have to consider the double-soft regulated term on the r. h. s. of Eq. (2.23). It reads

$$\left\langle \widetilde{[\mathrm{d}k_4][\mathrm{d}k_5]}\,(I-\mathbb{S})\,\overleftrightarrow{F_{\mathrm{LM}}}(1_{f_1},2_{f_2},X;4_{f_4},5_{f_5})\right\rangle . \tag{2.30}$$

In the case of gg emission, this term has an additional single-soft divergence, which arises when the energy of gluon $g(k_5)$ vanishes, $E_5 \to 0$. We emphasize at this point that the energy ordering in Eq. (2.22) prevents a similar soft singularity of gluon $g(k_4)$. To regulate the single-soft behaviour, we insert the identity $I = (I-S_5) + S_5$ into Eq. (2.30) and find

$$\begin{aligned}
&\left\langle \widetilde{[\mathrm{d}k_4][\mathrm{d}k_5]}\;(I-\mathbb{S})\;\overleftrightarrow{F_{\mathrm{LM}}}(1_{f_1},2_{f_2},X;4_g,5_g)\right\rangle \\
&= \left\langle \widetilde{[\mathrm{d}k_4][\mathrm{d}k_5]}\;(I-\mathbb{S})\;(I-S_5)\;\overleftrightarrow{F_{\mathrm{LM}}}(\ldots;4_g,5_g)\right\rangle \\
&+ \left\langle \widetilde{[\mathrm{d}k_4][\mathrm{d}k_5]}\;(I-\mathbb{S})\,S_5\;\overleftrightarrow{F_{\mathrm{LM}}}(\ldots;4_g,5_g)\right\rangle .
\end{aligned} \tag{2.31}$$

The operator S_5 is defined in analogy to $\mathbb{S}$, i. e. it removes k_5 from the momentum-conserving δ-function and the measurement function. It also extracts the most singular behaviour of the matrix element squared in the limit $E_5 \to 0$. Explicitly,

$$S_5|\mathcal{A}_g^{\mathrm{tree}}(\{p\};k_5)|^2 = -\,g_{s,b}^2 \sum_{i,j=1}^{n} \mathcal{S}_{ij}(k_5)|\mathcal{A}^{(ij)}(\{p\})|^2 , \tag{2.32}$$

where $\mathcal{S}_{ij}$ is given in Eq. (2.27). We find that gluon $g(k_5)$ decouples from the hard process up to color correlations.

The first term on the r. h. s. of Eq. (2.31) is regular in *all* soft limits but still contains collinear divergences. We discuss collinear regularisation of these divergences in Sec. 2.3. The second term on the r. h. s. of Eq. (2.31) is the double-soft regulated, single-soft subtraction term. Schematically, we can write this contribution as

$$\begin{aligned}
&\left\langle \widetilde{[\mathrm{d}k_4][\mathrm{d}k_5]}\;(I-\mathbb{S})\,S_5\;\overleftrightarrow{F_{\mathrm{LM}}}(1_{f_1},2_{f_2},X;4_g,5_g)\right\rangle \\
&\sim \left\langle [\mathrm{d}k_4]\;(I-S_4)\;\overleftrightarrow{F_{\mathrm{LM}}}(1_{f_1},2_{f_2},X;4_g)\times\int[\mathrm{d}k_5]\mathrm{Eik}(\{p\},k_5)\,\theta(E_4-E_5)\right\rangle ,
\end{aligned} \tag{2.33}$$

where we have used that $\mathbb{S}S_5 = S_4 S_5$ and omitted possible color correlations.[11] The single soft subtraction term in Eq. (2.33) still exhibits collinear singularities when gluon $g(k_4)$ becomes collinear to any of the hard partons. However, these singularities can be easily extracted in an NLO-like manner, see e. g. Refs. [1–4, 124]. The resulting terms contribute to the double-real cross section in Eq. (2.16) through the double-unresolved, Born-like contribution $\mathrm{d}\sigma_X^{RR}(\epsilon)$ (collinear $g(k_4)$) and through single-unresolved contribution $\mathrm{d}\sigma_{X+1}^{RR}(\epsilon)$(resolved $g(k_4)$).

11 In particular, we write "$\mathrm{Eik}(\{p\},k_5)$" instead of "$\mathcal{S}_{ij}(k_5)$".

2.2.2 *Uncorrelated double-soft singularities*

In the following Section we discuss the construction of subtraction terms for the emission of a gluon and a photon. We consider the partonic process $u(p_1) + \bar{d}(p_2) \to W^+(p_W) + g(k_4) + \gamma(k_5)$, which contributes to mixed QCD-EW corrections to W-boson hadroproduction [9] discussed in Part II of this thesis. We denote the differential cross section as

$$2s \cdot \mathrm{d}\sigma^{RR}_{Wg\gamma} = \left\langle [\mathrm{d}k_4][\mathrm{d}k_5]\; F_{\mathrm{LM}}\left(1_u, 2_{\bar{d}}, W^+; 4_g, 5_\gamma\right)\right\rangle , \tag{2.34}$$

following the notation introduced in Eq. (2.12). As already mentioned, the double-soft emission of a gluon-photon pair is *uncorrelated*; this means that instead of an entangled double-soft limit, only products of single-soft limits appear. Therefore, we can construct a simpler subtraction prescription than what was done in Sec. 2.2.1. To this end, we isolate *all* soft singularities by inserting the identity $I = \left[(I - S_g) + S_g\right] \times \left[(I - S_\gamma) + S_\gamma\right]$ into Eq. (2.34) and find

$$\begin{aligned}
&\left\langle [\mathrm{d}k_4][\mathrm{d}k_5]\; F_{\mathrm{LM}}\left(1_u, 2_{\bar{d}}, W^+; 4_g, 5_\gamma\right)\right\rangle \\
&= \left\langle [\mathrm{d}k_4][\mathrm{d}k_5] S_\gamma S_g\; F_{\mathrm{LM}}\left(1_u, 2_{\bar{d}}, W^+; 4_g, 5_\gamma\right)\right\rangle \\
&\;+ \left\langle [\mathrm{d}k_4][\mathrm{d}k_5]\left[\,(I - S_g)\, S_\gamma + (I - S_\gamma)\, S_g\right]\; F_{\mathrm{LM}}\left(1_u, 2_{\bar{d}}, W^+; 4_g, 5_\gamma\right)\right\rangle \\
&\;+ \left\langle [\mathrm{d}k_4][\mathrm{d}k_5]\; (I - S_\gamma)\; (I - S_g)\; F_{\mathrm{LM}}\left(1_u, 2_{\bar{d}}, W^+; 4_g, 5_\gamma\right)\right\rangle ,
\end{aligned} \tag{2.35}$$

where S_g (S_γ) denotes the soft gluon(photon) limit. Similarly to operator S_5, which is defined in Eq. (2.32), operators $S_{g,\gamma}$ extract the leading singular behaviour of the matrix element squared in the limit $k_{4,5} \to 0$ and remove $k_{4,5}$ from the momentum-conserving δ-function.

We begin our analysis of the various term in Eq. (2.35) by considering the soft-gluon limit. It reads

$$S_g\; F_{\mathrm{LM}}\left(1_u, 2_{\bar{d}}, W^+; 4_g, 5_\gamma\right) = 2 g_s^2 C_F\, \mathcal{S}_{12}(k_4)\; F_{\mathrm{LM}}\left(1_u, 2_{\bar{d}}, W^+; 5_\gamma\right) , \tag{2.36}$$

where $\mathcal{S}_{ij}$ is defined in Eq. (2.27), $C_F = (N_c^2 - 1)/(2N_c)$ is the $SU(N_c)$ Casimir invariant and $N_c = 3$ is the number of colors.

The soft-photon limit, on the other hand, is more involved due to the fact that the W boson carries electric charge. In diagrams that contribute to this limit, the photon is emitted from an external on-shell particle. The three relevant diagrams are

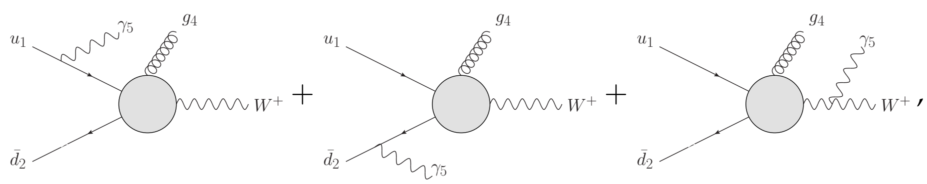

(2.37)

where the grey circle illustrates that the gluon is emitted from either the internal u or d quark. We extract the leading $1/E_5$ behaviour of the amplitude and obtain

$$\begin{aligned} & S_\gamma\, \mathcal{A}^{RR}_{u_1\bar{d}_2\to W^+ g_4\gamma_5} \\ &= e\left[Q_u \frac{p_1^\mu}{(p_1\cdot k_5)} - Q_d \frac{p_2^\mu}{(p_2\cdot k_5)} - Q_W \frac{p_W^\mu}{(p_W\cdot k_5)}\right] \varepsilon^*_\mu(k_5)\, \mathcal{A}^R_{u_1\bar{d}_2\to W^+ g_4}\,. \end{aligned} \tag{2.38}$$

In Eq. (2.38), $p_W = p_1 + p_2 - k_4$ is the momentum of the W boson and Q_u, Q_d, and $Q_W = Q_u - Q_d$ are the electric charges of up and down quarks, and the W boson, respectively. Upon squaring the expression in Eq. (2.38) and averaging over polarisations of the photon, we obtain

$$S_\gamma\, F_{\rm LM}(1_u, 2_{\bar{d}}, W^+; 4_g, 5_\gamma) = e^2\, \mathrm{Eik}_\gamma(p_1, p_2, p_W, k_5)\, F_{\rm LM}(1_u, 2_{\bar{d}}, W^+; 4_g)\ , \tag{2.39}$$

where

$$\begin{aligned} \mathrm{Eik}_\gamma(p_1, p_2, p_W, k_5) = \Big\{ & 2Q_u Q_d\, \mathcal{S}_{12}(k_5) - Q_W^2\, \mathcal{S}_{WW}(k_5) \\ & + 2Q_W\left[Q_u \mathcal{S}_{1W}(k_5) - Q_d \mathcal{S}_{W2}(k_5)\right]\Big\}\,. \end{aligned} \tag{2.40}$$

We note that the soft-gluon limit in Eq. (2.36) is independent of the photon four-momentum k_5. The soft-photon limit in Eq. (2.39), on the other hand, depends on p_W and, therefore, on the gluon four-momentum k_4 because of momentum conservation.

We are now in position to discuss the various terms on the r. h. s. of Eq. (2.35). The first term is the *uncorrelated* double-soft contribution, where both the gluon and the photon are soft. It reads

$$\begin{aligned} & \left\langle [\mathrm{d}k_4][\mathrm{d}k_5] S_\gamma S_g\, F_{\rm LM}(1_u, 2_{\bar{d}}, W^+; 4_g, 5_\gamma)\right\rangle \\ &= \int [\mathrm{d}k_5]\, \left[e^2\, \mathrm{Eik}_\gamma(p_1, p_2, p_1 + p_2, k_5)\right] \times \int [\mathrm{d}k_4]\, \left[2 g_s^2 C_F\, \mathcal{S}_{12}(k_4)\right] \\ &\quad \times \left\langle F_{\rm LM}(1_u, 2_{\bar{d}}, W^+)\right\rangle\,. \end{aligned} \tag{2.41}$$

In writing Eq. (2.41), we have used the fact that in the double-soft limit the soft-photon eikonal factor $\mathrm{Eik}_\gamma(\dots)$ does not depend on the momentum of the soft gluon, i. e. we set $p_W = p_1 + p_2$. Since both integrals in this formula exhibit poles starting at $1/\epsilon^2$, they have to be computed to $\mathcal{O}(\epsilon^2)$ to obtain finite contributions. We note that the integral over the soft-gluon eikonal function $\mathcal{S}_{12}$ can be calculated in a straightforward way. In fact, we find [9]

$$2 g_s^2 C_F \int [\mathrm{d}k_4]\, \mathcal{S}_{12}(k_4) = [\alpha_s] \frac{2 C_F\, (2\, E_{\rm max})^{-2\epsilon}}{\epsilon^2} \frac{\Gamma^2\,(1-\epsilon)}{\Gamma\,(1-2\epsilon)}\,, \tag{2.42}$$

where $[\alpha_s]$ is defined in Eq. (B.1). We will discuss the computation of the soft-photon integral in Sec. 3.1.2.

The second and the third term on the r. h. s. of Eq. (2.35) describe cases where the gluon is soft-regulated and the photon is soft ($\sim\ (I-S_g)\,S_\gamma$), and vice versa. We obtain

$$\begin{aligned}&\left\langle [dk_4][dk_5]\ (I-S_g)\,S_\gamma\ F_{LM}(1_u,2_{\bar d},W^+;4_g,5_\gamma)\right\rangle\\&=\left\langle (I-S_g)\int [dk_5]\ [e^2\,\mathrm{Eik}_\gamma(p_1,p_2,p_W,k_5)]\ F_{LM}(1_u,2_{\bar d},W^+;4_g)\right\rangle,\end{aligned}\tag{2.43}$$

and

$$\begin{aligned}&\left\langle [dk_4][dk_5]\ (I-S_\gamma)\,S_g\ F_{LM}(1_u,2_{\bar d},W^+;4_g,5_\gamma)\right\rangle\\&=\left[\int [dk_4]2g_s^2C_F\,\mathcal{S}_{12}(k_4)\right]\times\left\langle (I-S_\gamma)\ F_{LM}(1_u,2_{\bar d},W^+;5_\gamma)\right\rangle,\end{aligned}\tag{2.44}$$

respectively. We note that the soft-photon contribution in Eq. (2.43) is regulated in the soft-gluon limit but exhibits singularities when the gluon in the hard matrix element $F_{LM}(1_u,2_{\bar d},W^+;4_g)$ becomes collinear to one of the initial-state quarks. While the regularisation of these collinear divergences is NLO-like and for this reason straightforward,[12] it requires us to compute the soft-photon integral in Eq. (2.43) in case of a collinear gluon to higher orders in ϵ; we will present this computation in Sec. 3.1.2. Similarly, the matrix element $F_{LM}(1_u,2_{\bar d},W^+;5_\gamma)$ in Eq. (2.44) exhibits collinear singularities caused by the photon. These contribution multiply higher order ϵ-contributions of the integrated soft-gluon eikonal function Eq. (2.42). Finally, we note that the fourth term on the r. h. s. of Eq. (2.35) is regular in both soft limits.

2.2.3 *Processes with a single-soft singularity*

For the sake of completeness, we also consider partonic processes with $f_{4,5}=qg$, which only exhibit a single-soft but no double-soft divergence.[13] We write the corresponding contribution as

$$\left\langle [dk_4][dk_5]\ F_{LM}(1_{f_1},2_{f_2},X;4_q,5_g)\right\rangle.\tag{2.45}$$

Note that we did *not* introduce any energy ordering. Analogously to the extraction of the single-soft divergence in Eq. (2.31), we insert the identity $I=(I-S_5)+S_5$ and find

$$\begin{aligned}&\left\langle [dk_4][dk_5]\ F_{LM}(1_{f_1},2_{f_2},X;4_q,5_g)\right\rangle\\&=\left\langle [dk_4][dk_5]\ (I-S_5)\ F_{LM}(1_{f_1},2_{f_2},X;4_q,5_g)\right\rangle\\&+\left\langle [dk_4][dk_5]S_5\ F_{LM}(1_{f_1},2_{f_2},X;4_q,5_g)\right\rangle.\end{aligned}\tag{2.46}$$

The first term on the r. h. s. of Eq. (2.46) is soft-regulated. The second term is a single-soft subtraction term, which can be treated following the discussion below Eq. (2.31).

12 We will discuss this aspect in Sec. 4.2.2.

13 An example is the process $q\,g\to Zqg$, which contributes to double-real NNLO QCD corrections to $pp\to Z$.

2.3 COLLINEAR REGULARISATION

In the previous Section, we have sketched how to extract and regulate soft singularities appearing in double-real contributions. In this Section, we consider soft-regulated contributions, which we write as

$$\left\langle [\mathrm{d}k_4][\mathrm{d}k_5]\,\hat{O}_{\text{soft}}\; F_{\text{LM}}\big(1_{f_1}, 2_{f_2}, X; 4_{f_4}, 5_{f_5}\big)\right\rangle , \tag{2.47}$$

where $\hat{O}_{\text{soft}}$ denotes an appropriate combination of soft operators that regulates *all* soft singularities present in $F_{\text{LM}}\big(1_{f_1}, 2_{f_2}, X; 4_{f_4}, 5_{f_5}\big)$. More explicitly, $\hat{O}_{\text{soft}} = (I - \mathbb{S})\,(I - S_5)$ or $\hat{O}_{\text{soft}} = (I - S_4)\,(I - S_5)$ in case of correlated or uncorrelated double-soft singularities, respectively. In cases which only exhibit single-soft divergences, $\hat{O}_{\text{soft}} = (I - S_5)$.

In the following, we proceed with the extraction and regularisation of remaining *collinear* singularities. We emphasize again that this iterative formalism only works for gauge-invariant matrix elements whose soft and collinear singularities are disentangled thanks to color coherence. Hence, the collinear singularity structure and its regularisation do not depend on the energy parameterization, which is why we do not have to differ between the "standard" and the energy-ordered formulation on the l. h. s. and the r. h. s. of Eq. (2.22), respectively.

Collinear singularities in Eq. (2.47) occur, whenever partons $f_{4,5}$ become collinear partons $f_{1,2}$ in the initial state, to *massless* partons in the "hard" final-state X, or to each other. It can be shown that they factorize on external legs in physical gauges [123, 125].[14] However, the collinear limits can be approached in different ways, and it is beneficial to partition the phase space in order to uniquely identify how they are approached in a particular kinematic configuration.

2.3.1 *Collinear partitioning*

In general, there are two types of collinear singularities, since emitted partons $f_{4,5}$ can become collinear to *different* external partons, or to the *same* parton. To separate these cases, we follow the FKS approach [51, 52] and introduce energy-independent partition functions. We write

$$1 = \sum_{(i,j)\in\mathcal{DC}_p} \omega^{i4,j5}_{\mathcal{DC}} + \sum_{i\in\mathcal{TC}_p} \omega^{i4,o5}_{\mathcal{TC}}\,, \quad i \neq j\,, \tag{2.48}$$

where $\mathcal{DC}_p$ ($\mathcal{TC}_p$) denotes the set of so-called double-colllinear (triple-collinear) partitions. Weights are constructed to dampen the singular behaviour of matrix elements squared so that products $\omega^{ij,kl}_{\mathcal{DC}/\mathcal{TC}} \times F_{\text{LM}}$ only contain well-defined subsets of collinear limits.

14 In the physical (light-cone) gauge, a special case of axial gauge, the gluon propagator is proportional to "$-g^{\mu\nu} + (n^\mu p^\nu + n^\nu p^\mu)/(n\cdot p)$".

Double-collinear partitions $\omega_{\mathcal{DC}}^{i4,j5}$ are constructed in such a way that partons $f_{4,5}$ can only become collinear to external partons i and j, respectively; they dampen all but one collinear limit per emitted parton $f_{4,5}$. In particular, we require that double-collinear partition functions satisfy the following conditions

$$\begin{aligned} C_{4k}\, \omega_{\mathcal{DC}}^{i4,j5}\, F_{\rm LM} &\to \begin{cases} \sim 1/\eta_{4k}\,, & k=i\,, \\ \mathcal{O}\left(\eta_{4k}^{0}\right)\,, & \text{else}\,. \end{cases} \\ C_{5k}\, \omega_{\mathcal{DC}}^{i4,j5}\, F_{\rm LM} &\to \begin{cases} \sim 1/\eta_{5k}\,, & k=j\,, \\ \mathcal{O}\left(\eta_{5k}^{0}\right)\,, & \text{else}\,. \end{cases} \end{aligned} \tag{2.49}$$

Here, $i \neq j$ and the operator C_{4k} (C_{5k}) implies that the collinear limit $\eta_{4k} \to 0$ $(\eta_{5k} \to 0)$ should be taken.[15] Thanks to the conditions in Eq. (2.49), singularities can only appear when three-momenta $\boldsymbol{k}_{4,5}$ become collinear to the direction of *different* hard particles and, hence, *no* overlapping singularities occur.

Triple-collinear partitions $\omega_{\mathcal{TC}}^{i4,i5}$, on the other hand, select cases where singularities occur when partons $f_{4,5}$ become collinear to the same external parton i. They allow for singular configurations $\boldsymbol{k}_4 \parallel \boldsymbol{p}_i$, $\boldsymbol{k}_5 \parallel \boldsymbol{p}_i$, and $\boldsymbol{k}_4 \parallel \boldsymbol{k}_5$, which can be approached in various ways. We require that

$$\begin{aligned} C_{4j}\, \omega_{\mathcal{TC}}^{i4,i5}\, F_{\rm LM} &\to \begin{cases} \sim 1/\eta_{j4}\,, & j=i \vee j=5\,, \\ \mathcal{O}\left(\eta_{j4}^{0}\right)\,, & \text{else}\,. \end{cases} \\ C_{5j}\, \omega_{\mathcal{TC}}^{i4,i5}\, F_{\rm LM} &\to \begin{cases} \sim 1/\eta_{j5}\,, & j=i \vee j=4\,, \\ \mathcal{O}\left(\eta_{j4}^{0}\right)\,, & \text{else}\,. \end{cases}\,. \end{aligned} \tag{2.50}$$

We insert the partition of unity in Eq. (2.48) into the soft-regulated contribution in Eq. (2.47) and find

$$\begin{aligned} &\left\langle [dk_4][dk_5]\, \hat{O}_{\rm soft}\, F_{\rm LM}(1_{f_1},2_{f_2},X;4_{f_4},5_{f_5})\right\rangle \\ &= \sum_{(i,j)\in\mathcal{DC}_p} \left\langle [dk_4][dk_5]\, \hat{O}_{\rm soft}\, \omega_{\mathcal{DC}}^{i4,j5}\, F_{\rm LM}(1_{f_1},2_{f_2},X;4_{f_4},5_{f_5})\right\rangle \\ &+ \sum_{i\in\mathcal{TC}_p} \left\langle [dk_4][dk_5]\, \hat{O}_{\rm soft}\, \omega_{\mathcal{TC}}^{i4,i5}\, F_{\rm LM}(1_{f_1},2_{f_2},X;4_{f_4},5_{f_5})\right\rangle\,. \end{aligned} \tag{2.51}$$

We note that since partition functions are chosen to be energy-independent, they commute with the soft limits. Apart from the well-defined damping behaviour as explained above, the precise form of the partition functions $\omega_{\mathcal{DC}/\mathcal{TC}}^{ij,kl}$ is not important for the following discussion. We note that explicit constructions can be found in Refs. [1–4]. Here, we proceed by discussing contributions from double- and triple-collinear partition functions in Eq. (2.51) in Sec. 2.3.2 and Sec. 2.3.3, respectively.

15 Angular variables η_{ij} where introduced in Eq. (2.13).

2.3.2 *Double-collinear partitions*

A subtraction prescription for terms proportional to double-collinear partitions $\omega_{DC}^{i4,j5}$ is straightforward thanks to the absence of overlapping singularities. We use the identity $I = [\,(I - C_{4i}) + C_{4i}]\,[\,(I - C_{5j}) + C_{5j}]$ and write

$$\begin{aligned}
&\Big\langle [dk_4][dk_5]\,\hat{O}_{\rm soft}\;\omega_{DC}^{i4,j5}\,F_{\rm LM}(1_{f_1},2_{f_2},X;4_{f_4},5_{f_5})\Big\rangle = \\
&\Big\langle\,(I - C_{4i})\;(I - C_{5j})\,[dk_4][dk_5]\,\hat{O}_{\rm soft}\;\omega_{DC}^{i4,j5}\,F_{\rm LM}(1_{f_1},2_{f_2},X;4_{f_4},5_{f_5})\Big\rangle \\
&+\Big\langle\,[C_{4i} + C_{5j}]\,[dk_4][dk_5]\,\hat{O}_{\rm soft}\;\omega_{DC}^{i4,j5}\,F_{\rm LM}(1_{f_1},2_{f_2},X;4_{f_4},5_{f_5})\Big\rangle \\
&-\big\langle\,[C_{4i}C_{5j}]\,[dk_4][dk_5]\,\hat{O}_{\rm soft}\,F_{\rm LM}(1_{f_1},2_{f_2},X;4_{f_4},5_{f_5})\big\rangle\,.
\end{aligned}\tag{2.52}$$

When writing Eq. (2.52) we have used

$$C_{4i}C_{5j}\;\omega_{DC}^{i4,j5} = 1\,. \tag{2.53}$$

This identity holds because, thanks to definitions in Eq. (2.49) and Eq. (2.50), $\omega_{DC}^{i4,j5}$ is the only partition that yields a non-vanishing contribution in the $C_{4i}C_{5j}$ limit and since partitions need to add up to one (cf. Eq. (2.48)) in *all* kinematic configurations.

The first term on the r. h. s. of Eq. (2.52) is fully regulated and can be integrated numerically in $d = 4$ dimensions. It enters the double-real cross section in Eq. (2.16) through the fully-resolved contribution $d\sigma^{RR}_{X+2}$. The two terms in the second line on the r. h. s. of Eq. (2.52) are soft-regulated single-unresolved. The term proportional to C_{4i} requires a NLO-like regularisation of the remaining collinear singularities of parton f_5, and vice versa.[16] After this additional step, these subtraction terms contribute to $d\sigma^{RR}_{X+1}$ and $d\sigma^{RR}_{X}$ in Eq. (2.16). The term in the third line on the r. h. s. of Eq. (2.52) is the so-called soft-regulated double-unresolved double-collinear subtraction term, which contributes to $d\sigma^{RR}_{X}$ in Eq. (2.16). As will become clear later in Example 2, this term admits a factorization formula, in which the momenta of $k_{4,5}$ are not correlated. We conclude that the analytic computation of all these integrated subtraction terms is essentially NLO-like; we refer to Refs. [1–4] for further discussion.

All contributions to Eq. (2.52) are described by two different limits: the single-unresolved double-collinear limit C_{4i} (C_{5j}), and the double-unresolved double-collinear limit $C_{4i}C_{5j}$. At this point, a comment on the double-collinear operators C_{ab} is in order to unambiguously define Eq. (2.52). Operators C_{ab} are *defined* in such a way that they act on every function that appears to their right. This includes the partition weight $\omega_{DC}^{i4,j5}$, the function F_{LM} *and* the phase-space measure $[dk_4][dk_5]$. The precise prescription for operator C_{4i}, for example, is given as follows [2–4]:

i) extract the leading $\sim 1/\eta_{4i}$ behaviour of the term $\omega_{DC}^{i4,j5}[dk_4][dk_5]\,F_{LM}$ and enforce the $\eta_{4i} \to 0$ limit in the remaining expression;

16 Neither particle $f_{4,5}$ can cause a soft singularity at this point.

ii) replace $p_i \to z \cdot p_i$, where the precise definition of energy-fraction z is dependent on whether the hard parton i is in the initial or in the final state.

We explain how these limits act on the phase-space element $[dk_4][dk_5]$ in Appendix B.5.1. As an illustration, in Example 1 and Example 2, we present single- and double-unresolved double-collinear limits of some matrix elements squared, respectively.

Example 1 (*Single-unresolved double-collinear factorization*)

We consider the double-real correction $q(p_1)\bar{q}(p_2) \to Z\, g(k_4)g(k_5)$ to color-singlet production in the limit where gluon $g(k_4)$ is collinear to quark $q(p_1)$ and find

$$C_{41}\ F_{\rm LM}(1_q, 2_{\bar{q}}, Z; 4_g, 5_g) = g_{s,b}^2 \frac{P_{qq}(z_4)}{(p_1 \cdot k_4)} \times \frac{F_{\rm LM}(z_4 \cdot 1_q, 2_{\bar{q}}, Z; 5_g)}{z} . \tag{2.54}$$

Here, $z_4 = (E_1 - E_4)/E_1$ and the splitting function

$$P_{qq}(z) = C_F \left[\frac{1+z^2}{1-z} - \epsilon(1-z) \right] , \tag{2.55}$$

describes the collinear splitting $q \to q^* + g$. We note that Eqs. (2.54)-(2.55) are derived in Appendix B.3.

Example 2 (*Double-unresolved double-collinear factorization*)

The double-unresolved double-collinear limit for color singlet decay $Z \to q(p_a)\bar{q}(p_b)g(k_4)g(k_5)$ reads

$$\begin{aligned} &C_{4a}C_{5b}\ F_{\rm LM}(a_q, b_{\bar{q}}, Z; 4_g, 5_g) = \\ &g_{s,b}^4 \frac{P_{qq}(z_4)P_{qq}(z_5)}{(p_a \cdot k_4)\,(p_b \cdot k_5)} \times F_{\rm LM}(1/z_4 \cdot a_q, 1/z_5 \cdot b_{\bar{q}}, Z) . \end{aligned} \tag{2.56}$$

In this case, energy fractions of collinear splittings off final-state quarks are defined as

$$z_4 = \frac{E_a}{E_a + E_4}, \quad z_5 = \frac{E_b}{E_b + E_5} . \tag{2.57}$$

We note that momenta $k_{4,5}$ are not entangled in this double-unresolved limit, i. e. it is NLO-like. As a consequence, it is straightforward to integrate this subtraction term over the unresolved phase-space. The double-unresolved double-collinear limit in Eq. (2.56) can be derived following the steps described in Appendix B.3.

2.3.3 *Triple-collinear partitions*

As defined in Eq. (2.50), *triple-collinear* partitions $\omega_{TC}^{i4,i5}$ allow for singularities that arise in the limit where both partons f_4 and f_5 become collinear to the same external parton

i. This includes the triple-collinear singularity $\boldsymbol{k}_4 \parallel \boldsymbol{k}_5 \parallel \boldsymbol{p}_i$, which is extracted by a triple-collinear operator $\mathbb{C}_i$. The triple-collinear limit is approached by $\eta_{4i} \to 0$, $\eta_{5i} \to 0$ with $\eta_{4i} \sim \eta_{5i} \sim \eta_{45}$. Furthermore, overlapping double-collinear singularities can arise in the limits $\boldsymbol{k}_4 \parallel \boldsymbol{p}_i$, $\boldsymbol{k}_5 \parallel \boldsymbol{p}_i$, or $\boldsymbol{k}_4 \parallel \boldsymbol{k}_5$. In what follows, we show that these singularities can be disentangled by introducing sector functions that divide the phase space into non-overlapping regions.[17] First, we consider the general case, where all three double-collinear singularities are present. Then, we turn to the special case of $g\gamma$-emission for which the limit $\boldsymbol{k}_4 \parallel \boldsymbol{k}_5$ is not singular.

Triple-collinear sectors in the general case

In order to discuss the most general structure of singularities arising in contributions proportional to triple-collinear partion functions, we consider the emission of a gluon pair ($f_4 f_5 = gg$). In physical gauges, only three diagrams shown in Fig. 2.1 contribute to the singularities that are allowed by $\omega_{TC}^{i4,i5}$. In addition to the triple-collinear singularity in the limit $\boldsymbol{k}_4 \parallel \boldsymbol{k}_5 \parallel \boldsymbol{p}_i$, diagrams Fig. 2.1 (a), (b), and (c) have singularities in the limits $\boldsymbol{k}_4 \parallel \boldsymbol{p}_i$, $\boldsymbol{k}_5 \parallel \boldsymbol{p}_i$, and $\boldsymbol{k}_4 \parallel \boldsymbol{k}_5$, respectively. To isolate these overlapping singularities, we divide the phase space into four sectors θ^k, such that in each of these sectors the three angles η_{i4}, η_{i5}, and η_{45} have a well-defined hierarchy. We write

$$1 = \sum_{k \in \{a,b,c,d\}} \theta^k \,, \tag{2.58}$$

where

$$\theta^a = \theta(\eta_{i4}/2 - \eta_{i5}) \,, \tag{2.59}$$
$$\theta^b = \theta(\eta_{i5} - \eta_{i4}/2) \times \theta(\eta_{i4} - \eta_{i5}) \,, \tag{2.60}$$
$$\theta^c = \theta(\eta_{i5}/2 - \eta_{i4}) \,, \tag{2.61}$$
$$\theta^d = \theta(\eta_{i4} - \eta_{i5}/2) \times \theta(\eta_{i5} - \eta_{i4}) \,. \tag{2.62}$$

The four different phase-space regions are visualized in Fig. 2.2. Besides the triple-collinear singularity, each sector θ^k features a divergence in *one* double-collinear limit. We denote double-collinear operators that extract these limits in each sector k by C^k and write

$$C^a = C_{5i} \,, \quad C^b = C_{45} \,, \quad C^c = C_{4i} \,, \quad C^d = C_{45} \,. \tag{2.63}$$

17 We note that overlapping singularities can also be disentangled by introducing additional damping factors [101, 102].

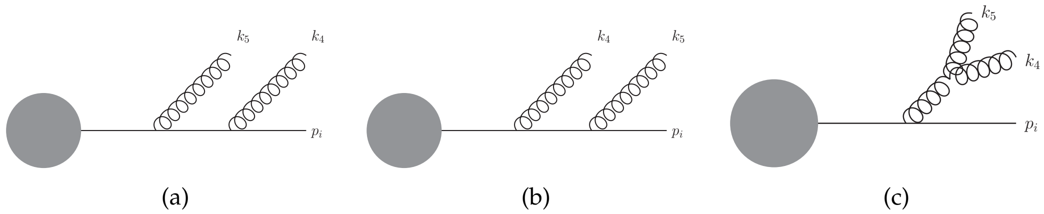

Figure 2.1: Diagrams that contribute to the singularity structure in the triple-collinear partition contribution in case of gg emission off a quark with momentum p_i.

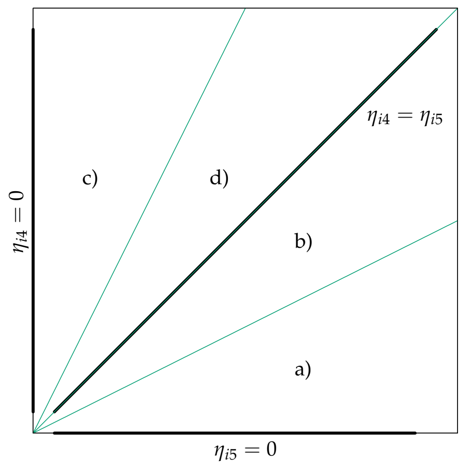

Figure 2.2: Visualization of the four sectors defined in Eqs. (2.59)-(2.62). Black lines correspond to double-collinear singularities, the triple-collinear singularity is at the origin.

Triple-collinear sectors in the case of $g\gamma$ emission

As mentioned above, simplifications arise in the case of $g\gamma$-emission. The two diagrams that contribute to collinear singularities in the triple-collinear partition are shown in Fig. 2.3, where, as in Sec. 2.2.2, gluon and photon carry momenta k_4 and k_5, respectively.[18] While both diagrams in Fig. 2.3 contribute to the triple collinear singularity, diagrams (a) and (b) have distinct double-collinear divergences in the limits $\boldsymbol{k}_4 \parallel \boldsymbol{p}_i$ (collinear gluon) and $\boldsymbol{k}_5 \parallel \boldsymbol{p}_i$ (collinear photon), respectively. However, there is no singular behaviour in the $\boldsymbol{k}_4 \parallel \boldsymbol{k}_5$ limit, and it is therefore sufficient to introduce only two sectors. Following Ref. [9] we define

$$1 = \sum_{k\in\{A,B\}} \theta^k \,, \tag{2.64}$$

where

$$\theta^A = \theta(\eta_{5i} - \eta_{4i}) \,, \tag{2.65}$$

$$\theta^B = \theta(\eta_{4i} - \eta_{5i}) \,, \tag{2.66}$$

and

$$C^A = C_{4i} \,, \quad C^B = C_{5i} \,. \tag{2.67}$$

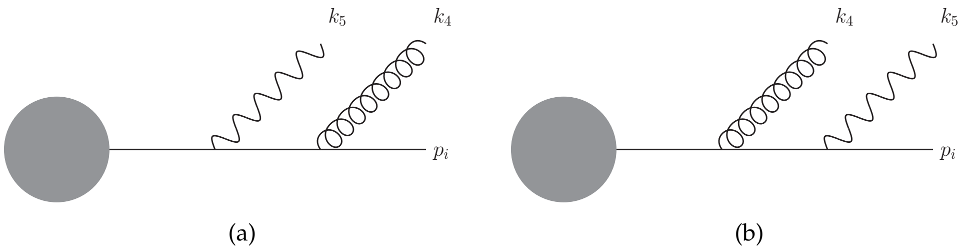

Figure 2.3: Diagrams that contribute to the triple-collinear partition in case of the $q^* \to g(k_4)\gamma(k_5)q(p_i)$ splitting.

Regularisation

We are now in position to regulate collinear singularities that appear in the terms in Eq. (2.51) that are proportional to triple-collinear partitions $\omega_{TC}^{i4,i5}$. For both definitions of

18 Again, this statement holds in physical gauges where collinear singularities factorize on external legs.

sectors ($\theta^{a..d}$ and $\theta^{A,B}$) discussed above, we insert partitions of unity (cf. Eq. (2.58) and Eq. (2.64)) and write

$$\begin{aligned}&\Big\langle [\mathrm{d}k_4][\mathrm{d}k_5]\,\hat{O}_{\rm soft}\;\;\omega^{i4,i5}_{\mathcal{TC}}\,F_{\rm LM}(1_{f_1},2_{f_2},X;4_{f_4},5_{f_5})\Big\rangle = \\ &\sum_k \Big\langle \theta^k [\mathrm{d}k_4][\mathrm{d}k_5]\,\hat{O}_{\rm soft}\;\;\omega^{i4,i5}_{\mathcal{TC}}\,F_{\rm LM}(1_{f_1},2_{f_2},X;4_{f_4},5_{f_5})\Big\rangle\,.\end{aligned} \tag{2.68}$$

Since each sector features only two overlapping collinear singularities, writing a subtraction formula is straightforward. We begin with extracting the double-collinear singularity by inserting the identity $\left(I - C^k\right) + C^k$ for each sector θ^k in Eq. (2.68). We obtain

$$\begin{aligned}&\sum_k \Big\langle \theta^k [\mathrm{d}k_4][\mathrm{d}k_5]\,\hat{O}_{\rm soft}\;\;\omega^{i4,i5}_{\mathcal{TC}}\,F_{\rm LM}(1_{f_1},2_{f_2},X;4_{f_4},5_{f_5})\Big\rangle = \\ &\sum_k \Big\{ \Big\langle \theta^k C^k [\mathrm{d}k_4][\mathrm{d}k_5]\,\hat{O}_{\rm soft}\;\;\omega^{i4,i5}_{\mathcal{TC}}\,F_{\rm LM}(1_{f_1},2_{f_2},X;4_{f_4},5_{f_5})\Big\rangle \\ &\quad + \Big\langle \theta^k\,\left(I - C^k\right)[\mathrm{d}k_4][\mathrm{d}k_5]\,\hat{O}_{\rm soft}\;\;\omega^{i4,i5}_{\mathcal{TC}}\,F_{\rm LM}(1_{f_1},2_{f_2},X;4_{f_4},5_{f_5})\Big\rangle\Big\}\,,\end{aligned} \tag{2.69}$$

where operators C^k were defined in Eq. (2.63) and Eq. (2.67). We define double-collinear operators in Eq. (2.69) in the same way as in the case of double-collinear partition, cf. Eq. (2.52). In the limit $\boldsymbol{a} \parallel \boldsymbol{b}$, these operators extract the leading behaviour in $1/\eta_{ab}$ from the matrix element squared and take the $\eta_{ab} \to 0$ limit everywhere else. In particular, they also act on the phase-space element $[\mathrm{d}k_4][\mathrm{d}k_5]$. We define the double-collinear limit of the phase space in Sec. B.5. Factorization of matrix elements squared in the single-collinear limit was illustrated in Example 1.

The first term on the r. h. s. of Eq. (2.69) is proportional to $\theta^k C^k$. We call it soft-regulated single-unresolved; it contains one unregulated collinear divergence that is particular to sector k.[19] The remaining collinear singularities are NLO-like and we do not discuss them further.

The second term on the r. h. s. of Eq. (2.69) is regular in the double-collinear limits; its only remaining singularity is the triple-collinear one. We insert the identity $I = (I - \mathbb{C}_i) + \mathbb{C}_i$ and obtain

$$\begin{aligned}&\sum_k \Big\langle \theta^k\,\left(I - C^k\right)[\mathrm{d}k_4][\mathrm{d}k_5]\,\hat{O}_{\rm soft}\;\;\omega^{i4,i5}_{\mathcal{TC}}\,F_{\rm LM}(1_{f_1},2_{f_2},X;4_{f_4},5_{f_5})\Big\rangle = \\ &\sum_k \Big\{ \Big\langle \theta^k\,\left(I - C^k\right)[\mathrm{d}k_4][\mathrm{d}k_5]\,\hat{O}_{\rm soft}\;(I - \mathbb{C}_i)\;\omega^{i4,i5}_{\mathcal{TC}}\,F_{\rm LM}(1_{f_1},2_{f_2},X;4_{f_4},5_{f_5})\Big\rangle \\ &\quad + \Big\langle \theta^k\,\left(I - C^k\right)[\mathrm{d}k_4][\mathrm{d}k_5]\,\hat{O}_{\rm soft}\;\mathbb{C}_i\;F_{\rm LM}(1_{f_1},2_{f_2},X;4_{f_4},5_{f_5})\Big\rangle\Big\}\,,\end{aligned} \tag{2.70}$$

19 For example in sector $k = b$, this term describes the emission of a gluon $g(k_{45})$ with momentum $k_4 + k_5$, which can become collinear to parton i. Or, as a second example, the term with sector $k = A$ describes the case where $\gamma(k_5)$ is still resolved and causes a singularity in the limit $\boldsymbol{k}_5 \parallel \boldsymbol{p}_i$.

where we have used that $\mathbb{C}_i\ \omega_{\mathcal{TC}}^{i4,i5} = 1$. This relation holds in analogy to Eq. (2.53), since $\omega_{\mathcal{TC}}^{i4,i5}$ is the only non-vanishing partition in the $\mathbb{C}_i$ limit.

We note that operators $\mathbb{C}_i$, in variance to double-collinear operators, do *not* act on the phase-space measure; this is why they appear to the right of $[dk_4][dk_5]$ in Eq. (2.70). However, they still act on matrix elements squared and momentum-conserving δ-functions, producing triple-collinear splitting functions $P_{f_i f_4 f_5}$ [123] and reduced matrix elements squared. Furthermore, it was shown in Refs. [2, 3] how to deal with spin-correlations in initial-state and final-state triple-collinear limits by averaging over azimuthal angles. For this reason, we only consider *spin-averaged* splitting functions in what follows.

In order to unambiguously define Eq. (2.70), it remains to specify the "genuine" triple-collinear limit $\mathbb{C}_i$ and its "strongly-ordered" counterpart $C^k\ \mathbb{C}_i$. To do so, we consider the most involved case of double-gluon emission in three different scenarios. First, we illustrate the triple-collinear limit $\mathbb{C}_i$ for initial- and final-state emissions in Example 3 and Example 4, respectively. Then, we consider an example of strongly-ordered triple-collinear emission off a final state particle in Example 5. For the detailed derivation of these formulas, we refer the reader to Ref. [123].

Example 3 (*Triple-collinear initial-state radiation*)

As an example of triple-collinear splitting in an initial state, we consider emission of partons $f_{4,5}$ collinear to parton f_1 and find

$$\begin{aligned}\mathbb{C}_1\ F_{\mathrm{LM}}(1_{f_1}, 2_{f_2}, X; 4_{f_4}, 5_{f_5}) = g_s^4 \left(\frac{2}{s_{145}}\right)^2 \times \\ P_{f_1 f_4 f_5}(-s_{14}, -s_{15}, s_{45}, z_1, z_4, z_5)\ F_{\mathrm{LM}}\left(\frac{E_1 - E_4 - E_5}{E_1} \cdot 1_f, 2_{f_2}, X\right) .\end{aligned} \tag{2.71}$$

Here $s_{145} = -s_{14} - s_{15} + s_{45}$ and energy fractions $z_{1,3,4}$ are given by

$$z_1 = (E_1 - E_4 - E_5)/E_1\,, \quad z_{4,5} = (E_4 + E_5 - E_1)/E_{4,5}\,, \tag{2.72}$$

such that the Born-like matrix element only depends on variable z_1. We note that the spin-averaged splitting function $P_{f_1 f_4 f_5}$ [123] describes triple-collinear splittings $f \to f_1 f_4 f_5$; the minus signs in its arguments in Eq. (2.71) reflect the fact that we crossed parton f_1 into the initial state.

Example 4 (***Triple-collinear final-state radiation***)

We consider emission of partons $f_{4,5}$ collinear to parton f_a in the decay $X \to f_a f_b + f_4 f_5$ and find

$$\mathbb{C}_a\; F_{\rm LM}(a_{f_a}, b_{f_b}, X; 4_{f_4}, 5_{f_5}) = g_s^4 \left(\frac{2}{s_{a45}}\right)^2 \\ \times P_{f_1 f_4 f_5}(s_{a4}, s_{a5}, s_{45}, z_a, z_4, z_5)\; F_{\rm LM}\left(\frac{E_a + E_4 + E_5}{E_a} \cdot a_f, b_{f_b}, X\right), \tag{2.73}$$

where $s_{a45} = s_{a4} + s_{a5} + s_{45}$ and $z_{a,4,5} = (E_a + E_4 + E_5)/E_{a,4,5}$.

Example 5 (***Strongly-ordered triple-collinear final-state radiation***)

We consider the strongly-ordered triple-collinear limit $\boldsymbol{k}_4 \parallel \boldsymbol{p}_1$ and $\boldsymbol{k}_4 \parallel \boldsymbol{k}_5 \parallel \boldsymbol{p}_1$ in the decay $Z \to q(p_1)\bar{q}(p_2) + g(k_4)g(k_5)$ and find

$$C_{41}\; \mathbb{C}_1\; F_{\rm LM}(1_q, 2_{\bar{q}}, Z; 4_g, 5_g) = \\ g_s^4\, \frac{P_{qq}(z)\, P_{qq}(\bar{z})}{(p_1 \cdot k_4)\, (p_1 \cdot k_5)}\; F_{\rm LM}\left(\frac{E_1 + E_4 + E_5}{E_1} \cdot 1_q, 2_{\bar{q}}, Z\right). \tag{2.74}$$

We note that in Eq. (2.74), $z = E_1/(E_1 + E_4)$ and $\bar{z} = (E_4 + E_1)/(E_1 + E_4 + E_5)$, and that momenta $k_{4,5}$ appear in an uncorrelated fashion.

We now return to the discussion of Eq. (2.70). The first term there is fully regulated and can be integrated numerically in $d = 4$ dimensions. It enters the double-real cross section in Eq. (2.16) through the fully-resolved contribution $\mathrm{d}\sigma^{RR}_{X+2}$. Regularisation of triple-collinear singularities marks the end of the nested regularisation procedure. We will summarize the required soft- and collinear subtractions in Sec. 2.4.

The second term on the r. h. s. of Eq. (2.70) is the so-called soft-regulated, triple-collinear subtraction term, which will be discussed in Sec. 2.6. It contributes to the double-real cross section in Eq. (2.16) through the double-unresolved contribution $\mathrm{d}\sigma^{RR}_{X}$. For now, we note that this subtraction term has been computed analytically in Ref. [5] for *all* possible partonic configurations for *both* initial- and final-state emissions.

2.4 REGULATED GLUON-EMISSION CONTRIBUTION IN Z-BOSON PRODUCTION

In what follows, we will summarize the results of the soft- and collinear subtraction procedure described in Sec. 2.2 and Sec. 2.3. To do so, we consider the emission of two gluons in color singlet (Z-boson) production, $q(p_1)\,\bar{q}(p_2) \to Z + g(k_4)g(k_5)$. We note that we choose this particular process because it possesses the most general structure of IR singularities.

Using the notation introduced in Eq. (2.12), we write the fully-differential cross section as

$$2s \cdot \mathrm{d}\sigma^{RR}_{Zgg} = \left\langle \widetilde{[\mathrm{d}k_4][\mathrm{d}k_5]}\; \overleftrightarrow{F_{\mathrm{LM}}}(1_q, 2_{\bar{q}}, Z; 4_g, 5_g) \right\rangle . \tag{2.75}$$

We follow the discussion in Sec. 2.2.1 to regulate and extract double- and single-soft singularities. In particular we adopted the energy-ordered notation of Eq. (2.20) and Eq. (2.21) in Eq. (2.75). Using the fact that the corresponding matrix element squared is symmetric under the exchange of two gluons $g(k_4) \leftrightarrow g(k_5)$, we write

$$\left\langle \widetilde{[\mathrm{d}k_4][\mathrm{d}k_5]}\; \overleftrightarrow{F_{\mathrm{LM}}}(1_q, 2_{\bar{q}}, Z; 4_g, 5_g) \right\rangle = 2 \left\langle \widetilde{[\mathrm{d}k_4][\mathrm{d}k_5]}\; F_{\mathrm{LM}}(1_q, 2_{\bar{q}}, Z; 4_g, 5_g) \right\rangle . \tag{2.76}$$

Collinear singularities in Eq. (2.76) are disentangled using partition functions as introduced in Eq. (2.48). For the case at hand, we need two double-collinear partitions $\mathcal{DC}_p = \{(1,2),(2,1)\}$ and two triple-collinear partitions $\mathcal{TC}_p = \{1,2\}$. We write

$$1 = \omega^{14,25}_{\mathcal{DC}} + \omega^{24,15}_{\mathcal{DC}} + \omega^{14,15}_{\mathcal{TC}} + \omega^{24,25}_{\mathcal{TC}} . \tag{2.77}$$

In partition $\omega^{14,25}_{\mathcal{DC}}$ $\left(\omega^{24,15}_{\mathcal{DC}}\right)$, a singularity arises when gluon $g(k_4)$ becomes collinear to quark $q(p_1)$ and gluon $g(k_5)$ becomes collinear to antiquark $\bar{q}(p_2)$ (and vice versa). In partition $\omega^{14,15}_{\mathcal{TC}}$ $\left(\omega^{24,25}_{\mathcal{TC}}\right)$ a singularity develops when gluons become collinear to quark $q(p_1)$ $\left(\text{antiquark } \bar{q}(p_2)\right)$ and to each other. Partitions are constructed in such a way that they supress all singularities except the ones that we mentioned explicitly. Collinear singularities in contributions stemming from triple-collinear partitions are disentangled by introducing the four sectors as defined in Eqs. (2.58)-(2.62).

Finally, we write the complete double-real cross section as

$$\left\langle \widetilde{[\mathrm{d}k_4][\mathrm{d}k_5]}\; F_{\mathrm{LM}}(1_q, 2_{\bar{q}}, Z; 4_g, 5_g) \right\rangle = \tag{2.78}$$

$$\left\langle \widetilde{[\mathrm{d}k_4][\mathrm{d}k_5]}\; \mathbb{S}\, F_{\mathrm{LM}}(1_q, 2_{\bar{q}}, Z; 4_g, 5_g) \right\rangle \tag{2.79}$$

$$+ \left\langle \widetilde{[\mathrm{d}k_4][\mathrm{d}k_5]}\; (I - \mathbb{S})\, S_5\, F_{\mathrm{LM}}(1_q, 2_{\bar{q}}, Z; 4_g, 5_g) \right\rangle \tag{2.80}$$

$$+ \sum_{\substack{i,j=1,2\\ i\neq j}} \left\langle [C_{4i} + C_{5j}]\; \widetilde{[\mathrm{d}k_4][\mathrm{d}k_5]}\; (I - \mathbb{S})\; (I - S_5)\; \omega^{i4,j5}_{\mathcal{DC}}\, F_{\mathrm{LM}}(1_q, 2_{\bar{q}}, Z; 4_g, 5_g) \right\rangle \tag{2.81}$$

$$+ \sum_{i=1,2} \sum_{k=a..d} \left\langle \theta^k C^k \widetilde{[\mathrm{d}k_4][\mathrm{d}k_5]}\; (I - \mathbb{S})\; (I - S_5)\; \omega^{i4,i5}_{\mathcal{TC}}\, F_{\mathrm{LM}}(1_q, 2_{\bar{q}}, Z; 4_g, 5_g) \right\rangle \tag{2.82}$$

$$- \sum_{\substack{i,j=1,2\\ i\neq j}} \left\langle C_{4i} C_{5j} \widetilde{[\mathrm{d}k_4][\mathrm{d}k_5]}\; (I - \mathbb{S})\; (I - S_5)\, F_{\mathrm{LM}}(1_q, 2_{\bar{q}}, Z; 4_g, 5_g) \right\rangle \tag{2.83}$$

$$+ \sum_{i=1,2} \sum_{k=a..d} \left\langle \theta^k \left(I - C^k\right) \widetilde{[\mathrm{d}k_4][\mathrm{d}k_5]}\; (I - \mathbb{S})\; (I - S_5)\; \mathbb{C}_i\, F_{\mathrm{LM}}(1_q, 2_{\bar{q}}, Z; 4_g, 5_g) \right\rangle \tag{2.84}$$

$$+\sum_{\substack{i,j=1,2\\ i\neq j}} \left\langle \hat{O}^{(i,j)}_{\rm NNLO}\, \widetilde{[dk_4][dk_5]}\; F_{\rm LM}(1_q,2_{\bar{q}},Z;4_g,5_g)\right\rangle \tag{2.85}$$

$$+\sum_{i=1,2}\sum_{k=a..d} \left\langle \hat{O}^{i,k}_{\rm NNLO}\, \widetilde{[dk_4][dk_5]}\; F_{\rm LM}(1_q,2_{\bar{q}},Z;4_g,5_g)\right\rangle . \tag{2.86}$$

The operators in Eqs. (2.79)-(2.86) are defined to extract leading singularities; we have discussed them in the preceding sections. They are summarized one more time in Table 2.1.

The contributions in Eq. (2.79), Eq. (2.83) and Eq. (2.84) denote the double-soft, double-collinear and triple-collinear subtraction terms, respectively. These double-unresolved contributions enter the double-real cross section in Eq. (2.16) through the Born-like term $d\sigma^{RR}_X(\epsilon)$. Contributions in Eq. (2.80), Eq. (2.81) and Eq. (2.82) are of the single-unresolved type. Each of these terms requires regularisation of the remaining NLO-like singularities caused by the respective resolved gluon, resulting in contributions to $d\sigma^{RR}_{X+1}(\epsilon)$ and $d\sigma^{RR}_X(\epsilon)$ in Eq. (2.16). Contributions in Eq. (2.85) and Eq. (2.86) are fully-regulated; the two operators that appear in these equations are defined as

$$\hat{O}^{(i,j)}_{\rm NNLO} = (I-C_{4i})\;(I-C_{5j})\;(I-\mathbb{S})\;(I-S_5)\;\omega^{i4,j5}_{\mathcal{DC}}\,, \tag{2.87}$$

$$\hat{O}^{i,k}_{\rm NNLO} = \theta^k\left(I-C^k\right)\;(I-\mathbb{C}_i)\;(I-\mathbb{S})\;(I-S_5)\;\omega^{i4,i5}_{\mathcal{TC}}\,. \tag{2.88}$$

We will continue with the discussion of the double-soft and the triple-collinear subtraction terms in Sec. 2.5 and Sec. 2.6, respectively.

name	symbol	limit	acts on phase-space
double-soft	$\mathbb{S}$	$E_4\to 0\,, E_5\to 0\,, E_4\sim E_5$	no
single-soft	S_i	$E_i\to 0$	no
triple-collinear	$\mathbb{C}_i$	$\eta_{4i}\to 0\,,\eta_{5i}\to 0\,,\eta_{4i}\sim\eta_{5i}\sim\eta_{45}$	no
double-collinear	$C_{ij}\;\left(C^k\right)$	$\eta_{ij}\to 0$	yes

Table 2.1: Summary of operators in the nested soft-collinear subtraction scheme.

2.5 DOUBLE-SOFT SUBTRACTION TERM

The double-soft subtraction term in Eq. (2.23) enters the double-real cross section in Eq. (2.16) through the Born-like contribution $d\sigma^{RR}_X(\epsilon)$. We summarize the above discussion by writing

$$\begin{aligned}&\left\langle \widetilde{[dk_4][dk_5]}\;\mathbb{S}\;F_{LM}(\ldots;4_{f_4},5_{f_5})\right\rangle\\ &\sim\left\langle F_{LM}(1_{f_1},2_{f_2},X)\times\int \widetilde{[dk_4][dk_5]}\,{\rm Eik}(\{p\},k_4,k_5)\right\rangle ,\end{aligned} \tag{2.89}$$

where we have omitted possible color-correlations between eikonal soft functions and the Born-like process.[20] We emphasize again that soft momenta $k_{4,5}$ decouple from the energy-momentum conservation, the measurement function and the matrix element squared. This allows us to obtain the double-soft subtraction term in a *universal* and *process-independent* manner by computing required double-soft integrals once and for all.

More specifically, we conclude that the double-soft subtraction term for an *arbitrary* process within the nested soft-collinear subtraction scheme can be constructed from the following three phase-space integrals

$$\mathcal{G}_{ij} = \int [\mathrm{d}k]\; \mathcal{S}_{ij}(k)\,, \tag{2.90}$$

$$\mathcal{G}\mathcal{G}_{ij} = \int [\mathrm{d}k_4][\mathrm{d}k_5]\, \theta(E_5 < E_4)\;\; \mathcal{S}_{ij}(k_4,k_5)\,, \tag{2.91}$$

$$\mathcal{Q}\bar{\mathcal{Q}}_{ij} = \int [\mathrm{d}k_4][\mathrm{d}k_5]\, \theta(E_5 < E_4)\;\; \mathcal{I}_{ij}(k_4,k_5)\,. \tag{2.92}$$

In Eqs. (2.90)-(2.92), indices i,j refer to the dependence of the soft integrals on two hard momenta p_i and p_j, respectively. Thanks to the properties of the integrands $\mathcal{S}_{ij}(k)$, $\mathcal{S}_{ij}(k_4,k_5)$, and $\mathcal{I}_{ij}(k_4,k_5)$, cf. Eq. (2.27), Eq. (2.28), and Eq. (B.15), the three quantities $\mathcal{G}_{ij}$, $\mathcal{G}\mathcal{G}_{ij}$, and $\mathcal{Q}\bar{\mathcal{Q}}_{ij}$ are symmetric under $i \leftrightarrow j$ exchange. Furthermore, the integrands are invariant under a re-scaling of hard momenta $p_{i,j} \to \lambda_{i,j} p_{i,j}$.[21] Hence, $\mathcal{G}_{ij}$, $\mathcal{G}\mathcal{G}_{ij}$, and $\mathcal{Q}\bar{\mathcal{Q}}_{ij}$ do not depend on the energies of hard emitters. Finally, we note that integrals over $\mathrm{d}E_4$ and $\mathrm{d}E_5$ in Eqs. (2.90)-(2.92) have decoupled from the energy-momentum conservation; therefore they are only restricted since we introduced the cut-off parameter $E_{\max}$ in Eq. (2.15).

The above discussion is valid for arbitrary processes. However, the functions $\mathcal{G}_{ij}$, $\mathcal{G}\mathcal{G}_{ij}$ and $\mathcal{Q}\bar{\mathcal{Q}}_{ij}$ in Eqs. (2.90)-(2.92) show important differences for massive and massless partons. One can distinguish three cases: *1)* both emitters are massless; *2)* both emitters are massive; and *3)* one emitter is massive and the other is massless. On top of that, masses of the two emitters can also differ. We discuss the different kinematic cases in what follows.

2.5.1 *Massless case*

In case the emitters are massless, $p_i^2 = p_j^2 = 0$, we can parameterize hard momenta as follows

$$p_{i,j} = E_{i,j} \times \begin{pmatrix} 1 \\ \boldsymbol{n}_{i,j} \end{pmatrix}\,. \tag{2.93}$$

20 In particular, we write "Eik($\{p\}, k_4, k_5$)" instead of fucntions $\mathcal{S}_{ij}(k_4)\mathcal{S}_{kl}(k_5)$, $\mathcal{S}_{ij}(k_4,k_5)$, or $\mathcal{I}_{ij}(k_1,k_2)$ that appear in Eq. (2.26) and Eq. (2.29).

21 For this counting to be valid, on has to consider that $m_{i,j}^2 = p_{i,j}^2 \to \lambda_{i,j}^2 m_{i,j}^2$.

Functions $\mathcal{G}_{ij}$, $\mathcal{GG}_{ij}$ and $\mathcal{Q}\bar{\mathcal{Q}}_{ij}$ in Eqs. (2.90)-(2.92) depend on the relative angle $\cos\theta_{ij} = \boldsymbol{n}_i \cdot \boldsymbol{n}_j$ between hard partons i and j, but, as discussed above, not on their energies. All phase-space integrals that are required in this case were computed analytically in Refs. [36, 37] and we present these results in Appendix C.1.

The double-soft subtraction term for massless emitters has been essential to demonstrate analytic cancellation of ϵ poles in color-singlet prodution [2], color-singlet decay [3] and deep-inelastic scattering [4]. Assuming that ϵ poles cancel with other contributions to cross sections, we schematically write the finite remainder in Eq. (2.89) as

$$\begin{aligned}&\left\langle F_{\mathrm{LM}}(1_{f_1}, 2_{f_2}, X) \times \int \widetilde{[\mathrm{d}k_4][\mathrm{d}k_5]}\, \mathrm{Eik}(\{p\}, k_4, k_5) \right\rangle \\ &\longrightarrow \sum_{i,j} \left\langle F_{\mathrm{LM}}(1_{f_1}, 2_{f_2}, X)_{ij} \times \mathcal{DS}(\cos\theta_{ij}) \right\rangle .\end{aligned} \tag{2.94}$$

In writing this equation, we denote the color-correlations of the Born-level matrix element by "$F_{LM}(1_{f_1}, 2_{f_2}, X)_{ij}$". From Eq. (2.94) it is evident that contributions to a physical cross section that involves an arbitrary number of massless colored partons at the Born level can be computed in a very efficient way. Indeed, according to Eq. (2.94) it suffices to generate Born-like events, weighted by the easy-to-evaluate function $\mathcal{DS}(\cos\theta_{ij})$ that can be constructed from results in Appendix C.1.

2.5.2 *Massive case*

In the case of massive emitters, $p_{i,j}^2 = m_{i,j}^2$, we can parameterize hard momenta as

$$p_{i,j} = \frac{m_{i,j}}{\sqrt{1-\beta_{i,j}^2}} \times \begin{pmatrix} 1 \\ \beta_{i,j}\boldsymbol{n}_{i,j} \end{pmatrix} , \tag{2.95}$$

where $\beta_{i,j}$ and $\boldsymbol{n}_{i,j}$ denote velocity and direction of flight of partons i and j, respectively. In this parametrization, the aforementioned independence of energies translates into an independence of masses $m_{i,j}$. Integrals in Eqs. (2.90)-(2.92) are then functions of velocities β_i, β_j and the relative angle $\cos\theta_{ij}$.

In this thesis, we discuss the analytic computation of $\mathcal{G}_{ij}$, $\mathcal{GG}_{ij}$ and $\mathcal{Q}\bar{\mathcal{Q}}_{ij}$ in the case where both emitters have the same mass ($m_i = m_j$) and are back-to-back ($\cos\theta_{ij} = 0$) [6]. The computation of $\mathcal{G}_{ij}$ is NLO-like and rather straightforward; we present it in Sec. 3.1.1. On the other hand, the functions $\mathcal{GG}_{ij}$ and $\mathcal{Q}\bar{\mathcal{Q}}_{ij}$ are genuinely NNLO-like, their computation is presented in Sec. 3.2.2. The results fully characterize the integrated double-soft subtraction term to describe the decay process of a colour singlet into two massive fermions, e. g. $H \to b\bar{b}$. Furthermore, they are important ingredients to describe more complex processes such as heavy-quark pair production within the nested soft-collinear subtraction scheme.

2.5.3 *Massive-massless case*

In the case where one emitter (e. g. parton i) is massive and the other is massless, integrals in Eqs. (2.90)-(2.92) are functions of $\cos\theta_{ij}$ and β_i. For example, such integrals would be required to describe single-top or heavy-quark pair production within the NSS. We plan to address this case in the future.

2.6 triple-collinear subtraction term

In the following Section, we discuss the triple-collinear subtraction term that was defined in Eq. (2.70); it is convenient to split it into the difference of two contributions

$$\begin{aligned}\mathcal{I}_{TC} &= \sum_k \left\langle \theta^k \left(I - C^k\right) [dk_4][dk_5]\, \hat{O}_{\rm soft}\; \mathbb{C}_i\; F_{\rm LM}(1_{f_1}, 2_{f_2}, X; 4_{f_4}, 5_{f_5}) \right\rangle \\ &= \langle [dk_4][dk_5]\, \hat{O}_{\rm soft}\; \mathbb{C}_i\; F_{\rm LM}(1_{f_1}, 2_{f_2}, X; 4_{f_4}, 5_{f_5}) \rangle \\ &\quad - \sum_k \left\langle \theta^k\, C^k [dk_4][dk_5]\, \hat{O}_{\rm soft}\; \mathbb{C}_i\; F_{\rm LM}(1_{f_1}, 2_{f_2}, X; 4_{f_4}, 5_{f_5}) \right\rangle . \end{aligned} \tag{2.96}$$

The term in the first line on the r. h. s. of Eq. (2.96),

$$\mathcal{I}_{TC}^{\rm gen} = \langle [dk_4][dk_5]\, \hat{O}_{\rm soft}\; \mathbb{C}_i\; F_{\rm LM}(1_{f_1}, 2_{f_2}, X; 4_{f_4}, 5_{f_5}) \rangle \,, \tag{2.97}$$

is of "genuine" triple-collinear nature and *independent* of how sectors are defined. Terms in the second line on the r. h. s. of Eq. (2.96),

$$\mathcal{I}_{TC}^{\rm s.o.} = \sum_k \left\langle \theta^k\, C^k [dk_4][dk_5]\, \hat{O}_{\rm soft}\; \mathbb{C}_i\; F_{\rm LM}(1_{f_1}, 2_{f_2}, X; 4_{f_4}, 5_{f_5}) \right\rangle , \tag{2.98}$$

on the other hand, are proportional to double-collinear operators C^k. These so-called *strongly-ordered* contributions depend on how sectors are defined.

The factorization formulas for the matrix element squared in the triple-collinear limit $\mathbb{C}_i$ for initial- and final-state splittings are given in Eq. (2.71) and Eq. (2.73), respectively. We use them to write the subtraction terms in Eqs. (2.97)-(2.98) as[22]

$$\begin{aligned}\mathcal{I}_{TC}^{\rm gen} &= 4g^4 \Bigg\langle [dk_4][dk_5]\, \hat{O}_{\rm soft}\, \frac{P_{f_i,f_4,f_5}(\pm s_{i4}, \pm s_{i5}, s_{45}, \pm E_i, E_4, E_5)}{s_{i45}^2} \\ &\quad \times F_{\rm LM}\left(\frac{\mp E_i - E_4 - E_5}{\mp E_i} \cdot (p_i)_f\, , .. \right) \Bigg\rangle , \\ \mathcal{I}_{TC}^{\rm s.o.} &= 4g^4 \sum_k \Bigg\langle \theta^k C^k [dk_4][dk_5]\, \hat{O}_{\rm soft}\, \frac{P_{f_i,f_4,f_5}(\pm s_{i4}, \pm s_{i5}, s_{45}, \pm E_i, E_4, E_5)}{s_{i45}^2} \end{aligned} \tag{2.99}$$

22 The sign convention for incoming (outgoing) partons f_i is $-$" ("$+$") in the argument of P_{f_i,f_4,f_5} and "$+E_i$" ("$-E_i$") in the argument of $F_{\rm LM}$.

$$\times\, F_{\mathrm{LM}}\left(\frac{\mp E_i - E_4 - E_5}{\mp E_i}\cdot (p_i)_f\,,..\right)\Big\rangle\,, \tag{2.100}$$

where $g^4 = g_s^4$ in case of NNLO QCD corrections and $g^4 = g_s^2 e^2$ in case of mixed QCD-EW corrections. We note that it was shown in Refs. [2, 3] that we only have to consider spin-averaged splitting functions in Eq. (2.99) and Eq. (2.100). Furthermore, we note that the appearance of the propagator $1/s_{i45}$ in Eq. (2.99) emphasises the double-unresolved nature of this subtraction term, complicating the phase-space integration. In the strongly-ordered limit in Eq. (2.100), this propagator factorizes into a product of two-particle kinematic invariants, as can be seen, for example, in Example 5.

In what follows, we will discuss genuine and strongly-ordered triple-collinear subtraction terms in Sec. 2.6.1 and Sec. 2.6.2, respectively. We will provide a summary of all triple-collinear subtraction terms by listing required splitting functions that have to be considered in Sec. 2.6.3.

2.6.1 *Genuine triple-collinear subtraction terms*

We begin with the discussion of the genuine triple-collinear term $\mathcal{I}_{TC}^{\mathrm{gen}}$ in Eq. (2.99),

$$\begin{aligned}\mathcal{I}_{TC}^{\mathrm{gen}} &= 4g^4\Big\langle [\mathrm{d}k_4][\mathrm{d}k_5]\,\hat{O}_{\mathrm{soft}}\,\frac{P_{f_i,f_4,f_5}(\pm s_{i4},\pm s_{i5},s_{45},\pm E_i,E_4,E_5)}{s_{i45}^2}\\ &\times\, F_{\mathrm{LM}}\left(\frac{\mp E_i - E_4 - E_5}{\mp E_i}\cdot (p_i)_f\,,..\right)\Big\rangle\,. \end{aligned}\tag{2.101}$$

We note that, in variance to double-collinear operators C^k, the triple-collinear operator $\mathbb{C}_i$ does *not* act on the phase-space measure, leaving the unresolved phase space intact. This implies that taking this limit does *not* modify the scalar products s_{ij} (or s_{ijk}) that appear in Eq. (2.101). With this definition, the triple-collinear limit is independent of the precise phase-space parameterization. This was *not* the case in the original formulation of the nested soft-collinear subtraction scheme [1], where operator $\mathbb{C}_i$ was defined to act on the phase-space measure, and integrated triple-collinear subtraction terms were obtained numerically. In fact, the original prescription was changed precisely to facilitate the *analytic* integration of the triple-collinear subtraction terms [5].

In the new formulation, the triple-collinear subtraction term in Eq. (2.101) has to be integrated over the full, unresolved phase space.[23] We separate integration over energies and angles and write

$$\begin{aligned}\mathcal{I}_{TC}^{\mathrm{gen}} &= \int \mathrm{d}E_4\,\mathrm{d}E_5\,(E_4E_5)^{1-2\epsilon}\Phi_E(E_4,E_5)\,\hat{O}_{\mathrm{soft}}\,\mathcal{T}^{\pm}(E_i,E_4,E_5)\\ &\times\Big\langle\, F_{\mathrm{LM}}\left(\frac{\mp E_i - E_4 - E_5}{\mp E_i}\cdot (p_i)_f\,,..\right)\Big\rangle\,, \end{aligned}\tag{2.102}$$

23 We note that the phase-space is constrained by the $E_{\max}$ cut-off in Eq. (2.15) and might be energy-ordered.

where the operator $\hat{O}_{\rm soft}$ and the energy constraint function Φ_E depend on whether the soft singularity structure of the partonic process warrants energy ordering. In writing Eq. (2.102) we have defined the angular integral

$$\mathcal{T}^{\pm}(E_i, E_4, E_5) = 4g^4 \int \mathrm{d}\Omega_{45}^{(d-1)} \, \frac{P_{f_i,f_4,f_5}(\pm s_{i4}, \pm s_{i5}, s_{45}, \pm E_i, E_4, E_5)}{s_{i45}^2} \,, \tag{2.103}$$

with $\mathrm{d}\Omega_{45}^{(d-1)} = \mathrm{d}\Omega_4^{(d-1)}\,\mathrm{d}\Omega_5^{(d-1)}$. We note that, thanks to the new definition of $\mathbb{C}_i$, the integrand in Eq. (2.103) is a rotationally invariant function in $d-1$ spatial dimensions.

It follows from Eq. (2.102) that the hard matrix element squared depends *only* on the sum of energies $E_4 + E_5$. It is therefore possible to integrate over directions $\boldsymbol{n}_{4,5}$ in Eq. (2.103) and over ratio of energies E_4/E_5 in Eq. (2.102) in a *universal* manner. In fact, we will explain in Sec. 3.2.3 how angular integrals $\mathcal{T}^{\pm}$ in Eq. (2.103) can be obtained using methods of multi-loop calculations, and how resulting expressions can be integrated over energies.

In order to facilitate integration over energies in Eq. (2.102), we need to introduce convenient parameterizations. Below, we shortly explain how this can be done so that the following two requirements are met: *i)* the factorization of $F_{\rm LM}$ is ensured, and *ii)* the regularisation of soft singularities becomes explicit. To this end, we consider the cases of initial-state splittings $f_i \to f^* f_4 f_5$ with and without energy ordering, as well as final-state splittings $f^* \to f_i f_4 f_5$.

Parameterization for initial-state splittings with energy-ordering

The case of initial-state splittings that requires energy-ordering, e. g. $g \to g^* + gg$ or $q \to q^* + gg$ was discussed in Ref. [1] and we briefly summarize it here. The domain of integration over energies in Eq. (2.102) is defined by the function Φ_E. In the energy-ordered case, it reads

$$\Phi_E = \theta(E_{\rm max} - E_4)\,\theta(E_4 - E_5)\;. \tag{2.104}$$

The operator $\hat{O}_{\rm soft}$ that regulates all soft-singularities reads

$$\hat{O}_{\rm soft} = (I - \mathbb{S})\,(I - S_5) = I - S_5 - \mathbb{S} + \mathbb{S}S_5\,. \tag{2.105}$$

Altogether, we find the triple-collinear subtraction term

$$\begin{aligned}\mathcal{I}_{TC}^{\rm ISR} = & \int_0^{E_{\rm max}} \mathrm{d}E_4 \int_0^{E_4} \mathrm{d}E_5\,(E_4E_5)^{1-2\epsilon}\,[I - S_5 - \mathbb{S} + \mathbb{S}S_5]\,\mathcal{T}^-(E_i,E_4,E_5) \\ & \times \left\langle F_{\rm LM}\left(\frac{E_i - E_4 - E_5}{E_i}\cdot(p_i)_f,..\right)\right\rangle ,\end{aligned} \tag{2.106}$$

where the function $\mathcal{T}^-(E_i, E_4, E_5)$ is defined in Eq. (2.103). In order to decouple the matrix element squared in the term in Eq. (2.106) that is proportional to the identity operator I from remaining integrations over energies, we apply the change of variables

$$E_4 = E_i(1-z)(1-r/2)\,, \quad E_5 = E_i(1-z)r/2\,, \quad r \in [0,1]\,, \quad z \in [z_{\rm min}, 1]\,, \tag{2.107}$$

where

$$z_{\min} = 1 - \frac{E_{\max}/E_i}{1 - r/2} > 1 - E_{\max}/E_i\,. \tag{2.108}$$

Indeed, in this parameterization the matrix element squared reads

$$F_{\text{LM}}\left(\frac{E_i - E_4 - E_5}{E_i} \cdot (p_i)_f, ..\right) = F_{\text{LM}}\Big(z \cdot (p_i)_f, ..\Big)\,, \tag{2.109}$$

and has decoupled from the integration over r. Since the matrix element squared in Eq. (2.109) vanishes for $z < z_{\min}$ due to energy conservation [1], we can extend integration over z by replacing $z_{\min}$ with zero. This allows us to write the hard contribution to Eq. (2.106) as

$$\begin{aligned} \mathcal{I}_{TC}^{\text{ISR}}\Big|_{I} &= \frac{E_i^{4-4\epsilon}}{2} \int_0^1 \mathrm{d}z\,(1-z)^{3-4\epsilon} \int_0^1 \mathrm{d}r \left[\left(1 - \frac{r}{2}\right)\frac{r}{2}\right]^{1-2\epsilon} \\ &\times \mathcal{T}^{-}\left(E_i, E_i(1-z)\left(1 - \frac{r}{2}\right), E_i(1-z)\frac{r}{2}\right) \Big\langle F_{\text{LM}}\Big(z \cdot (p_i)_f, ..\Big)\Big\rangle\,. \end{aligned} \tag{2.110}$$

We now turn to the discussion of the contribution proportional to the single-soft operator S_5 in Eq. (2.106). We note that the parameterization in Eq. (2.107) is not suited to describe this limit, which requires us to take $E_5 \to 0$ at fixed E_4. In order to describe the single-soft contribution to the triple-collinear subtraction term, we choose the following parameterization

$$E_4 = E_i(1-z)\,, \quad E_5 = E_i(1-z)r\,, \quad r \in [0,1]\,, \quad z \in [z_{\min}, 1]\,. \tag{2.111}$$

The single-soft limit requires us to extract the leading $1/r$ behavior in the $r \to 0$ limit. Upon doing this, we find

$$\begin{aligned} \mathcal{I}_{TC}^{\text{ISR}}\Big|_{S_5} &= E_i^{4-4\epsilon} \int_0^1 \mathrm{d}z(1-z)^{3-4\epsilon} \int_0^1 \frac{\mathrm{d}r}{r^{1+2\epsilon}} \\ &\times \left[\lim_{r\to 0} r^2 \mathcal{T}^{-}(E_i, E_i(1-z), E_i(1-z)r)\right] \Big\langle F_{\text{LM}}\Big(z \cdot (p_i)_f, ..\Big)\Big\rangle\,. \end{aligned} \tag{2.112}$$

We note that when writing Eq. (2.112), we have again replaced $z_{\min}$ with zero, and that the product $r^2 \cdot \mathcal{T}(\dots)$ is regular at $r = 0$. Furthermore, we note that the single-soft contribution in Eq. (2.112) can be integrated over r, rendering the respective ϵ pole explicit.

The parameterization in Eq. (2.111) is also suitable for the discussion of the double-soft limit, since $z \to 1$ sends both $E_{4,5} \to 0$ while the ratio E_4/E_5 is kept fixed. Accordingly, we write the remaining two contributions to Eq. (2.106) as

$$\mathcal{I}_{TC}^{\text{ISR}}\Big|_{\cancel{S}} = E_i^{4-4\epsilon} \int_{z_{\min}}^1 \frac{\mathrm{d}z}{(1-z)^{1+4\epsilon}} \int_0^1 \mathrm{d}r\, r^{1-2\epsilon}$$

$$\times \left[\lim_{z\to 1}(1-z)^4 \mathcal{T}^-(E_i, E_i(1-z), E_i(1-z)r)\right] \left\langle F_{\rm LM}\Big((p_i)_f, ..\Big)\right\rangle, \qquad (2.113)$$

$$\mathcal{I}_{TC}^{\rm ISR}\Big|_{\mathbb{S}S_5} = E_i^{4-4\epsilon} \int_{z_{\rm min}}^1 \frac{{\rm d}z}{(1-z)^{1+4\epsilon}} \int_0^1 \frac{{\rm d}r}{r^{1+2\epsilon}}$$

$$\times \left[\lim_{r\to 0}\lim_{z\to 1}(1-z)^4 r^2 \mathcal{T}^-(E_i, E_i(1-z), E_i(1-z)r)\right] \left\langle F_{\rm LM}\Big((p_i)_f, ..\Big)\right\rangle. \qquad (2.114)$$

Here, we had to keep $z_{\rm min}$; the reason for this is that energies $E_{4,5}$ decouple from the energy conservation in F_{LM} in the double-soft limit, so that the region $z \in [0, z_{\rm min}]$ is not automatically cut off in Eqs. (2.113)-(2.114). We note that the double-soft contribution in Eq. (2.113) can be explicitly integrated over z, while the strongly-ordered contribution in Eq. (2.114) can be integrated over both r and z.

Upon adding the contributions Eq. (2.110) and Eqs. (2.112)-(2.114) and carrying out integrations over r and z where possible, we arrive at the following result

$$\mathcal{I}_{TC}^{\rm ISR} = E_i^{-4\epsilon} \int_0^1 {\rm d}z \left[R_\delta\, \delta(1-z) + \frac{R_+}{[(1-z)^{1+4\epsilon}]_+} + R_{\rm reg}(z)\right]$$
$$\times \left\langle \frac{F_{\rm LM}\Big(z\cdot(p_i)_f, ..\Big)}{z}\right\rangle. \qquad (2.115)$$

The definition of the so-called plus prescription $[\ldots]_+$, used in the above formula, is given in Eq. (B.4). The three functions $R_{\delta,+,\,{\rm reg}}$ in Eq. (2.115) read

$$\begin{aligned} R_\delta =& \frac{(E_{\rm max}/E_i)^{-4\epsilon} - 1}{4\epsilon} A_3 - \int_0^1 \frac{{\rm d}r}{r^{1+2\epsilon}} \frac{[(1+r)^{4\epsilon} - 1]}{4\epsilon} F(r), \\ R_+ =& A_1(1) + A_2(1), \\ R_{\rm reg}(z) =& \frac{A_1(z) + A_2(z) - A_1(1) - A_2(1)}{(1-z)^{1+4\epsilon}}, \end{aligned} \qquad (2.116)$$

where

$$\begin{aligned}
A_1(z) &= \frac{z(1-z)^4}{2^{-2\epsilon}} \int_0^1 \frac{\mathrm{d}r}{r^{1+2\epsilon}} \left(1-\frac{r}{2}\right)^{-1-2\epsilon} (I - \hat{L}_r) \\
&\quad \times \left[\left(\frac{r}{2}\right)^2 \left(1-\frac{r}{2}\right)^2 E_i^4 \, \mathcal{T}^- \left(E_i, E_i(1-z)\left(1-\frac{r}{2}\right), E_i(1-z)\frac{r}{2}\right) \right], \\
A_2(z) &= \frac{z(1-z)^4}{2\epsilon} \left[1 - \frac{\Gamma^2(1-2\epsilon)}{\Gamma(1-4\epsilon)}\right] \\
&\quad \times \hat{L}_r \left[E_i^4 r^2 \, \mathcal{T}^- (E_i, E_i(1-z), E_i(1-z)r) \right], \\
A_3 &= \int_0^1 \frac{\mathrm{d}r}{r^{1+2\epsilon}} \, \hat{L}_{1-z} (I - \hat{L}_r) \\
&\quad \times \left[E_i^4 (1-z)^4 r^2 \, \mathcal{T}^- (E_i, E_i(1-z), E_i(1-z)r) \right], \\
F(r) &= \hat{L}_{1-z} \left[E_i^4 (1-z)^4 r^2 \, \mathcal{T}^- (E_i, E_i(1-z), E_i(1-z)r) \right],
\end{aligned} \tag{2.117}$$

and

$$\hat{L}_x \, g(\ldots, x, \ldots) = \lim_{x\to 0} g(\ldots, x, \ldots) \,. \tag{2.118}$$

We postpone the computation of the three quantities $R_{\delta,+,\,\mathrm{reg}}$ in Eq. (2.116) until Sec. 3.2.3.

Parameterization for initial-state splittings without energy-ordering

Some partonic processes are free of double-soft or soft singularities in general. The former is the case for the $f_{4,5} = qg$ final state,[24] whereas the latter is the case for the $f_{4,5} = qq'$ final state. In these cases, we do not introduce any energy ordering. Then, the integration in Eq. (2.102) is constrained by

$$\Phi_E = \theta(\, E_{\max} - E_4)\, \theta(\, E_{\max} - E_5) \,, \tag{2.119}$$

and the operator $\hat{O}_{\mathrm{soft}}$ that regulates the (potential) single-soft singularity reads

$$\hat{O}_{\mathrm{soft}} = I - S_5 \,. \tag{2.120}$$

To describe the hard contribution proportional to the identity operator I, we choose the parameterization

$$E_4 = E_i(1-z)(1-r) \,, \quad E_5 = E_i(1-z) r \,, \tag{2.121}$$

24 We note that the regularization of single-soft singularities was discussed in Sec. 2.2.3. In particular, we assign momentum k_5 (k_4) to the particle that can (cannot) become soft.

where $z, r \in [0,1]$. For the single-soft contribution, proportional to S_5, we employ the parameterization in Eq. (2.111). Following steps similar to the ones in the previous section, we obtain

$$\mathcal{I}_{TC}^{\text{ISR}} = E_i^{-4\epsilon} \int_0^1 \mathrm{d}z \; \widetilde{R}_{\text{reg}}(z) \left\langle \frac{F_{\text{LM}}\Big(z \cdot (p_i)_f, ..\Big)}{z} \right\rangle . \tag{2.122}$$

In writing Eq. (2.122), we have defined

$$\widetilde{R}_{\text{reg}}(z) = z(1-z)^{3-4\epsilon} \left[\tilde{A}_1(z) + \tilde{A}_2(z)\right] , \tag{2.123}$$

where

$$\begin{aligned}
\tilde{A}_1(z) &= \int_0^1 \frac{\mathrm{d}r}{r^{1+2\epsilon}} (1-r)^{1-2\epsilon} \\
&\quad \times (1-\hat{L}_r) \Bigg[r^2 E_i^4 \, \mathcal{T}^-(E_i, E_i(1-z)(1-r), E_i(1-z)r) \Bigg], \\
\tilde{A}_2(z) &= \frac{1}{2\epsilon} \left[\left(\frac{E_{\max}}{E_i} \right)^{-2\epsilon} (1-z)^{2\epsilon} - \frac{(1-2\epsilon)}{(1-4\epsilon)} \frac{\Gamma^2(1-2\epsilon)}{\Gamma(1-4\epsilon)} \right] \\
&\quad \times \hat{L}_r \left[r^2 E_1^4 \, \mathcal{T}^-(E_i, E_i(1-z), E_i(1-z)r) \right] .
\end{aligned} \tag{2.124}$$

The computation of the quantity $\widetilde{R}_{\text{reg}}(z)$ in Eq. (2.123) is described in Sec. 3.2.3.

Parameterization for final-state splittings

Up to now, we have focused on triple-collinear splittings in initial-state radiation as discussed in Refs. [1, 2]. In what follows, we focus on final-state triple-collinear splittings. The corresponding subtraction terms were discussed in Refs. [3, 126]. We begin with the subtraction term for the final-state emission, cf. Eq. (2.102), and write

$$\begin{aligned}
\mathcal{I}_{TC}^{\text{FSR}} &= \int \mathrm{d}E_4 \, \mathrm{d}E_5 \, (E_4 E_5)^{1-2\epsilon} \, \theta(E_4 - E_5) \, \theta(E_{\max} - E_4) \, (I - \mathbb{S}) \, (I - S_5) \\
&\times S(E_i) \, \mathcal{T}^+(E_i, E_4, E_5) \left\langle \frac{\mathrm{d}^{d-1} \boldsymbol{p}_i}{(2\pi)^{d-1} 2E_i} \, F_{\text{LM}}\left(\frac{E_i + E_4 + E_5}{E_i} \cdot (p_i)_f, .. \right) \right\rangle .
\end{aligned} \tag{2.125}$$

We note that $\mathcal{T}^+$ in Eq. (2.125) was defined in Eq. (2.103) and that we have restored the dependence on the damping factor $S(E_i)$, which was mentioned in Sec. 2.1 after Eq. (2.17). Furthermore, in Eq. (2.125) we have included the final-state phase-space volume in order to emphasize that it can be part of a re-definition of energies.

The function F_{LM} in Eq. (2.125) that describes the hard process depends on the total energy of the final-state particles $E = E_i + E_4 + E_5$. We parametrize energies accordingly, and write

$$E_4 = E\, x_1, \quad E_5 = E\, x_1 x_2, \quad E_i = E\,(1 - x_1 - x_1 x_2) \, . \tag{2.126}$$

In this parameterization the hard matrix element becomes independent of $x_{1,2}$ and we find

$$F_{\rm LM}\left(\frac{E_i + E_4 + E_5}{E_i} \cdot (p_i)_f, ..\right) = F_{\rm LM}\Big(E \cdot (n_i)_f, ..\Big)\,, \tag{2.127}$$

where the four-vector $n_i = (1, \boldsymbol{n}_i)$ denotes the direction-of-flight of hard parton i. Hence, the subtraction term in Eq. (2.125) is simply a number that depends on ϵ.

We note that the double-soft (single-soft) limit corresponds to the $x_1 \to 0$ ($x_2 \to 0$) limit in this parameterization, while the energy ordering $E_5 < E_4$ implies $x_2 < 1$. We employ the parametrization in Eq. (2.125) and obtain[25]

$$\begin{aligned} \mathcal{I}_{TC}^{\rm FSR} &= E^{-4\epsilon}\int_0^1 \frac{{\rm d}x_1}{x_1^{1+4\epsilon}}\frac{{\rm d}x_2}{x_2^{1+2\epsilon}}\,\theta(\,E_{\rm max}/E - x_1)\,\theta(1-x_1-x_1x_2) \\ &\times\,\left(I - \hat{L}_{x_1}\right)\left(I - \hat{L}_{x_2}\right)\,(1-x_1-x_1x_2)^{n-2\epsilon} \\ &\times\,\Big[E^4 x_1^4 x_2^2 \mathcal{T}^+(E\,(1-x_1-x_1x_2), E\,x_1, E\,x_1x_2)\Big]\,. \end{aligned} \tag{2.128}$$

In Eq. (2.128), the function $\theta(1-x_1-x_1x_2)$ enforces positivity of the hard-parton energy $E_i > 0$ and we have assumed that the damping factor S is homogeneous in E_i. More specifically, we find

$$\begin{aligned} &{\rm d}E_4\,{\rm d}E_5\,{\rm d}E_i\,S(E_i)\,(E_iE_4E_5)^{1-2\epsilon} = {\rm d}E E^{1-2\epsilon} \\ &\quad\times E^{4-4\epsilon}\,{\rm d}x_1\,{\rm d}x_2 x_1^{3-4\epsilon}x_2^{1-2\epsilon}(1-x_1-x_1x_2)^{n-2\epsilon}\,, \end{aligned} \tag{2.129}$$

where we assumed that the damping factors has the form $S(E_i) = E_i^{n-1} \times S(1)$. It will become clear in Sec. 3.2.3 that the factor $(1-x_1-x_1x_2)^{n-2\epsilon}$ in Eq. (2.128) does not complicate the actual integration over $x_{1,2}$.

The $E_{\rm max}$ dependence in Eq. (2.128) arises from the cut-off $\theta(\,E_{\rm max}/E - x_1) = \theta^E$. However, this cut-off is only relevant for terms in the double-soft limit $\hat{L}_{x_1}$. For other terms, the condition $\theta(1-x_1-x_1x_2)$ provides a stronger bound on the integration variables. This allows us to split the integrand as follows

$$\begin{aligned} &\theta^E\,\left(I - \hat{L}_{x_1}\right)\,\left(I - \hat{L}_{x_2}\right) = \Big[\,\left(I - \hat{L}_{x_2}\right) - \theta^E\,\hat{L}_{x_1}\,\left(I - \hat{L}_{x_2}\right)\Big] \\ &= \Big[\,\left(I - \hat{L}_{x_1}\right)\,\left(I - \hat{L}_{x_2}\right)\Big] - (\theta^E - 1)\,\hat{L}_{x_1}\,\left(I - \hat{L}_{x_2}\right)\,. \end{aligned} \tag{2.130}$$

25 We do not show the Born-like factor $\langle F_{LM}\rangle$ because it is immaterial for the $x_{1,2}$ integration.

We insert the identity in Eq. (2.130) into the subtraction term in Eq. (2.128), integrate the double-soft contribution over x_1, and find

$$
\begin{aligned}
\mathcal{I}_{TC}^{\rm FSR} = E^{-4\epsilon}\Bigg\{ & \int_0^1 \frac{{\rm d}x_1}{x_1^{1+4\epsilon}} \frac{{\rm d}x_2}{x_2^{1+2\epsilon}} \left(I - \hat{L}_{x_1}\right) \left(I - \hat{L}_{x_2}\right) \theta(1 - x_1 - x_1 x_2) \\
& \times (1 - x_1 - x_1 x_2)^{n-2\epsilon} \left[E^4 x_1^4 x_2^2 \mathcal{T}^+(E\,(1 - x_1 - x_1 x_2), E\,x_1, E\,x_1 x_2)\right] \\
& - \frac{(E_{\rm max}/E)^{-4\epsilon} - 1}{-4\epsilon} \int\limits_0^1 \frac{{\rm d}x_2}{x_2^{1+2\epsilon}}\, \hat{L}_{x_1} \left(I - \hat{L}_{x_2}\right) \\
& \times \left[E^4 x_1^4 x_2^2 \mathcal{T}^+(E\,(1 - x_1 - x_1 x_2), E\,x_1, E\,x_1 x_2)\right] \Bigg\}\,.
\end{aligned}
\tag{2.131}
$$

We will discuss the analytical computation of the integral in Eq. (2.131) in Sec. 3.2.3.

2.6.2 *Strongly-ordered triple-collinear subtraction terms*

It remains to discuss strongly-ordered triple-collinear contributions in Eq. (2.100). Again, we separate integration over energies and angles and write

$$
\begin{aligned}
\mathcal{I}_{TC}^{\rm s.o.} = & \int {\rm d}E_4\, {\rm d}E_5\, (E_4 E_5)^{1-2\epsilon} \Phi_E(E_4, E_5)\, \hat{O}_{\rm soft}\, \mathcal{T}_{\rm s.o.}^{\pm}(E_i, E_4, E_5) \\
\times & \left\langle F_{\rm LM}\left(\frac{\mp E_i - E_4 - E_5}{\mp E_i} \cdot (p_i)_f\,, ..\right)\right\rangle\,.
\end{aligned}
\tag{2.132}
$$

In Eq. (2.132), we have defined the strongly-ordered angular integral

$$
\mathcal{T}_{\rm s.o.}^{\pm}(E_i, E_4, E_5) = 4g^4 \sum_k \int \theta^k C^k\, {\rm d}\Omega_{45}^{(d-1)}\, \frac{P_{f_i, f_4, f_5}(\pm s_{i4}, \pm s_{i5}, s_{45}, \pm E_i, E_4, E_5)}{s_{i45}^2}\,. \tag{2.133}
$$

We note that we parameterize the integral over energies in Eq. (2.132) following the same steps as in Sec. 2.6.1. In variance with the genuine triple-collinear contribution, the strongly-ordered angular integral in Eq. (2.133) depends on the angular phase-space parameterization. This is the case, since operators $\theta^k C^k$ act on - and constrain - the angular part of the unresolved phase space. However, once the double-collinear limit is taken, all resulting terms have a NLO-like structure, cf. Eq. (2.74), and are simple enough to allow for a straightforward integration in terms of gamma functions. We will explain how to compute such integrals in Sec. 3.1.3.

2.6.3 *Overview of the required partonic splittings*

We have discussed three variants of energy parameterizations for both initial-state and final-state emissions that apply to genuine and strongly-ordered contributions to the triple-collinear subtraction terms. These parameterizations were chosen to ensure that integration of triple-collinear splitting functions decouples from the matrix element squared to an extent possible. Furthermore, we explained how to make integrations over energy-like variables finite. In summary, we can write the triple-collinear subtraction term in Eq. (2.96) as follows

$$\mathcal{I}_{TC} = \int \mathrm{d}E_4 \, \mathrm{d}E_5 \, (E_4 E_5)^{1-2\epsilon} \Phi_E(E_4, E_5) \, \hat{O}_{\text{soft}} \, \left[\mathcal{T}^{\pm}(E_i, E_4, E_5) - \mathcal{T}^{\pm}_{\text{s.o.}}(E_i, E_4, E_5)\right] \\ \times \left\langle F_{\text{LM}}\left(\frac{\mp E_i - E_4 - E_5}{\mp E_i} \cdot (p_i)_f \, , ..\right)\right\rangle . \tag{2.134}$$

The splitting functions $P_{f_i f_4 f_5}$ that have to be considered in order to describe *all* possible initial-state and final-state splittings are listed in Table 2.2 and Table 2.3, respectively. There, we also specify the type of energy parameterization that was used for initial-state splittings and the power n that was defined in the context of final-state splittings in Eq. (2.128).

We will explain how to obtain (strongly-ordered) angular integrals $\mathcal{T}^{\pm}$ ($\mathcal{T}^{\pm}_{\text{s.o.}}$), as well as the respective energy integrals in Sec. 3.2.3 (Sec. 3.1.3). As will become clear in Sec. 3.1.3, NLO-like integrals can be obtained in a straightforward way by parametric integration, irrespective of the energy parameterization or the specific definition of sectors.

Splitting	EO	P_{abc}	Name in supplementary material
$q \to ggq^*$	✓	$1/2\left(P_{g_4 g_5 q_1} + 4 \leftrightarrow 5\right)$	ISR[z,1]
$g \to ggg^*$	✓	$1/2\left(P_{g_1 g_4 g_5} + 4 \leftrightarrow 5\right)$	ISR[z,2]
$q \to \bar{q}'q'q^*$	✓	$P_{\bar{q}'_4 q'_5 q_1} + 4 \leftrightarrow 5$	ISR[z,3]
$q \to qq'\bar{q}'^*$	✓	$P_{\bar{q}'_1 q'_4 q_5} + 4 \leftrightarrow 5$	ISR[z,4]
$q \to \bar{q}qq^*$	✓	$P^{\mathrm{id}}_{\bar{q}_4 q_5 q_1} + 4 \leftrightarrow 5$	ISR[z,5]
$q \to qq\bar{q}^*$	✓	$1/2\left(P^{\mathrm{id}}_{\bar{q}_1 q_4 q_5} + 4 \leftrightarrow 5\right)$	ISR[z,6]
$g \to q\bar{q}g^*$	✓	$P_{g_1 q_4 \bar{q}_5} + 4 \leftrightarrow 5$	ISR[z,7]
$q \to qgg^*$	X	$P_{g_5 q_1 \bar{q}_4}$	ISR[z,8]
$g \to qgq*$	X	$P_{g_1 g_5 q_4}$	ISR[z,9]

Table 2.2: List of all required splittings in the case of initial-state radiation. In the first column we define the partons that take part in the splitting. In the second column, we indicate whether the energy-ordered parametrization in Eq. (2.115) or the parameterization in Eq. (2.122) is used. In the third column, we identify the corresponding triple-collinear splitting functions of Ref. [123] that have to be used in Eq. (2.103). Energy-ordered contributions are symmetrized in $f_4 \leftrightarrow f_5$ according to Eq. (2.21). We include an additional symmetry factor where required by the formulation of the subtraction scheme. Finally, the last column provides the name of the corresponding expression in the `Mathematica` readable supplementary material of Ref. [5].

Splitting	P_{abc}	n	Name in supplementary material
$q^* \to ggq$	$1/2\left(P_{g_4 g_5 q_1} + 4 \leftrightarrow 5\right)$	1	FSR[1]
$q^* \to \bar{q}'q'q$	$P_{\bar{q}'_4 q'_5 q_1} + 4 \leftrightarrow 5$	1	FSR[2]
$q^* \to \bar{q}qq$	$P^{\mathrm{id}}_{\bar{q}_4 q_1 q_5} + 4 \leftrightarrow 5$	1	FSR[3]
$g^* \to gq\bar{q}$	$P_{g_1 q_4 \bar{q}_5} + P_{g_4 q_1 \bar{q}_5} + P_{g_5 q_1 \bar{q}_4}$	2	FSR[4]
$g^* \to ggg$	$P_{g_1 g_4 g_5}$	2	FSR[5]

Table 2.3: List of all required splittings in the case of final-state radiation. In the first column we define the partonic splitting. In the second column, we identify the corresponding triple-collinear splitting functions of Ref. [123] that have to be used in Eq. (2.103). We include an additional symmetry factor where required. The third column denotes the power n as defined in Eq. (2.128). Finally, the last column provides the name of the corresponding expression in the supplementary material of Ref. [5].

3 INTEGRATED SUBTRACTION TERMS

In this Chapter, we present analytic computations of the integrated subtraction terms that emerged in the course of the regularisation procedure with the nested soft-collinear subtraction scheme, as described in Chapter 2. Although subtraction terms can be integrated numerically, deriving analytic formulas for them is advantageous for two reasons. First, they allow for an analytic cancellation of IR poles, a welcome cross-check of the correctness of the subtraction procedure. Second, use of analytic expressions instead of multidimensional numerical integration, makes calculations of physical cross sections both more efficient and numerically stable.

LAYOUT OF THE CHAPTER This Chapter is organized as follows. First, we consider NLO-like subtraction terms in Sec. 3.1. This includes computation of single-soft integrals in Sec. 3.1.1 and Sec. 3.1.2, as well as strongly-ordered triple-collinear subtraction terms in Sec. 3.1.3. As will become clear in Sec. 3.1, all NLO-like integrals that we have to consider can be obtained in a closed form in terms of gamma functions and hypergeometric functions for arbitrary ϵ. We manipulate these special functions using their properties listed in Appendix A. Their ϵ-expansion can be obtained with the help of `HypExp` [127, 128].

We then turn to genuinely NNLO-like subtraction terms in Sec. 3.2. As already discussed, these contributions arise from regulating double-soft and triple-collinear singularities. We begin by outlining the computational strategy for the required phase-space integrals in Sec. 3.2.1. We then explain how to obtain analytic results for the double-soft phase-space integrals $\mathcal{G}\mathcal{G}_{ij}$ and $\mathcal{Q}\bar{\mathcal{Q}}_{ij}$ (cf. Eq. (2.91) and Eq. (2.92)) in Sec. 3.2.2. In Sec. 3.2.3 we proceed with the calculation of triple-collinear integrals (cf. Eq. (2.99)) that are required to describe all possible partonic splittings in initial and final states.

3.1 NLO-LIKE SUBTRACTION TERMS

In this Section, we present computations of NLO-like integrated subtraction terms that were introduced earlier in Chapter 2.

3.1.1 *Soft subtraction term for massive back-to-back emitters*

We begin with the computation of the quantity $\mathcal{G}_{ij}$ as defined in Eq. (2.90) for two massive emitters. We denote their momenta by $p_A^2 = p_B^2 = m^2$; they are assumed to be back-to-back. Since the function $\mathcal{G}_{ij}$ is symmetric under the exchange $i \leftrightarrow j$, we only need to compute $\mathcal{G}_{AB}$ and $\mathcal{G}_{AA}$. The first integral reads

$$\begin{aligned}\mathcal{G}_{AB} &= \int [\mathrm{d}k]\, \frac{(p_A \cdot p_B)}{(p_A \cdot k)(p_B \cdot k)} \\ &= \frac{(1+\beta^2)}{2} \int_0^{E_{\max}} \frac{\mathrm{d}E}{E^{1+2\epsilon}} \int \frac{\mathrm{d}\Omega_k^{(d-1)}}{(1-\beta \boldsymbol{n}\cdot\boldsymbol{n}_k)(1+\beta \boldsymbol{n}\cdot\boldsymbol{n}_k)}\,,\end{aligned} \tag{3.1}$$

where we have parameterised the gluon four momentum as $k = E(1, \boldsymbol{n}_k)$ and $p_{A,B}$ as $p_{A,B} = E_{A,B}(1, \pm\beta\boldsymbol{n})$. In order to simplify the angular integration, we choose the reference frame where $\boldsymbol{n} = \boldsymbol{e}_z$. We find $(1 \pm \beta\boldsymbol{n}\cdot\boldsymbol{n}_k) = (1 \pm \beta\cos\theta)$. Introducing $\eta = (1-\cos\theta)/2$ and changing integration variables from θ to η, we obtain

$$\mathcal{G}_{AB} = -\frac{(1+\beta^2)\; E_{\max}^{-2\epsilon}\Omega^{(d-2)}}{4\epsilon} \int_0^1 \mathrm{d}\eta \left(\frac{[4\eta(1-\eta)]^{-\epsilon}}{[1-\beta(1-2\eta)]} + \frac{[4\eta(1-\eta)]^{-\epsilon}}{[1+\beta(1-2\eta)]} \right). \tag{3.2}$$

The integral in Eq. (3.2) can be written as a sum of hypergeometric functions. We find

$$\begin{aligned}\mathcal{G}_{AB} = &-\frac{(1+\beta^2)\; E_{\max}^{-2\epsilon}\,\Omega^{(d-1)}}{8\epsilon}\times \\ &\left\{ \frac{{}_2F_1\left[\{1, 1-\epsilon\}, \{2-2\epsilon\}; \frac{-2\beta}{1-\beta}\right]}{1-\beta} + \frac{{}_2F_1\left[\{1, 1-\epsilon\}, \{2-2\epsilon\}; \frac{2\beta}{1+\beta}\right]}{1+\beta} \right\}.\end{aligned} \tag{3.3}$$

Following similar steps, we compute the self-correlated emission integral $\mathcal{G}_{AA}$. The result reads

$$\begin{aligned}\mathcal{G}_{AA} &= \int [\mathrm{d}k]\, \frac{m^2}{(p_A \cdot k)^2} \\ &= -\frac{E_{\max}^{-2\epsilon}\,\Omega^{(d-1)}}{4\epsilon} \times \left\{ 1 - 2\epsilon \left({}_2F_1\left[\{1, \frac{1}{2}\}, \{\frac{3}{2}-\epsilon\}; \beta^2\right] - 1 \right) \right\}.\end{aligned} \tag{3.4}$$

We apply the quadratic transformation of hypergeometric functions given in Eq. (A.9) to the result in Eq. (3.3), and write $\mathcal{G}_{AA}, \mathcal{G}_{AB}$ as

$$\mathcal{G}_{AA} = -\frac{E_{\max}^{-2\epsilon}\,\Omega^{(d-1)}}{4\epsilon} \times \left\{ 1 - 2\epsilon \left({}_2F_1\left[\{1, \frac{1}{2}\}, \{\frac{3}{2}-\epsilon\}; \beta^2\right] - 1 \right) \right\}, \tag{3.5}$$

$$\mathcal{G}_{AB} = -\frac{(1+\beta^2)\; E_{\max}^{-2\epsilon}\,\Omega^{(d-1)}}{4\epsilon} \times {}_2F_1\left[\{1, \frac{1}{2}\}, \{\frac{3}{2}-\epsilon\}; \beta^2\right]. \tag{3.6}$$

We note that the hypergeometric function ${}_2F_1\left[\{1, 1/2\}, \{3/2-\epsilon\}; \beta^2\right]$, which appears in Eqs. (3.5)-(3.6) has half-integer parameters. Its expansion in powers of ϵ therefore yields classical polylogarithms with arguments that involve square roots of β. In order to find a simpler expansion, we *first* rewrite the hypergeometric function using the quadratic transformation in Eq. (A.10) and then apply the linear transformation in Eq. (A.7). We find

$$
\begin{aligned}
&{}_2F_1\left[\{1,1/2\},\{\tfrac{3}{2}-\epsilon\};\beta^2\right] = \frac{1-2\epsilon}{2\epsilon\beta}\left(\frac{2\beta}{1+\beta}\right)^{2\epsilon} \times \\
&\left\{\left(\frac{1-\beta}{1+\beta}\right)^{-\epsilon}\frac{\Gamma(1-2\epsilon)\,\Gamma(1+\epsilon)}{\Gamma(1-\epsilon)} - {}_2F_1\left[\{\epsilon,2\epsilon\},\{1+\epsilon\};\frac{1-\beta}{1+\beta}\right]\right\}.
\end{aligned}
\tag{3.7}
$$

The expansion of the hypergeometric function in Eq. (3.7) is free of square roots. It can be easily obtained with `HypExp`; the result reads

$$
\begin{aligned}
&{}_2F_1\left[\{\epsilon,2\epsilon\},\{1+\epsilon\};\frac{1-\beta}{1+\beta}\right] \\
&= 1 + 2\epsilon^2\,\mathrm{Li}_2\left(\frac{1-\beta}{1+\beta}\right) + \epsilon^3\left[4\zeta_3 + \frac{2\pi^2}{3}\ln\left(\frac{2\beta}{1+\beta}\right) - 2\ln\left(\frac{1-\beta}{1+\beta}\right)\ln^2\left(\frac{2\beta}{1+\beta}\right)\right. \\
&\left. - 4\ln\left(\frac{2\beta}{1+\beta}\right)\mathrm{Li}_2\left(\frac{1-\beta}{1+\beta}\right) - 2\,\mathrm{Li}_3\left(\frac{1-\beta}{1+\beta}\right) - 4\,\mathrm{Li}_3\left(\frac{2\beta}{1+\beta}\right)\right] + \mathcal{O}\left(\epsilon^4\right).
\end{aligned}
\tag{3.8}
$$

We note that soft integrals shown in Eq. (3.3) and Eq. (3.4) were obtained earlier in the literature [67, 129].

3.1.2 *Soft-photon subtraction terms for W boson production*

As we have mentioned earlier, we will compute mixed QCD-EW corrections to W-boson hadroproduction in Part II of this thesis. In the following, we consider phase-space integrals that are required to describe soft-photon contributions to these corrections. In particular, we need to integrate the soft-photon eikonal function, shown in Eq. (2.39), over the unresolved phase space of the photon. More specifically, we require the integral

$$
e^2\int[\mathrm{d}p_\gamma]\mathrm{Eik}_\gamma(p_1,p_2,p_W,p_\gamma)\,,
\tag{3.9}
$$

where the soft-photon eikonal function $\mathrm{Eik}_\gamma(p_1,p_2,p_W,p_\gamma)$ is defined in Eq. (2.40) and $p_W = p_1 + p_2 - p_g$. As was already pointed out in Sec. 2.2.2, we need the integral in Eq. (3.9) in three cases where the gluon is *1)* resolved, *2)* collinear to one of the incoming quarks, or *3)* soft.

RESOLVED GLUON In case of a resolved gluon, it is sufficient to compute the integral in Eq. (3.9) in an ϵ expansion including finite terms. The result can be found in Ref. [67]. It reads

$$
e^2\int[\mathrm{d}p_\gamma]\mathrm{Eik}_\gamma(p_1,p_2,p_W,p_\gamma) = [\alpha](2\,E_{\max})^{-2\epsilon}\frac{\Gamma^2(1-\epsilon)}{\Gamma(1-2\epsilon)}J_\gamma(1,2,W)\,,
\tag{3.10}
$$

where $[\alpha]$ is given in Eq. (B.2) and

$$
\begin{aligned}
J_\gamma(1,2,W) &= \frac{Q_1^2+Q_2^2}{\epsilon^2} \\
&+ \frac{Q_W}{\epsilon}\left(Q_W - 2Q_1 \ln\left(\frac{\kappa_{1W}}{\sqrt{1-\beta^2}}\right) + 2Q_2 \ln\left(\frac{\kappa_{2W}}{\sqrt{1-\beta^2}}\right)\right) \\
&- Q_W^2\left[\frac{1}{\beta}\ln\frac{1-\beta}{1+\beta} - \frac{1}{2}\ln^2\frac{1-\beta}{1+\beta}\right] \\
&- 2Q_W\sum_{i=1}^{2} Q_i(-1)^i \ln\left(\frac{\kappa_{iW}}{1-\beta}\right)\ln\left(\frac{\kappa_{iW}}{1+\beta}\right) \\
&- 2Q_W\sum_{i=1}^{2} Q_i(-1)^i \left[\mathrm{Li}_2\left(1-\frac{\kappa_{iW}}{1-\beta}\right) + \mathrm{Li}_2\left(1-\frac{\kappa_{iW}}{1+\beta}\right)\right] + \mathcal{O}(\epsilon)\,.
\end{aligned}
\tag{3.11}
$$

In Eq. (3.11) the electric charges of the two colliding quarks in the process $q_1(p_1)\bar{q}(p_2) \to W^\pm$ are denoted as $Q_{1,2}$, such that the charge of the W boson is $Q_W = Q_1 - Q_2$. We also note that $\beta = \sqrt{1 - M_W^2/E_W^2}$ and $\kappa_{iW} = (p_i p_W)/(E_i E_W)$.

UNRESOLVED GLUON In case of a soft or collinear gluon, we need to evaluate the integral in Eq. (3.9) to higher orders in the ϵ-expansion in order to obtain all finite contributions to the cross section in Eq. (2.35). It is technically convenient to *first* take the respective limit of the integrand in Eq. (3.9) and *then* integrate over the unresolved phase space of the photon. The relevant limits of the soft-photon eikonal function are

$$S_g \mathrm{Eik}_\gamma(p_1,p_2,p_W,p_\gamma) = \mathrm{Eik}_\gamma(p_1,p_2,p_1+p_2,p_\gamma)\,, \tag{3.12}$$

$$C_{g1} \mathrm{Eik}_\gamma(p_1,p_2,p_W,p_\gamma) = \mathrm{Eik}_\gamma(p_1,p_2,(E_1-E_g)/E_1\cdot p_1+p_2,p_\gamma)\,, \tag{3.13}$$

$$C_{g2} \mathrm{Eik}_\gamma(p_1,p_2,p_W,p_\gamma) = \mathrm{Eik}_\gamma(p_1,p_2,p_1+(E_2-E_g)/E_2\cdot p_2,p_\gamma)\,. \tag{3.14}$$

It is straightforward to see that these three cases can be accommodated by computing the integral in Eq. (3.9) with the constraint $p_W = p_1 + p_2$ in a reference frame that is boosted along the collision axis $\boldsymbol{p}_1 \sim \boldsymbol{p}_2 \sim \boldsymbol{e}_z$ relative to the partonic center-of-mass frame. We denote such an expression by

$$e^2 \int [\mathrm{d}p_\gamma] \mathrm{Eik}_\gamma(p_1,p_2,p_W,p_\gamma)\bigg|_{p_W=p_1+p_2} = \sum_{(\alpha,\beta)\in \boldsymbol{E}} \mathcal{I}^{\gamma,(\alpha,\beta)}_{\text{boost}}\,, \tag{3.15}$$

where the set of emitters reads

$$\boldsymbol{E} = \{(1,2),(1,W),(W,2),(W,W)\}\,. \tag{3.16}$$

We write the individual contributions to Eq. (3.15) as

$$\mathcal{I}^{\gamma,(1,2)}_{\text{boost}} = 2e^2 Q_1 Q_2 \int \frac{[\mathrm{d}k]\,(p_1\cdot p_2)}{(p_1\cdot k)(p_2\cdot k)} = 4Q_1Q_2 \widetilde{\mathcal{I}}^\gamma(1,1)\,, \tag{3.17}$$

$$\mathcal{I}^{\gamma,(1,W)}_{\text{boost}} = 2e^2 Q_W Q_1 \int \frac{[\mathrm{d}k]\,(p_1\cdot p_{12})}{(p_1\cdot k)(p_{12}\cdot k)} = 2Q_W Q_1 (1-\beta_E)\widetilde{\mathcal{I}}^{\gamma}(1,\beta_E)\,, \tag{3.18}$$

$$\mathcal{I}^{\gamma,(W,2)}_{\text{boost}} = -2e^2 Q_W Q_2 \int \frac{[\mathrm{d}k]\,(p_{12}\cdot p_2)}{(p_{12}\cdot k)(p_2\cdot k)} = -2Q_W Q_2 (1+\beta_E)\widetilde{\mathcal{I}}^{\gamma}(\beta_E,1)\,, \tag{3.19}$$

$$\mathcal{I}^{\gamma,(W,W)}_{\text{boost}} = -e^2 Q_W^2 \int \frac{[\mathrm{d}k]\,(p_{12}\cdot p_{12})}{(p_{12}\cdot k)(p_{12}\cdot k)} = -Q_W^2 (1-\beta_E^2)\widetilde{\mathcal{I}}^{\gamma}(\beta_E,\beta_E)\,, \tag{3.20}$$

where $p_{12} = p_1 + p_2$. Furthermore, we have defined

$$\beta_E = \frac{E_1 - E_2}{E_1 + E_2}\,, \tag{3.21}$$

and introduced a new integral

$$\widetilde{\mathcal{I}}^{\gamma}(\beta_1,\beta_2) = [\alpha](2\,E_{\max})^{-2\epsilon}\frac{\Gamma^2(1-\epsilon)}{\Gamma(1-2\epsilon)} \int \frac{\mathrm{d}\Omega_k^{(d-1)}}{(1-\beta_1 \boldsymbol{n}\cdot\boldsymbol{n}_k)(1+\beta_2 \boldsymbol{n}\cdot\boldsymbol{n}_k)}\,. \tag{3.22}$$

The angular integral in Eq. (3.22) can be computed following steps described in Sec. 3.1.1. We obtain

$$e^2 \int [\mathrm{d}p_\gamma]\mathrm{Eik}_\gamma(p_1,p_2,p_W,p_\gamma)\Big|_{p_W=p_1+p_2} = [\alpha](2\,E_{\max})^{-2\epsilon}\frac{\Gamma^2(1-\epsilon)}{\Gamma(1-2\epsilon)}\tilde{J}_\gamma(E_1,E_2)\,, \tag{3.23}$$

where the function $\tilde{J}_\gamma(E_1,E_2)$ reads

$$\begin{aligned}\tilde{J}_\gamma(E_1,E_2) = {}& \frac{Q_1^2+Q_2^2}{\epsilon^2} + \frac{Q_W^2}{\epsilon(1-2\epsilon)} + \frac{Q_W}{\epsilon^2}\left\{Q_1\left[\left(\frac{E_1}{E_2}\right)^{\epsilon} - 1\right] - Q_2\left[\left(\frac{E_2}{E_1}\right)^{\epsilon} - 1\right]\right\} \\ & + \frac{Q_W}{\epsilon^2}\left\{Q_1\left(\frac{E_1}{E_2}\right)^{\epsilon}\left[{}_2F_1\left[\{-\epsilon,-2\epsilon\},\{1-2\epsilon\};1-\frac{E_2}{E_1}\right] - 1\right]\right. \\ & \left. -Q_2\left(\frac{E_2}{E_1}\right)^{\epsilon}\left[{}_2F_1\left[\{-\epsilon,-2\epsilon\},\{1-2\epsilon\};1-\frac{E_1}{E_2}\right] - 1\right]\right\} \\ & + \frac{Q_W^2}{\epsilon(1-2\epsilon)}\left(\frac{E_2}{E_1}\right)^{\epsilon}\left[{}_2F_1\left[\{-2\epsilon,1-\epsilon\},\{2-2\epsilon\};1-\frac{E_1}{E_2}\right] - 1\right].\end{aligned} \tag{3.24}$$

We note that the ϵ-expansion of this result is straightforward and can be obtained with `HypExp`.

3.1.3 *Strongly-ordered triple-collinear subtraction terms*

In the following, we explain how to analytically calculate soft-regulated and strongly-ordered triple-collinear subtraction terms, $\mathcal{I}_{TC}^{\text{s.o.}}$, which were defined in Eq. (2.100). Following the notation introduced in Sec. 2.6.2, they can be written as

$$\begin{aligned}\mathcal{I}_{TC}^{\text{s.o.}} &= \int \mathrm{d}E_4\, \mathrm{d}E_5\, (E_4E_5)^{1-2\epsilon}\Phi_E(E_4,E_5)\, \hat{O}_{\text{soft}}\, \mathcal{T}_{\text{s.o.}}^{\pm}(E_i,E_4,E_5)\\ &\times \left\langle F_{LM}\left(\frac{\mp E_i - E_4 - E_5}{\mp E_i}\cdot (p_i)_f,..\right)\right\rangle ,\end{aligned} \tag{3.25}$$

where

$$\mathcal{T}_{\text{s.o.}}^{\pm}(E_i,E_4,E_5) = 4g^4 \sum_k \int \theta^k C^k\, \mathrm{d}\Omega_{45}^{(d-1)}\, \frac{P_{f_i,f_4,f_5}(\pm s_{i4},\pm s_{i5},s_{45},\pm E_i,E_4,E_5)}{s_{i45}^2}\,. \tag{3.26}$$

We note, that the limit C^k acts on both the measure $\mathrm{d}\Omega_{45}^{(d-1)}$ and the splitting function P_{f_i,f_4,f_5}. This produces a NLO-like integrand,[1] making the integration particularly straightforward. The goal is to compute all strongly-ordered subtraction terms that contribute to all possible splittings listed in Table 2.2 and Table 2.3. To do so, we have implemented the following procedure in `Mathematica`:

- parameterise the angular phase space in each sector (cf. Eq. (2.58)) in Eq. (3.26) in terms of variables x_3, x_4, and λ as suggested in Ref. [95];[2]
- parameterise energies in Eq. (3.26) as described in Sec. 2.6;
- take the strongly-ordered limit C^k in Eq. (3.26). In the $\{x_3, x_4, \lambda\}$-parametrization this limit corresponds to extracting the leading $1/x_4$ behaviour of the integrand at fixed x_3, λ;
- integrate over x_3 and λ; the result is expressed in terms of gamma functions that depend on ϵ.

Following these steps, we obtain all relevant strongly-ordered integrals in Eq. (3.26) in a straightforward manner. We have also used this setup in Ref. [9] to compute the strongly-ordered contribution for $g\gamma$-emission for mixed QCD-EW corrections to W boson production, employing simplified sector definitions discussed in Eq. (2.64). We note that we explain how to perform the remaining integrations over energies in Sec. 3.2.3.

1 As can be seen in Example 5, momenta $k_{4,5}$ are decorrelated in the strongly-ordered limit.
2 All relevant formulas can be found in Appendix B.5.2 of this thesis and in Appendix B of Ref. [1].

3.2 GENUINELY DOUBLE-UNRESOLVED SUBTRACTION TERMS

While the NLO-like subtraction terms that we considered in the previous Section could be directly integrated in a closed form for arbitrary ϵ, this approach becomes unfeasible in case of NNLO-like subtraction terms. Indeed, it turns out that it is beneficial to use the idea of *reverse unitarity* [39] in order to make required phase-space integrals amenable to methods of multi-loop calculations such as integration-by-parts (IBP) relations [130, 131] and the method of differential equations [132–136].

This Section is organized as follows. In Sec. 3.2.1, we explain how genuinely double-unresolved integrals can be computed. We then describe specific details pertinent to the calculation of integrated double-soft and triple-collinear subtraction terms in Sec. 3.2.2 and Sec. 3.2.3, respectively.

3.2.1 *Double-unresolved subtraction terms and reverse unitarity*

It is interesting to realize, that both double-soft and triple-collinear subtraction terms can be obtained following one and the same procedure [5, 6, 36, 37]. Indeed, it is straightforward to see[3] that these subtraction terms can be written in a similiar way, namely

$$\mathcal{I}^{\mathrm{du}} = \int [\mathrm{d}k_4][\mathrm{d}k_5]\; \mathcal{K}(\{p\},k_4,k_5) \otimes F_{\mathrm{LM}}(\{p\},E_4,E_5)\;. \tag{3.27}$$

Here, integrand $\mathcal{K}$ describes either double-soft gluon or double-soft quark emission, or the triple-collinear emission of partons f_4, f_5 off the parton f_r. Therefore, depending on the type of contribution that we are interested in, the function $\mathcal{K}$ may read[4]

$$\mathcal{K} \in \left\{ \mathcal{S}_{ij}(k_4,k_5)\;,\; \mathcal{I}_{ij}(k_4,k_5)\;,\; P_{f_r,f_4,f_5}(\pm s_{r4}, \pm s_{r5}, s_{45}, \pm E_r, E_4, E_5)/s_{r45}^2 \right\}\;. \tag{3.28}$$

As can be seen in Eq. (3.28), $\mathcal{K}$ is a function of one (or two) external momenta $p_r\big(\{p_i,p_j\}\big)$, light-like momenta $k_{4,5}$ and energies $E_{4,5}$ carried by unresolved partons. We note that the energy-dependence of the Born-like matrix element $F_{\mathrm{LM}}(\{p\},E_4,E_5)$ on $E_{4,5}$ in Eq. (3.27) only occurs for the triple-collinear subtraction term. Double-soft subtraction terms, on the other hand, exhibit color correlations, which we denoted with the symbol "$\otimes$" in Eq. (3.27).

The energy integration that has to be carried out in Eq. (3.27) is constrained by the cut-off $E_{\max}$, cf. Eq. (2.15), and possibly by an energy-ordering condition $E_5 <$

3 Cf. Eq. (2.91), Eq. (2.92) and Eq. (2.99).
4 The sign convention in the argument of P_{f_r,f_4,f_5} is "$-$" for incoming and "$+$" for outgoing partons f_r.

E_4, cf. Eq. (2.20).[5] Switching from integrations over energies $E_{4,5}$ to integrations over dimensionless variables $\boldsymbol{x} = \{x_4, x_5\}$, we write $\mathcal{I}^{\rm du}$ as

$$\mathcal{I}^{\rm du} = \int_0^1 {\rm d}\boldsymbol{x}\, g(\boldsymbol{x}) \times F_{\rm LM}(\{p\}, \boldsymbol{x}') \int {\rm d}\Omega_{45}^{(d-1)}\, \mathcal{K}(\{p\}, \boldsymbol{n}_4, \boldsymbol{n}_5, \boldsymbol{x})\,, \tag{3.29}$$

where ${\rm d}\Omega_{45}^{(d-1)} = {\rm d}\Omega_4^{(d-1)}\,{\rm d}\Omega_5^{(d-1)}$. In Eq. (3.29), $\boldsymbol{x}' \subseteq \boldsymbol{x}$ denotes a subset of $\boldsymbol{x}$ and the function $g(\boldsymbol{x})$ collects both the Jacobian of the transformation and possible constraints on the phase space.

We note that the function $\mathcal{K}$ in Eq. (3.28) is rotationally invariant in $d-1$ spatial dimensions. We can use this fact, together with *reverse unitarity* [39] to establish a connection between the angular integrals in Eq. (3.29) and loop integrals. To this end, we first express angular integration through an integration over loop-momenta, constrained by additional δ-functions. We find

$${\rm d}\Omega_i^{(d-1)} = 2\,{\rm d}^d k_i\, \delta^+(k_i^2)\, \delta((k_i \cdot N) - x_i)\, x_i^{-1+2\epsilon}\,, \quad i = 4, 5\,, \tag{3.30}$$

where $N = (1, \boldsymbol{0})$. We then write [137]

$$-(2\pi {\rm i})\, \delta(q^2 - m^2) = \lim_{\sigma \to 0}\left[\frac{1}{q^2 - m^2 + {\rm i}\sigma} - \frac{1}{q^2 - m^2 - {\rm i}\sigma}\right] \equiv \frac{1}{[q^2 - m^2]_c}\,, \tag{3.31}$$

to identify δ-functions with *cut propagators*. We use Eq. (3.30) and Eq. (3.31) and write the integral in Eq. (3.29) as

$$\mathcal{I}^{\rm du} = \int_0^1 {\rm d}\boldsymbol{x}\, g(\boldsymbol{x}) (x_4 x_5)^{-1+2\epsilon}\; F_{\rm LM}(\{p\}, \boldsymbol{x}') \times G(\{p\}, x_4, x_5)\,, \tag{3.32}$$

where

$$G(\{p\}, x_4, x_5) = \int \frac{{\rm d}^d k_4\, {\rm d}^d k_5\, \mathcal{K}(\{p\}, k_4, k_5, \boldsymbol{x})}{[k_4^2]_c\, [k_5^2]_c\, [(k_4 \cdot N) - x_4]_c\, [(k_5 \cdot N) - x_5]_c}\,. \tag{3.33}$$

Our goal is to calculate the integral over $k_{4,5}$ that appears in Eq. (3.33) as a function of $\boldsymbol{x}$. To explain how this is done, we will introduce two commonly-used techniques: integration-by-parts relations and the method of differential equations. We will then show how to apply these methods to compute cut loop integrals in Eq. (3.33).

Integration-by-parts relations

Dimensionally regularized loop integrals are not independent. In fact, many relations between such integrals can be found using integration-by-parts (IBP) and Lorentz invariance (LI) identities. Scalar integrals at L-loops with E independent external momenta can be conveniently classified into classes that we refer to as *topologies*. We write integrals as

$$I_{\vec{\alpha}}^{\mathcal{T}}(s_{ij}) = \int \prod_{l=1}^{L} {\rm d}^d k_l \prod_{n=1}^{N} D_n^{-\alpha_n}\,, \quad \vec{\alpha} \in \mathbb{Z}^N\,. \tag{3.34}$$

5 Not all partonic configurations that contribute to triple-collinear subtraction terms require energy ordering. However, whether or not the phase space is energy-ordered is not important for the following discussion.

We note that the set of $N = L(L+1)/2 + L \cdot E$ linearly independent propagators $1/D_n$ defines the topology $\mathcal{T}$, where each D_n is a linear function of scalar products build from external momenta $\{p_1, .., p_E\}$ and loop momenta $\{k_1, .., k_L\}$. As indicated in Eq. (3.34), integrals $I^{\mathcal{T}}_{\vec{\alpha}}(s_{ij})$ are functions of all scalar invariants $s_{ij} = 2(p_i \cdot p_j)$ that can be constructed from external momenta. Requiring that these integrals do not change under an infinitesimal Lorentz transformation yields the Lorentz invariance identity [136]

$$\sum_{e=1}^{E} \left[p_i^\mu \frac{\partial}{\partial p_i^\nu} - p_i^\nu \frac{\partial}{\partial p_i^\mu} \right] I^{\mathcal{T}}_{\vec{\alpha}}(s_{ij}) = 0 . \tag{3.35}$$

Contracting Eq. (3.35) with all possible anti-symmetric combinations of external momenta yields $E(E-1)/2$ independent equations. Furthermore, dimensionally regulated integrals are invariant under shifts of the loop momenta. This implies that [130, 131]

$$\int \prod_{l=1}^{L} \mathrm{d}^d k_l \, \frac{\partial}{\partial k_i^\mu} \left[q^\mu \, \mathcal{I}' \right] = 0 , \quad q \in \{k_1, .., k_L, p_1, \ldots, p_E\} , \tag{3.36}$$

where

$$\mathcal{I}' = \prod_{n=1}^{N} D_n^{-\alpha_n} , \tag{3.37}$$

is an integrand of the same form as in Eq. (3.34). The identity in Eq. (3.36) yields $L(L+E)$ independent equations. Acting with derivatives w. r. t. $p_i^{\mu,\nu}$ and k_i^μ in Eq. (3.35) and Eq. (3.36) produces integrals that can be expressed through the *same* topology as the seed integral. Hence, these identities provide linear relations between integrals with different indices α in the same topology $\mathcal{T}$.[6]

One way to make use of IBP and LI identities is to generate a large system of linear equations and to assign a "weight" as a measure of complexity to all integrals that appear in it [139]. Generation of linear relations and a subsequent *reduction* that expresses all "complicated" integrals in terms of a small set of so-called master integrals (MIs) has been automated in a large number of publicly-available computer programs [140–146]. We note that sets of master integrals were proven to be finite in Ref. [147]. Furthermore, we note that another approach [148, 149] implements an heuristic search to find reduction rules for generic integrals of a given topology, see also Ref. [150].

Method of differential equations

Besides the fact, that the IBP technique allows us to algebraically reduce the number of loop integrals that need to be computed, it also serves as a starting point for the so-called differential equation method [132–136]. To introduce this method, we consider the vector of master integrals $\boldsymbol{I}$ and differentiate it w. r. t. any of the kinematic invariants denoted by

6 In fact, it was shown that LI identities are not independent from IBP identities [138].

$s \in \{s_{ij}\}$. Using IBP relations, the result of the differentiation can be expressed through the same set of master integrals $\boldsymbol{I}$. This allows us to obtain a closed set of first-order linear differential equations

$$\frac{\partial}{\partial s}\boldsymbol{I} = \hat{M}_s(\{s_{ij}\},\epsilon) \times \boldsymbol{I}\,, \quad s \in \{s_{ij}\}\,. \tag{3.38}$$

The entries of the matrix $\hat{M}$ are rational functions of kinematic invariants and regularisation parameter ϵ. Using the fact that integrals have a definite mass dimension, we introduce dimensionless variables $\boldsymbol{Y}$.[7] Repeating the above argument for all variables $y \in \boldsymbol{Y}$, we write

$$\mathrm{d}\boldsymbol{I} = \sum_{y\in\boldsymbol{Y}} \hat{M}_y(\boldsymbol{Y},\epsilon) \times \boldsymbol{I}\,\mathrm{d}y\,. \tag{3.39}$$

In practical applications, one is usually interested in computing master integrals as an expansion in the dimensional parameter ϵ. We can write

$$\boldsymbol{I}\,(\boldsymbol{Y},\epsilon) = \sum_{n=0}^{n_{\max}} \epsilon^n \boldsymbol{I}^{(n)}\,(\boldsymbol{Y})\;, \tag{3.40}$$

where we have chosen a normalization such that all integrals start at ϵ^0 and $n_{\max}$ denotes the highest power of ϵ that is required in a computation. With the ansatz in Eq. (3.40), we can write the differential equation (DEQ) in Eq. (3.39) as

$$\sum_{n=0}^{n_{\max}} \epsilon^n\,\mathrm{d}\boldsymbol{I}^{(n)} = \sum_{n=0}^{n_{\max}} \epsilon^n \sum_{y\in\boldsymbol{Y}} \hat{M}_y(\boldsymbol{Y},\epsilon) \times \boldsymbol{I}^{(n)}\,\mathrm{d}y\,. \tag{3.41}$$

If matrices $\hat{M}_y(\boldsymbol{Y},\epsilon)$ are strictly lower triangular in the $\epsilon \to 0$ limit, the DEQ in Eq. (3.41) decouples as an expansion in ϵ. Then, solutions can be found by simply integrating the r. h. s. of Eq. (3.41) order by order in ϵ. Particular simplifications arise, if the differential equations are brought into the so-called ϵ-homogeneous or *canonical* form [151]. There, the DEQ takes the form

$$\mathrm{d}\boldsymbol{J} = \epsilon\,\mathrm{d}\hat{A}_y(\boldsymbol{Y})\,\boldsymbol{J}\,, \tag{3.42}$$

where $\boldsymbol{J}$ denotes master integrals in the canonical basis. The matrix $\mathrm{d}\hat{A}_y(\boldsymbol{Y})$ in Eq. (3.42) can be written in the so-called "dlog" form

$$\mathrm{d}\hat{A}_y(\boldsymbol{Y},\epsilon) = \sum_{k=0}^{N} \hat{a}_k\;\mathrm{dln}(R_k)\,, \tag{3.43}$$

where matrices $\hat{a}^k$ contain rational numbers, and functions $R_k(\boldsymbol{Y})$ constitute the so-called *alphabet*. Solutions to a DEQ that admits the form in Eq. (3.42) can be written as Chen

7 We note that this step also reduces the total number of variables by one.

iterated integrals [152]. These solutions are said to have *uniform weight*, which basically means that powers of ϵ coincide with the number of integrations. If the functions R_k are linear,[8] the matrix $\mathrm{d}\hat{A}_y(\boldsymbol{Y},\epsilon)$ has only simple poles. It reads

$$\mathrm{d}\hat{A}_y(\boldsymbol{Y},\epsilon) = \epsilon \times \sum_{y\in\boldsymbol{Y}} \sum_{\tilde{k}} \frac{\hat{a}_{\tilde{k}}\,\mathrm{d}y}{y - y_{\tilde{k}}}\,, \tag{3.44}$$

where the sum over $\tilde{k}$ only runs over the y-dependent part of the alphabet. In this case, the ϵ-expansion of the DEQ in Eq. (3.41) simplifies considerably. Order-by order in ϵ, we find

$$\mathrm{d}\boldsymbol{J}^{(n)} = \sum_{y\in\boldsymbol{Y}} \sum_{\tilde{k}} \frac{\hat{a}_{\tilde{k}}\boldsymbol{J}^{(n-1)}\,\mathrm{d}y}{y - y_{\tilde{k}}}\,, \quad n \geq 0\,. \tag{3.45}$$

Equivalently, we can write Eq. (3.45) as

$$\frac{\partial}{\partial y}\boldsymbol{J}^{(n)} = \sum_{\tilde{k}} \frac{\hat{a}_{\tilde{k}}\boldsymbol{J}^{(n-1)}\,\mathrm{d}y}{y - y_{\tilde{k}}}\,, \quad y \in \boldsymbol{Y}\,, n \geq 0\,. \tag{3.46}$$

Solutions to Eq. (3.46) can be expressed through a special class of iterated integrals, the so-called Goncharov polylogarithms (GPLs) [154, 155] which we review in Appendix A.5. We note that there are examples, where solutions to Eq. (3.42) can be written in terms of GPLs even in the case of a non-rationalizable alphabet [156]. However, this is not the case in general [157].

Finding a canonical basis $\boldsymbol{J}$ such that $\hat{A}_y$ has the from of Eq. (3.42) is usually a complicated task. A recent proposal, for example, is to construct the basis $\boldsymbol{J}$ by starting with integrands with an ansatz for the numerator and adjusting it to reach a dlog form[9] for the maximal residue [158].[10] Such integrals are conjectured to evaluate to functions of uniform weight and thus obey canonical differential equations.

Another approach is to find the canonical basis from the DEQ itself. The idea is to start with some basis of master integrals $\boldsymbol{I}$ and construct a transformation

$$\boldsymbol{I} = \hat{T}(\boldsymbol{Y},\epsilon)\boldsymbol{J}\,, \tag{3.47}$$

where the entries of the transformation matrix $\hat{T}(\boldsymbol{Y},\epsilon)$ are rational functions in $y \in \boldsymbol{Y}$ and ϵ. For a suitable $\hat{T}$, the new basis $\boldsymbol{J}$ is canonical and the DEQ reads

$$\frac{\partial}{\partial y}\boldsymbol{J} = \epsilon\hat{A}_y\,\boldsymbol{J}\,, \quad \hat{A}_y = \hat{T}^{-1}\left[\hat{M}_y(\boldsymbol{Y},\epsilon) - \frac{\partial}{\partial y}\right]\hat{T}\,. \tag{3.48}$$

8 There are algorithmic approaches to rationalize square roots appearing in algebraic R_k, e. g. in Ref. [153].
9 An integrand is said to have "dlog" form if it locally behaves as $\mathrm{d}x/x$ for $x \approx 0$ in every integration variable x [158].
10 Another implementation of the calculation of multivariate residues can be found in Ref. [159].

Depending on details of the DEQ in basis $\boldsymbol{I}$, there are various ways to construct the transformation $\hat{T}$ in Eq. (3.47) such that Eq. (3.48) is canonical [160–163]. An algorithmic solution applicable to single-variable problems has been proposed in Refs. [164, 165] and implemented in various computer programs [166–168]. Another approach, which is suitable for multi-scale problems, was proposed in Ref. [169] and implemented as a `Mathematica` package [170]. In this case, an ansatz for the transformation in Eq. (3.47) is made and constrained to fulfill Eq. (3.48).

Application to double-unresolved integrals

We note that both IBP reductions and the DEQ method can be used to compute cut loop integrals as in Eq. (3.33). This is the case because derivatives w. r. t. momenta or kinematic invariants are independent of the $\pm i\sigma$ prescription in Eq. (3.31). Hence, we can interpret δ-functions as propagators while applying these methods. In intermediate stages of such computations, one might encounter integrals for which a cut propagator is either absent or appears in its numerator. Such integrals do not contribute to the discontinuity, since they vanish in the $\sigma \to 0$ limit of Eq. (3.31). Cut propagators in the denominator that are raised to a power higher than one can not be replaced by δ-functions[11] and we will avoid them when choosing a basis of master integrals.

We will discuss the computation in case of double-soft and triple-collinear subtraction terms in Sec. 3.2.2 and Sec. 3.2.3, respectively. There, we will employ IBP relations to express $G(\{p\}, x_4, x_5)$ in Eq. (3.33) through a small set of master integrals. We will then use differential equations to compute these master integrals, and subsequently $G(\{p\}, x_4, x_5)$, as a function of $\{x_4, x_5\}$ and kinematic invariants in both cases. As we will see, it will be possible to write $G(\{p\}, x_4, x_5)$ in a convenient way, which will allow for a straightforward integration over parameters $\{x_4, x_5\}$ in Eq. (3.32) that do *not* appear in the Born-like matrix element $F_{\mathrm{LM}}(\{p\}, \boldsymbol{x}')$.

3.2.2 *Integrated double-soft subtraction terms*

In the following, we compute double-soft subtraction terms $\mathcal{GG}_{ij}$ and $\mathcal{Q}\bar{\mathcal{Q}}_{ij}$ defined in Eq. (2.91) and Eq. (2.92), respectively. As discussed in Sec. 2.5 and Sec. 3.1.1, we are interested in the case where both emitters are massive and their momenta are back-to-back. We denote momenta of hard particles as $p_{A,B}$, such that $p_A^2 = p_B^2 = m^2$. Thanks to the $i \leftrightarrow j$ symmetry, we only need to compute $\mathcal{GG}_{AA}, \mathcal{GG}_{AB}, \mathcal{Q}\bar{\mathcal{Q}}_{AA}$, and $\mathcal{Q}\bar{\mathcal{Q}}_{AB}$.

We begin with the observation that both integrands, $\mathcal{S}_{ij}(k_4, k_5)$ and $\mathcal{I}_{ij}(k_4, k_5)$, are homogeneous under the scaling $k_4 \sim k_5 \sim \lambda$. We use this fact and parameterize energies of unresolved partons as

$$E_4 = E_{\max} \cdot x\,, \qquad\qquad E_5 = E_{\max} \cdot x \cdot z\,. \tag{3.49}$$

11 In fact we can identify such expressions with derivatives of δ-functions, i. e. $[x]_c^{-n} = \delta^{(n-1)}(x)$ where $n \geq 1$.

Integration over x factorizes and yields

$$\mathcal{G}\mathcal{G}_{ij} = -\frac{E_{\max}^{-4\epsilon}}{16\epsilon}\int_0^1 \mathrm{d}z\, z^{1-2\epsilon}\int \mathrm{d}\Omega_{45}^{(d-1)}\, \mathcal{S}_{ij}(n_4, z\cdot n_5)\,, \tag{3.50}$$

$$\mathcal{Q}\bar{\mathcal{Q}}_{ij} = -\frac{E_{\max}^{-4\epsilon}}{16\epsilon}\int_0^1 \mathrm{d}z\, z^{1-2\epsilon}\int \mathrm{d}\Omega_{45}^{(d-1)}\, \mathcal{I}_{ij}(n_4, z\cdot n_5)\,, \tag{3.51}$$

where $n_i = (1, \boldsymbol{n}_i)$. Both integrals in Eq. (3.50) and Eq. (3.51) are of the form displayed in Eq. (3.29), and we compute them following the discussion in Sec. 3.2.1.[12]

It is important to realize that the case of gluon emission exhibits a singularity in the so-called strongly-ordered limit, where the gluon with momentum k_5 is much softer than the gluon with momentum k_4.[13] Such a behavior translates into a logarithmic $z = 0$ endpoint singularity in the integral in Eq. (3.50). We regulate and extract the divergent part of the integrand by defining

$$\mathcal{S}_{ij}^{\mathrm{s.o.}}(n_4, n_5) = z^{-2}\lim_{z\to 0}\left[z^2\mathcal{S}_{ij}(n_4, z\cdot n_5)\right]\,. \tag{3.52}$$

Following the discussion in Sec. 3.2.1, we define cut loop integrals[14]

$$\begin{aligned}
\mathcal{E}_{ij}^{\mathcal{G}\mathcal{G}}(z,\beta,\epsilon) &= \int \frac{\mathrm{d}^d k_4\, \mathrm{d}^d k_5\;\; \mathcal{S}_{ij}\,(k_4, k_5)}{[k_4^2]_c[k_5^2]_c[k_4\cdot p_{AB} - 2E^2]_c[k_5\cdot p_{AB} - 2E^2 z]_c}\,,\\
\mathcal{E}_{ij}^{\mathcal{G}\mathcal{G},\mathrm{s.o.}}(z,\beta,\epsilon) &= \int \frac{\mathrm{d}^d k_4\, \mathrm{d}^d k_5\;\; \mathcal{S}_{ij}^{\mathrm{s.o.}}\,(k_4, k_5)}{[k_4^2]_c[k_5^2]_c[k_4\cdot p_{AB} - 2E^2]_c[k_5\cdot p_{AB} - 2E^2 z]_c}\,,\\
\mathcal{E}_{ij}^{\mathcal{Q}\bar{\mathcal{Q}}}(z,\beta,\epsilon) &= \int \frac{\mathrm{d}^d k_4\, \mathrm{d}^d k_5\;\; \mathcal{I}_{ij}\,(k_4, k_5)}{[k_4^2]_c[k_5^2]_c[k_4\cdot p_{AB} - 2E^2]_c[k_5\cdot p_{AB} - 2E^2 z]_c}\,,
\end{aligned} \tag{3.53}$$

where the momentum p_{AB} is defined as

$$p_A + p_B = p_{AB} = E(1, \boldsymbol{\beta}) + E(1, -\boldsymbol{\beta}) = (2E, \boldsymbol{0})\,. \tag{3.54}$$

We use Eq. (3.53), Eq. (3.50) and Eq. (3.51) and write

$$\begin{aligned}
\mathcal{G}\mathcal{G}_{ij} = -\frac{1}{\epsilon}\left(\frac{E_{\max}}{E}\right)^{-4\epsilon}\Bigg[\int_0^1 \mathrm{d}z\,\Big(\mathcal{E}_{ij}^{\mathcal{G}\mathcal{G}}(z,\beta,\epsilon) - \mathcal{E}_{ij}^{\mathcal{G}\mathcal{G},\mathrm{s.o.}}(z,\beta,\epsilon)\Big)&\\
+\int_0^1 \mathrm{d}z\,\mathcal{E}_{ij}^{\mathcal{G}\mathcal{G},\mathrm{s.o.}}(z,\beta,\epsilon)\Bigg]\,,&
\end{aligned} \tag{3.55}$$

$$\mathcal{Q}\bar{\mathcal{Q}}_{ij} = -\frac{1}{\epsilon}\left(\frac{E_{\max}}{E}\right)^{-4\epsilon}\int_0^1 \mathrm{d}z\,\mathcal{E}_{ij}^{\mathcal{Q}\bar{\mathcal{Q}}}(z,\beta,\epsilon)\,. \tag{3.56}$$

---

12 We note that in the double-soft limit, the Born-level matrix element F_{LM} does not depend on the energies of unresolved partons.

13 Thanks to the energy ordering, the opposite is not possible.

14 We note that the energy-fraction z plays the role of an internal mass.

We note that when writing Eq. (3.55), we have subtracted and added back the $z \to 0$ limit of the integrand. Furthermore, we note that it is beneficial to perform this subtraction at the level of the full integrand and not, for example, at the level of individual integrals. This way, we fully account for gauge properties of QCD amplitudes and hence, no unphysical singularities can appear.

While the first term in Eq. (3.55) can be expanded in ϵ prior to integration over z, in the second term, $\mathcal{E}_{ij}^{\mathcal{G}\mathcal{G},\text{s.o.}}(z,\beta,\epsilon)$ is a homogeneous function of z and therefore can be trivially integrated. We note that the quark-pair contribution in Eq. (3.56) does not exhibit the strongly ordered singularity, so no endpoint subtraction is required.

IBP reduction

Following the computational setup outlined in Sec. 3.2.1, we apply the IBP method to the integrands of Eq. (3.55) and Eq. (3.56). We express all integrals in terms of topologies T^{a_1,a_2,a_3}

$$T^{a_1,a_2,a_3}(\alpha_1,\alpha_2,\alpha_3) = \left(E^2\right)^{-d+4+\sum_{i=1}^{3}\alpha_i} \int \frac{\mathrm{d}^d k_4\,\mathrm{d}^d k_5}{D_{\text{cut}}\,D_{a_1}^{\alpha_1}\,D_{a_2}^{\alpha_2}\,D_{a_3}^{\alpha_3}} \equiv \left\langle \prod_{i=1}^{3} \frac{1}{D_{a_i}^{\alpha_i}} \right\rangle, \tag{3.57}$$

where we choose a convenient normalisation to render integrals dimensionless. The first four inverse cut propagators in each topology read

$$D_{\text{cut}} = [k_4^2]_c\,[k_5^2]_c\,[k_4\cdot p_{AB} - 2E^2]_c\,[k_5\cdot p_{AB} - 2E^2 z]_c\,. \tag{3.58}$$

The three inverse ordinary propagators D_{a_i} define topologies T^{a_1,a_2,a_3}; they are drawn from the set

$$D_{1,\ldots,7} = \{(p_A\!\cdot\! k_4),\,(p_B\!\cdot\! k_4),\,(p_A\!\cdot\! k_5),\,(p_B\!\cdot\! k_5),\,(k_4\!\cdot\! k_5),\,(p_A\!\cdot\! k_{12}),\,(p_B\!\cdot\! k_{12})\}\,. \tag{3.59}$$

Inverse propagators in Eq. (3.59) fulfill a number of linear relations; they read

$$\begin{aligned} &D_1 + D_3 = D_6\,, \qquad D_2 + D_4 = D_7\,,\\ &D_1 + D_2 = 2E^2\,, \qquad D_3 + D_4 = 2E^2\,z\,, \end{aligned} \tag{3.60}$$

where the last two relations follow from cut constraints. We use these relations to obtain a partial fraction decomposition of Eq. (3.53), so that the result can be expressed through the topologies in Eq. (3.57). We derive and solve IBP relations with `Reduze2` [144] and express integrals in Eq. (3.53) through thirteen master integrals $\boldsymbol{I}(z,\beta,\epsilon)$ grouped into five topologies. The first MI is the phase-space volume

$$I_1 = \left\langle 1 \right\rangle = z^{1-2\epsilon}\,\frac{\left(\Omega^{(d-1)}\right)^2}{16}\,, \tag{3.61}$$

where $\Omega^{(d)}$ is defined in Eq. (B.3) and the notation $\langle \ldots \rangle$ is introduced in Eq. (3.57). The remaining twelve MI can be found in Eq. (C.5) in Appendix C.2.1.

Differential equations

As explained in Sec. 3.2.1, it is practical to compute MI using differential equations. We derive a closed system of first order partial differential equations for master integrals $\boldsymbol{I}$ as functions of β and z, which we cast into a canonical form by changing the basis of MI

$$\boldsymbol{I} = \hat{T}_{\text{can}} \boldsymbol{J} \,. \tag{3.62}$$

We find a suitable transformation by using both the program CANONICA [170] and the program Libra [168].[15] Since Libra is designed for single-variable problems, we apply it sequentially by first transforming the DEQ in z and then the one in β, while making sure that the second step does not spoil the ϵ-homogeneous form reached in the first step. We present the transformation matrix $\hat{T}_{\text{can}}$ in Eq. (C.6). The DEQ in the canonical basis $\boldsymbol{J}$ can be written as

$$\partial_x \boldsymbol{J} = \epsilon\, \hat{M}_x\, \boldsymbol{J} \,, \quad x \in \{z, \beta\} \,, \tag{3.63}$$

where matrices $\hat{M}_{z,\beta}$ feature only simple poles

$$\hat{M}_x = \sum_{x_i \in \mathcal{A}_x} \frac{\hat{m}_{x_i}}{x - x_i} \,, \tag{3.64}$$

with coefficients $\hat{m}_{x_i}$ being rational numbers. When writing Eq. (3.64), we have defined two alphabets

$$\mathcal{A}_z = \left\{ 0,\, -1,\, \frac{-2}{1 \pm \beta},\, -\frac{(1 \pm \beta)}{2},\, -\frac{1-\beta}{1+\beta},\, -\frac{1+\beta}{1-\beta} \right\} , \tag{3.65}$$

$$\mathcal{A}_\beta = \left\{ 0,\, \pm 1,\, \pm(1+2z),\, \pm\frac{1+z}{1-z},\, \pm\frac{2+z}{z} \right\} . \tag{3.66}$$

We note that the differential equations are given in Appendix C.2.2.

As discussed in Sec. 3.2.1, solutions to fuchsian differential equations in ϵ-homogeneous form, as in Eqs. (3.63)-(3.64), can be obtained by recursively integrating their right-hand-side. However, eventually, we will also need to integrate over the energy fraction z, as can be seen in Eq. (3.55) and Eq. (3.56). This integration dramatically simplifies if we write master integrals $\boldsymbol{J}$ in such a way that z appears *only* as an argument of GPLs. To satisfy this condition, at each order in ϵ, we proceed in the following way: First, we integrate the DEQ w. r. t. variable z such that

$$\boldsymbol{J}^n\,(z,\beta) = \sum_{z_i \in \mathcal{A}_z} \int \frac{\hat{m}_{z_i}\, \mathrm{d}z}{z - z_i} \boldsymbol{J}^{n-1}\,(z,\beta) + \boldsymbol{J}_0^n\,(\beta) \,. \tag{3.67}$$

15 We thank Roman Lee for providing access to the Libra package prior to publication.

In order to compute the function $J_0^n(\beta)$, we insert the solution in Eq. (3.67) into the DEQ in β in Eqs. (3.63)-(3.64) and find

$$\frac{\partial}{\partial\beta} J_0^n(\beta) = \sum_{\beta_i \in \mathcal{A}_\beta} \frac{\hat{m}_{\beta_i}\,\mathrm{d}\beta}{\beta-\beta_i} J^{n-1}(z,\beta) - \frac{\partial}{\partial\beta} \sum_{z_i \in \mathcal{A}_z} \int \frac{\hat{m}_{z_i}\,\mathrm{d}z}{z-z_i} J^{n-1}(z,\beta)\,. \tag{3.68}$$

We then verify analytically that the r. h. s. of Eq. (3.68) is independent of z. Denoting the β-dependent remnant of the DEQ in Eq. (3.68) by tilde, we write

$$J_0^n(\beta) = \sum_{\beta_i \in \tilde{\mathcal{A}}_\beta} \int \frac{\widetilde{m}_{\beta_i}\,\mathrm{d}\beta}{\beta-\beta_i} \widetilde{J}^{n-1}(\beta) + C^n\,, \tag{3.69}$$

where C^n are constants of integration and $\tilde{\mathcal{A}}_\beta = \{0,-1,+1\}$ is the z-independent part of the alphabet $\mathcal{A}_\beta$ in Eq. (3.66). The integrals in Eq. (3.67) and Eq. (3.69) can be expressed in terms of $\mathrm{G}(\{\vec{z}_0\};z)$ and $\mathrm{G}(\{\vec{\beta}_0\};\beta)$, respectively, where letters in $\vec{z}_0$ stem from the full alphabet $\mathcal{A}_z$ and letters in $\vec{\beta}_0$ stem from the constant alphabet $\tilde{\mathcal{A}}_\beta$. We will explain how to obtain the remaining constants C^n in what follows.

Boundary conditions

In the previous paragraph, we explained how to obtain master integrals

$$J^n = J^n(z,\beta) + C^n \tag{3.70}$$

up to a vector of integration constants C^n. These constants can be obtained by considering the relation

$$C = \hat{T}_{\mathrm{can}}^{-1} \cdot I - J(z,\beta)\,, \tag{3.71}$$

in a suitable limit. We note that the transformation matrix $\hat{T}_{\mathrm{can}}$ in Eq. (3.71) was introduced in Eq. (3.62), and have defined

$$C = \sum_n \epsilon^n C^n\,, \quad J(z,\beta) = \sum_n \epsilon^n J^n(z,\beta)\,. \tag{3.72}$$

For our purposes, it turns out that the threshold limit $\beta \to 0$ is particularly convenient to determine boundary constants. This is the case, since in the limit $\beta \to 0$, the dependencies of integrands on the direction of hard momenta disappear. For example, we find that

$$p_A \cdot (k_1 + k_2) = E^2[(1+z) - \beta \boldsymbol{n}(\boldsymbol{n}_1 + z\boldsymbol{n}_2)] \xrightarrow{\beta\to 0} E^2(1+z)\,. \tag{3.73}$$

We also find that the master integrals I, cf. Eq. (C.5), have a constant limit as β goes to zero

$$\lim_{\beta\to 0} I(z,\beta,\epsilon) = F(z,\epsilon) + \mathcal{O}(\beta)\,. \tag{3.74}$$

Moreover, all but the first entry of the inverse transformation matrix $\hat{T}_{\text{can}}^{-1}$ in Eq. (3.71) are suppressed by powers of β, so that

$$\lim_{\beta\to 0} \hat{T}_{\text{can}}^{-1} = \begin{pmatrix} 1/z & 0 & \cdots & 0 \\ 0 & 0 & \cdots & 0 \\ \vdots & \vdots & \ddots & \\ 0 & 0 & & 0 \end{pmatrix} + \mathcal{O}(\beta)\,. \tag{3.75}$$

This implies, that Eq. (3.71) simplifies to

$$\boldsymbol{C} = \left(\frac{I_1}{z}, 0, \ldots, 0\right) - \lim_{\beta\to 0} \boldsymbol{J}(z,\beta) + \mathcal{O}(\beta)\,, \tag{3.76}$$

in the limit $\beta \to 0$. Hence, we only need the phase-space volume I_1, cf. Eq. (3.61), to fix all constants $\boldsymbol{C}$. We note that we have checked the solutions for master integrals in the $\boldsymbol{I}$-basis for several values of β and z by comparing them to numerical integration with `Mathematica`.[16]

Integration over z

Having computed all required master integrals, we can express the integrands $\mathcal{E}_{ij}^{\mathcal{X}\mathcal{X}}(z,\beta,\epsilon)$ in Eq. (3.55) and Eq. (3.56) through rational functions of z, β and GPLs $\mathrm{G}(\{\vec{z}_0\};z)$ and $\mathrm{G}(\{\vec{\beta}_0\};\beta)$. As discussed earlier, z only appears in the argument of GPLs, i. e. the letters in $\vec{\beta}_0$ are *independent* of z. This representation allows us to carry out the final z integration in Eq. (3.55) and Eq. (3.56) using the recursive definition of GPLs in Eq. (A.14). We note, that the antiderivative contains spurious $1/z^n$ poles at the lower endpoint $z = 0$. Those poles cancel upon expanding all GPLs with `PolyLogTools` [171]. We use a private implementation of the so-called *super-shuffle* identities [172], cf. Appendix A.5, Example 7, to translate the results into a *fibration* basis, where only GPLs of argument β appear.

Results

Having carried out the final integration over z, we are ready to present results for integrated double-soft subtraction terms (cf. Eq. (2.91) and Eq. (2.92)) for massive back-to-back emitters. We write

$$\begin{aligned} \mathcal{G}\mathcal{G}_{ij} &= \frac{E_{\text{max}}^{-4\epsilon}}{16}\left(\Omega^{(d-1)}\right)^2 \times f_{ij}^{gg}(\beta,\epsilon)\,, \\ \mathcal{Q}\bar{\mathcal{Q}}_{ij} &= \frac{E_{\text{max}}^{-4\epsilon}}{16}\left(\Omega^{(d-1)}\right)^2 \times f_{ij}^{q\bar{q}}(\beta,\epsilon)\,, \end{aligned} \tag{3.77}$$

where $\Omega^{(d)}$ is defined in Eq. (B.3) and $ij \in \{AA, AB\}$. We note that, thanks to the strongly-ordered singularity, functions f_{AA}^{gg} and f_{AB}^{gg}, that describe soft gluon-pair emission, feature

16 We thank Arnd Behring for providing help with this.

$1/\epsilon^3$ poles. Functions $f_{AA}^{q\bar{q}}$ that describe the emission of a soft quark-antiquark pair, on the other hand, only start at $1/\epsilon^2$.[17] Our results for the four functions $f_{ij}^{gg,q\bar{q}}(\beta,\epsilon)$ can be found in the ancillary file provided with Ref. [6].[18] The results are expressed through GPLs of β of up to weight four, with integer letters drawn from the alphabet $\mathcal{A} = \{0, \pm 1, \pm 3\}$. We note that these expressions are manifestly real in the physical region $\beta \in [0,1]$. We present the pole-structure of the functions f_{ij}^{gg} and $f_{ij}^{q\bar{q}}$, as well as their threshold $\beta \to 0$ expansion and their high-energy $\beta \to 1$ expansion in Appendix C.2.3.

3.2.3 *Integrated triple-collinear subtraction terms*

In the following section, we analytically compute integrated triple-collinear subtraction terms, which were defined in Eq. (2.96). We note that in Sec. 3.1.3 we already described how to obtain strongly-ordered angular integrals $\mathcal{T}^{\pm}_{\text{s.o.}}$, defined in Eq. (2.133). To obtain *complete* results for triple-collinear subtraction terms, we *1)* compute genuine triple-collinear angular integrals $\mathcal{T}^{\pm}$ defined in Eq. (2.103) and *2)* perform the remaining integrations over energies in Eq. (2.134).

Angular integration

In the following, we explain how to compute angular integrals $\mathcal{T}^{\pm}$ defined in Eq. (2.103). They read

$$\mathcal{T}^{\pm}(E_i, E_4, E_5) = 4g^4 \int \mathrm{d}\Omega_{45}^{(d-1)} \frac{P_{f_i,f_4,f_5}(\pm s_{i4}, \pm s_{i5}, s_{45}, \pm E_i, E_4, E_5)}{s_{i45}^2} \,. \tag{3.78}$$

In this formula, the integrand is rotationally invariant in $d-1$ dimensions and we have to integrate over the full solid angle $\mathrm{d}\Omega_{45}^{(d-1)}$ of particles $f_{4,5}$. In particular, angular integration is *not* constrained to the collinear region, thanks to the new definition of operator $\mathbb{C}_i$ as explained in Sec. 2.3.3. Hence, these integrals have the form of Eq. (3.29) and we can proceed as discussed in Sec. 3.2.1 in order to compute $\mathcal{T}^{\pm}$ as a function of energies.

We re-introduce integration over four-momenta $k_{4,5}$ and write

$$\mathcal{T}^{\pm}(E_i, E_4, E_5) = \int \frac{\mathrm{d}^d k_4\, \mathrm{d}^d k_5\; \delta\big(k_4^2\big)\, \delta\big(k_5^2\big)\, \delta\big(k_4^0 - E_4\big)\, \delta\big(k_5^0 - E_5\big)\, P_{f_i f_4 f_5}}{(E_4 E_5)^{1-2\epsilon}\, s_{i45}^2} \,, \tag{3.79}$$

where for brevity we do not show arguments for $P_{f_i f_4 f_5}$. We re-write partonic energies k_i^0 through scalar products

$$\delta\big(k_i^0 - E_i\big) = \delta\big((N{\cdot}k_i) - E_i\big) \,, \tag{3.80}$$

17 Matrix elements describing the emission of a quark-antiquark pair are not singular in the limit where one quark is softer than the other.

18 We note that these results were checked numerically for several values of β using adapted numerical routines from Ref. [173].

where the auxiliary vector N reads $N = (1, \mathbf{0})$. We replace δ-functions by cut propagators and obtain

$$\mathcal{T}^{\pm}(E_i, E_4, E_5) = (E_4 E_5)^{-1+2\epsilon} \int \frac{\mathrm{d}^d k_4 \, \mathrm{d}^d k_5 \, P_{f_i f_5 f_5}}{D_1 D_2 D_3 D_4 \, s_{i45}^2} \,. \tag{3.81}$$

The first four propagators in Eq. (3.81) are the cut ones; they read

$$D_1 = k_4^2 \,, \; D_2 = k_5^2 \,, \; D_3 = (N \cdot k_4) - E_4 \,, \; D_4 = (N \cdot k_5) - E_5 \,. \tag{3.82}$$

All integrals that contribute to Eq. (3.81) belong to the following class of integrals

$$I_{a_5, a_6, a_7, a_8}(E_i, E_4, E_5) = (E_4 E_5)^{-1+2\epsilon} \int \frac{\mathrm{d}^d k_4 \, \mathrm{d}^d k_5}{D_1 D_2 D_3 D_4 D_5^{a_5} D_6^{a_6} D_7^{a_7} D_8^{a_8}} \,. \tag{3.83}$$

The ordinary inverse propagators $D_{5,\ldots,8}$ in Eq. (3.83) read

$$D_5 = (p_i + k_4)^2 \,, \; D_6 = (p_i + k_5)^2 \,, \; D_7 = (k_4 + k_5)^2 \,, \; D_8 = (p_i + k_4 + k_5)^2 \,. \tag{3.84}$$

We use `Reduze2` [144] to express all integrals that appear in Eq. (3.83) through four master integrals $\boldsymbol{I}$, for which we choose the basis

$$\boldsymbol{I} = \left\{ I_{0,0,0,0}, I_{0,0,0,1}, I_{-1,0,0,2}, I_{0,-1,0,2} \right\} . \tag{3.85}$$

In particular, in the integrals in Eq. (3.85), all cut propagators are raised to first power.

To derive differential equations, it is convenient to introduce two dimensionless variables $\omega_{4,5} = E_{4,5}/E_i$. This allows us to factor the overall mass dimension

$$I_{a_5, a_6, a_7, a_8}(E_i, E_4, E_5) = E_i^{2d-6-2(a_5+a_6+a_7+a_8)} \, \bar{I}_{a_5, a_6, a_7, a_8}(\omega_4, \omega_5) \,, \tag{3.86}$$

and study the dependence of the integrals $\bar{I}$ on $\omega_{4,5}$. To proceed further, we note that the phase-space MI $\bar{I}_1$ is straightforward to compute; it reads

$$\bar{I}_{0,0,0,0} = \frac{(\omega_4 \omega_5)^{1-2\epsilon}}{16} \left[\Omega^{(d-1)} \right]^2 . \tag{3.87}$$

With the help of `Reduze2`, we derive a set of differential equations in $\omega_{4,5}$ for integrals $\bar{I}$. As discussed in Sec. 3.2.1, it is beneficial to choose a basis of MI $\bar{\boldsymbol{J}}$ that makes differential equations canonical. Original integrals $\bar{\boldsymbol{I}}$ and canonical integrals are related by a linear transformation

$$\bar{\boldsymbol{I}} = \hat{T}_{\mathrm{can}} \bar{\boldsymbol{J}} \,. \tag{3.88}$$

To find this transformation, we applied the algorithmic approach of Ref. [164] sequentially in both variables $\omega_{4,5}$. The resulting transformation matrix is given in Eq. (C.46).

In this new basis, differential equations take the form

$$\mathrm{d}\bar{\boldsymbol{J}} = \frac{\epsilon}{20} \sum_{i=4,5} \mathrm{d}\hat{M}_{\omega_i}(\omega_4, \omega_5, \epsilon)\, \bar{\boldsymbol{J}}\,, \tag{3.89}$$

where the matrices $\mathrm{d}\hat{M}_{\omega_i}$ read

$$\mathrm{d}\hat{M}_{\omega_i} = \sum_{r_j \in \mathcal{A}_{\omega_i}} \hat{m}_{\omega_i}^{r_j}\, \mathrm{dln}(r_j)\,, \tag{3.90}$$

and the two alphabets are defined as follows

$$\mathcal{A}_{\omega_i} = \{\omega_i,\, \omega_i - 1,\, \omega_4 + \omega_5,\, \omega_4 + \omega_5 - 1\}\;. \tag{3.91}$$

We note that the coefficient matrices $\hat{m}_{\omega_i}^{r_j}$ in Eq. (3.90) can be found in Eq. (C.47) and Eq. (C.48).

As we have argued in Sec. 3.2.1, it is straightforward to write solutions to such differential equations in terms of GPLs. However, to fully determine master integrals $\bar{\boldsymbol{J}}$, we need to compute boundary constants in a suitable limit. To this end, we consider the limit $\omega_4 \sim \omega_5 \sim \omega \to 0$ of the inverse of Eq. (3.88),

$$\lim_{\omega_4 \sim \omega_5 \to 0} \bar{\boldsymbol{J}} = \lim_{\omega_4 \sim \omega_5 \to 0} \left[\hat{T}_{\mathrm{can}}^{-1} \bar{\boldsymbol{I}}\right]\;. \tag{3.92}$$

We denote master integrals in this limit by[19]

$$\bar{\boldsymbol{I}}^{\mathrm{lim}} = \lim_{\omega_4 \sim \omega_5 \to 0} \bar{\boldsymbol{I}}\,, \tag{3.93}$$

and observe that

$$\bar{I}^{\mathrm{lim}}_{-1,0,0,2} = \bar{I}^{\mathrm{lim}}_{0,-1,0,2} = \frac{1}{2} \times \bar{I}^{\mathrm{lim}}_{0,0,0,1}\,. \tag{3.94}$$

It follows that, apart from phase-space $\bar{I}_{0,0,0,0}$, we need one additional boundary constant, $\bar{I}_{0,0,0,1}$ in the $\omega \to 0$ limit. We find

$$\bar{I}^{\mathrm{lim}}_{0,0,0,1} = \bar{I}^{\mathrm{lim}}_{0,0,0,0}\, \omega^{-1} \times \mathcal{I}_{\mathrm{b.c.}} + \mathcal{O}\left(\omega^0\right)\;, \tag{3.95}$$

where

$$\mathcal{I}_{\mathrm{b.c.}} = \int \frac{\mathrm{d}\Omega_{45}^{(d-1)}}{\left[\Omega^{(d-1)}\right]^2} \frac{1}{[\eta_{i4} + \eta_{i5}]}\,. \tag{3.96}$$

19 We note that the limit $\omega_4 \sim \omega_5 \to 0$ of $\hat{T}_{\mathrm{can}}^{-1}$ is such that we only need the leading contribution of each master integral.

We explain how to compute this integral in Appendix C.3.2, the result reads

$$\begin{aligned}\mathcal{I}_{\text{b.c.}} = &\frac{4^{-\epsilon}(1-2\epsilon)^2}{\epsilon(1-4\epsilon)} \frac{\Gamma^4(1-2\epsilon)\,\Gamma(1+\epsilon)}{\Gamma(1-4\epsilon)\,\Gamma^3(1-\epsilon)} \\ &- \frac{(1-2\epsilon)}{\epsilon}\,{}_3F_2\left[\{1,1-\epsilon,2\epsilon\},\{2(1-\epsilon),1+\epsilon\};-1\right] .\end{aligned} \tag{3.97}$$

This allows us to fix boundary conditions for $\bar{J}$ in the limit $\omega_4 = \omega_5 = \omega \to 0$ using

$$\lim_{\omega_4 \sim \omega_5 \to 0} \bar{J} = \left[\lim_{\omega_4 \sim \omega_5 \to 0} \hat{T}^{-1}_{\text{can}}\right] \bar{I}^{\text{lim}}_{0,0,0,0} \left(1, \frac{\mathcal{I}_{\text{b.c.}}}{\omega}, \frac{\mathcal{I}_{\text{b.c.}}}{2\omega}, \frac{\mathcal{I}_{\text{b.c.}}}{2\omega}\right) + \mathcal{O}(\omega^0) \,. \tag{3.98}$$

We are now in position to compute $\mathcal{T}^{\pm}$ in Eq. (3.81) for *any* splitting $f^* \to f_i f_4 f_5$ ($f_i \to f^* f_4 f_5$) and *any* energy parameterization in a few simple steps:

- first, we express the angular integral $\mathcal{T}^{-(+)}$, which describes emission off the initial state (final state), through master integrals $\boldsymbol{J}$ and rational coefficients that depend on r, z ($x_{1,2}$);
- second, we perform the change of variables $\{\omega_{4,5}\} \to \{r, z\}$ ($\{\omega_{4,5}\} \to \{x_{1,2}\}$) in canonical differential equations in Eq. (3.89) and boundary conditions in Eq. (3.98);
- third, we compute $\boldsymbol{J}$ by integrating differential equations order-by-order in ϵ in terms of GPLs. At each order, we solve the differential equation in r (x_2) first, so that this variable *only* appears in arguments of GPLs;
- finally, we fix boundary conditions using Eq. (3.98).

We note that we have checked analytic results for master integrals for a few values of energy variables using Mellin-Barnes methods. Numerical Mellin-Barnes integrations were performed with the help of the `Mathematica` package `MB.m` [174].

Energy integration

In the previous section, we have computed $\mathcal{T}^{\pm}$ for all energy parameterizations that we discussed in Sec. 2.6. The ϵ-expansion of this quantitiy starts at $1/\epsilon^2$. However, the $1\epsilon^2$-pole has to cancel when the difference with the strongly-ordered counterpart $\mathcal{T}^{\pm}_{\text{s.o.}}$ in Eq. (2.134) is computed. This cancellation provides a welcome consistency check of our calculations.

INITIAL-STATE RADIATION In case of initial-state radiation, we have to consider the various splittings in two different energy parameterizations as summarised in Table 2.2. In each case, integrals over r, which enter the quantities R_δ, R_+, $R_{\text{reg}}(z)$, and $\widetilde{R}_{\text{reg}}(z)$ defined in Eq. (2.116) and Eq. (2.123), consist of GPLs in which r only appears in the argument. This feature allows us to carry out the final integration over r using the recursive definition of GPLs in Eq. (A.14).

FINAL-STATE RADIATION In case of final-state radiation, we have to consider the various splittings shown in Table 2.3 in the $x_{1,2}$-parameterization. We split the integral in Eq. (2.131) as follows

$$\begin{aligned}
&\int_0^1 \mathrm{d}x_1 \int_0^1 \mathrm{d}x_2\; \theta(1 - x_1 - x_1 x_2) \\
&= \int_0^{1/2} \mathrm{d}x_1 \int_0^1 \mathrm{d}x_2 + \int_{1/2}^1 \mathrm{d}x_1 \int_0^{(1-x_1)/x_1} \mathrm{d}x_2\,,
\end{aligned} \tag{3.99}$$

and express its integrand through GPLs where x_2 only appears in the argument. Then, the x_2 integration is straightforward; the result is expressed in terms of GPLs, which contain constants and rational functions of x_1 in both the letters and the arguments. We map these GPLs onto a fibration basis, where x_1 only appears in the argument and all letters are constant, using a `Mathematica` implementation of the "super-shuffle" procedure that we explain in Appendix A.5. After this step, the remaining integration over x_1 is straightforward, the result can be expressed through GPLs of weight four with rational letters and arguments. Finally, we evaluate these expressions with `GiNaC` [175, 176] and use the PSLQ algorithm [177, 178] to express them through linear combinations of a few transcendental[20] and rational numbers.

Results

The complete list of analytic results for triple-collinear subtraction terms can be found in the supplementary material of Ref. [5], see also Table 2.2 and Table 2.3. We note that all results have been checked numerically. We present some exmamples for initial-state and final-state integrated triple-collinear subtraction terms in Appendix C.3.3.

20 Appearing transcendental numbers are π, $\ln(2)$, $\mathrm{Li}_4(1/2)$, and ζ_3.

Part II

MIXED QCD-EW CORRECTIONS TO VECTOR BOSON PRODUCTION

In the second part of this thesis, we present the computation of mixed QCD-EW NNLO corrections to on-shell Z- and W-boson production at the LHC. We begin by describing technical details of these computations in Chapter 4. In the case of Z-boson production, QCD-QED corrections are obtained by abelianising NNLO QCD calculations. Additionally, calculation of mixed QCD-EW corrections requires inclusion of one-loop weak and two-loop QCD-weak corrections. In the case of W-boson production, we discuss computation of previously unknown two-loop contributions, as well as details of the regularisation of IR singularities employing the nested soft-collinear subtraction scheme. In Chapter 5, we study how these corrections affect inclusive and fiducial cross sections and kinematic distributions of Z- and W-boson production at the LHC. We also estimate the impact of QCD-EW initial-initial corrections on the W-boson mass extraction at the LHC.

4 VECTOR BOSON PRODUCTION AT THE LHC

After early experimental indications of the neutral-current interaction [179], the discovery of EW gauge bosons $W^{\pm}$ and Z [180–183] played an important role in establishing the validity of the Standard Model. Since then, the infamous Drell-Yan (DY) process [184] $pp \to \gamma^*/Z^* \to l\bar{l}$ ($pp \to W^* \to l\bar{\nu}_l$) has become a standard candle at the LHC [185–189]: its large cross section and clean signature make it useful for luminosity monitoring [190–192] and detector calibration [193]. Besides that, the DY process is used in measurements of the weak mixing angle [193, 194], the determination of PDFs [195–198] and for searches of New physics at high energies [199].

MEASURING THE W-BOSON MASS AT THE LHC One of the ultimate goals of precision electroweak physics at the LHC is the direct measurement of the mass of the W-boson with a precision of $\mathcal{O}(10)$ MeV [28], an astonishing relative uncertainty of $\mathcal{O}(10^{-2})$ percent! If achieved, such a precision would challenge the precision of M_W that is reached in EW fits, where the most recent result is $M_W = 80358 \pm 8\text{MeV}$ [29, 30]. A comparison of direct and indirect determinations of M_W will allow for a strong consistency check of the SM.

Since energies of initial partons are not fixed at hadron colliders and produced neutrinos escape undetected, it is in fact impossible to fully reconstruct the W-boson mass in a single event. The way out is to consider observables that are sensitive to M_W. One example of such an observable is the so-called transverse mass[1]

$$M_W^{\perp} = \sqrt{2p_\ell^{\perp}p_{\text{miss}}^{\perp}(1-\cos\Delta\phi)} \leq M_W\,, \tag{4.1}$$

where $p^{\perp}_{\ell(\text{miss})}$ is the absolute value of the momentum of the charged lepton (neutrino) transverse to the beam axis $\boldsymbol{e}_z$ and $\Delta\phi = \sphericalangle\left(\boldsymbol{p}_\ell^{\perp}, \boldsymbol{p}_{\text{miss}}^{\perp}\right)$ is the opening angle between leptons in the transverse plane.[2] Since for stable W bosons, the transverse mass is always smaller than the W-boson mass, $M_W^{\perp} \leq M_W$, the kinematic distribution in the transverse mass features a sharp edge which can be used to determine M_W. We note that, although the edge at $M_W^{\perp} = M_W$ is shifted due to the finite width of the W boson and detector effects [200], additional initial-state or final-state radiation plays only a minor role for this observable.

The second useful observable is the transverse momentum of the lepton $p_\ell^{\perp}$, which exhibits a Jacobian peak at $p_\ell^{\perp} = M_W/2$. In contrast to the transverse-mass distribution,

1 We adapt the definition of Ref. [25] for massless leptons ℓ, ν.

2 The so-called transverse "missing" momentum $\boldsymbol{p}_{\text{miss}}^{\perp}$ that is carried by the neutrino is inferred using momentum conservation in the transverse plane.

the transverse-momentum distribution is strongly affected by additional QCD and QED radiation in the initial and final state. In fact, it is impossible to predict the $p_\ell^\perp$ spectrum with the required $\mathcal{O}(10^{-2})$ precision, since state-of-the-art fixed-order predictions in the framework of collinear factorization typically only reach a precision of $\mathcal{O}(1\%)$, even when augmented with parton showers and resummation.

To circumvent this problem, in the experimental analyses in Ref. [25] well-understood Z-boson samples were used to describe the $p_\ell^\perp$ distribution in W-boson production. This procedure relies on – and is rather sensitive to – the theoretical modelling of differences between Z- and W-boson production. These differences originate, for example, in the flavor of initial-state partons implying uncertainties from PDFs [201–203],[3] massive quark effects [205, 206], or the fact that the contribution $g\,g \to Z\,g$ does not exist in the W-boson case.

Another difference are fixed-order NLO electroweak and mixed QCD-EW corrections, which need to be accounted for in order to enable extraction of the W-boson mass with $\mathcal{O}(10)$ MeV precision.

In what follows, we will give a brief overview of the theoretical predictions for the (on-shell) DY process. In Sec. 4.1 and Sec. 4.2, we discuss computation of mixed QCD-EW corrections to on-shell Z- and W-boson production [7–9]. Finally, in Chapter 5 we present inclusive and differential cross sections at the QCD-EW NNLO level and assess the impact of these corrections on the extraction of the W-boson mass from the $p_\ell^\perp$ distribution [10].

THEORETICAL PREDICTIONS FOR DRELL-YAN PROCESS Corrections to the inclusive DY cross section were computed with NLO (NNLO) QCD accuracy fourty (thirty) years ago [207–210]. Recently, a further step in the quest for high-precision description of the DY process has been accomplished with the computation of N3LO QCD corrections [211, 212].[4] Distributions for arbitrary IR safe observables for dilepton production are available through NNLO QCD [71, 80, 215–221] and NLO EW [222–231].

Given the relative magnitude of strong and electroweak coupling constants, the availability of N3LO QCD computations, and the demanding precision physics programme at the LHC, it becomes important to know mixed QCD-EW $\mathcal{O}(\alpha_s\alpha)$ corrections as well.[5] Required two-loop master integrals were computed in Ref. [232]; the complete double-virtual amplitude for $pp \to \ell\bar{\ell}$ was obtained in Ref. [156]. Only very recently, these results where combined with real-emission contributions in Ref. [233] to describe QCD-EW corrections to the DY process $pp \to \ell\bar{\ell}$.

In the absence of a full calculation, various approximations have been used to estimate differential QCD-EW corrections. For example, in Ref. [234], NNLO QCD and NLO EW corrections have been combined additively, a leading-logarithmic approximation was presented in Ref. [235], including matching to QCD parton showers and multiple photon

3 A recent study showed how these uncertainties can be halfed using LHCb data [204].
4 Threshold effects at N3LO were studied in Refs. [213, 214].
5 We note that numerically $\alpha_s^3 \sim \alpha_s\alpha$ so one would expect both contributions to be of a comparable magnitude.

emission. More recently, QCD-QED corrections have been computed for the process $pp \to Z^* \to \nu\bar{\nu}$ [236].[6] Differential predictions at order $\mathcal{O}(n_f \alpha_s \alpha_{\mathrm{EW}})$ for both neutral- and charged current DY have been obtained in Ref. [237].[7] Some of the off-shell effects for the process $pp \to W^{(*)} \to \ell\nu$ were also covered in the computation in Ref. [238], where double-virtual corrections were obtained by reweighing the on-shell form factor computed in Ref. [9].

THEORETICAL PREDICTIONS FOR ON-SHELL GAUGE BOSON PRODUCTION Despite the fact, that the generic DY process $pp \to \ell\bar{\ell}(\ell\bar{\nu})$ is the target of many experimental analyses, the theoretical description of the production of an *on-shell* vector boson yields significant simplifications while being accurate enough for many purposes and various observables. In fact, in the limit where the intermediate vector boson becomes on-shell, real and virtual contributions that connect incoming partons and outgoing leptons are suppressed by the ratio of the boson's width to its mass Γ_V/M_V [239], and, for this reason, can be neglected. It is therefore possible to divide mixed QCD-EW corrections into *initial-initial* and *initial-final* corrections

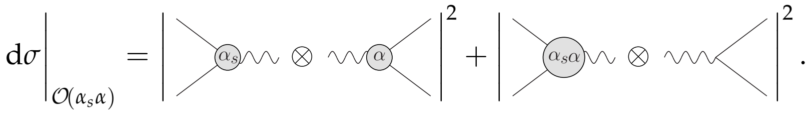

(4.2)

The first term on the r. h. s. of Eq. (4.2) denotes NLO-like initial-final contributions that arise from NLO QCD corrections to the production and NLO EW corrections to the decay stage of the process. The second term denotes genuine NNLO initial-initial contributions that were, in fact, unknown up to now. Initial-final contributions were argued to be numerically dominant in Ref. [240]. Furthermore, $\mathcal{O}(\Gamma_V/M_V)$-suppressed soft-photon contributions were computed in this work and found to be negligible. Subsequently, initial-final contributions, as well as corrections to the decay that originate from renormalization, were studied in Ref. [241].

Initial-initial mixed QCD-QED corrections to the inclusive cross section of on-shell Z-boson production were studied in [38], where results were obtained by "abelianizing" the well-known NNLO QCD results of Ref. [208]. Surprisingly, in the setup of Ref. [38], these corrections turn out to be only about a factor of ~ 3.5 smaller than NNLO QCD corrections. We note that we will address this observation again in Sec. 5.1, where we compare our findings to the results of Ref. [38]. QCD-QED corrections are a gauge-invariant subset of mixed QCD-EW corrections, which where studied in Refs. [242–244].

6 We note that since this particular final state is color- and electrically neutral, corrections only affect the production vertex.

7 We note that in the approximation, where only n_f-enhanced contributions are considered, double-real contributions vanish by color conservation and the subtraction procedure is NLO-like. Analogously, no genuine vertex corrections can occur in this approximation.

THIS WORK As mentioned in the beginning of this Chapter, it is commonly believed that mixed QCD-EW corrections are important for a precise measurement of the W-boson mass at the LHC. Because of that, we have computed all missing QCD-EW initial-initial corrections to on-shell vector-boson production cross sections. In Ref. [7], we studied QCD-QED initial-initial corrections at the fully-differential level for the first time. This computation is interesting for three reasons. First, the rather modest suppression of the results in Ref. [38] w. r. t. NNLO QCD mentioned above makes it worthwhile to extend these studies to exclusive observables. Second, understanding the IR structure of mixed corrections to $pp \to Z$ allows us to add QCD-EW corrections to this process in a straightforward way and is an important step towards the more involved case of $pp \to W^{\pm}$. Finally, it allows us to quantitatively compare our results to corresponding initial-final corrections of Ref. [241]. In Ref. [8], we added additional real-virtual and double-virtual QCD-*weak* corrections and obtained the full set of QCD-EW corrections to Z-boson production. We computed initial-initial QCD-EW corrections to on-shell W-boson production at the fully-differential level in Ref. [9].

LAYOUT OF THE CHAPTER In the remainder of this Chapter, we present technical aspects of the computations of mixed QCD-EW corrections to vector boson production at the LHC. In Sec. 4.1, we describe calculation of QCD-QED corrections to Z-boson production, which were obtained in Ref. [7] by applying an "abelianization" procedure [38] to NNLO QCD corrections computed with the nested soft-collinear subtraction scheme in Refs. [1, 2]. We also explain how to include required QCD-weak corrections in order to obtain the full set of QCD-EW corrections [8]. In Sec. 4.2, we present mixed QCD-EW corrections to W-boson production that were originally computed in Ref. [9]. Since W bosons are electrically charged, the IR singularity structure of mixed QCD-EW corrections is different from the structure of NNLO QCD corrections. We discuss how to accommodate these differences in the construction of subtraction terms for double-real contributions in the framework of nested soft-collinear subtractions. We note that we discuss the computation of master integrals for the previously unknown two-loop $q\bar{q}' \to W$ form factor and present required double-real matrix elements in spinor-helicity formalism in Appendix D.

4.1 MIXED QCD-EW CORRECTIONS TO Z-BOSON PRODUCTION

4.1.1 *Preliminary remarks*

In the following Section, we discuss technical aspects of the computation of QCD-EW corrections to the on-shell Z-boson production in hadron collisions at the fully-differential level. Initial-final corrections, corresponding to the first term on the r. h. s. of Eq. (4.2), are NLO-like $\mathcal{O}(\alpha_s)$ and $\mathcal{O}(\alpha)$ corrections to production and decay stages, respectively.

We deal with the IR singularities that appear in these contributions using the well-known FKS scheme [51, 52].

Genuine NNLO initial-initial corrections, on the other hand, are more complicated. They require the following ingredients:

- tree-level partonic processes $q\bar{q} \to Zg\gamma$, $q\bar{q} \to Zq\bar{q}$, $qq \to Zqq$, $qg \to Zq\gamma$, $q\gamma \to Zqg$, $g\gamma \to Zq\bar{q}$;
- one-loop EW corrections to partonic processes $q\bar{q} \to Zg$ and $qg \to Zq$;
- one-loop QCD corrections to partonic processes $q\bar{q} \to Z\gamma$ and $q\gamma \to Zq$;
- two-loop QCD-EW corrections to partonic processes $q\bar{q} \to Z$.

Phase-space integration over unresolved regions of final-state particles causes soft and collinear singularities. They need to be regulated, extracted, and properly cancelled against explicit $1/\epsilon$-poles from loop integrals at a fully-differential level. It is convenient to divide the contributions mentioned above into two gauge-invariant subsets: QED and *weak* contributions. Out of these two, only mixed QCD-QED corrections have NNLO-like IR singularities: these are very similar to QCD corrections. In fact, it was observed in Ref. [38] that these contributions can be obtained by a set of replacement rules for various color factors.[8] Once QED corrections are understood, weak corrections are obtained by adding renormalized one-loop weak and two-loop QCD-weak contributions. Up to NLO-like QCD IR singularities, these corrections are IR finite, since, by definition, they include virtual exchanges of massive gauge bosons.

4.1.2 *QED corrections to Z-boson production*

Following the abelianisation procedure of Ref. [38], we obtain initial-initial QCD-QED corrections at a fully differential level by modifying QCD color factors C_F^2, $C_F C_A$, and $C_F T_R$, which appear in the corresponding NNLO QCD calculation [1, 2]. These color factors arise, when in calculations of spin and helicity averaged matrix elements squared, the following color traces are evaluated[9]

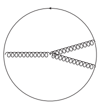 $\sim C_A C_F\,,$ 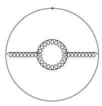 $\sim C_A C_F\,,$ 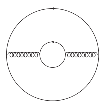 $\sim C_F T_R\,,$ (4.3)

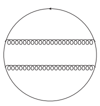 $\sim C_F^2\,,$ 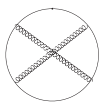 $\sim C_F\,(C_F - C_A/2)\,.$ (4.4)

8 In essence, replacement rules follow from the change of color factors under the exchange of gluons with photons.

9 In this notation, we do not show the Z boson and we do not distinguish between virtual and real particles.

As an example, we consider the interference of a particular two-loop NNLO QCD diagram with the tree-level diagram and find

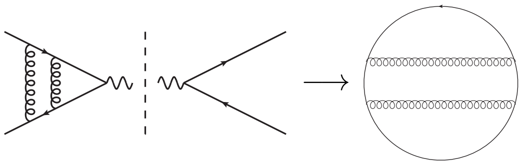

$$. \tag{4.5}$$

An example of a double-real interference term at NNLO QCD is

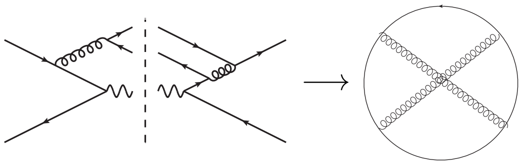

$$. \tag{4.6}$$

It is straightforward to see, that all contributions in Eq. (4.3) vanish if one gluon is replaced by a photon: for the first two diagrams, this happens because there is no gluon-photon coupling; the last diagram vanishes since it becomes proportional to $\mathrm{Tr}(T^a T^b)\mathrm{Tr}(T^a T^b) \to \mathrm{Tr}(T^a)\mathrm{Tr}(T^a) = 0$. Accordingly, we have to remove color factors $C_A \to 0$ and $T_R \to 0$. Diagrams in Eq. (4.4), on the other hand, do not vanish. In fact, they yield

$$\begin{aligned}
&\mathrm{Tr}(T^a T^a T^b T^b) \to n_{\mathrm{ex}}\,\mathrm{Tr}(T^a T^a) e_q^2 = n_{\mathrm{ex}}\, C_F Q_q^2\,,\\
&\mathrm{Tr}(T^a T^b T^a T^b) \to n_{\mathrm{ex}}\,\mathrm{Tr}(T^a T^a) e_q^2 = n_{\mathrm{ex}}\, C_F Q_q^2\,,
\end{aligned} \tag{4.7}$$

where n_{ex} denotes the number of indistinguishable gluons that can be exchanged with a photon and Q_q is the electric charge of the quark. In what follows, we discuss how color factors have to be changed in case of quark-quark, quark-gluon and gluon-gluon initiated contributions, respectively.

QUARK-INITIATED PROCESSES Quark-initiated contributions in NNLO QCD are tree-level processes $q\bar{q} \to Zgg$, $q\bar{q} \to Zq\bar{q}$, and $q_i q_j \to Z q_i q_j$, as well as one-loop corrections to $q\bar{q} \to Zg$ and two-loop corrections to $q\bar{q} \to Z$. For these processes, any of the two gluons can be replaced with a photon ($n_{\mathrm{ex}} = 2$) and up to two independent color traces appear. We note that a special case arises only in the situation $q\bar{q} \to Zg(k_4)g(k_5)$, where both gluons appear in the final state. Upon replacing either gluon, these contributions are mapped onto two distinct contributions in the QCD-QED case, $q\bar{q} \to Zg(k_4)\gamma(k_5)$ and $q\bar{q} \to Z\gamma(k_4)g(k_5)$. Naively, one might think that $n_{\mathrm{ex}} = 1$ in Eq. (4.7) and that the correct replacement rule should be $C_F^2 \to C_F e_q^2$.

However, the extra factor of two accounts for the symmetry factor $1/2!$ that is present in the gg, but not in the $g\gamma$ case. We conclude that the replacement rules for quark-initated partonic channels are

$$C_F^2 \to 2C_F e_q^2\,, \quad C_A \to 0\,, \quad T_R \to 0\,. \tag{4.8}$$

QUARK-GLUON INITIATED PROCESSES Quark-initiated contributions in NNLO QCD are the tree-level processes $qg \to Zqg$ and the one-loop QCD correction to $qg \to Zq$. For these cases we can replace only one gluon with a photon. This can either be an initial-state gluon, in which case we obtain the tree-level contribution $q\gamma \to Zqg$ and the one-loop QCD contribution $q\gamma \to Zq$, or the final-state gluon, in which case we obtain $qg \to Zq\gamma$. Finally, we can also replace the virtual gluon with a photon. In this case, we obtain the one-loop QED contribution to $qg \to Zq$. All these changes amount to the replacement

$$C_F^2 \to C_F e_q^2 \,, \quad C_A \to 0 \,. \tag{4.9}$$

We note that we also have to replace the averaging factor over color charges when an initial-state gluon is replaced by a photon.

GLUON-GLUON INITIATED PROCESSES The gluon-induced process receives only tree-level contributions $gg \to Zq\bar{q}$. In this case, we replace one of the two initial-state gluons with a photon and obtain the two processes $g\gamma \to Zq\bar{q}$ and $\gamma g \to Zq\bar{q}$. The replacement rules in this case read

$$C_F^2 \to C_F e_q^2 \,, \quad C_A \to 0 \,. \tag{4.10}$$

We note that also in this case we have to change the averaging factor over the color of the initial-state gluon.

Applying these rules to the calculation of on-shell Z-boson production through NNLO QCD in Ref. [2], we obtain a fully-differential description of initial-initial QCD-QED corrections. This includes regulated double- and single-real contributions, integrated subtraction terms, and finite remainders of virtual corrections, and allows us to compute arbitrary IR safe observables to on-shell Z-boson production. We discuss phenomenological implications of these corrections in Chapter 5.

CHECKS We note that we have checked this calculation in the following way. We followed the procedure described above to abelianise the analytic NNLO QCD corrections to inclusive Z-boson production [208] and compared these results to that of Ref. [38]. We then used the fully-differential setup described above to compute the *inclusive* cross section and found agreement with the analytic results presented in Ref. [38] within the numerical precision.

4.1.3 *Weak corrections to Z-boson production*

Having discussed computation of initial-initial QCD-QED corrections in Sec. 4.1.2, we now turn to *weak* corrections and summarize briefly what was done in Ref. [8]. There, two-loop QCD-weak corrections to the $q\bar{q} \to Z$ vertex[10] were re-computed, confirming results

10 We note that we disregard top-quark contributions.

presented earlier in Ref. [245].[11] One-loop weak corrections to the partonic processes $q\bar{q} \to Zg$ and $qg \to Zq$ were obtained using the `OpenLoops` package [247–251].

We note, that we will study phenomenological impact of QED and weak corrections in Chapter 5. Before that, we discuss calculation of mixed QCD-EW corrections to the production of electrically charged W bosons in the next section.

4.2 MIXED QCD-EW CORRECTIONS TO W-BOSON PRODUCTION

4.2.1 *Preliminary remarks*

The computation of mixed QCD-EW initial-initial corrections to W-boson production was presented in Ref. [9]. It is considerably more involved than the Z-boson case. In fact, since the W boson carries electric charge, the IR behaviour of matrix elements changes, as compared to the case of Z-boson production. For this reason, QCD-QED corrections to W-boson production cannot be obtained by abelianising NNLO QCD corrections to this process and a new calculation is required.[12]

To fully describe initial-initial $\mathcal{O}(\alpha_s\alpha)$ corrections to on-shell W-boson production, the following double-real, real-virtual and double-virtual matrix elements have to be computed[13]

- $q\bar{q}'$-channel:
  - tree-level contributions $q\bar{q}' \to W + g + \gamma$ and $q\bar{q}' \to W + q + \bar{q}$;
  - one-loop QCD contribution $q\bar{q}' \to W + \gamma$;
  - one-loop EW contribution $q\bar{q}' \to W + g$;
  - two-loop QCD-EW contribution $q\bar{q}' \to W$;
- qq-channel with the tree-level contribution $qq \to W + qq'$;
- qq'-channel with the tree-level contribution $qq' \to W + qq$;
- qg-channel:
  - tree-level contribution $qg \to W + q' + \gamma$;
  - one-loop EW contribution $qg \to W + q'$;
- $q\gamma$-channel:
  - tree-level contribution $q\gamma \to W + q' + g$;
  - one-loop QCD contribution $q\gamma \to W + q'$;

11 The renormalized form-factor was obtained using results in Ref. [246].
12 We note that it was demonstrated in Ref. [238] how to obtain a valid subtraction scheme by abelianising QCD corrections to heavy-quark production.
13 Further contributions from PDF renormalization are not displayed here, they can be found in Ref. [9].

- $g\gamma$-channel with the tree-level contribution $g\gamma \to W + q\bar{q}'$.

For the sake of brevity, from now on we will restrict ourselves to the case of W^+ production.[14] We denote up- and down-type quarks by u and d and assume that the CKM matrix is an identity matrix, $V_{\text{CKM}} = \mathbb{1}_{3x3}$.

DOUBLE-VIRTUAL CORRECTIONS The two-loop QCD-EW form factor $u\bar{d} \to W^+$ was computed in Ref. [9]. In this thesis, we describe the computation of ten previously unknown master integrals in Appendix D.1.

REAL-VIRTUAL CORRECTIONS We note that finite one-loop EW and QCD remainders are obtained in Ref. [9] numerically with the `OpenLoops` package. Furthermore, we note that one-loop QCD corrections to $q\bar{q}' \to W^+ + \gamma$ and $qg \to W^+ + q' + \gamma$ require particular care since the photon couples to the W boson. The required subtraction terms can be extracted from the results in Sec. 3.1.2. Details can be found in Ref. [9].

DOUBLE-REAL CORRECTIONS All double-real corrections listed above can be expressed through two types of tree-level amplitudes: they contain the W-boson and either four quarks or two quarks and a photon and a gluon. We present these quantities in Appendix D.2. In the following Section, we explain how to properly regulate and extract all soft and collinear singularities. In particular, we comment on the modifications to the nested soft-collinear subtraction scheme that were made to simplify this calculation.[15]

4.2.2 *Regularisation of infrared singularities in double-real corrections*

In this section, we discuss the regularisation of IR singularities in double-real contributions. In particular, we show how to regulate and extract IR divergences for each of the partonic channels listed in the beginning of Sec. 4.2 using the nested soft-collinear subtraction scheme. We follow the procedure that was presented in Sec. 2.2 and Sec. 2.3 and iteratively subtract soft and collinear singularities. In contrast to previous computations [1, 2], we work in a reference frame in which the initial-state partons $f_{1,2}$ are back-to back but carry *arbitrary* energies $E_{1,2}$, demonstrating the flexibility of the subtraction scheme. We begin by discussing processes with quarks in the initial state, and then turn to quark-gluon (-photon) and gluon-photon initiated processes, respectively.

Quark-initiated processes

QUARK EMISSION We start with processes that have quarks both in the initial and in the final state. We consider two representative examples for quark emission, $u\,\bar{d} \to W\,q\,\bar{q}$ and $u\,d \to W^+\,d\,d$, where $q\bar{q}$ denotes a generic light quark-antiquark pair. In case

14 Results for the case of W^- production can be obtained by changing charges and PDFs appropriately.
15 We note that several aspects have already been touched upon in Part I of this thesis.

of mixed QCD-EW corrections, only interference terms with a *continuous* quark line contribute. All other terms vanish since the are proportional to $\sim \mathrm{Tr}(T^a) = 0$.[16] It follows that $q\bar{q}$ is either $u\bar{u}$ or $d\bar{d}$.

An example for an interference term with a continuous quark line for the case $u\,\bar{d} \to W^+\,u\,\bar{u}$ is

$$\left|\mathcal{A}_{u\bar{d}\to W^+u\bar{u}}\right|^2\Big|_{\mathcal{O}(\alpha_s\alpha)} \supset \qquad (4.11)$$

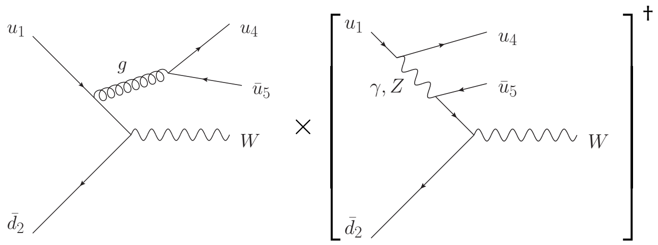

We note that the case of $d\bar{d}$-emission can be obtained from Eq. (4.11) by replacing the s-channel splitting $g \to u\bar{u}$ with the splitting $g \to d\bar{d}$ in the left diagram and by moving the t-channel boson exchange to the lower line in the right diagram.

The left diagram in Eq. (4.11) could, in principle, cause a double-soft singularity in the limit $k_{4,5} \to 0$, a double-collinear singularity in the limit $\boldsymbol{k}_4 \parallel \boldsymbol{k}_5$ and a triple-collinear singularity when $\boldsymbol{k}_4 \parallel \boldsymbol{k}_5 \parallel \boldsymbol{p}_1$. However, the photon contribution in the right diagram in Eq. (4.11) only develops collinear singularities when $\boldsymbol{k}_4 \parallel \boldsymbol{p}_1$ and when $\boldsymbol{k}_4 \parallel \boldsymbol{k}_5 \parallel \boldsymbol{p}_1$.[17] Hence, the interference term shown in Eq. (4.11) is *only* singular in the triple-collinear limit $\boldsymbol{k}_4 \parallel \boldsymbol{k}_5 \parallel \boldsymbol{p}_1$. In fact, it is straightforward to check that *all* double-real contributions with two quarks both in the initial and in the final state stem from s-channel and t-channel interferences, like the one in Eq. (4.11), and exhibit *only* triple-collinear singularities.

For the process $u\,d \to W^+\,d\,d$, an example for an interference with a continuous quark line is

$$\left|\mathcal{A}_{u\,d\to W^+dd}\right|^2\Big|_{\mathcal{O}(\alpha_s\alpha)} \supset \qquad (4.12)$$

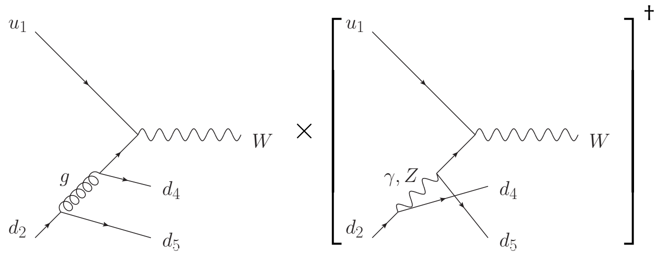

For the same reasons discussed below Eq. (4.11), the contribution shown in Eq. (4.12) is only singular in the triple-collinear limit $\boldsymbol{k}_4 \parallel \boldsymbol{k}_5 \parallel \boldsymbol{p}_2$.

Adopting the notation of Sec. 2.1, we write

$$\mathrm{d}\sigma^{RR}_{u\bar{d}\to W^+q\bar{q}} = \left\langle [\mathrm{d}k_4][\mathrm{d}k_5]\; F_{\mathrm{LM}}\left(1_u, 2_{\bar{d}}, W^+; 4_q, 5_{\bar{q}}\right)\right\rangle , \qquad (4.13)$$

16 See also Appendix D.2. Equivalently, this observation corresponds to taking $T_R \to 0$ in the Z-boson case, see Eq. (4.3) and the discussion below that equation.

17 We note that the contribution with a Z-boson is finite.

$$\mathrm{d}\sigma^{RR}_{ud\to W^+dd} = \left\langle [\mathrm{d}k_4][\mathrm{d}k_5]\ F_{\mathrm{LM}}(1_u, 2_d, W^+; 4_d, 5_d) \right\rangle , \tag{4.14}$$

where we note that the rather simple singularity structure, which has in fact no overlapping limits, does not require us to introduce partition functions or sectors. Hence, in case of $q\bar{q}$ emission, cf. Eq. (4.13), we can extract all divergences by inserting the following partition of unity $I = (I - \mathbb{C}_1 - \mathbb{C}_2) + \mathbb{C}_1 + \mathbb{C}_2$ into Eq. (4.13). We note that the triple-collinear limit $\boldsymbol{k}_4 \parallel \boldsymbol{k}_5 \parallel \boldsymbol{p}_1$ is relevant for $q\bar{q} = u\bar{u}$, whereas $\boldsymbol{k}_4 \parallel \boldsymbol{k}_5 \parallel \boldsymbol{p}_2$ is relevant for the contribution $q\bar{q} = d\bar{d}$. The process in Eq. (4.14), on the other hand, has only one triple-collinear singularity so it suffices to insert $I = (I - \mathbb{C}_2) + \mathbb{C}_2$. We obtain

$$\mathrm{d}\sigma^{RR}_{u\bar{d}\to W^+q\bar{q}} = \left\langle [\mathrm{d}k_4][\mathrm{d}k_5]\ (I - \mathbb{C}_1 - \mathbb{C}_2)\ F_{\mathrm{LM}}(1_u, 2_{\bar{d}}, W^+; 4_q, 5_{\bar{q}}) \right\rangle \tag{4.15}$$
$$+ \left\langle [\mathrm{d}k_4][\mathrm{d}k_5]\,[\mathbb{C}_1 + \mathbb{C}_2]\ F_{\mathrm{LM}}(1_u, 2_{\bar{d}}, W^+; 4_q, 5_{\bar{q}}) \right\rangle , \tag{4.16}$$

and

$$\mathrm{d}\sigma^{RR}_{ud\to W^+dd} = \left\langle [\mathrm{d}k_4][\mathrm{d}k_5]\ (I - \mathbb{C}_2)\ F_{\mathrm{LM}}(1_u, 2_d, W^+; 4_d, 5_d) \right\rangle \tag{4.17}$$
$$+ \left\langle [\mathrm{d}k_4][\mathrm{d}k_5]\ \mathbb{C}_2\ F_{\mathrm{LM}}(1_u, 2_d, W^+; 4_d, 5_d) \right\rangle , \tag{4.18}$$

respectively.

Finally, we note that the required genuine triple-collinear subtraction terms in Eq. (4.16) and Eq. (4.18) are independent of the phase-space parametrization. This is the case since triple-collinear operators $\mathbb{C}_i$ are defined in a way that they only act on matrix elements squared and momentum-conserving δ-functions and *not* on the unresolved phase-space, cf. Sec. 2.3.3. We obtain results for subtraction terms in case of triple-collinear splittings $u \to u\bar{u}u^*$, $d \to d\bar{d}d^*$ and $d \to dd\bar{d}^*$ at $\mathcal{O}(\alpha_s\alpha)$ by abelianising the NNLO QCD result for the splitting $q \to \bar{q}qq^*$ and $q \to qq\bar{q}^*$ computed in Ref. [5].[18]

EMISSION OF A PHOTON AND A GLUON We now turn to the other quark-initiated double-real correction, which is the emission of a gluon-photon pair $u\bar{d} \to W^+\,g\,\gamma$. We write the corresponding fully-differential cross section as

$$2s \cdot \mathrm{d}\sigma^{RR}_{u\bar{d}\to Wg\gamma} = \left\langle [\mathrm{d}k_4][\mathrm{d}k_5]\ F_{\mathrm{LM}}(1_u, 2_{\bar{d}}, W^+; 4_g, 5_\gamma) \right\rangle . \tag{4.19}$$

As we have discussed in Chapter 2, the singularity structure in the case of $g\gamma$-emission is simpler than the gg case in NNLO QCD. Indeed,

- as we have discussed in Sec. 2.2.2, the double-soft limit S_gS_γ is uncorrelated, meaning that the matrix element factorizes into a product of NLO-like eikonal functions. However, we need to account for the fact that the charged W-boson appears as a massive radiator in the soft-photon eikonal function. We presented analytic results for the integrated soft-photon subtraction term for a resolved, a soft, and a collinear gluon in Sec. 3.1.2;[19]

18 See also Table 2.2.
19 We note that the integrated subtraction term for a soft gluon is trivial to obtain, see Eq. (2.42).

- in Sec. 2.3.3 we noticed the absence of a singularity in the limit where the photon and the gluon become collinear to each other. We have used this fact to divide the phase space into two (instead of four) sectors, see Eq. (2.64) and the discussion around it.

With theses simplifications in mind, we write the double-real cross section in Eq. (4.19) as

$$\begin{aligned}
&\big\langle [\mathrm{d}k_4][\mathrm{d}k_5]\; F_{\mathrm{LM}}\big(1_u,2_{\bar{d}},W^+;4_g,5_\gamma\big)\big\rangle \\
&= \big\langle [\mathrm{d}k_4][\mathrm{d}k_5] S_\gamma S_g\; F_{\mathrm{LM}}\big(1_u,2_{\bar{d}},W^+;4_g,5_\gamma\big)\big\rangle \\
&+ \big\langle [\mathrm{d}k_4][\mathrm{d}k_5]\,\big[\,(I-S_g)\,S_\gamma + (I-S_\gamma)\,S_g\big]\; F_{\mathrm{LM}}\big(1_u,2_{\bar{d}},W^+;4_g,5_\gamma\big)\big\rangle \\
&+ \big\langle [\mathrm{d}k_4][\mathrm{d}k_5]\;(I-S_\gamma)\;(I-S_g)\; F_{\mathrm{LM}}\big(1_u,2_{\bar{d}},W^+;4_g,5_\gamma\big)\big\rangle\;.
\end{aligned} \tag{4.20}$$

We note that we have derived results for the integrated soft-gluon and soft-photon subtraction terms in Eq. (2.42) and Sec. 3.1.2, respectively. In particular, we have found that the soft-gluon integral is independent of the photon momentum, while the soft-photon integral was computed for three distinct cases that involve resolved, soft, or collinear gluons. With these results, we can compute the double-soft and single-soft subtraction terms in Eq. (4.20).

We begin with the double-soft contribution to Eq. (4.20) and obtain

$$\begin{aligned}
&\big\langle [\mathrm{d}k_4][\mathrm{d}k_5] S_\gamma S_g\; F_{\mathrm{LM}}\big(1_u,2_{\bar{d}},W^+;4_g,5_\gamma\big)\big\rangle = [\alpha][\alpha_s]\left[(2\,E_{\max})^{-2\epsilon}\frac{\Gamma^2\,(1-\epsilon)}{\Gamma\,(1-2\epsilon)}\right]^2 \\
&\times \frac{2C_F}{\epsilon^2}\,\big\langle \tilde{J}_\gamma(E_1,E_2)\; F_{\mathrm{LM}}\big(1_u,2_{\bar{d}},W^+\big)\big\rangle\;.
\end{aligned} \tag{4.21}$$

The function $\tilde{J}_\gamma(E_1,E_2)$ can be found in Eq. (3.24).

As we explained in Sec. 2.2.2, single-soft contributions in which either the gluon or the photon is soft, exhibit singularities when the remaining resolved emission becomes collinear to one of the initial-state quarks. However, these singularities can be dealt with in a straightforward NLO-like manner. Indeed, for the soft-gluon emission we insert the partition of unity $I = (I-C_{\gamma 1}-C_{\gamma 2}) + C_{\gamma 1} + C_{\gamma 2}$ and write[20]

$$\begin{aligned}
&\big\langle [\mathrm{d}k_4][\mathrm{d}k_5]\;(I-S_\gamma)\,S_g\; F_{\mathrm{LM}}\big(1_u,2_{\bar{d}},W^+;4_g,5_\gamma\big)\big\rangle \\
&= [\alpha_s](2\,E_{\max})^{-2\epsilon}\,\frac{2C_F\,\Gamma^2\,(1-\epsilon)}{\epsilon^2\,\Gamma\,(1-2\epsilon)} \times \Big\{ \big\langle \hat{O}^{\gamma}_{\mathrm{NLO}}[\mathrm{d}k_5]\; F_{\mathrm{LM}}\big(1_u,2_{\bar{d}},W^+;5_\gamma\big)\big\rangle \\
&+ \big\langle\,(I-S_\gamma)\,\big[C_{\gamma 1}+C_{\gamma 2}\big]\,[\mathrm{d}k_5]\; F_{\mathrm{LM}}\big(1_u,2_{\bar{d}},W^+;5_\gamma\big)\big\rangle\Big\}.
\end{aligned} \tag{4.22}$$

In Eq. (4.22), the first term on the r. h. s. denotes the fully-regulated contribution with a resolved photon, proportional to

$$\hat{O}^{\gamma}_{\mathrm{NLO}} = (I-S_\gamma)\;(I-C_{\gamma 1}-C_{\gamma 2})\;. \tag{4.23}$$

20 Again, we note that the soft-gluon eikonal function is independent of the photon momentum.

Terms in the last line of Eq. (4.22) are subtraction terms for collinear singularities caused by the photon. We focus on the term proportional to $C_{\gamma 1}$ and consider collinear and soft-collinear limits. We find

$$C_{\gamma 1}\, F_{\rm LM}(1_u, 2_{\bar d}, W^+; 5_\gamma) = \frac{e^2 Q_u^2}{E_5^2 \rho_{51}} \times (1-z)\bar{P}_{qq}(z) \frac{F_{\rm LM}(z\cdot 1_u, 2_{\bar d}, W^+)}{z}\,, \tag{4.24}$$

$$S_\gamma C_{\gamma 1}\, F_{\rm LM}(1_u, 2_{\bar d}, W^+; 5_\gamma) = \frac{e^2 Q_u^2}{E_5^2 \rho_{51}} \times 2\; F_{\rm LM}(1_u, 2_{\bar d}, W^+)\,, \tag{4.25}$$

where $E_5 = (1-z)E_1$ and

$$\bar{P}_{qq}(z) = \left[\frac{1+z^2}{1-z} - \epsilon(1-z)\right]\,, \tag{4.26}$$

is the conventional splitting function given in Eq. (2.55) without color factor C_F. We integrate over angle ρ_{51} and obtain

$$\begin{aligned}
&\left\langle (I-S_\gamma)\, C_{\gamma 1}[dk_5]\; F_{\rm LM}(1_u, 2_{\bar d}, W^+; 5_\gamma)\right\rangle \\
&= -\frac{[\alpha]\,\Gamma^2(1-\epsilon)}{\epsilon\,\Gamma(1-2\epsilon)} Q_u^2 (2E_1)^{-2\epsilon}\left[\int_0^1 {\rm d}z\, \frac{\bar{P}_{qq}(z)}{(1-z)^{2\epsilon}} \left\langle \frac{F_{\rm LM}(z\cdot 1_u, 2_{\bar d}, W^+)}{z}\right\rangle \right.\\
&\qquad \left. -2\int_{z_{\rm min}}^1 {\rm d}z (1-z)^{-1-2\epsilon} \left\langle F_{\rm LM}(1_u, 2_{\bar d}, W^+)\right\rangle\right] \\
&= -\frac{[\alpha]\,\Gamma^2(1-\epsilon)}{\epsilon\,\Gamma(1-2\epsilon)} Q_u^2 (2E_1)^{-2\epsilon}\int_0^1 {\rm d}z \left[\frac{\bar{P}_{qq}(z)}{(1-z)^{2\epsilon}} + \frac{1}{\epsilon}\delta(1-z) e^{-2\epsilon L_1}\right] \\
&\qquad \times \left\langle \frac{F_{\rm LM}(z\cdot 1_u, 2_{\bar d}, W^+)}{z}\right\rangle\,,
\end{aligned} \tag{4.27}$$

where $L_i = E_{\rm max}/E_i$. The term proportional to $C_{\gamma 2}$ in Eq. (4.22) can be computed in a similar way; we obtain

$$\begin{aligned}
&\left\langle [dk_4][dk_5]\; (I-S_\gamma)\, S_g\; F_{\rm LM}(1_u, 2_{\bar d}, W^+; 4_g, 5_\gamma)\right\rangle \\
&= [\alpha_s](2\,E_{\rm max})^{-2\epsilon}\, \frac{2C_F\,\Gamma^2(1-\epsilon)}{\epsilon^2\,\Gamma(1-2\epsilon)} \left\{ \left\langle \hat{O}^{\gamma}_{\rm NLO}[dk_5]\; F_{\rm LM}(1_u, 2_{\bar d}, W^+; 5_\gamma)\right\rangle \right.\\
&\quad - \frac{[\alpha]\,\Gamma^2(1-\epsilon)}{\epsilon\,\Gamma(1-2\epsilon)} \int_0^1 {\rm d}z \left[Q_u^2\, P_{qq}^{\rm NLO}(z, L_1)\, (2E_1)^{-2\epsilon} \left\langle \frac{F_{\rm LM}(z\cdot 1_u, 2_{\bar d})}{z}\right\rangle \right.\\
&\quad \left.\left. + Q_d^2\, P_{qq}^{\rm NLO}(z, L_2)\, (2E_2)^{-2\epsilon} \left\langle \frac{F_{\rm LM}(1_u, z\cdot 2_{\bar d})}{z}\right\rangle \right]\right\}\,,
\end{aligned} \tag{4.28}$$

for the whole expression Eq. (4.22). We note that in Eq. (4.28) we have used $J_\gamma(1,2,W)$ as given in Eq. (3.11) and that we abbreviated

$$P_{qq}^{\rm NLO}(z, L) = (1-z)^{-2\epsilon}\left[\frac{1+z^2}{1-z} - \epsilon(1-z)\right] + \frac{1}{\epsilon}\,\delta(1-z)\, e^{-2\epsilon L}\,. \tag{4.29}$$

For the soft-photon contribution to Eq. (4.20), we find

$$
\begin{aligned}
&\big\langle [\mathrm{d}k_4][\mathrm{d}k_5]\ (I-S_g)\, S_\gamma\ F_{\mathrm{LM}}\big(1_u,2_{\bar d},W^+;4_g,5_\gamma\big)\big\rangle \\
&= [\alpha](2\,E_{\max})^{-2\epsilon}\,\frac{\Gamma^2\,(1-\epsilon)}{\Gamma\,(1-2\epsilon)}\times\bigg\{\,\langle \hat{O}^{g}_{\mathrm{NLO}}[\mathrm{d}k_4] J_\gamma(1,2,W)\ F_{\mathrm{LM}}\big(1_u,2_{\bar d},W^+;4_g\big)\rangle \\
&\quad -\frac{[\alpha_s]C_F\,\Gamma^2\,(1-\epsilon)}{\epsilon\,\Gamma\,(1-2\epsilon)}\int_0^1 \mathrm{d}z\,\bigg[P^{\mathrm{NLO}}_{qq}(z,L_1)\,(2E_1)^{-2\epsilon}\,\tilde{J}_\gamma(z\cdot E_1,E_2) \\
&\quad \times\bigg\langle\frac{F_{\mathrm{LM}}(z\cdot 1_u,2_{\bar d})}{z}\bigg\rangle + P^{\mathrm{NLO}}_{qq}(z,L_2)\,(2E_2)^{-2\epsilon}\,\tilde{J}_\gamma(E_1,z\cdot E_2) \\
&\quad \times\bigg\langle\frac{F_{\mathrm{LM}}(1_u,z\cdot 2_{\bar d})}{z}\bigg\rangle\bigg]\bigg\}\,,
\end{aligned}
\tag{4.30}
$$

where

$$
\hat{O}^{g}_{\mathrm{NLO}} = (I-S_g)\ (I-C_{g1}-C_{g2})\ . \tag{4.31}
$$

We note that the collinear subtraction terms in Eq. (4.30) are more involved than in the soft-gluon case, since the soft-photon eikonal function has a residual dependence on the gluon momentum k_4. We have shown in Sec. 3.1.2 how to integrate the soft-photon eikonal function in case of a unresolved gluon. In particular, we found that $C_{g1}\,J_\gamma(1,2,W) = \tilde{J}_\gamma(z\cdot E_1,E_2)$ and $C_{g2}\,J_\gamma(1,2,W) = \tilde{J}_\gamma(E_1,z\cdot E_2)$, where $z = (E_{1,2} - E_4)/E_{1,2}$ and $\tilde{J}_\gamma(E_1,E_2)$ is given in Eq. (3.24).

In the following, we regulate remaining collinear singularities in the soft-regulated term in Eq. (4.20)

$$
\big\langle [\mathrm{d}k_4][\mathrm{d}k_5]\ (I-S_\gamma)\ (I-S_g)\ F_{\mathrm{LM}}\big(1_u,2_{\bar d},W^+;4_g,5_\gamma\big)\big\rangle\ , \tag{4.32}
$$

following the discussion in Sec. 2.3 and making use of the fact that there is no double-collinear $\boldsymbol{k}_4 \parallel \boldsymbol{k}_5$ singularity. In particular, we introduce partition functions

$$
1 = \omega^{14,25}_{\mathcal{DC}} + \omega^{24,15}_{\mathcal{DC}} + \omega^{14,15}_{\mathcal{TC}} + \omega^{24,25}_{\mathcal{TC}}\,, \tag{4.33}
$$

where we define double-collinear partitions

$$
\omega^{14,25}_{\mathcal{DC}} = \frac{\rho_{15}\rho_{24}}{4}\,,\qquad \omega^{24,15}_{\mathcal{DC}} = \frac{\rho_{14}\rho_{25}}{4}\,, \tag{4.34}
$$

and triple-collinear partitions

$$
\omega^{14,15}_{\mathcal{TC}} = \frac{\rho_{24}\rho_{25}}{4}\,,\qquad \omega^{24,25}_{\mathcal{TC}} = \frac{\rho_{14}\rho_{15}}{4}\,. \tag{4.35}
$$

Furthermore, we employ definitions of sectors as in Eq. (2.64). We then write the soft-regulated contribution in Eq. (4.32) as[21]

$$
\begin{aligned}
&\big\langle [\mathrm{d}k_4][\mathrm{d}k_5]\ (I-S_\gamma)\ (I-S_g)\ F_{\mathrm{LM}}\big(1_u,2_{\bar d},W^+;4_g,5_\gamma\big)\big\rangle \\
&= \sum_{n=1}^{4}\Big\langle \Xi^{q\bar q}_n[\mathrm{d}k_4][\mathrm{d}k_5]\ (I-S_\gamma)\ (I-S_g)\ F_{\mathrm{LM}}\big(1_u,2_{\bar d},W^+;4_g,5_\gamma\big)\Big\rangle\,,
\end{aligned}
\tag{4.36}
$$

21 We recall that double-collinear operators C_{ij} act on the phase space $[\mathrm{d}k_4][\mathrm{d}k_5]$, whereas triple-collinear operators $\mathbb{C}_i$ do not.

where operators $\Xi_n^{q\bar{q}}$ read[22]

$$\Xi_1^{q\bar{q}} = \sum_{\substack{i,j=1,2\\ i\neq j}} (I - C_{4i})\ (I - C_{5j})\ \omega_{\mathcal{DC}}^{i4,j5} + \sum_{i=1,2}\sum_{k=A,B} \left(I - C^k\right)\ (I - \mathbb{C}_i)\ \omega_{\mathcal{TC}}^{i4,i5}\,, \tag{4.37}$$

$$\Xi_2^{q\bar{q}} = \sum_{i=1,2}\sum_{k=A,B} \left(I - C^k\right)\ \mathbb{C}_i\,, \tag{4.38}$$

$$\Xi_3^{q\bar{q}} = -\sum_{\substack{i,j=1,2\\ i\neq j}} C_{4i} C_{5j}\,, \tag{4.39}$$

$$\Xi_4^{q\bar{q}} = \sum_{\substack{i,j=1,2\\ i\neq j}} \left[C_{4i} + C_{5j}\right]\ \omega_{\mathcal{DC}}^{i4,j5} + \sum_{i=1,2}\sum_{k=A,B} \theta^k C^k\ \omega_{\mathcal{TC}}^{i4,i5}\,. \tag{4.40}$$

We note that the term proportional to operator $(I - S_\gamma)\ \left(I - S_g\right)\ \Xi_1^{q\bar{q}}$ in Eq. (4.36) describes the fully-regulated contribution, which is computed numerically in $d = 4$ dimensions. The operator $\Xi_2^{q\bar{q}}$ in Eq. (4.38) describes the triple-collinear contribution. We find

$$\begin{aligned}
&\left\langle \left(I - S_g\right)\ (I - S_\gamma)\ \Xi_2^{q\bar{q}}\ F_{\mathrm{LM}}(1_u, 2_{\bar{d}}, W, 4_g, 5_\gamma;) \right\rangle \\
&= -2[\alpha][\alpha_s] C_F \int_0^1 \mathrm{d}z\, P_{qq}^{\mathrm{trc}}(z) \left[Q_u^2 (2E_1)^{-4\epsilon} \left\langle \frac{F_{\mathrm{LM}}(z\cdot 1_u, 2_{\bar{d}}, W^+)}{z} \right\rangle \right. \\
&\quad \left. + Q_{\bar{d}}^2 (2E_2)^{-4\epsilon} \left\langle \frac{F_{\mathrm{LM}}(1_u, z\cdot 2_{\bar{d}}, W^+)}{z} \right\rangle \right].
\end{aligned} \tag{4.41}$$

We compute the the strongly-ordered and the genuine contributions to the triple-collinear subtraction term in Eq. (4.41) following the discussion in Sec. 3.1.3 and Sec. 3.2.3, respectively. We note that in contrast to the triple-collinear subtraction terms obtained in the context of NNLO QCD computations [5], we have to take the abelian limit $C_A \to 0$ and consider *modified* sectors $k = A, B$. We obtain

$$\begin{aligned}
P_{qq}^{\mathrm{trc}}(z) = \frac{1}{\epsilon}&\left[\frac{3}{2}(1-z) + z\ln(z) + \frac{3+z^2}{4(1-z)}\ln^2(z)\right] \\
&+ \left(\frac{11}{2} - 6\ln(1-z)\right)(1-z) - \frac{2\pi^2 z}{3} - \frac{z}{2}\ln^2(z) \\
&- \frac{(19+9z^2)}{12(1-z)}\ln^3(z) + 4z\,\mathrm{Li}_2(z) \\
&- \left(z + \frac{\pi^2(5+3z^2)}{3(1-z)} + \frac{2(1+z^2)}{1-z}\mathrm{Li}_2(z)\right)\ln(z) \\
&+ \frac{2(5+3z^2)}{1-z}\left(\mathrm{Li}_3(z) - \zeta_3\right)\,.
\end{aligned} \tag{4.42}$$

22 We note that we can neglect partition functions $\omega_{\mathcal{DC}/\mathcal{TC}}^{ij,kl}$ in double-unresolved contributions $n = 2, 3$, since they become unity in these limits.

The remaining contributions $\Xi_{3,4}^{q\bar{q}}$ describe NLO-like unresolved collinear subtraction terms. In particular, $\Xi_3^{q\bar{q}}$ in Eq. (4.39) describes the double-unresolved contribution that originates from the double-collinear partitions, where both the gluon and the photon are collinear to different initial-state quarks. Operator $\Xi_4^{q\bar{q}}$ in Eq. (4.40) describes all contributions in which either the gluon or the photon is collinear. The computation of these integrated subtraction terms is NLO-like and can be found in Ref. [9].

Quark-gluon and quark-photon initiated processes

In the following, we turn to the regularisation of IR singularities in the quark-gluon initiated process. In particular, we consider the double-real correction $g\bar{d} \to W^+\bar{u}\gamma$, the respective cross section reads

$$2s \cdot \mathrm{d}\sigma^{RR}_{g\bar{d}\to W\bar{u}\gamma} = \big\langle [\mathrm{d}k_4][\mathrm{d}k_5]\; F_{LM}\big(1_g, 2_{\bar{d}}, W^+; 4_{\bar{u}}, 5_\gamma\big)\big\rangle\;. \tag{4.43}$$

We begin with the regularisation of the soft singularity caused by the photon and write

$$\begin{aligned}&\big\langle [\mathrm{d}k_4][\mathrm{d}k_5]\; F_{LM}\big(1_g, 2_{\bar{d}}, W^+; 4_{\bar{u}}, 5_\gamma\big)\big\rangle\\ =\;& \big\langle [\mathrm{d}k_4][\mathrm{d}k_5] S_\gamma\; F_{LM}\big(1_g, 2_{\bar{d}}, W^+; 4_{\bar{u}}, 5_\gamma\big)\big\rangle\\ &+ \big\langle [\mathrm{d}k_4][\mathrm{d}k_5]\; (I - S_\gamma)\; F_{LM}\big(1_g, 2_{\bar{d}}, W^+; 4_{\bar{u}}, 5_\gamma\big)\big\rangle\;.\end{aligned} \tag{4.44}$$

The single-soft contribution can be obtained following the same steps as in the case of $g\gamma$-emission. We arrive at

$$\begin{aligned}&\big\langle [\mathrm{d}k_4][\mathrm{d}k_5] S_\gamma\; F_{LM}\big(1_g, 2_{\bar{d}}, W^+; 4_{\bar{u}}, 5_\gamma\big)\big\rangle\\ =&[\alpha](2\,E_{\max})^{-2\epsilon}\frac{\Gamma^2(1-\epsilon)}{\Gamma(1-2\epsilon)}\bigg\{ \big\langle \hat{O}^{\bar{u}}_{\mathrm{NLO}} J_\gamma(2,4,W)[\mathrm{d}k_4]\; F_{LM}\big(1_g, 2_{\bar{d}}, W^+; 4_{\bar{u}},\big)\big\rangle\\ &-\frac{[\alpha_s]T_R\,\Gamma^2(1-\epsilon)\,(2E_1)^{-2\epsilon}}{\epsilon\,\Gamma(1-2\epsilon)}\int_0^1 \mathrm{d}z\; P^{\mathrm{NLO}}_{qg}(z)\,\tilde{J}_\gamma(z\cdot E_1, E_2)\left\langle \frac{F_{LM}(z\cdot 1_u, 2_{\bar{d}})}{z}\right\rangle\bigg\}\,,\end{aligned} \tag{4.45}$$

where $\hat{O}^{\bar{u}}_{\mathrm{NLO}} = (I - C_{51})$, the splitting function $P^{\mathrm{NLO}}_{qg}(z)$ can be found in Eq. (D.43) and $J_\gamma(2,4,W)$ is given in Eq. (D.41).

We now analyse collinear singularities of the soft-regulated contribution proportional to $\langle [\mathrm{d}k_4][\mathrm{d}k_5]\; (I - S_\gamma)\; F_{LM}(1_g, 2_{\bar{d}}, W^+; 4_{\bar{u}}, 5_\gamma)\rangle$ in Eq. (4.44). Double-collinear divergences can arise when the final-state quark $\bar{u}(k_4)$ becomes collinear to the gluon, and when the final state photon $\gamma(k_5)$ becomes collinear either to $\bar{u}(k_4)$ or to $\bar{d}(p_2)$. A triple collinear singularity arises in the limit $\boldsymbol{k}_4 \parallel \boldsymbol{k}_5 \parallel \boldsymbol{p}_1$. We follow the same steps as in the case of $g\gamma$-emission and write

$$\begin{aligned}&\big\langle [\mathrm{d}k_4][\mathrm{d}k_5]\; (I - S_\gamma)\; F_{LM}\big(1_g, 2_{\bar{d}}, W^+; 4_{\bar{u}}, 5_\gamma\big)\big\rangle\\ =& \sum_{n=1}^{4} \big\langle \Xi^{gq}_n [\mathrm{d}k_4][\mathrm{d}k_5]\; (I - S_\gamma)\; F_{LM}\big(1_g, 2_{\bar{d}}, W^+; 4_{\bar{u}}, 5_\gamma\big)\big\rangle\;,\end{aligned} \tag{4.46}$$

where[23]

$$\Xi_1^{gq} = (I - C_{41})\,(I - C_{52})\,\omega_{\mathcal{DC}}^{25} + \sum_{k=a,b,c,d} \left(I - C^k\right)\,(I - \mathbb{C}_1)\,\omega_{\mathcal{TC}}^{45}\,, \tag{4.47}$$

$$\Xi_2^{gq} = \sum_{k=a,b,c,d} \left(I - C^k\right)\,\mathbb{C}_1\,, \tag{4.48}$$

$$\Xi_3^{gq} = -C_{41}C_{52}\,, \tag{4.49}$$

$$\Xi_4^{gq} = [C_{41} + C_{52}]\,\omega_{\mathcal{DC}}^{25} + \sum_{k=a,b,c,d} \theta^k C^k\,\omega_{\mathcal{TC}}^{45}\,, \tag{4.50}$$

and

$$\omega_{\mathcal{DC}}^{25} = \frac{\rho_{45}}{\rho_{24} + \rho_{45}}\,, \qquad \omega_{\mathcal{TC}}^{45} = \frac{\rho_{24}}{\rho_{24} + \rho_{45}}\,. \tag{4.51}$$

We note that due to the presence of the $\boldsymbol{k}_4 \parallel \boldsymbol{k}_5$ singularity, we have used the four sectors $k = a..d$ that appear in NNLO QCD computations, cf. Eq. (2.58), to disentangle strongly-ordered limits in the triple-collinear contribution. Although, strictly speaking, sector $k = a$ is redundant, since there is no singularity when initial-state gluon and final-state photon become collinear in the limit $\boldsymbol{k}_5 \parallel \boldsymbol{k}_1$, we include $k = a$ in Eqs. (4.47)-(4.50) but note that $C^a\, F_{\rm LM}\left(1_g, 2_{\bar{d}}, W^+; 4_{\bar{u}}, 5_\gamma\right) = 0$.

The operators $\Xi_{1,\ldots,4}^{gq}$ in Eqs. (4.47)-(4.50) are defined similarly to those in case of $g\gamma$ emission, given in Eqs. (4.37)-(4.40). Contribution $(I - S_\gamma)\,\Xi_1^{gq}$ in Eq. (4.46) is fully regulated, we compute it numerically in $d = 4$ dimensions. We note that the triple-collinear contribution Ξ_2^{gq} in Eq. (4.48) is obtained by abelianising the NNLO QCD result for the splitting $g \to qgq^*$ computed in Ref. [5].[24] The remaining contributions Ξ_3^{gq} and Ξ_4^{gq} in Eq. (4.49) and Eq. (4.50) involve double-unresolved double-collinear limits, as well as single-unresolved collinear subtraction terms. A discussion of these NLO-like contributions can be found in Ref. [9].

Finally, we note that the contribution of the quark-photon initiated partonic channel $\gamma\bar{d} \to W^+\bar{u}g$ can be computed along the lines discussed above. It turns out that results for this channel can be found by a straightforward abelianisation of the contribution of the process $g\bar{d} \to W^+\bar{u}\gamma$, where additionally, one has to set Q_W to zero.

Gluon-photon initiated processes

The last remaining double-real contribution refers to the partonic process $g\gamma \to W^+\bar{u}d$. We write the differential cross section in the standard way

$$2s \cdot \mathrm{d}\sigma_{g\gamma \to W\bar{u}d}^{RR} = \left\langle [\mathrm{d}k_4][\mathrm{d}k_5]\; F_{\rm LM}\left(1_g, 2_\gamma, W^+; 4_{\bar{u}}, 5_d\right)\right\rangle\,. \tag{4.52}$$

---

23 As before, partition functions $\omega_{\mathcal{DC}/\mathcal{TC}}^{ij}$ in double-unresolved contributions Ξ_2^{gq} and Ξ_3^{gq} are equal to one.
24 See also Table 2.2.

This contribution has no soft or triple-collinear singularities, it only exhibits double-collinear singularities when the final-state (anti-)quark becomes collinear to either the photon or the gluon in the initial state. These collinear divergences are not entangled; for example when $\bar{u}(k_4)$ becomes collinear to $g(p_1)$, the remaining quark $d(k_5)$ can only become collinear to $\gamma(p_2)$. Hence, there is no need to split the phase space with partition functions or sectors. We write

$$\begin{aligned} &\left\langle [dk_4][dk_5]\, F_{LM}(1_g, 2_\gamma, W^+; 4_{\bar{u}}, 5_d)\right\rangle \\ &= \left\langle \hat{O}^{g\gamma}_{\rm NNLO}[dk_4][dk_5]\, F_{LM}(1_g, 2_\gamma, W^+; 4_{\bar{u}}, 5_d)\right\rangle \\ &+ \left\langle [C_{41}+C_{42}+C_{51}+C_{52}]\,[dk_4][dk_5]\, F_{LM}(1_g, 2_\gamma, W^+; 4_{\bar{u}}, 5_d)\right\rangle \\ &- \left\langle [C_{41}C_{52}+C_{42}C_{51}]\,[dk_4][dk_5]\, F_{LM}(1_g, 2_\gamma, W^+; 4_{\bar{u}}, 5_d)\right\rangle\,, \end{aligned} \tag{4.53}$$

where the fully-regulated contribution is proportional to

$$\hat{O}^{g\gamma}_{\rm NNLO} = I - C_{41} - C_{42} - C_{51} - C_{52} + C_{41}C_{52} + C_{42}C_{51}\,. \tag{4.54}$$

We note that all single- and double-unresolved subtraction terms in Eq. (4.53) are NLO-like and can be obtained by abelianising the NNLO QCD calculations for the gg-channel in Refs. [1, 2]. Results can be found in Ref. [9].

4.2.3 *Summary*

To obtain complete a description of mixed QCD-EW corrections to W-boson production, we have to combine different building blocks discussed in Sec. 4.2.1. To this end, we implemented all one- and two-loop finite remainders, contributions from the renormalization of PDFs, as well as double-real matrix elements, presented in Appendix D.2, and finite remainders of the integrated subtraction terms that we discussed in Sec. 4.2.2, in a `Fortran` computer code [9]. This code can be used to compute mixed QCD-EW corrections to arbitrary IR safe observables in the process $pp \to W^\pm + X$.

Our results pass several checks. First, we note that we achieve an analytic cancellation of all IR poles. Second, the double-real matrix elements squared presented in Appendix D.2 have been checked to be regularised by the formulas in Sec. 4.2.2. Third, the same matrix elements have been used to compute the cross section of the process $pp \to W + \gamma + \text{jet}$, which then was compared to `MADGRAPH` [252] results for different partonic channels. Fourth, we have considered the limit of equal up- and down quark charges $Q_u = Q_d \Leftrightarrow Q_W = 0$ in several unresolved contributions and compared results with the results for Z-boson production in Ref. [8]. This approach is particularly useful to check modified partition functions and phase-space sectors described in the previous section.

In the next Chapter, we will study phenomenological impact of mixed QCD-EW corrections to Z- and W-boson hadroproduction. In particular, we will assess the impact of these corrections on the extraction of the W-boson mass at the LHC.

5 NUMERICAL RESULTS FOR ON-SHELL VECTOR BOSON PRODUCTION

In this Chapter, we discuss numerical results for the production of on-shell Z- and W bosons at the LHC focusing on NNLO QCD-EW corrections. We present inclusive cross sections and kinematic distributions of a few selected observables in Sec. 5.1. The main focus of this Chapter, however, is to study how mixed corrections affect lepton transverse-momenta distributions in Z and W production that are used to determine the W-boson mass at the LHC. In Sec. 5.2, we describe a simple but transparent model, which allows us to investigate this question.

5.1 INCLUSIVE CROSS-SECTIONS AND KINEMATIC DISTRIBUTIONS

In this section, we present numerical results for Z- and W-boson production at the LHC. Originally, these results have been presented in Refs. [7–9]. We begin by describing the numerical setup of our calculations.

5.1.1 *The setup*

The computational setup for both cases is as follows. We consider the LHC with a center-of-mass collision energy of 13 TeV. The strong coupling constant is renormalized in the $\overline{\text{MS}}$ scheme; for electroweak corrections we employ the G_μ input-parameter and on-shell renormalization schemes. We set $\mu_F = \mu_R \equiv \mu$ in all numerical computations. We use

$$\begin{aligned} &G_F = 1.16639 \times 10^{-5}\ \text{GeV}^{-2} \quad M_Z = 91.1876\ \text{GeV}\,, \quad M_W = 80.398\ \text{GeV}\,, \\ &\quad M_t = 173.2\ \text{GeV}\,, \quad M_H = 125\ \text{GeV}\,, \end{aligned} \tag{5.1}$$

as input parameters in the G_μ scheme, from which we derive the weak mixing angle

$$\sin^2\theta_W = 1 - \frac{M_W^2}{M_Z^2} \approx 0.222646\,, \tag{5.2}$$

and the fine-structure constant

$$\alpha = \frac{\sqrt{2}G_F M_W^2}{\pi}\left(1 - \frac{M_W^2}{M_Z^2}\right) \approx 1/132.338\,. \tag{5.3}$$

We note that the G_μ input scheme is particularly suited for describing processes involving W and Z bosons, since it re-absorbs contributions to the on-shell renormalization of the weak mixing angle [253], resulting in numerically small EW corrections.

We use the NNLO NNPDF3.1luxQED [254–256] PDFs with five active flavors for *all* numerical computations. The value of the strong coupling constant, as provided by this PDF set, is $\alpha_s(M_Z) = 0.118$.

As we discussed in Chapter 4, we compute corrections to Z- and W-boson production in the narrow-width approximation, where the square of the propagator of an intermediate vector boson is replaced by a δ-function

$$\frac{1}{(Q^2 - M_V^2)^2 + M_V^2 \Gamma_V^2} \to \frac{\pi}{M_V \Gamma_V} \delta(Q^2 - M_V^2)\,. \tag{5.4}$$

We then incorporate perturbative corrections to the width of the vector boson Γ_V, by writing the hadronic cross section, cf. Eq. (1.1), as follows

$$\mathrm{d}\sigma_{pp\to V\to\ell\bar{\ell}(\ell\bar{\nu})} = \frac{\mathrm{d}\sigma_{pp\to V}\,\mathrm{d}\Gamma_{V\to\ell\bar{\ell}(\ell\bar{\nu})}}{\Gamma_V} = \mathrm{Br}_{V\to\ell\bar{\ell}(\ell\bar{\nu})} \times \mathrm{d}\sigma_{pp\to V} \times \frac{\mathrm{d}\Gamma_{V\to\ell\bar{\ell}(\ell\bar{\nu})}}{\Gamma_{V\to\ell\bar{\ell}(\ell\bar{\nu})}}\,. \tag{5.5}$$

We treat branching fractions $\mathrm{Br}_{V\to\ell\bar{\ell}(\ell\bar{\nu})}$ as experimental input parameters[1] and expand all other quantities in α_s and α.

Since we work with massless leptons, we need to define an IR-safe observable by combining collinear leptons and photons into lepton "jets", similar to QCD jets. To this end, we choose a simplified version of the standard recipe [257] and define $R_{\ell\gamma} = \sqrt{(y_\ell - y_\gamma)^2 + (\varphi_\ell - \varphi_\gamma)^2}$ where $y_{\ell,\gamma}$ and $\varphi_{\ell,\gamma}$ are the rapidities and azimuthal angles of leptons and photons, respectively. We choose to recombine particles for which $R_{\ell\gamma} < R_{\min} = 0.1$ [257].

We find it convenient to normalize results relative to cross sections computed through NLO QCD. Hence, we define relative corrections for inclusive cross sections and on a differential bin-by-bin level as

$$\Delta^i = \frac{\sigma^i}{\sigma^{\mathrm{LO}} + \sigma^{\mathrm{QCD}}_{\mathrm{NLO}}}\,, \quad \mathrm{d}\Delta^i = \frac{\mathrm{d}\sigma^i}{\mathrm{d}\sigma^{\mathrm{LO}} + \mathrm{d}\sigma^{\mathrm{QCD}}_{\mathrm{NLO}}}\,, \tag{5.6}$$

where σ^i denotes the different contributions that appear on the r. h. s. of the following equation

$$\sigma = \sigma_{\mathrm{LO}} + \sigma^{\mathrm{QCD}}_{\mathrm{NLO}} + \sigma^{\mathrm{EW}}_{\mathrm{NLO}} + \sigma^{\mathrm{QCD\text{-}QCD}}_{\mathrm{NNLO}} + \sigma^{\mathrm{QCD\text{-}EW}}_{\mathrm{NNLO}} + \mathcal{O}\left(\alpha_s^3, \alpha^3\right)\,. \tag{5.7}$$

We note that in case of Z-boson production, we split EW corrections into QED and *weak* corrections. In what follows, we present numerical results for Z- and W-boson production separately.

1 In particular, we do *not* consider perturbative corrections to branching fractions.

5.1.2 *Z-boson production*

QED corrections

We begin with the discussion of QED corrections to Z-boson production at the LHC. We use the numerical setup descibed in Sec. 5.1.1 and choose $\mu = M_Z$. We obtain the following results for inclusive cross sections

$$\Delta_{\text{NLO}}^{\text{QED}} = 3.2 \cdot 10^{-3}\,, \qquad \Delta_{\text{NNLO}}^{\text{QCD-QCD}} = -6.4 \cdot 10^{-3}\,, \qquad \sigma_{\text{NNLO}}^{\text{QCD-QED}} = 2.9 \cdot 10^{-4}\,. \quad (5.8)$$

We note that the inclusive cross sections in Eq. (5.8) only describe corrections to the production stage of the process, $pp \to Z$. As can be seen form Eq. (5.5), corrections to the *decay* stage of the process cancel in inclusive cross sections since the factor $\mathrm{d}\Gamma_{Z\to\ell\bar{\ell}}/\Gamma_{Z\to\ell\bar{\ell}}$ always integrates to one. The results in Eq. (5.8) follow the expected hierarchy based on the relative magnitude of strong and electroweak coupling constants. In particular, QCD-QED corrections are factors of ten and twenty smaller than QED and NNLO QCD corrections, respectively.

We note that the results presented here differ from the ones obtained in Ref. [38], where QCD-QED corrections were found to only be a factor ~ 3.5 smaller than NNLO QCD ones. However, this difference is due to a different setup, since the authors of Ref. [38] used only four active flavors u, d, c, and s as initial-state quarks. We note that we confirm their results if we use the same input and that the strong sensitivity to input parameters is a peculiar consequence of a large cancellation between $q\bar{q}$- and qg-initiated channels.

In order to study fiducial cross section, we employ the following set of standard kinematic selection conditions

$$p_{\ell_1}^{\perp} > 24\ \text{GeV}\,, \quad p_{\ell_2}^{\perp} > 16\ \text{GeV}\,, \quad |y_{\ell_i}| < 2.4\,, \quad 50\ \text{GeV} < m_{\ell\bar{\ell}} < 120\ \text{GeV}\,, \qquad (5.9)$$

where $p_{\ell_{1(2)}}^{\perp}$ denotes the transverse momentum of the harder (softer) lepton *jet* and $m_{\ell\bar{\ell}}$ is the invariant mass of the lepton system.

Furthermore, we split QED corrections to the cross section in Eq. (5.5) into three categories: corrections to the production $\mathrm{d}\sigma_{pp\to Z}$ (P), corrections to the decay $\mathrm{d}\Gamma_{Z\to\ell\bar{\ell}}$ (D), and corrections to the leptonic width $\Gamma_{Z\to\ell\bar{\ell}}$ (W). We find

$$\begin{aligned}
\Delta_{\text{NLO}}^{\text{QED}} &= (3.0 \cdot 10^{-3})_P - (7.2 \cdot 10^{-3})_D - (1.6 \cdot 10^{-3})_W\,, \\
\Delta_{\text{NNLO}}^{\text{QCD-QCD}} &= -\,(1.2 \cdot 10^{-2})_{P\otimes P}\,, \\
\Delta_{\text{NNLO}}^{\text{QCD-QED}} &= -\,(1.5 \cdot 10^{-4})_{P\otimes P} - (4.9 \cdot 10^{-3})_{P\otimes D} - (0.3 \cdot 10^{-3})_{P\otimes W}\,.
\end{aligned} \qquad (5.10)$$

We note that, as in the inclusive case, fiducial corrections to the production stage in Eq. (5.10) are consistent with expectations based on relative sizes of couplings. Compared to the inclusive case, shown in Eq. (5.8), NNLO QCD corrections to fiducial cross sections are a factor of two *larger*, while QCD-QED corrections are a factor of two *smaller*.

channel	$\Delta^{\text{QCD-QED}}_{\text{NNLO}}\big\|_{P\otimes P} \cdot 10^4$
$q\bar{q}$	5.60
qq	0.13
$qg + gq$	-7.01
$q\gamma + \gamma q$	-0.32
γg	0.06
total	-1.54

Table 5.1: QCD-QED initial-initial contributions $\Delta^{\text{QCD-QED}}_{\text{NNLO}}\big|_{P\otimes P}$, see Eq. (5.10), split into different partonic channels.

To understand the reason behind that, it is interesting to split mixed QCD-QED corrections to the production stage $pp \to Z$ into the different partonic channels, see Table 5.1. The results there show almost an order of magnitude cancellation between $q\bar{q}$- and qg-initiated contributions.[2] Another interesting observation from Table 5.1 is, that despite the fact that photon-induced channels are rather small, they contribute significantly to the total result because of this cancellation. Interestingly, the contribution of photon-induced channels is larger than that of the qq-initiated process. We conclude that these exotic channels cannot be neglected when mixed corrections are computed.

Electroweak corrections

We now turn to the discussion of QCD-EW corrections to Z-boson production. We employ the numerical setup described in Sec. 5.1.1, set $\mu = M_Z/2$ and obtain results for (NNLO) QCD, EW and QCD-EW corrections given in Table 5.2. We note that the second column in Table 5.2 shows inclusive results, the third column shows results where we imposed the fiducial cuts displayed in Eq. (5.9), and the forth column shows fiducial results where only corrections to the production stage $pp \to Z$ are considered.

We begin with the discussion of inclusive results, where we observe that NLO-*weak* corrections in fact exceed NLO-QED ones, and that there is a cancellation between the two, resulting in mixed QCD-EW corrections at the level of one per mille.

We also note that the NNLO QCD corrections in this case are a factor of two larger and have changed sign w.r.t. those shown in Eq. (5.8), which can be traced back to the different scale choice and further underlines the sensitivity of these corrections to chosen input parameters. In fact, scale uncertainties in the theoretical description of Z-boson production are dominated by NNLO QCD corrections, while QCD-EW corrections play a negligible role. However, scale uncertainties reduce substantially once N3LO QCD corrections are considered [211].

2 We note that a similar cancellation affects NNLO QCD corrections.

We now turn to the fiducial cross sections, shown in the third column in Table 5.2, which we compute applying the cuts in Eq. (5.9). Similarly to what we observed for QED corrections in the previous section, we find that NNLO QCD corrections change rather strongly w. r. t. inclusive results. They become a factor of two smaller due to an increased cancellation of $q\bar{q}$ and qg channels for the scale choice $\mu = M_Z/2$. We also observe that (QCD-)QED corrections are strongly affected by the kinematic constraints and even flip sign. In total, fiducial QCD-EW corrections may even exceed NNLO QCD ones.

If we consider fiducial corrections to the production stage $pp \to Z$, we obtain the results shown in the fourth column in Table 5.2. Apart from the relative sizes of NLO EW and mixed QCD-EW corrections, numerical results are consistent with expectations based on the relative magnitude of coupling constants.

correction	inclusive	fiducial	fiducial (production)
$\Delta_{\text{NLO}}^{\text{QED}}$	$+2.3 \times 10^{-3}$	-5.3×10^{-3}	$+2.2 \times 10^{-3}$
$\Delta_{\text{NLO}}^{\text{weak}}$	-5.5×10^{-3}	-5.0×10^{-3}	-5.0×10^{-3}
$\Delta_{\text{NLO}}^{\text{EW}}$	-3.2×10^{-3}	-1.0×10^{-2}	-2.8×10^{-3}
$\Delta_{\text{NNLO}}^{\text{QCD-QCD}}$	$+1.3 \times 10^{-2}$	$+5.8 \times 10^{-3}$	$+5.8 \times 10^{-3}$
$\Delta_{\text{NNLO}}^{\text{QCD-QED}}$	$+5.5 \times 10^{-4}$	-5.9×10^{-3}	$+1.4 \times 10^{-4}$
$\Delta_{\text{NNLO}}^{\text{QCD-weak}}$	-1.6×10^{-3}	-2.1×10^{-3}	-2.1×10^{-3}
$\Delta_{\text{NNLO}}^{\text{QCD-EW}}$	-1.1×10^{-3}	-8.0×10^{-3}	-2.0×10^{-3}

Table 5.2: Corrections to the cross section of $pp \to Z \to \ell\bar{\ell}$.

Kinematic distributions

In the following, we turn to the presentation of kinematic distributions. In Fig. 5.1, we present QCD-weak, QCD-QED and combined QCD-EW corrections to the rapidity and transverse momentum distribution of the dilepton system in the upper and lower panes, respectively. In the left panes, we show corrections to the full process $pp \to Z \to \ell\bar{\ell}$, while right panes only include corrections to the production stage. For reference, we also show NNLO QCD corrections which we divide by a factor of 10.

We observe that, while mixed corrections are in general quite small, their relative importance w. r. t. NNLO QCD corrections depends on the observable and the kinematic region. For example, mixed corrections exceed NNLO QCD corrections for central rapidities $|y_{\ell\bar{\ell}}| < 1.2$ while the situation is the opposite at large rapidities $|y_{\ell\bar{\ell}}| > 1.2$. We note that kinematic edges at $|y_{\ell\bar{\ell}}| = 1.2$ appear because the selection criteria in Eq. (5.9) do not allow for Born-level contributions outside this region. As can be seen in Fig. 5.1, mixed corrections to the production stage of the Z boson (right plots) are smaller than initial-final ones (left plots), as expected [240], and are rather flat.

In Fig. 5.2, we present corrections to distributions of the transverse momentum of the harder lepton and the Collins-Soper angle θ^*. The angle θ^* is defined as [258]

$$\cos\theta^* = \frac{\mathrm{sgn}(p^z_{\ell\bar{\ell}})(P^+_{\ell} P^-_{\bar{\ell}} - P^-_{\ell} P^+_{\bar{\ell}})}{\sqrt{m^2_{\ell\bar{\ell}}\left(m^2_{\ell\bar{\ell}} + (p^{\perp}_{\ell\bar{\ell}})^2\right)}}\,, \tag{5.11}$$

where $P^{\pm}_i = E_i \pm p^z_i$, $m^2_{\ell\bar{\ell}} = (p_\ell + p_{\bar{\ell}})^2$ is the invariant mass of the di-lepton system, and $p^{\perp}_{\ell\bar{\ell}}$ is its transverse momentum. All quantities in Eq. (5.11) are measured in the laboratory frame. The Collins-Soper angle is used to define the forward-backward asymmetry [193]

$$A_{\mathrm{FB}} = \frac{F-B}{F+B}\,, \tag{5.12}$$

where

$$F = \int_0^1 \frac{\mathrm{d}\sigma}{\mathrm{d}\cos\theta^*}\,\mathrm{d}\cos\theta^*\,, \quad B = \int_{-1}^0 \frac{\mathrm{d}\sigma}{\mathrm{d}\cos\theta^*}\,\mathrm{d}\cos\theta^*\,. \tag{5.13}$$

The definition of θ^* in Eq. (5.11) minimizes the impact of QCD corrections to A_{FB} and, for vanishing transverse momentum $p^{\perp}_{\ell,\bar{\ell}} = 0$, coincides with the angle between the lepton and the incoming proton in the di-lepton rest-frame [259].

We observe in the left panes in Fig. 5.2 that mixed corrections to production and decay are sizable for these observables and may play a dominant role depending on the kinematic region. Mixed corrections to the production stage only, on the other hand, give contributions only at the per mille level. This concludes our discussion of numerical results for Z-boson production, we turn to the case of W-boson production in the next section.

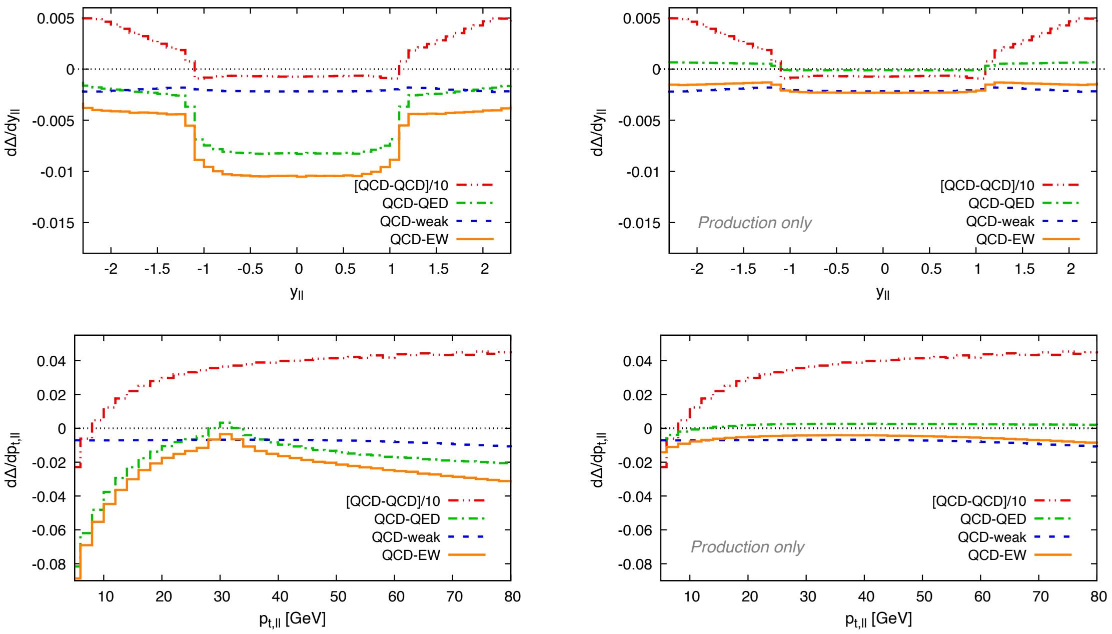

Figure 5.1: Mixed QCD-EW corrections to distributions of the dilepton rapidity and transverse momentum in Z-boson production.

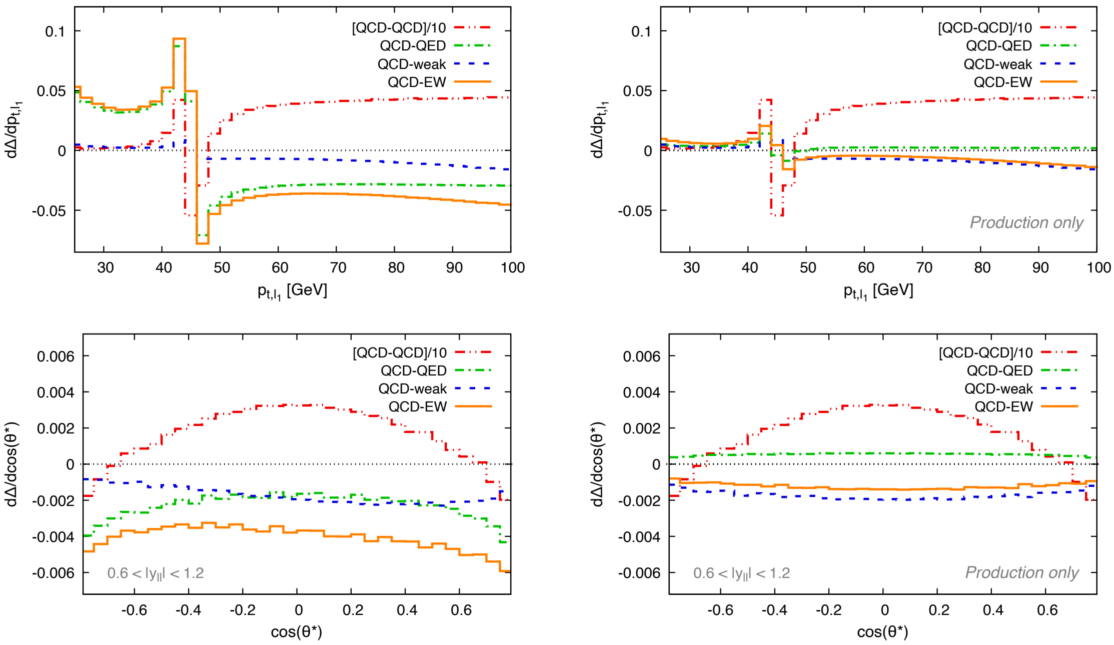

Figure 5.2: Mixed QCD-EW corrections to distributions of the transverse momentum of the harder lepton and the Collins-Soper angle in Z-boson production.

5.1.3 *W-boson production*

In the following, we briefly discuss numerical results for *initial-initial* mixed QCD-EW corrections to W^+-boson production at the LHC. In contrast to the Z-boson case, we only consider initial corrections to the production stage $pp \to W^+$. We use the numerical setup described in Sec. 5.1.1 and choose the central scale $\mu = M_W/2$. Furthermore, we apply the following kinematic constraints

$$p_{\bar{\ell}}^{\perp} > 15\text{ GeV}\,, \quad p_{\nu}^{\perp} > 15\text{ GeV}\,, \quad |y_{\ell_i}| < 2.4\,. \tag{5.14}$$

Using these cuts, we obtain corrections to the fiducial cross section for the process $pp \to W$ shown in Table 5.3. We observe that NLO EW corrections are tiny, and that mixed QCD-EW corrections actually exceed them.

We now turn to mixed corrections to differential distributions of the rapidity and the transverse momentum of the charged lepton $\bar{\ell}$, and of the transverse momentum and the transverse mass of the $\bar{\ell}\nu$ system. These distributions are shown in the upper and lower panes in Fig. 5.3, respectively.[3] For each of the four distributions, we show the size of NLO QCD corrections in the upper part of the plots. Following Eq. (5.6), we use NLO QCD corrections as a baseline, and show initial-initial QCD-EW corrections, as well as initial NLO-EW relative to them in lower panes. Again, we observe small NLO EW corrections such that mixed corrections become comparable or, as in case of the y_ℓ distribution, dominant. Furthermore, we note that both types of corrections have, in contrast to the Z-boson case, quite different shapes.

Discussion of mixed corrections to W-boson production conclude our presentation of numerical results. In summary, we have observed that mixed QCD-EW corrections are small as expected, of the order of a few per mille. However, these feeble effects may impact the very precise W-boson mass extraction at the LHC. We address this question in the next Section.

3 We note that the Jacobian peaks at $p_{\bar{\ell}}^{\perp} = M_W/2$ and $M_W^{\perp} = M_W$, mentioned in the beginning of Chapter 4, are clearly visible there.

σ[pb]	channel	$\mu = M_W$	$\mu = M_W/2$	$\mu = M_W/4$
σ_{LO}		6007.6	5195.0	4325.9
$\sigma_{\text{NLO}}^{\text{QCD}}$	$q\bar{q}'$	1455.2	1126.7	839.2
	$qg + gq$	-946.4	10.3	943.0
	total	508.8	1137.0	1782.2
$\sigma_{\text{NLO}}^{\text{EW}}$	$q\bar{q}'$	-2.2	-5.2	-6.7
	$q\gamma + \gamma q$	4.2	4.2	4.04
	total	2.1	-1.0	-2.6
$\sigma_{\text{NNLO}}^{\text{QCD-EW}}$	$q\bar{q}' + qq'$	-1.0	-1.2	-1.0
	$qg + gq$	-1.4	-1.2	-2.1
	$q\gamma + \gamma q$	0.06	0.03	-0.04
	$g\gamma + \gamma g$	-0.12	0.04	0.30
	total	-2.4	-2.3	-2.8

Table 5.3: Corrections to the fiducial cross section of $pp \to W^+ \to \bar{\ell}\nu$ with cuts defined in Eq. (5.14).

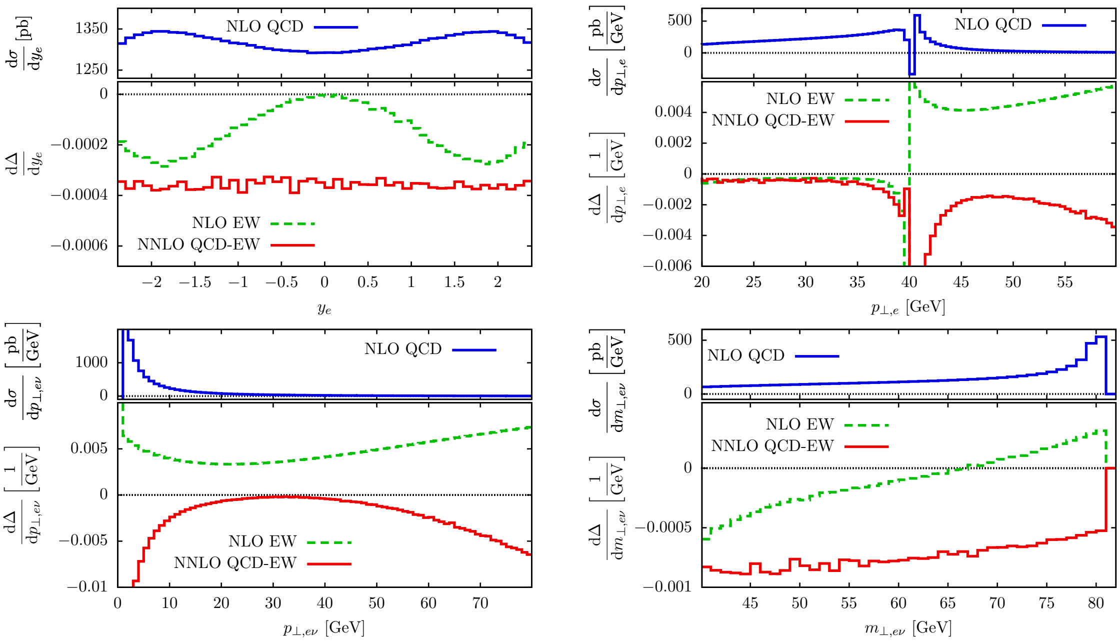

Figure 5.3: Mixed QCD-EW corrections to kinematic distributions of rapidity and transverse momentum of the charged lepton $\bar{\ell}$, as well as transverse momentum and transverse mass of the $\bar{\ell}\nu$ system in W^+-boson production.

5.2 IMPLICATIONS FOR THE W-BOSON MASS MEASUREMENT

The impact of mixed QCD-EW corrections on the W-boson mass measurement at the LHC has been studied quite extensively in the past. While the effect of initial-final contributions, which arise from NLO QCD corrections to the production and NLO EW corrections to the decay stage of the process, was studied in Ref. [241], initial-initial corrections were not available so far. Various approximations of these corrections were computed in Refs. [235, 260]. An extensive review of many theoretical approaches relevant for the W-boson mass extraction from LHC data can be found in Ref. [261].

In the following, we describe how we use the fully-differential description of mixed *initial-initial* QCD-EW corrections to Z- and W-boson production at the LHC [7–9] to estimate the impact of these contributions on the measurement of M_W from $p_\ell^\perp$ distributions [10]. As already mentioned in the beginning of Chapter 4, experimental analyses similar to that of the ATLAS collaboration in Ref. [25], extract the W-boson mass by performing *template fits* to the transverse-momentum distribution of the lepton. The correctness of the template is ensured by making use of similarities between Z- and W-boson production at the LHC and the very precisely known Z-boson mass. We incorporate the main features of this approach and construct a simple, physically transparent model that allows us to *estimate* the impact of initial-initial QCD-EW effects. We describe our setup in Sec. 5.2.1 and present results in Sec. 5.2.2.

5.2.1 *Setup*

Instead of utilizing the actual lepton transverse-momentum distribution itself, we consider its first moment, the normalized *average* transverse momentum $\left\langle p_{\ell,V}^\perp \right\rangle$. More precisely, for an observable $\mathcal{O}$, we define

$$\langle \mathcal{O} \rangle = \frac{\int \mathrm{d}\sigma_V \times \mathcal{O}}{\int \mathrm{d}\sigma_V}\,, \tag{5.15}$$

and study the quantity

$$\left\langle p_{\ell,V}^\perp \right\rangle = \frac{\int \frac{\mathrm{d}\sigma_V}{\mathrm{d}p_{\ell,V}^\perp} \times p_{\ell,V}^\perp \; \mathrm{d}p_{\ell,V}^\perp}{\int \mathrm{d}\sigma_V}\,. \tag{5.16}$$

In Eqs. (5.15)-(5.16), $\mathrm{d}\sigma_V$ denotes the fully-differential cross section of the process $pp \to V \to \ell\bar{\ell}(\bar{\ell}\nu)$, where $V = Z, W$ indicates the vector boson that decays into the lepton pair.

In order to understand how the average transverse-momentum of the lepton, given in Eq. (5.16), is correlated with the mass of the respective vector boson, we compute it at LO. At *parton* level, the normalized differential cross section for the production of an on-shell vector boson and the subsequent decay into leptons reads

$$\frac{1}{\hat{\sigma}_0}\frac{\mathrm{d}\hat{\sigma}_{f_1 f_2\to V\to \ell\bar{\ell}(\bar{\ell}\nu)}}{\mathrm{d}p^{\perp}_{\ell,V}} = \frac{6\kappa}{M_V}\frac{1-2\kappa^2}{\sqrt{1-4\kappa^2}}\,, \tag{5.17}$$

where $\kappa = p^{\perp}_{\ell,V}/M_V$ and $\hat{\sigma}_0$ denotes the inclusive partonic cross section at LO. We note that the formula in Eq. (5.17) illustrates the Jacobian peak at $p^{\perp}_{\ell,V} = M_V/2$ mentioned in the beginning of Chapter 4.

We are interested to find out how kinematic cuts $p^{\perp}_{\ell,V} > p^{\perp}_{\mathrm{cut}}$ influence the average transverse momentum. We define

$$\left\langle p^{\perp}_{\ell,V}\,\theta\left(p^{\perp}_{\ell,V} - p^{\perp}_{\mathrm{cut}}\right)\right\rangle = M_V \times f(r)\,, \quad r = \frac{p^{\perp}_{\mathrm{cut}}}{M_V}\,, \tag{5.18}$$

where the function f quantifies the dependence on the imposed transverse-momentum cut $p^{\perp}_{\mathrm{cut}}$ and $0 \le r \le 1/2$. To compute it, we need to convolute the parton-level cross section in Eq. (5.17) with PDFs and integrate over the transverse momentum of the lepton as defined in Eq. (5.16). It is straightforward to see that for the Born-level process $pp \to V \to \ell\bar{\ell}(\bar{\ell}\nu)$ the transverse momentum of the lepton does not depend on momentum fractions $x_{1,2}$, cf. Eq. (1.1). Hence the dependence on PDFs in Eq. (5.16) cancels out and a compact, analytic expression for the fraction $f^{\mathrm{LO}}(r)$ is obtained; we find

$$f^{\mathrm{LO}}(r) = \left[\frac{3r(5-8r^2)}{32(1-r^2)} + \frac{15\mathrm{ArcSin}\left(\sqrt{1-4r^2}\right)}{64(1-r^2)\sqrt{1-4r^2}}\right]\,. \tag{5.19}$$

This result fully quantifies the dependence of the normalized lepton transverse-momentum average on the cut constraint $p^{\perp}_{\mathrm{cut}}$ at the LHC at leading order in perturbation theory. We note that $f^{\mathrm{LO}}(r)$ in Eq. (5.19) is a slowly changing, monotone function, which varies between the inclusive value $f^{\mathrm{LO}}(0) = 15\pi/128 \approx 0.368$ and $f^{\mathrm{LO}}(1/2) = 0.5$.

Using the average transverse-momentum of leptons in Z- and W-boson production, we *define* the following observable for the W-boson mass [10]

$$M_W^{\mathrm{meas}} = \frac{\left\langle p^{\perp}_{\ell,W}\right\rangle^{\mathrm{meas}}}{\left\langle p^{\perp}_{\ell,Z}\right\rangle^{\mathrm{meas}}}\, M_Z\, C_{\mathrm{th}}\,, \tag{5.20}$$

where the theoretical correction factor

$$C_{\mathrm{th}} = \frac{M_W}{M_Z}\frac{\left\langle p^{\perp}_{\ell,Z}\right\rangle^{\mathrm{th}}}{\left\langle p^{\perp}_{\ell,W}\right\rangle^{\mathrm{th}}}\,, \tag{5.21}$$

accounts for calculable differences in the Z- and W-boson distributions.

We use the definitions in Eqs. (5.20)-(5.21) to estimate how a *refined* theoretical modeling of C_{th} shifts the extracted W-boson mass. To this end, we write [10]

$$\frac{\delta M_W^{\text{meas}}}{M_W^{\text{meas}}} = \frac{\delta C_{\text{th}}}{C_{\text{th}}} = \frac{\delta \left\langle p_{\ell,Z}^{\perp} \right\rangle^{\text{th}}}{\left\langle p_{\ell,Z}^{\perp} \right\rangle^{\text{th}}} - \frac{\delta \left\langle p_{\ell,W}^{\perp} \right\rangle^{\text{th}}}{\left\langle p_{\ell,W}^{\perp} \right\rangle^{\text{th}}} , \tag{5.22}$$

where δX denotes the change of quantity X due to changes in the theoretical framework. The r. h. s. of Eq. (5.22) clearly shows that shifts in the extracted W-boson mass originate from effects that affect Z- and W-boson production *differently*.

In what follows, we study how initial-initial mixed QCD-EW corrections affect the quantities in Eq. (5.22). To do so, we compare the value of C_{th} computed including mixed QCD-EW corrections, as well as initial NLO QCD and initial NLO EW corrections, against a "baseline" value for C_{th} computed *without* mixed corrections. More specifically, we write quantities in Eq. (5.22) as

$$\left\langle p_{\ell,V}^{\perp} \right\rangle^{\text{th}} = \frac{F_{\text{base}}\left(p_{\ell,V}^{\perp}, V\right)}{F_{\text{base}}(1, V)} , \tag{5.23}$$

$$\delta \left\langle p_{\ell,V}^{\perp} \right\rangle^{\text{th}} = \frac{F_{\text{mixed}}\left(p_{\ell,V}^{\perp}, V\right)}{F_{\text{mixed}}(1, V)} - \frac{F_{\text{base}}\left(p_{\ell,V}^{\perp}, V\right)}{F_{\text{base}}(1, V)} , \tag{5.24}$$

where

$$\begin{aligned} F_{\text{base}}(\mathcal{O}, V) &= F(0,0,\mathcal{O},V) + F(0,1,\mathcal{O},V) + F(1,0,\mathcal{O},V) , \\ F_{\text{mixed}}(\mathcal{O}, V) &= F_{\text{base}}(\mathcal{O},V) + F(1,1,\mathcal{O},V) , \end{aligned} \tag{5.25}$$

with

$$F(i,j,\mathcal{O},V) = \alpha_s^i \alpha^j \int \mathrm{d}\sigma_V^{i,j} \times \mathcal{O} . \tag{5.26}$$

We will also study the impact that NLO EW corrections have; to estimate it, we compare C_{th} computed including corrections through NLO EW to the baseline, where only NLO QCD corrections are considered. More specifically, in this case we define

$$\begin{aligned} \tilde{F}_{\text{base}}(\mathcal{O}, V) &= F(0,0,\mathcal{O},V) + F(1,0,\mathcal{O},V) , \\ F_{\text{NLO-EW}}(\mathcal{O}, V) &= \tilde{F}_{\text{base}}(\mathcal{O},V) + F(0,1,\mathcal{O},V) , \end{aligned} \tag{5.27}$$

and use these quantities instead of $F_{\text{base,mixed}}$ in Eqs. (5.23)-(5.24).

5.2.2 *Results*

In what follows, we use the model described in the preceding Section, as well as the numerical setup as discussed in Sec. 5.1.1, to study shifts in the extracted W-boson mass.

For definiteness, we will focus on the case of W^+-boson production. That is, we consider the processes $pp \to Z \to \ell\bar{\ell}$ and $pp \to W^+ \to \bar{\ell}\nu$, where $\ell(\bar{\ell})$ denotes the charged, massless (anti-)lepton and ν the neutrino.

INCLUSIVE LEVEL We begin by estimating shifts of the extracted W-boson mass when no kinematic cuts are applied. To estimate uncertainties, we compute all quantities in Eq. (5.22) performing a three-point scale variation $\mu = \mu_F = \mu_R = \{M_V/4, M_V/2, M_V\}$, where $V = Z, W$ as appropriate. We find that mixed corrections cause a shift

$$(\delta M_W)^{\text{mixed}} = 7 \pm 2 \text{ MeV}. \tag{5.28}$$

We repeat the same analysis to study the shift caused by NLO EW corrections using Eq. (5.27), and find $(\delta M_W)^{\text{NLO-EW}} = 1$ MeV. It follows that the impact of mixed QCD-EW corrections actually *exceeds* the impact of NLO EW on the measurement of M_W in our setup.

To appreciate that the result in Eq. (5.28) entails enormous cancellations between QCD-EW effects in Z- and W-boson production, we only consider the second term on the r. h. s. of Eq. (5.22), $\delta \left\langle p^{\perp}_{\ell,W} \right\rangle / \left\langle p^{\perp}_{\ell,W} \right\rangle$, and set $\delta \left\langle p^{\perp}_{\ell,Z} \right\rangle / \left\langle p^{\perp}_{\ell,Z} \right\rangle$ to zero. In fact, we find that both mixed QCD-EW and NLO EW corrections cause rather large shifts of the order 54 MeV and -31 MeV, respectively. We note that, since the impact of mixed QCD-EW corrections on the extracted W-boson mass is greater than the one from NLO EW corrections, we conclude that the transverse-momentum distributions for Z- and W-boson production are stronger correlated in the NLO EW case, leading to a slightly larger cancellation between the two terms in Eq. (5.22).

ATLAS CUTS Using the fully-differential setup that we described in Chapter 4, we repeat the above analysis employing cuts used in Ref. [25]. In case of W^+-boson production, we require the transverse-momentum of the lepton and the neutrino to exceed 30 GeV. Furthermore, we require a minimal transverse mass $M_W^{\perp} > 60$ GeV and a charged lepton in the central rapidity region $\left|y^{\ell}\right| < 2.4$. In case of Z-boson production, we require each of the charged leptons to be harder than 25 GeV and to have rapidities $\left|y^{\ell,\bar{\ell}}\right| < 2.4$. We obtain[4]

$$(\delta M_W)^{\text{mixed}} = -17 \pm 2 \text{ MeV}. \tag{5.29}$$

In this case, NLO EW corrections cause a shift of $\mathcal{O}(3)$ MeV.

We note that the selection criteria of Ref. [25] described above impose a *higher* $p^{\perp}_{\ell}$ cut in case of the lighter (W-)boson, which effectively gives more weight to events with higher $p^{\perp}$. In fact, if we *only* employ a cut in $p^{\perp}_{\ell}$, we can use Eqs. (5.18)-(5.19) to compute the normalized average momentum at LO. We obtain

$$f^{\text{LO}}\left(\frac{25}{91.1876}\right) \approx 0.422\,, \quad f^{\text{LO}}\left(\frac{30}{80.398}\right) \approx 0.459\,, \tag{5.30}$$

4 Again, uncertainties are estimated with a three-point variation.

for the Z- and the W-boson, respectively. This effect leads to a decorrelation of Z- and W-boson production distributions and eventually causes larger shift in the extracted value of the W-boson mass.

TUNED CUTS Since the large shift in Eq. (5.29) is caused by particularities of cuts used by the ATLAS collaboration in the analyses in Ref. [25], it is interesting to ask, whether one can *tune* these cuts leading to a stronger correlation of $p_{\ell,V}^{\perp}$ distributions in Z- and W-boson production. To this end, we keep the kinematic cuts in the case of Z-boson production as chosen by ATLAS and *lower* $p_{\ell,W}^{\perp}$ until $C_{\text{th}} = 1$ at leading order. We find that we have to choose $p_{\ell,W}^{\perp} > 25.44$ GeV instead of $p_{\ell,W}^{\perp} > 30$ GeV. For the refined cut value, we obtain a shift in the extracted W-boson mass of

$$(\delta M_W)^{\text{mixed}} = -1 \pm 5\ \text{MeV}\,, \tag{5.31}$$

where uncertainties are estimated by three-point scale variation. For the refined cut, the NLO EW correction shifts the extracted value for M_W by $\mathcal{O}(-3)$ MeV.

SUMMARY We have used the average transverse momentum of leptons from decays of on-shell Z and W bosons to study the impact of mixed initial-initial QCD-EW corrections on the extraction of the W-boson mass at the LHC. From the three different scenarios that we considered in our simplified approach, we conclude that mixed QCD-EW corrections affect the extracted value of the W-boson mass at the level of $\mathcal{O}(10)$ MeV and that kinematic selection criteria do matter.[5] In fact, we find that mixed initial-initial QCD-EW corrections, which are not fully accounted for in Ref. [25], may shift M_W^{meas} by up to 17 MeV; a value that is comparable to the target precision. While these results are only estimates, they point to the need to study mixed initial-initial QCD-EW effects in a way that is aligned with the experimental strategies of the W-boson mass measurement, such as e. g. template fits.

5 See also Ref. [262].

6 CONCLUSION

This thesis is devoted to the development and application of theoretical methods that facilitate high-precision description of hard scattering processes at the LHC. We described analytic computations of important building blocks of the nested soft-collinear subtraction scheme, including integrated triple-collinear and double-soft subtraction terms. We used these results to compute fully-differential mixed QCD-EW corrections to Z- and W-boson production at hadron colliders and discussed the potential impact of these corrections on the W-boson mass measurements at the LHC.

In the first part of this thesis, we studied technical aspects of the nested soft-collinear subtraction scheme. In Chapter 2, we explained how subtraction terms needed for the regularisation and extraction of soft and collinear singularities are defined in the nested soft-collinear subtraction scheme. We presented analytic results for various integrated subtraction terms in Chapter 3. Besides the direct integration of NLO-like subtraction terms, we computed two double-unresolved integrated subtraction terms:

- double-soft subtraction terms for equal mass back-to-back hard emitters. Such contributions arise in the fully differential description of colour singlet decays into massive quarks, e. g. for Higgs-boson decays into bottom quarks or in heavy-quark production;
- triple-collinear subtraction terms for all possible partonic splittings in initial and final states.

Analytic results for subtraction terms improve the efficiency and numerical stability of practical computations. Additionally, they will enable the derivation of a general NNLO QCD subtraction formula for arbitrary hard processes at the LHC. We expect the approach described in this thesis to be well suited to tackle the computation of remaining double-soft subtraction terms, for example those needed for single-top or top pair production.

In the second part of this thesis, we studied fully-differential mixed QCD-EW corrections to on-shell vector boson production at the LHC. In particular, we obtained the so-far unknown initial-initial contributions to mixed QCD-EW corrections to Z- and W-boson production. Technical details of these computations were presented in Sec. 4.1 and Sec. 4.2. There, we explained how to compute QCD-QED corrections to Z-boson production by starting from the known QCD NNLO calculation [1, 2] and considering the abelian limit. We combined this result with the finite remainder of one-loop weak corrections and the analytical finite remainder of two-loop QCD-weak corrections.

In the case of W-boson production, we discussed the regularisation of IR singularities of double-real contributions within the nested soft-collinear subtraction scheme. We adapted the scheme to accommodate simplifications that arise due to the abelian nature of mixed $\mathcal{O}(\alpha_s\alpha)$ corrections. We presented analytic formulas for double-real tree-level helicity amplitudes, as well as several two-loop master integrals that are required for the evaluation of the QCD-EW on-shell W-boson form factor in Appendix D.

We implemented results in a `Fortan` computer code that allows us to study QCD-EW corrections to inclusive and fiducial cross sections, as well as kinematic distributions related to on-shell Z- and W-boson production at the LHC. We found that mixed QCD-EW initial-initial corrections to fiducial cross sections are small, of the order of one per mille.

However, these small corrections may become relevant for the direct W-boson mass measurement at the LHC, since in this case precision of $\mathcal{O}(10)$ MeV is expected to be achieved. In Sec. 5.2, we have used a simple but transparent model to study how initial-initial mixed QCD-EW corrections affect Z and W boson $p_\ell^\perp$-distributions. We have found that induced shifts in the measured value for M_W depend rather strongly on kinematic cuts and that there are cases where they are comparable to the target precision of $\mathcal{O}(10)$ MeV or even larger. This result calls for more detailed studies of the impact of mixed QCD-EW corrections on the W-boson mass measurement that incorporate details of experimental analyses.

Part III

APPENDIX

A SPECIAL FUNCTIONS

In this Appendix, we define various special functions that we use throughout this thesis.

A.1 GAMMA FUNCTION

The gamma function is defined by the Euler integral [263]

$$\Gamma(\alpha) = \int_0^\infty \mathrm{d}x\, x^{\alpha-1} e^{-x}\,, \quad \mathrm{Re}(\alpha) > 0\,. \tag{A.1}$$

By analytical continuation, it can be defined as an meromorphic function $\Gamma(z)$, having simple poles at integer values $z = -n$ with residue $(-1)^n/n!$. The gamma function obeys the recursion relation [263]

$$\Gamma(z+1) = z\,\Gamma(z)\,, \tag{A.2}$$

and the Legendre duplication formula [263]

$$\Gamma(z)\,\Gamma\left(z+\frac{1}{2}\right) = 2^{1-2z}\sqrt{\pi}\,\Gamma(2z)\,, \tag{A.3}$$

which can be applied to shift arguments of gamma functions such that ϵ-poles become explicit.

A.2 BETA FUNCTION

The beta function is defined by the Euler integral [263]

$$B(\alpha,\beta) = \int_0^1 \mathrm{d}t\, t^{\alpha-1}(1-t)^{\beta-1} = \frac{\Gamma(\alpha)\Gamma(\beta)}{\Gamma(\alpha+\beta)}\,, \quad \mathrm{Re}(\alpha) > 0 \wedge \mathrm{Re}(\beta) > 0\,. \tag{A.4}$$

Analytic continuation of the beta function is defined by continuing the gamma functions on the r. h. s. of Eq. (A.4).

A.3 HYPERGEOMETRIC FUNCTION

DEFINITION The hypergeometric series reads [263]

$${}_2F_1\left[\{a,b\},\{c\};z\right] = \frac{\Gamma(c)}{\Gamma(a)\,\Gamma(b)} \sum_{n=0}^{\infty} \frac{\Gamma(a+n)\,\Gamma(b+n)}{\Gamma(c+n)} \frac{z^n}{n!}\,, \tag{A.5}$$

with radius of convergence $|z| = 1$. The principal branch is obtained by a cut along the real axis $z \in [1, \infty]$, or equivalently $|\arg(1-z)| \le \pi$. For $\mathrm{Re}(c) > \mathrm{Re}(b) > 0$, the integral representation reads [263]

$$ {}_2F_1\left[\{a,b\},\{c\};z\right] = \frac{\Gamma(c)}{\Gamma(b)\Gamma(c-b)} \int_0^1 \mathrm{d}u\; u^{b-1}(1-u)^{c-b-1}(1-z\,u)^{-a}\,. \tag{A.6} $$

LINEAR TRANSFORMATIONS Linear transformations that are used in this thesis read [263]

$$ \begin{aligned} &{}_2F_1\left[\{a,b\},\{c\};z\right] \\ &= \frac{\Gamma(c)\,\Gamma(c-a-b)}{\Gamma(c-a)\,\Gamma(c-b)}\; {}_2F_1\left[\{a,b\},\{a+b-c+1\};1-z\right] \\ &+ (1-z)^{c-a-b}\frac{\Gamma(c)\,\Gamma(a+b-c)}{\Gamma(a)\,\Gamma(b)}\; {}_2F_1\left[\{c-a,c-b\},\{c-a-b+1\};1-z\right]\,, \end{aligned} \tag{A.7} $$

and

$$ \begin{aligned} &{}_2F_1\left[\{a,b\},\{c\};z\right] \\ &= \frac{(-z)^{-a}\,\Gamma(b-a)\,\Gamma(c)}{\Gamma(b)\,\Gamma(c-a)}\; {}_2F_1\left[\{a,1+a-c\},\{1+a-b\};1/z\right] \\ &\quad + \frac{(-z)^{-b}\,\Gamma(a-b)\,\Gamma(c)}{\Gamma(a)\,\Gamma(c-b)}\; {}_2F_1\left[\{b,1+b-c\},\{1-a+b\};1/z\right]\,. \end{aligned} \tag{A.8} $$

QUADRATIC TRANSFORMATIONS Two useful quadratic transformations read [263]

$$ {}_2F_1\left[\{a,b\},\{2b\};z\right] = \left(1-\frac{z}{2}\right)^{-a} {}_2F_1\left[\{\frac{a}{2},\frac{a+1}{2}\},\{b+\frac{1}{2}\};\frac{z^2}{4(1-z/2)^2}\right]\,, \tag{A.9} $$

and

$$ {}_2F_1\left[\{a,a+\frac{1}{2}\},\{c\};z\right] = \left(1\pm\sqrt{z}\right)^{-2a} {}_2F_1\left[\{2a,c-\frac{1}{2}\},\{2c-1\};\frac{\pm 2\sqrt{z}}{1\pm\sqrt{z}}\right]\,. \tag{A.10} $$

GENERALIZED HYPERGEOMETRIC FUNCTION By Euler's recursion formula, we can express certain integrals over hypergeometric functions as generalized hypergeometric functions. In particular, we have [263]

$$ \begin{aligned} &{}_{p+1}F_{q+1}\left[\{a_1\ldots a_{p+1}\},\{b_1\ldots b_{q+1}\};z\right] \\ &= \frac{\Gamma\left(b_{q+1}\right)}{\Gamma\left(a_{p+1}\right)\Gamma\left(b_{q+1}-a_{p+1}\right)}\times \\ &\quad \int_0^1 \mathrm{d}x\; x^{a_{p+1}-1}(1-x)^{b_{q+1}-a_{p+1}-1}\; {}_pF_q\left[\{a_1\ldots a_p\},\{b_1\ldots b_q\};x\,z\right]\,. \end{aligned} \tag{A.11} $$

A.4 CLAUSEN FUNCTION

We define Clausen functions as [263]

$$\mathrm{Cl}_n(z) = \begin{cases} \frac{1}{2}\left[\mathrm{Li}_n\left(e^{\mathrm{i}z}\right) + \mathrm{Li}_n\left(e^{-\mathrm{i}z}\right)\right], & n \text{ odd}, \\ \frac{1}{2\mathrm{i}}\left[\mathrm{Li}_n\left(e^{\mathrm{i}z}\right) - \mathrm{Li}_n\left(e^{-\mathrm{i}z}\right)\right], & n \text{ even}. \end{cases} \tag{A.12}$$

A.5 GONCHAROV POLYLOGARITHM

DEFINITION Goncharov polylogarithms (GPLs) [154, 155] are a special case of Chen iterated integrals [152]. We define them via an integral representation

$$\mathrm{G}_{\vec{\sigma}}(x) = \mathrm{G}(\{\sigma_n, \dots, \sigma_1\}; x) = \int_0^x \frac{\mathrm{d}t_n}{t_n - \sigma_n} \int_0^{t_n} \frac{\mathrm{d}t_{n-1}}{t_{n-1} - \sigma_{n-1}} \cdots \int_0^{t_2} \frac{\mathrm{d}t_1}{t_1 - \sigma_1}, \tag{A.13}$$

where the so-called *letters* σ_i are arbitrary complex numbers and $\sigma_1 \neq 0$. We call the n-tuple $\{\sigma_n, \dots, \sigma_1\}$ a *word* of *weight* n. We can write Eq. (A.13) recursively as

$$\mathrm{G}(\{a, \vec{\sigma}\}; x) = \int_0^x \frac{\mathrm{d}t}{t-a} \mathrm{G}(\{\vec{\sigma}\}; t), \quad \mathrm{G}(\{\}; x) = 1. \tag{A.14}$$

Integral representations in Eq. (A.13) and Eq. (A.14) diverge whenever the word $\vec{\sigma}$ ends with (several) zero(es). To cover this case, we extend the definition by

$$\mathrm{G}(\{\underbrace{0, \dots, 0}_{n \text{ times}}\}; x) = \frac{\ln^n(x)}{n!}. \tag{A.15}$$

SPECIAL CASES GPLs are related to harmonic polylogarithms (HPLs) [264] via

$$\mathrm{H}(\{\vec{\omega}\}; x) = (-1)^{n_{-1}(\vec{\omega})} \times \mathrm{G}(\{\vec{\omega}\}; x), \tag{A.16}$$

where letters ω_i are drawn from the alphabet $\{0, 1, -1\}$ and $n_{-1}(\vec{\omega})$ counts the appearances of letter "-1" in $\vec{\omega}$. Classical polylogarithms can be expressed through GPLs as

$$\mathrm{Li}_n(x) = -\mathrm{G}(\{\underbrace{0, \dots, 0}_{n \text{ times}}, 1\}; x). \tag{A.17}$$

NUMERICAL EVALUATION Numerical evaluation of GPLs is, for example, discussed in Refs. [176, 265].

SHUFFLE ALGEBRA GPLs obey the so-called *shuffle* identity

$$G(\{\vec{\sigma}_1\};x) \times G(\{\vec{\sigma}_2\};x) = \sum_{\vec{s}\,\in\,\vec{\sigma}_1 \sqcup\!\sqcup\, \vec{\sigma}_2} G(\{\vec{s}\};x)\,, \tag{A.18}$$

where the sum runs over all possible shuffles $\vec{\sigma}_1 \sqcup\!\sqcup\, \vec{\sigma}_2$. A shuffle of two words $\vec{\sigma}_{1,2}$ of lengths $n_{1,2}$ is the set of $(n_1+n_2)!/n_1!/n_2!$ words, for which the ordering of letters is the same as in the original words $\vec{\sigma}_i$.

Example 6 (*Shuffle*)

As a straightforward example, we compute

$$\begin{aligned} &\mathrm{G}_{a,b}\,(t) \times \mathrm{G}_{c,d}\,(t) \\ &= 2\,\mathrm{G}_{a,b,c,d}\,(t) + \mathrm{G}_{a,c,b,d}\,(t) + \mathrm{G}_{a,c,d,b}\,(t) + \mathrm{G}_{c,a,b,d}\,(t) + \mathrm{G}_{c,a,d,b}\,(t)\;. \end{aligned} \tag{A.19}$$

FIBRATION BASIS A (multi-variable) GPL is said to be in a so-called *fibration basis*, if it admits the from $G(\{\vec{\sigma}\};x)$, where the word $\vec{\sigma}$ is independent of x. In practical applications, it might be desirable to bring GPLs into a certain fibration basis. Here, we describe such procedure, which is sometimes referred to as "super-shuffle" [172]. Consider a GPL of weight n,

$$G(\{\vec{R}(x)\};\tilde{R}(x)) \tag{A.20}$$

where $\vec{R}$ ($\tilde{R}$) denotes a rational word (function) of x and suppose we want to find the fibration basis in x. Up to a constant, we can write this function as the primitive of its derivative,

$$G(\{\vec{R}(x)\};\tilde{R}(x)) = \int^x \mathrm{d}t \left[\frac{\partial}{\partial t} G(\{\vec{R}(t)\};\tilde{R}(t))\right] + \text{const}\,. \tag{A.21}$$

After taking the derivative in Eq. (A.21), the integrand contains *only* GPLs of weight $n-1$, and we can use the relation to recursively derive a fibration basis. The recursion starts with the natural logarithm at weight one,

$$G(\{f(x)\};g(x)) = \ln\left(1 - \frac{g(x)}{f(x)}\right)\,, \quad G(\{0\};g(x)) = \ln\left(g(x)\right)\,, \tag{A.22}$$

where f and g are rational functions of x. Using standard identities, we can always bring Eq. (A.22) into a fibration basis in x. We note that during this procedure, constants of integration in Eq. (A.21) have to be fixed in a suitable limit $x \to a$ for each weight.

Example 7 (*Fibration basis*)

We demonstrate the recursive super-shuffle algorithm re-writing the weight-three expression $G_{-1,1/x,1/x}((1-x)/x)$*. Using Eq. (A.21), we write*

$$\begin{aligned} & G_{-1,1/x,1/x}((1-x)/x) \\ &= \int^x \mathrm{d}t \, \frac{G_{-1,1/t}((1-t)/t) - G_{1/t,1/t}((1-t)/t)}{1+t} + c_3 \,. \end{aligned} \tag{A.23}$$

Using Eq. (A.21) again, we re-write the two weight-two expressions in the integrand as

$$\begin{aligned} G_{-1,1/x}\left(\frac{1-x}{x}\right) &= \int^x \mathrm{d}t \, \frac{G_{-1}((1-t)/t) - G_{1/t}((1-t)/t)}{1+t} + c_2^a \,, \\ G_{1/x,1/x}\left(\frac{1-x}{x}\right) &= \int^x \mathrm{d}t \, \frac{G_{1/t}((1-t)/t)}{t} + c_2^b \,. \end{aligned} \tag{A.24}$$

We are now in the position to re-write the weight-one integrand in Eq. (A.24) as

$$\begin{aligned} G_{-1}((1-t)/t) &= -\ln(t) = -G_0(t) \,, \\ G_{1/t}((1-t)/t) &= \ln(t) = G_0(t) \,. \end{aligned} \tag{A.25}$$

We use Eq. (A.25) in Eq. (A.24) and find

$$\begin{aligned} G_{-1,1/x}\left(\frac{1-x}{x}\right) &= -2\int^x \mathrm{d}t \, \frac{G_0(t)}{1+t} + c_2^a = -2\, G_{-1,0}(x) + c_2^a \,, \\ G_{1/x,1/x}\left(\frac{1-x}{x}\right) &= \int^x \mathrm{d}t \, \frac{G_0(t)}{t} + c_2^b = G_{0,0}(x) + c_2^b \,. \end{aligned} \tag{A.26}$$

To compute constants c_2^i*, we take the (regular) limit* $x \to 1$ *in Eq. (A.26). We obtain*

$$c_2^a = -\frac{\pi^2}{6} \,, \quad c_2^b = 0 \,. \tag{A.27}$$

Using the above formulas, we can express the integrand in Eq. (A.23) through a fibration basis and integrate. We find

$$\begin{aligned} & G_{-1,1/x,1/x}((1-x)/x) \\ &= \int^x \mathrm{d}t \, \frac{-2\, G_{-1,0}(t) - \frac{\pi^2}{6} - G_{0,0}(t)}{1+t} + c_3 \\ &= -2G_{-1,-1,0}(x) - \frac{\pi^2}{6} G_{-1}(x) - G_{-1,0,0}(x) + c_3 \,. \end{aligned} \tag{A.28}$$

Finally, we fix the constant c_3 *in the regular limit* $x \to 1$ *and find* $c_3 = \zeta_3$*.*

B NESTED SOFT-COLLINEAR SUBTRACTIONS

In this Appendix, we collect some of the definitions used in Chapter 2.

B.1 GENERAL DEFINITIONS

B.1.1 *Coupling constants*

We use the following abbreviations for bare coupling constants

$$[\alpha_s] = \frac{g_s^2 \Omega^{(d-2)}}{2(2\pi)^{d-1}} = \frac{g_s^2}{8\pi^2} \frac{(4\pi)^\epsilon}{\Gamma(1-\epsilon)}, \tag{B.1}$$

and

$$[\alpha] = \frac{e^2 \Omega^{(d-2)}}{2(2\pi)^{d-1}} = \frac{e^2}{8\pi^2} \frac{(4\pi)^\epsilon}{\Gamma(1-\epsilon)}. \tag{B.2}$$

In Eqs. (B.1)-(B.2), $\Omega^{(n)}$ denotes the volume of a unit sphere *embedded* in n dimensions. Its definition reads

$$\int \mathrm{d}\Omega^{(n)} = \Omega^{(n)} = \frac{2\pi^{n/2}}{\Gamma(n/2)}. \tag{B.3}$$

B.1.2 *Plus prescription*

We define the *plus prescription* as

$$\int_0^1 \mathrm{d}z\, [f(z)]_+\, g(z) = \int_0^1 \mathrm{d}z\, f(z)\, [g(z) - g(1)]\,, \tag{B.4}$$

where g is a function that is regular at $z = 1$. In soft-regulated collinear contributions, we will encounter integrals of the form

$$\int_0^1 \mathrm{d}z\, \frac{g(z) - g(1)}{(1-z)^{1+j\epsilon}} = \int_0^1 \mathrm{d}z \left[\sum_{n=0}^{\infty} \frac{(-1)^n (j\epsilon)^n}{n!} \mathcal{D}_n(z) \right] g(z)\,, \tag{B.5}$$

where the r. h. s. follows from Taylor expansion in ϵ and we used the abbreviation

$$\mathcal{D}_n(z) = \left[\frac{\ln^n(1-z)}{1-z} \right]_+. \tag{B.6}$$

It is useful to re-write Eq. (B.5) in the following way; we integrate the second term on the l. h. s. and find

$$\int_0^1 \mathrm{d}z \left[\frac{1}{(1-z)^{1+j\epsilon}} + \frac{\delta(1-z)}{j\epsilon}\right] g(z) = \int_0^1 \mathrm{d}z \left[\sum_{n=0}^{\infty} \frac{(-1)^n (j\epsilon)^n}{n!} \mathcal{D}_n(z)\right] g(z)\,, \tag{B.7}$$

which we write as

$$\frac{1}{(1-z)^{1+j\epsilon}} = \sum_{n=0}^{\infty} \frac{(-1)^n (j\epsilon)^n}{n!} \mathcal{D}_n(z) - \frac{\delta(1-z)}{j\epsilon}\,. \tag{B.8}$$

The relation in Eq. (B.8) should be understood in a distributional sense: it is only valid when multiplied with a test function that is regular at $z = 1$ and integrated over $z \in [0,1]$.

B.2 EIKONAL FUNCTIONS

B.2.1 *Color notation*

We adopt color notations of Ref. [53] and write a generic matrix element as

$$\mathcal{M}_{c_1,\ldots,c_n}(p_1,\ldots,p_n) = \big\langle c_1,\ldots,c_n \big| \mathcal{M}(p_1,\ldots,p_n) \big\rangle\,, \tag{B.9}$$

where c_i are color indices. We denote the color charge of a gluon emitted from a parton i by an operator $\boldsymbol{T}_i$. This operator acts on the color space as

$$\big\langle c_1,\ldots,c_i,\ldots,c_m,a \big| \boldsymbol{T}_i \big| b_1,\ldots,b_i,\ldots,b_m \big\rangle = \delta_{c_1 b_1} \ldots T^a_{c_i b_i} \ldots \delta_{c_n b_n}\,, \tag{B.10}$$

where a is the index of the gluon. We have

$$T^a_{c_i b_i} = \begin{cases} \mathrm{i} f_{a c_i b_i} & i \text{ is a gluon} \\ t^a_{c_i b_i} & i \text{ is a quark} \\ -t^a_{c_i b_i} & i \text{ is a antiquark} \end{cases}\,, \tag{B.11}$$

where f_{abc} and t^a_{bc} are the $SU(N_c)$ color generators in the adjoint and fundamental representation, respectively. To describe eikonal functions up to $\mathcal{O}(\alpha_s^2)$, we require the following two correlations

$$\begin{aligned} |\mathcal{A}^{(ij)}(\{p\})|^2 &= \langle \mathcal{A}(p_1,\ldots,p_n)| \boldsymbol{T}_i \cdot \boldsymbol{T}_j |\mathcal{A}(p_1,\ldots,p_n)\rangle\,, \\ |\mathcal{A}^{\{(ij),(kl)\}}(\{p\})|^2 &= \langle \mathcal{A}(p_1,\ldots,p_n)| \{\boldsymbol{T}_i \cdot \boldsymbol{T}_j, \boldsymbol{T}_k \cdot \boldsymbol{T}_l\} |\mathcal{A}(p_1,\ldots,p_n)\rangle\,, \end{aligned} \tag{B.12}$$

where $\{\cdot,\cdot\}$ denotes the anticommutator in colour space.

B.2.2 *Gluon emission*

The double-soft function $\mathcal{S}^0_{ij}(k_1,k_2)$ for gluon emission off massless emitters reads [123]

$$\begin{aligned}
\mathcal{S}^0_{ij}(k_1,k_2) &= \frac{(1-\epsilon)}{(k_1\cdot k_2)^2}\frac{\left[(p_i\cdot k_1)(p_j\cdot k_2)+i\leftrightarrow j\right]}{(p_i\cdot k_{12})(p_j\cdot k_{12})} \\
&- \frac{(p_i\cdot p_j)^2}{2(p_i\cdot k_1)(p_j\cdot k_2)(p_i\cdot k_2)(p_j\cdot k_1)}\left[2-\frac{\left[(p_i\cdot k_1)(p_j\cdot k_2)+i\leftrightarrow j\right]}{(p_i\cdot k_{12})(p_j\cdot k_{12})}\right] \\
&+ \frac{(p_i\cdot p_j)}{2(k_1\cdot k_2)}\left[\frac{2}{(p_i\cdot k_1)(p_j\cdot k_2)}+\frac{2}{(p_j\cdot k_1)(p_i\cdot k_2)}-\frac{1}{(p_i\cdot k_{12})(p_j\cdot k_{12})}\right. \\
&\left.\times\left(4+\frac{\left[(p_i\cdot k_1)(p_j\cdot k_2)+i\leftrightarrow j\right]^2}{(p_i\cdot k_1)(p_j\cdot k_2)(p_i\cdot k_2)(p_j\cdot k_1)}\right)\right],
\end{aligned} \tag{B.13}$$

where $k_{12} = k_1+k_2$. The double-soft function $\mathcal{S}^m_{ij}(k_1,k_2)$ for massive emitters was derived in Ref. [96], building on the fact that eikonal currents are *identical* for massive and massless emitters. The result is given by [96]

$$\begin{aligned}
\mathcal{S}^m_{ij}(k_1,k_2) &= -\frac{1}{4(k_1\cdot k_2)(p_i\cdot k_1)(p_i\cdot k_2)} \\
&+ \frac{(p_i\cdot p_j)(p_j\cdot k_{12})}{2(p_i\cdot k_1)(p_j\cdot k_2)(p_i\cdot k_2)(p_j\cdot k_1)(p_i\cdot k_{12})} \\
&- \frac{1}{2(k_1\cdot k_2)(p_i\cdot k_{12})(p_j\cdot k_{12})}\left(\frac{(p_j\cdot k_1)^2}{(p_i\cdot k_1)(p_j\cdot k_2)}+\frac{(p_j\cdot k_2)^2}{(p_i\cdot k_2)(p_j\cdot k_1)}\right).
\end{aligned} \tag{B.14}$$

B.2.3 *Quark emission*

The soft function $\mathcal{I}_{ij}(k_1,k_2)$ for quark-antiquark pair emission is given by [123]

$$\mathcal{I}_{ij}(k_1,k_2) = \frac{\left[(p_i\cdot k_1)\left(p_j\cdot k_2\right)+i\leftrightarrow j\right]-\left(p_i\cdot p_j\right)(k_1\cdot k_2)}{(k_1\cdot k_2)^2\left(p_i\cdot k_{12}\right)\left(p_j\cdot k_{12}\right)}. \tag{B.15}$$

B.3 DERIVATION OF DOUBLE-COLLINEAR GLUON EMISSION

In this Section, we derive the factorization formula given in Example 1. We consider the double-real correction $q(p_1)\bar{q}(p_2)\to Z\,g(k_4)g(k_5)$ to color-singlet production and take the limit $\boldsymbol{k}_4 \parallel \boldsymbol{p}_1$. The tree-level diagrams that contribute to this process can be split in two classes,

$$\mathcal{A}_{q\bar{q}\to Zgg} = \mathcal{A}_c + \mathcal{A}_f = \tag{B.16}$$

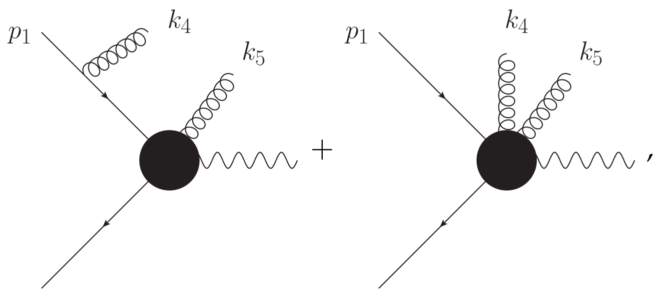

where the black disc summarizes the various ways in which the gluon(s) can be attached. On the r. h. s. of Eq. (B.16), the first diagram class, $\mathcal{A}_c$, contains the singular propagator $1/\left(p_1 - k_4\right)^2$, while all other diagrams, in class $\mathcal{A}_f$, are finite in the limit $\boldsymbol{k}_4 \parallel \boldsymbol{p}_1$.

We begin with the first class and write

$$\mathcal{A}_c = g_{s,b} \mathcal{A}_{\text{blob},i} \frac{\widehat{p}_1 - \widehat{k}_4}{\left(p_1 - k_4\right)^2} T_{ij}\, \widehat{\varepsilon}_4 u_1^j\,, \tag{B.17}$$

where the quark spinor u_1^j, the gluon polarisation $\widehat{\varepsilon}_4$, the quark propagator "$\widehat{q}/q^2$", as well as the quark-gluon coupling are given explicitly and the remainder is summarized in the object $\mathcal{A}_{\text{blob},i}$. We parameterize

$$k_4^\mu = \alpha p_1 - q_\perp^\mu - \frac{q_\perp^2}{\alpha} \frac{n^\mu}{2(p_1 \cdot n)}\,, \tag{B.18}$$

where $n^2 = (q_\perp \cdot n) = (q_\perp \cdot p_1) = 0$. In this parameterization, n is an auxiliary vector that defines the transverse component $q_\perp$ and $\boldsymbol{k}_4 \parallel \boldsymbol{p}_1$ corresponds to the limit $q_\perp \to 0$; we find

$$\left(p_1 - k_4\right)^2 = \frac{q_\perp^2}{\alpha}\,. \tag{B.19}$$

In the following, we extract the singular behaviour in Eq. (B.16) that contributes to the non-integrable $\mathcal{O}\left(1/q_\perp^2\right)$ singularity of the matrix element squared. We insert parameterization Eq. (B.18) into Eq. (B.17) and obtain

$$\begin{aligned} \mathcal{A}_c &\underset{q_\perp \to 0}{\sim} g_{s,b} T_{ij} \mathcal{A}_{\text{blob},i} \frac{(1-\alpha)\widehat{p}_1 + \widehat{q}_\perp}{\left(p_1 - k_4\right)^2}\, \widehat{\varepsilon}_4 u_1^j \\ &= g_{s,b} T_{ij} \mathcal{A}_{\text{blob},i} \frac{2(1-\alpha)(p_1 \cdot \varepsilon_4) + \widehat{q}_\perp \widehat{\varepsilon}_4}{\left(p_1 - k_4\right)^2}\, u_1^j\,, \end{aligned} \tag{B.20}$$

where we neglected the $\mathcal{O}\left(q_\perp^2\right)$ contribution in the numerator and used the Dirac equation $\widehat{p}_1 u_1^j = 0$. Since we work in the physical (light-cone) gauge, the following transversality relation holds

$$0 = (k_4 \cdot \varepsilon_4) = \alpha (p_1 \cdot \varepsilon_4) - (q_\perp \cdot \varepsilon_4) + \mathcal{O}\left(q_\perp^2\right)\,. \tag{B.21}$$

Inserting the relation above into Eq. (B.20), we obtain

$$\mathcal{A}_c \underset{q_\perp\to 0}{\sim} \frac{g_{s,b}T_{ij}}{(p_1-k_4)^2}\mathcal{A}_{\text{blob},i}\left[\frac{2(1-\alpha)}{\alpha}(q_\perp\cdot\varepsilon_4)+\widehat{q}_\perp\widehat{\varepsilon}_4\right]u_1^j \equiv \mathcal{A}_c^{\text{lim}}\,. \tag{B.22}$$

From Eq. (B.19) and Eq. (B.22), we find that $\mathcal{A}_c^{\text{lim}} \sim 1/q_\perp$. Hence, the non-integrable contribution to the matrix element squared reads

$$\left|\mathcal{A}_c+\mathcal{A}_f\right|^2 = \left|\mathcal{A}_c^{\text{lim}}\right|^2 + \mathcal{O}(1/q_\perp)\;. \tag{B.23}$$

We conclude that, due to the physical gauge, the singularity factorizes on the external leg such that no interference terms between singular and non-singular diagrams contribute in Eq. (B.23).

We now turn to the computation of the singularity of the matrix element squared.[1] We find

$$\begin{aligned}\overline{|\mathcal{A}_c^{\text{lim}}|^2} = \frac{g_{s,b}^2 C_F}{(p_1-k_4)^4}\sum_{\lambda_4}\text{Tr}\Big\{\mathcal{A}_{\text{blob}}\left[\frac{2(1-\alpha)}{\alpha}(q_\perp\cdot\varepsilon_4)+\widehat{q}_\perp\widehat{\varepsilon}_4\right]\widehat{p}_1 \\ \times\left[\frac{2(1-\alpha)}{\alpha}(q_\perp\cdot\varepsilon_4^*)+\widehat{\varepsilon}_4^*\widehat{q}_\perp\right]\mathcal{A}_{\text{blob}}^\dagger\Big\}\,.\end{aligned} \tag{B.24}$$

The sum over polarisations of the gluon yields

$$\sum_{\lambda_4}\varepsilon_{4,\mu}\varepsilon_{4,\nu}^* = -g_{\mu,\nu} + \frac{k_{4,\mu}n_\nu + k_{4,\nu}n_\mu}{(k_4\cdot n)}\,. \tag{B.25}$$

We use that

$$\sum_{\lambda_4}(q_\perp\cdot\varepsilon_4)\text{Tr}\Big\{\mathcal{A}_{\text{blob}}\,\widehat{p}_1\widehat{\varepsilon}_4^*\widehat{q}_\perp\,\mathcal{A}_{\text{blob}}^\dagger\Big\} = -\,q_\perp^2\,\text{Tr}\Big\{\mathcal{A}_{\text{blob}}\,\widehat{p}_1\,\mathcal{A}_{\text{blob}}^\dagger\Big\}\,, \tag{B.26}$$

$$\sum_{\lambda_4}\text{Tr}\Big\{\mathcal{A}_{\text{blob}}\,\widehat{q}_\perp\widehat{\varepsilon}_4\widehat{p}_1\widehat{\varepsilon}_4^*\widehat{q}_\perp\,\mathcal{A}_{\text{blob}}^\dagger\Big\} = -\,(d-2)q_\perp^2\,\text{Tr}\Big\{\mathcal{A}_{\text{blob}}\,\widehat{p}_1\,\mathcal{A}_{\text{blob}}^\dagger\Big\}\,, \tag{B.27}$$

and arrive at

$$\overline{|\mathcal{A}_c^{\text{lim}}|^2} = \frac{g_{s,b}^2 C_F}{(p_1\cdot k_4)}\times\left[\frac{1+z^2}{1-z}-\epsilon(1-z)\right]\times\overline{|\mathcal{A}_{\text{red}}\,[p_1-k_4]|^2}\,, \tag{B.28}$$

where $z = 1-\alpha$. The reduced matrix element squared in Eq. (B.28) reads

$$\begin{aligned}&\overline{|\mathcal{A}_{\text{red}}\,[p_1-k_4]|^2} \\ &= (1-\alpha)\text{Tr}\Big\{\mathcal{A}_{\text{blob}}\,\widehat{p}_1\,\mathcal{A}_{\text{blob}}^\dagger\Big\} \\ &= \text{Tr}\Big\{\mathcal{A}_{\text{blob}}u\,[(1-\alpha)p_1]\,\bar{u}\,[(1-\alpha)p_1]\,\mathcal{A}_{\text{blob}}^\dagger\Big\}\,.\end{aligned} \tag{B.29}$$

1 More precisely, we average over spin and colour of the incoming quark and sum over helicity and colour of the outgoing gluon

As can be seen from Eq. (B.29), $\mathcal{A}_{\text{red}}$ describes $\mathcal{A}_c$ in a situation where $g(k_4)$ is absent and the incoming quark carries momentum $(1-\alpha)p_1 = zp_1 = p_1 - k_4 + \mathcal{O}(q_\perp)$ instead of momentum p_1.

B.4 COLOR COHERENCE IN THE SOFT-COLLINEAR LIMIT

In the following, we explain how the coherence of soft emission forbids the appearance of entangled soft-collinear singularities. The absence of this type of singularity is used in the formulation of the nested soft-collinear subtraction scheme [1], where soft and collinear singularities are regulated iteratively and independent of each other. In this thesis, the regularisation is described in Chapter 2.

To understand how entangled soft-collinear singularities could arise, consider, for example, the diagram

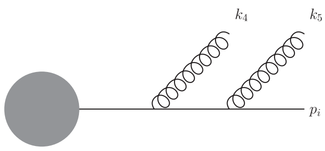

(B.30)

In the limit $k_5 \to 0$ and $\boldsymbol{k}_4 \parallel \boldsymbol{p}_i$, this diagram behaves like

$$\frac{1}{\underbrace{(p_i\cdot k_4)}_{\text{collinear}} + \underbrace{(p_i\cdot k_5) + (k_4\cdot k_5)}_{\text{soft}}} \to \infty\,. \tag{B.31}$$

In the following, we employ arguments of Section 3.4 in Ref. [123] to explain the absence of overlapping soft-collinear singularities in double-real corrections, using the example of gluon-emission corrections to Higgs boson decay, $H \to b(p_1)\bar{b}(p_2) + g(k_4)g(k_5)$. Specifically, we consider the limit where one gluon becomes soft ($k_5 \to 0$) and the other gluon becomes collinear to the b quark ($\boldsymbol{k}_4 \parallel \boldsymbol{p}_1$). The four diagrams that contribute to the divergence in this particular limit are

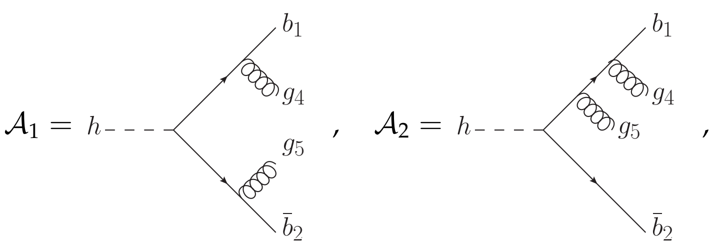

(B.32)

$\mathcal{A}_3 =$ 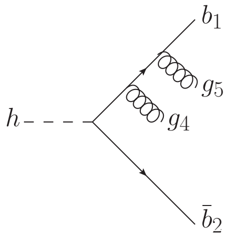

$,\quad \mathcal{A}_4 =$ 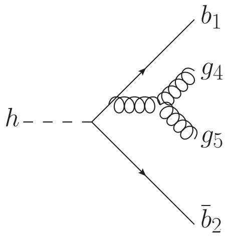

$. \qquad \text{(B.33)}$

In the limit $k_5 \to 0$ and $\boldsymbol{k}_4 \parallel \boldsymbol{p}_1$, diagrams $\mathcal{A}_{2,3,4}$ in Eq. (B.32) have an entangled soft-collinear divergence as displayed in Eq. (B.31) upon identifying $p_1 = p_i$. However, such overlapping soft-collinear singularities *only* appear on the level of individual diagrams – they are absent in gauge-invariant matrix elements due the fact soft emission in QCD is *coherent*.

To verify this statement at the example of Higgs decay, we turn to the sum of diagrams in Eqs. (B.32)-(B.33). We begin by extracting the leading singular behaviour in the soft limit $k_5 \to 0$ and obtain

$$\mathcal{A}^{h\to b_1\bar{b}_2 g_4 g_5} \underset{k_5\to 0}{\sim} \mathcal{A}_1 + \cdots + \mathcal{A}_4 \underset{k_5\to 0}{\sim} \frac{g_{s,b}^2 \boldsymbol{J}^\mu(k_5)\, \varepsilon_\mu^*(k_5)}{(p_1+k_4)^2} \times \mathcal{A}^{h\to b_1\bar{b}_2}\,, \tag{B.34}$$

where $\mathcal{A}^{h\to b_1\bar{b}_2}$ is the Born-level amplitude. The soft current $\boldsymbol{J}^\mu(k_5)$ in Eq. (B.34) reads[2]

$$\begin{aligned}\boldsymbol{J}^\mu(k_5) = &\underbrace{\boldsymbol{T}_2 \frac{p_2^\mu}{(p_2\cdot k_5)}}_{\mathcal{A}_1} + \underbrace{(\boldsymbol{T}_4+\boldsymbol{T}_1)\frac{2(p_1+k_4)^\mu}{(p_1+k_4+k_5)^2}}_{\mathcal{A}_2} \\ &+ \frac{(p_1+k_4)^2}{(p_1+k_4+k_5)^2}\left[\underbrace{\boldsymbol{T}_1\frac{p_1^\mu}{(p_1\cdot k_5)}}_{\mathcal{A}_3} + \underbrace{\boldsymbol{T}_4\frac{k_4^\mu}{(k_4\cdot k_5)}}_{\mathcal{A}_4}\right] .\end{aligned} \tag{B.35}$$

To simplify the computation of the collinear limit $\boldsymbol{k}_4 \parallel \boldsymbol{p}_1$, we re-arrange terms in Eq. (B.35) and write the soft current as

$$\boldsymbol{J}^\mu(k_5) = \boldsymbol{J}^\mu_{\text{cs}}(k_5) + \boldsymbol{J}^\mu_{\text{cf}}(k_5)\,, \tag{B.36}$$

where

$$\boldsymbol{J}^\mu_{\text{cs}}(k_5) = \boldsymbol{T}_2\frac{p_2^\mu}{(p_2\cdot k_5)} + (\boldsymbol{T}_1+\boldsymbol{T}_4)\frac{(p_1+k_4)^\mu}{(p_1+k_4)\cdot k_5}\,, \tag{B.37}$$

and

$$\begin{aligned}\boldsymbol{J}^\mu_{\text{cf}}(k_5) = &\frac{(p_1+k_4)^2}{(p_1+k_4+k_5)^2} \\ &\times\left[\boldsymbol{T}_1\frac{p_1^\mu}{(p_1\cdot k_5)} + \boldsymbol{T}_4\frac{k_4^\mu}{(k_4\cdot k_5)} - (\boldsymbol{T}_1+\boldsymbol{T}_4)\frac{(p_1+k_4)^\mu}{(p_1+k_4)\cdot k_5}\right] .\end{aligned} \tag{B.38}$$

2 We employ the color notation of Sec. B.2 and retain all terms that cause singularities in $k_5 \to 0$, $\boldsymbol{k}_4 \parallel \boldsymbol{p}_1$.

In writing Eqs. (B.36)-(B.38), we have used that

$$\frac{2(p_1+k_4)^\mu}{(p_1+k_4+k_5)^2} = \frac{(p_1+k_4)^\mu}{(p_1+k_4)\cdot k_5}\left[1-\frac{(p_1+k_4)^2}{(p_1+k_4+k_5)^2}\right]. \tag{B.39}$$

We note the currents in Eqs. (B.37)-(B.38) are *separately* gauge invariant, since $k_{5,\mu}\boldsymbol{J}^\mu_{\mathrm{cs,cf}}(k_5) = 0$. For this reason, the decomposition in Eq. (B.36) does not spoil gauge invariance. Furthermore, we note that both $\boldsymbol{J}^\mu_{\mathrm{cs}}(k_5)$ and $\boldsymbol{J}^\mu_{\mathrm{cf}}(k_5)$ show the expected soft behavior $\mathcal{O}(1/k_5)$.

We now turn to the discussion of the collinear limit $\boldsymbol{k}_4 \parallel \boldsymbol{p}_1$. To this end, we parameterize momenta p_1 and k_4 as [123]

$$\begin{aligned} p_1^\mu &= z\,q^\mu + q_\perp^\mu - \frac{q_\perp^2}{z}\frac{n^\mu}{2(q\cdot n)}\,, \\ k_4^\mu &= (1-z)\,q^\mu - q_\perp^\mu - \frac{q_\perp^2}{1-z}\frac{n^\mu}{2(q\cdot n)}\,, \end{aligned} \tag{B.40}$$

where $q^2 = n^2 = (q_\perp\cdot n) = (q_\perp\cdot q) = 0$. In this parameterization, q denotes the momentum to which p_1 and k_4 become parallel, n is an auxiliary vector needed to define the transverse component $q_\perp$, and $\boldsymbol{k}_4 \parallel \boldsymbol{p}_1$ corresponds to the limit $q_\perp \to 0$.

It is straightforward to see that in the limit $q_\perp \to 0$ the soft current $\boldsymbol{J}^\mu_{\mathrm{cf}}(k_5)$ in Eq. (B.38) is suppressed by $\mathcal{O}(q_\perp)$ w. r. t. the soft current $\boldsymbol{J}^\mu_{\mathrm{cs}}(k_5)$ in Eq. (B.37). Hence, we can neglect $\boldsymbol{J}^\mu_{\mathrm{cf}}(k_5)$ in the soft-collinear limit and find

$$\begin{aligned} \mathcal{A}^{h\to b_1\bar{b}_2 g_4 g_5} \underset{\boldsymbol{k}_4\parallel \boldsymbol{p}_1}{\overset{k_5\to 0}{\sim}} \frac{g_{s,b}^2}{2(p_1\cdot k_4)}\left[\boldsymbol{T}_2\frac{p_2^\mu}{(p_2\cdot k_5)} + (\boldsymbol{T}_1+\boldsymbol{T}_4)\frac{(p_1+k_4)^\mu}{(p_1+k_4)\cdot k_5}\right] \\ \times\, \varepsilon^*_\mu(k_5)\,\mathcal{A}^{h\to b_1\bar{b}_2}\,. \end{aligned} \tag{B.41}$$

The factorization formula in Eq. (B.41) describes the emission of a soft gluon $g(k_5)$ by anti-quark $\bar{b}(p_2)$ and the *coherent* soft emission by a particle with momentum $p_1 + k_4$ and charge $\boldsymbol{T}_4 + \boldsymbol{T}_1$. We emphasize again that the overlapping soft-collinear singularity is absent on the level of the gauge-invariant amplitude, as can be seen from Eq. (B.41).

We note that the discussion above can be generalized to show the absence of overlapping soft-collinear singularities in tree-level amplitudes describing the scattering of n massless partons in cases where arbitrarily many particles become soft and arbitrarily many particles become collinear [123].

B.5 PHASE-SPACE PARAMETRIZATION

In the following, we briefly summarize the angular phase-space parameterization and define double-collinear limits. We begin by separating energies and angles in Eq. (2.15) and write

$$[\mathrm{d}k_4][\mathrm{d}k_5] = \frac{\mathrm{d}^{d-1}\boldsymbol{k}_4}{(2\pi)^{d-1}2E_4}\frac{\mathrm{d}^{d-1}\boldsymbol{k}_5}{(2\pi)^{d-1}2E_5} = \frac{\mathrm{d}E_4\,\mathrm{d}E_5}{(E_4E_5)^{-1+2\epsilon}}\frac{\mathrm{d}\Omega_4^{(d-1)}}{2(2\pi)^{d-1}}\frac{\mathrm{d}\Omega_5^{(d-1)}}{2(2\pi)^{d-1}}\,. \tag{B.42}$$

We will present the parameterization of the angular phase-space in case of double-collinear and triple-collinear partitions in Appendix B.5.1 and Appendix B.5.2, respectively.

B.5.1 *Double-collinear partitions*

Double-collinear partitions $\omega_{\mathcal{DC}}^{i4,j5}$, $i \neq j$, are defined to dampen all but the singular limits $\boldsymbol{k}_4 \parallel \boldsymbol{p}_i$ and $\boldsymbol{k}_5 \parallel \boldsymbol{p}_j$, see Eq. (2.49). To simplify double-collinear limits, we parameterize the direction-of-flight of partons $f_{4,5}$ relative to Born-particles i and j, respectively. We write

$$n_4^\mu = t^\mu + \cos\theta_{4i}\, e_i^\mu + \sin\theta_{4i}\, b_i^\mu\,, \tag{B.43}$$
$$n_5^\mu = t^\mu + \cos\theta_{5j}\, e_j^\mu + \sin\theta_{5j}\, b_j^\mu\,, \tag{B.44}$$

where $t = (1, \boldsymbol{0})$ and $e_{i,j} = \big(0, \boldsymbol{n}_{i,j}\big)$. Vectors $b_{i,j}$ fulfill the condition

$$t \cdot b_m = 0\,, \quad e_m \cdot b_m = 0\,, \quad m \in \{i, j\}\,. \tag{B.45}$$

With this parameterization, the angular phase space in Eq. (B.42) reads

$$\frac{\mathrm{d}\Omega_4^{(d-1)}}{2(2\pi)^{d-1}}\frac{\mathrm{d}\Omega_5^{(d-1)}}{2(2\pi)^{d-1}} = \frac{\mathrm{d}\Omega_{b_i}^{(d-2)}}{(2\pi)^{d-1}}\frac{\mathrm{d}\Omega_{b_j}^{(d-2)}}{(2\pi)^{d-1}} \tag{B.46}$$
$$\times\, \mathrm{d}\eta_{4i}\,[4\eta_{4i}(1-\eta_{4i})]^{-\epsilon}\, \mathrm{d}\eta_{5j}\,\big[4\eta_{5j}(1-\eta_{5j})\big]^{-\epsilon}\,, \tag{B.47}$$

where $\eta_{lm} = (1-\cos\theta_{lm})/2 \in [0,1]$. Double-collinear limits are defined to extract the leading $1/\eta$-behaviour; in this parameterization we find

$$\begin{aligned} C_{4i}\,\frac{\mathrm{d}\Omega_4^{(d-1)}}{2(2\pi)^{d-1}} &= \frac{\mathrm{d}\Omega_{b_i}^{(d-2)}}{(2\pi)^{d-1}}\,\mathrm{d}\eta_{4i}\,[4\eta_{4i}]^{-\epsilon}\,, \\ C_{5j}\,\frac{\mathrm{d}\Omega_5^{(d-1)}}{2(2\pi)^{d-1}} &= \frac{\mathrm{d}\Omega_{b_j}^{(d-2)}}{(2\pi)^{d-1}}\,\mathrm{d}\eta_{5j}\,\big[4\eta_{5j}\big]^{-\epsilon}\,. \end{aligned} \tag{B.48}$$

B.5.2 *Triple-collinear partitions*

Triple-collinear partitions $\omega_{\mathcal{TC}}^{i4,i5}$ are defined to dampen all but the double-collinear singular limits $\boldsymbol{k}_4 \parallel \boldsymbol{p}_i$, $\boldsymbol{k}_5 \parallel \boldsymbol{p}_i$, and $\boldsymbol{k}_4 \parallel \boldsymbol{k}_5$, as well as the triple-collinear divergence $\boldsymbol{k}_4 \parallel \boldsymbol{k}_5 \parallel \boldsymbol{p}_i$, see Eq. (2.50). To simplify the extraction of these singularities, we adopt the parameterization of Ref. [95].[3] We write

$$n_4^\mu = t^\mu + \cos\theta_{4i}\, e_i^\mu + \sin\theta_{4i}\, b_i^\mu\,, \tag{B.49}$$

3 Relevant formulas can also be found in Appendix B of Ref. [1].

$$n_5^\mu = t^\mu + \cos\theta_{5i}\, e_i^\mu + \sin\theta_{5i}\left(\cos\varphi_{45}\, b_i^\mu + \sin\varphi_{45}\, a_i^\mu\right)\,, \tag{B.50}$$

where

$$t\cdot a_i = t\cdot b_i = e_i\cdot a_i = e_i\cdot b_i = a_i\cdot b_i = 0\,. \tag{B.51}$$

We obtain

$$\begin{aligned}\frac{\mathrm{d}\Omega_4^{(d-1)}}{2(2\pi)^{d-1}}\frac{\mathrm{d}\Omega_5^{(d-1)}}{2(2\pi)^{d-1}} &= \frac{\mathrm{d}\Omega_{b_i}^{(d-2)}\,\mathrm{d}\Omega_{a_i}^{(d-3)}}{2^{6\epsilon}(2\pi)^{2d-2}}\\ &\times \eta_{45}^{1-2\epsilon}\frac{\mathrm{d}\eta_4}{[\eta_4(1-\eta_4)]^{\epsilon}}\frac{\mathrm{d}\eta_5}{[\eta_5(1-\eta_5)]^{-\epsilon}}\frac{\mathrm{d}\lambda}{[\lambda(1-\lambda)]^{1/2+\epsilon}}\,.\end{aligned} \tag{B.52}$$

In writing Eq. (B.52), we have defined

$$\sin^2\varphi_{45} = 4\lambda(1-\lambda)\eta_{45}^2\,,\quad \eta_{45} = \frac{|\eta_4-\eta_5|}{D}\,,\quad \eta_{4,5} = \frac{1-\cos\theta_{4i,5i}}{2}\,, \tag{B.53}$$

where

$$D = \eta_4+\eta_5-2\eta_4\eta_5+2(2\lambda-1)\sqrt{\eta_4\eta_5(1-\eta_4)(1-\eta_5)}\,. \tag{B.54}$$

In Sec. 2.3.3, we have discussed how to split the phase space into sectors for two cases: the general case, that admits a $\boldsymbol{k}_4 \parallel \boldsymbol{k}_5$ singularity, and the case without. We will explain how to parameterize angles in both cases in what follows.

Parameterization in the general case

In the general case, which admits the $\boldsymbol{k}_4 \parallel \boldsymbol{k}_5$ singularity, we have split the phase space into four sectors, see Eqs. (2.59)-(2.62). In these four sectors, we choose the following parameterization

$$(a)\quad \eta_4 = x_3\,,\qquad \eta_5 = x_3\,x_4/2\,, \tag{B.55}$$

$$(b)\quad \eta_4 = x_3\,,\qquad \eta_5 = x_3(1-x_4/2)\,, \tag{B.56}$$

$$(c)\quad \eta_4 = x_3\,x_4/2\,,\qquad \eta_5 = x_3\,, \tag{B.57}$$

$$(d)\quad \eta_4 = x_3(1-x_4)/2\,,\qquad \eta_5 = x_3\,. \tag{B.58}$$

Since the measure in Eq. (B.52) is symmetric in $\eta_4 \leftrightarrow \eta_5$, angular phase spaces for sectors a, c and b, d are identical. We write

$$\begin{aligned}\frac{\mathrm{d}\Omega_4^{(d-1)}}{2(2\pi)^{d-1}}\frac{\mathrm{d}\Omega_5^{(d-1)}}{2(2\pi)^{d-1}}\times\theta^{a,c} &= \frac{\mathrm{d}\Omega_{b_i}^{(d-2)}\,\mathrm{d}\Omega_{a_i}^{(d-3)}}{2^{6\epsilon}(2\pi)^{2d-2}}\left[(1-x_3)F_\epsilon^{(a,c)}\right]^{-\epsilon}F_0^{(a,c)}x_3^2x_4\\ &\times\frac{\mathrm{d}x_3}{x_3^{1+2\epsilon}}\frac{\mathrm{d}x_4}{x_4^{1+\epsilon}}\frac{\mathrm{d}\lambda}{[\lambda(1-\lambda)]^{1/2+\epsilon}}\,,\end{aligned} \tag{B.59}$$

$$\frac{d\Omega_4^{(d-1)}}{2(2\pi)^{d-1}}\frac{d\Omega_5^{(d-1)}}{2(2\pi)^{d-1}}\times\theta^{b,d}=\frac{d\Omega_{b_i}^{(d-2)}\,d\Omega_{a_i}^{(d-3)}}{2^{6\epsilon}(2\pi)^{2d-2}}\left[(1-x_3)F_\epsilon^{(b,d)}\right]^{-\epsilon}F_0^{(b,d)}x_3^2x_4^2$$
$$\times\frac{dx_3}{x_3^{1+2\epsilon}}\frac{dx_4}{x_4^{1+2\epsilon}}\frac{d\lambda}{[\lambda(1-\lambda)]^{1/2+\epsilon}}\,, \tag{B.60}$$

where

$$F_\epsilon^{(a,c)}=\frac{(1-x_3x_4/2)(1-x_4/2)^2}{2N(x_3,x_4/2,\lambda)^2}\,,\qquad F_0^{(a,c)}=\frac{(1-x_4/2)}{2N(x_3,x_4/2,\lambda)}\,, \tag{B.61}$$
$$F_\epsilon^{(b,d)}=\frac{(1-x_4/2)(1-x_3(1-x_4/2))}{4N(x_3,1-x_4/2,\lambda)^2}\,,\qquad F_0^{(b,d)}=\frac{1}{4N(x_3,1-x_4/2,\lambda)}\,, \tag{B.62}$$

and

$$N(x_3,x_4,\lambda)=1+x_4(1-2x_3)-2(1-2\lambda)\sqrt{x_4(1-x_3)(1-x_3x_4)}\,. \tag{B.63}$$

In sectors a and c, double-collinear singularities $\boldsymbol{k}_5\parallel\boldsymbol{p}_i$ and $\boldsymbol{k}_4\parallel\boldsymbol{p}_i$ are present. With the parameterization Eq. (B.55) and Eq. (B.55), these limits correspond to the limit $x_4\to 0$. We find

$$C^k\left[\frac{d\Omega_4^{(d-1)}}{2(2\pi)^{d-1}}\frac{d\Omega_5^{(d-1)}}{2(2\pi)^{d-1}}\times\theta^{a,c}\right]=\frac{d\Omega_{b_i}^{(d-2)}\,d\Omega_{a_i}^{(d-3)}}{2^{6\epsilon}(2\pi)^{2d-2}}\left[\frac{1-x_3}{2}\right]^{-\epsilon}\frac{x_3^2x_4}{2}$$
$$\times\frac{dx_3}{x_3^{1+2\epsilon}}\frac{dx_4}{x_4^{1+\epsilon}}\frac{d\lambda}{[\lambda(1-\lambda)]^{1/2+\epsilon}}\,, \tag{B.64}$$

where $k=a,c$.

In sectors b and d, the double-collinear singularity $\boldsymbol{k}_4\parallel\boldsymbol{k}_5$ is present. As can be seen from Eq. (B.56) and Eq. (B.58), this limit again corresponds to taking $x_4\to 0$. We find

$$C^k\left[\frac{d\Omega_4^{(d-1)}}{2(2\pi)^{d-1}}\frac{d\Omega_5^{(d-1)}}{2(2\pi)^{d-1}}\times\theta^{a,c}\right]=\frac{d\Omega_{b_i}^{(d-2)}\,d\Omega_{a_i}^{(d-3)}}{2^{6\epsilon}(2\pi)^{2d-2}}\left[\frac{1}{64\lambda^2}\right]^{-\epsilon}\frac{x_3^2x_4^2}{16(1-x_3)\lambda}$$
$$\times\frac{dx_3}{x_3^{1+2\epsilon}}\frac{dx_4}{x_4^{1+2\epsilon}}\frac{d\lambda}{[\lambda(1-\lambda)]^{1/2+\epsilon}}\,, \tag{B.65}$$

where $k=b,d$.

Parameterization in the case of $g\gamma$ emission

In the case of $g\gamma$ emission, no singularity arises in the limit when the gluon and the photon become collinear, $\boldsymbol{k}_4\parallel\boldsymbol{k}_5$. Accordingly, we have split the phase space into only two sectors, see Eqs. (2.65)-(2.66). We parameterize

$$(A)\quad \eta_4=x_3\,x_4\,,\quad \eta_5=x_3\,, \tag{B.66}$$
$$(B)\quad \eta_4=x_3\,,\quad \eta_5=x_3\,x_4\,, \tag{B.67}$$

and find

$$\frac{\mathrm{d}\Omega_4^{(d-1)}}{2(2\pi)^{d-1}}\frac{\mathrm{d}\Omega_5^{(d-1)}}{2(2\pi)^{d-1}}\times\theta^{A,B}=\frac{\mathrm{d}\Omega_{b_i}^{(d-2)}\,\mathrm{d}\Omega_{a_i}^{(d-3)}}{2^{6\epsilon}(2\pi)^{2d-2}}\left[(1-x_3)F_\epsilon^{(A,B)}\right]^{-\epsilon}F_0^{(A,B)}x_3^2x_4$$
$$\times\frac{\mathrm{d}x_3}{x_3^{1+2\epsilon}}\frac{\mathrm{d}x_4}{x_4^{1+\epsilon}}\frac{\mathrm{d}\lambda}{[\lambda(1-\lambda)]^{1/2+\epsilon}}\,, \tag{B.68}$$

where

$$F_\epsilon^{(A,B)}=\frac{(1-x_3x_4)(1-x_4)^2}{2N(x_3,x_4,\lambda)^2}\,,\quad F_0^{(A,B)}=\frac{(1-x_4)}{N(x_3,x_4,\lambda)}\,. \tag{B.69}$$

Also in this case, the double collinear limits correspond to $x_4\to 0$. We find

$$C^k\left[\frac{\mathrm{d}\Omega_4^{(d-1)}}{2(2\pi)^{d-1}}\frac{\mathrm{d}\Omega_5^{(d-1)}}{2(2\pi)^{d-1}}\times\theta^{A,B}\right]=\frac{\mathrm{d}\Omega_{b_i}^{(d-2)}\,\mathrm{d}\Omega_{a_i}^{(d-3)}}{2^{6\epsilon}(2\pi)^{2d-2}}\left[\frac{1-x_3}{2}\right]^{-\epsilon}x_3^2x_4$$
$$\times\frac{\mathrm{d}x_3}{x_3^{1+2\epsilon}}\frac{\mathrm{d}x_4}{x_4^{1+\epsilon}}\frac{\mathrm{d}\lambda}{[\lambda(1-\lambda)]^{1/2+\epsilon}}\,, \tag{B.70}$$

where $k=A,B$.

C INTEGRATED DOUBLE-UNRESOLVED SUBTRACTION TERMS

In this Appendix, we collect formulas relevant to integrated subtraction terms discussed in Chapter 3. We present double-soft subtraction terms for massless emitters [36, 37] in Appendix C.1. In case of massive back-to-back emitters, we present master integrals, differential equations and results for double-soft subtraction terms in Apps. C.2.1 - C.2.3, respectively. In Appendix C.3, we present triple-collinear subtraction terms. In particular, we show differential equations, computation of boundary constants and a few explicit results in Apps. C.3.1 - C.3.3, respectively.

C.1 DOUBLE-SOFT SUBTRACTION TERMS FOR MASSLESS EMITTERS

In the following, we repeat the results of Refs. [36, 37] for double-soft subtraction terms in case of massless emitters at an arbitrary angle. Adopting the notation used there, we define

$$\mathcal{S}_{ij}^{(gg)} = 2\mathcal{G}\mathcal{G}_{ij} - \mathcal{G}\mathcal{G}_{ii} - \mathcal{G}\mathcal{G}_{jj}\,, \tag{C.1}$$

$$\mathcal{S}_{ij}^{(q\bar{q})} = -2 \times \left[2\mathcal{Q}\bar{\mathcal{Q}}_{ij} - \mathcal{Q}\bar{\mathcal{Q}}_{ii} - \mathcal{Q}\bar{\mathcal{Q}}_{jj}\right]\,, \tag{C.2}$$

where $\mathcal{G}\mathcal{G}_{ij}$ and $\mathcal{Q}\bar{\mathcal{Q}}_{ij}$ are given in Eq. (2.91) and Eq. (2.92), respectively. To display results in a compact form, we abbreviate $s = \sin\delta$ and $c = \cos\delta$, where $\delta = \theta_{ij}/2$ denotes half of the relative angle between emitters i and j. We find [36, 37]

$$\begin{aligned}
\mathcal{S}_{ij}^{(gg)} &= (2\,E_{\max})^{-4\epsilon}\left[\frac{1}{8\pi^2}\frac{(4\pi)^\epsilon}{\Gamma(1-\epsilon)}\right]^2\left\{\frac{1}{2\epsilon^4} + \frac{1}{\epsilon^3}\left[\frac{11}{12} - \ln(s^2)\right]\right.\\
&+ \frac{1}{\epsilon^2}\left[2\,\mathrm{Li}_2(c^2) + \ln^2(s^2) - \frac{11}{6}\ln(s^2) + \frac{11}{3}\ln 2 - \frac{\pi^2}{4} - \frac{16}{9}\right]\\
&+ \frac{1}{\epsilon}\left[6\,\mathrm{Li}_3(s^2) + 2\,\mathrm{Li}_3(c^2) + \left(2\ln(s^2) + \frac{11}{3}\right)\mathrm{Li}_2(c^2) - \frac{2}{3}\ln^3(s^2)\right.\\
&\quad + \left(3\ln(c^2) + \frac{11}{6}\right)\ln^2(s^2) - \left(\frac{22}{3}\ln 2 + \frac{\pi^2}{2} - \frac{32}{9}\right)\ln(s^2)\\
&\quad \left. - \frac{45}{4}\zeta_3 - \frac{11}{3}\ln^2 2 - \frac{11}{36}\pi^2 - \frac{137}{18}\ln 2 + \frac{217}{54}\right]\\
&+ 4\mathrm{G}(\{-1,0,0,1\};s^2) - 7\mathrm{G}(\{0,1,0,1\};s^2) + \frac{22}{3}\mathrm{Cl}_3(2\delta) + \frac{1}{3\tan(\delta)}\mathrm{Cl}_2(2\delta)\\
&+ 2\,\mathrm{Li}_4(c^2) - 14\,\mathrm{Li}_4(s^2) + 4\,\mathrm{Li}_4\left(\frac{1}{1+s^2}\right) - 2\,\mathrm{Li}_4\left(\frac{1-s^2}{1+s^2}\right)
\end{aligned}$$

$$
\begin{aligned}
&+2\,\mathrm{Li}_4\left(\frac{s^2-1}{1+s^2}\right)+\mathrm{Li}_4\left(1-s^4\right)+\Big[10\ln(s^2)-4\ln\left(1+s^2\right)\\
&+\frac{11}{3}\Big]\,\mathrm{Li}_3\left(c^2\right)+\Big[14\ln(c^2)+2\ln(s^2)+4\ln\left(1+s^2\right)+\frac{22}{3}\Big]\,\mathrm{Li}_3\left(s^2\right)\\
&+4\ln(c^2)\,\mathrm{Li}_3\left(-s^2\right)+\frac{9}{2}\,\mathrm{Li}_2^2\left(c^2\right)-4\,\mathrm{Li}_2\left(c^2\right)\mathrm{Li}_2\left(-s^2\right)+\Big[7\ln(c^2)\ln(s^2)\\
&-\ln^2(s^2)-\frac{5}{2}\pi^2+\frac{22}{3}\ln 2-\frac{131}{18}\Big]\,\mathrm{Li}_2\left(c^2\right)+\left[\frac{2}{3}\pi^2-4\ln(c^2)\ln(s^2)\right]\times\\
&\mathrm{Li}_2\left(-s^2\right)+\frac{\ln^4(s^2)}{3}+\frac{\ln^4\left(1+s^2\right)}{6}-\ln^3(s^2)\left[\frac{4}{3}\ln(c^2)+\frac{11}{9}\right]\\
&+\ln^2(s^2)\left[7\ln^2(c^2)+\frac{11}{3}\ln(c^2)+\frac{\pi^2}{3}+\frac{22}{3}\ln 2-\frac{32}{9}\right]-\frac{\pi^2}{6}\ln^2\left(1+s^2\right)\\
&+\zeta_3\left[\frac{17}{2}\ln(s^2)-11\ln(c^2)+\frac{7}{2}\ln\left(1+s^2\right)-\frac{21}{2}\ln 2-\frac{99}{4}\right]+\ln(s^2)\times\\
&\left[-\frac{7\pi^2}{2}\ln(c^2)+\frac{22}{3}\ln^2 2-\frac{11}{18}\pi^2+\frac{137}{9}\ln 2-\frac{208}{27}\right]-12\,\mathrm{Li}_4\left(\frac{1}{2}\right)\\
&+\frac{143}{720}\pi^4-\frac{\ln^4 2}{2}+\frac{\pi^2}{2}\ln^2 2-\frac{11}{6}\pi^2\ln 2+\frac{125}{216}\pi^2+\frac{22}{9}\ln^3 2\\
&+\frac{137}{18}\ln^2 2+\frac{434}{27}\ln 2-\frac{649}{81}+\mathcal{O}(\epsilon)\Bigg\},
\end{aligned}
\tag{C.3}
$$

and

$$
\begin{aligned}
\mathcal{S}_{ij}^{(q\bar{q})}&=(2\,E_{\max})^{-4\epsilon}\left[\frac{1}{8\pi^2}\frac{(4\pi)^\epsilon}{\Gamma(1-\epsilon)}\right]^2\Bigg\{-\frac{1}{3\epsilon^3}+\frac{1}{\epsilon^2}\left[\frac{2}{3}\ln(s^2)-\frac{4}{3}\ln 2\right.\\
&\left.+\frac{13}{18}\right]+\frac{1}{\epsilon}\left[-\frac{4}{3}\mathrm{Li}_2\left(c^2\right)-\frac{2}{3}\ln^2(s^2)+\ln(s^2)\left(\frac{8}{3}\ln 2-\frac{13}{9}\right)+\frac{\pi^2}{9}\right.\\
&\left.+\frac{4}{3}\ln^2 2+\frac{35}{9}\ln 2-\frac{125}{54}\right]-\frac{8}{3}\mathrm{Cl}_3(2\delta)-\frac{2}{3\tan(\delta)}\mathrm{Cl}_2(2\delta)-\frac{4}{3}\mathrm{Li}_3\left(c^2\right)\\
&-\frac{8}{3}\mathrm{Li}_3\left(s^2\right)+\mathrm{Li}_2\left(c^2\right)\left[\frac{29}{9}-\frac{8}{3}\ln 2\right]+\frac{4}{9}\ln^3(s^2)+\ln^2(s^2)\left[-\frac{4}{3}\ln(c^2)\right.\\
&\left.-\frac{8}{3}\ln 2+\frac{13}{9}\right]+\ln(s^2)\left[-\frac{8}{3}\ln^2 2-\frac{70}{9}\ln 2+\frac{2}{9}\pi^2+\frac{107}{27}\right]+9\zeta_3\\
&+\frac{2\pi^2}{3}\ln 2-\frac{8}{9}\ln^3 2-\frac{23}{108}\pi^2-\frac{35}{9}\ln^2 2-\frac{223}{27}\ln 2+\frac{601}{162}+\mathcal{O}(\epsilon)\Bigg\},
\end{aligned}
\tag{C.4}
$$

where Clausen functions $\mathrm{Cl}_n(z)$ are defined in Eq. (A.12).

C.2 DOUBLE-SOFT SUBTRACTION TERMS FOR MASSIVE EMITTERS

In the following Section, we present formulas for the computation of double-soft subtraction with massive emitters that are back-to-back, discussed in Sec. 3.2.2.

C.2.1 *Master integrals*

We find the following set of thirteen master integrals

$$\begin{aligned}
I_1 &= \left\langle 1 \right\rangle , \\
I_{2,\ldots,4} &= \left\{ \left\langle \frac{1}{D_3} \right\rangle, \left\langle \frac{1}{D_2 D_3} \right\rangle, \left\langle \frac{1}{D_2 D_3 D_5} \right\rangle \right\} \subset T^{2,3,5} , \\
I_{5,\ldots,9} &= \left\{ \left\langle \frac{D_2}{D_6} \right\rangle, \left\langle \frac{D_5}{D_6} \right\rangle, \left\langle \frac{1}{D_6} \right\rangle, \left\langle \frac{1}{D_2 D_6} \right\rangle, \left\langle \frac{1}{D_2 D_5 D_6} \right\rangle \right\} \subset T^{2,5,6} , \\
I_{10} &= \left\{ \left\langle \frac{1}{D_2 D_7} \right\rangle \right\} \subset T^{2,5,7} , \\
I_{11,12} &= \left\{ \left\langle \frac{1}{D_4 D_6} \right\rangle, \left\langle \frac{1}{D_4 D_5 D_6} \right\rangle \right\} \subset T^{4,5,6} , \\
I_{13} &= \left\{ \left\langle \frac{1}{D_4 D_7} \right\rangle \right\} \subset T^{4,5,7} ,
\end{aligned} \tag{C.5}$$

where topologies T^{a_1,a_2,a_3} are defined in Eq. (3.57).

C.2.2 *Differential equations*

In order to display the transformation matrix $\hat{T}_{\mathrm{can}}$, which was defined in Eq. (3.62), we write

$$\hat{T}_{\mathrm{can}} = \hat{T}_{\mathrm{can}}^{\mathrm{diag}} + \hat{T}_{\mathrm{can}}^{\mathrm{extra}} , \tag{C.6}$$

where

$$\begin{aligned}
\hat{T}_{\mathrm{can}}^{\mathrm{diag}} = \mathrm{diag}\Bigg(& z, \frac{1-2\epsilon}{3\beta\epsilon}, \frac{(1-2\epsilon)^2}{9\beta^2\epsilon^2}, \frac{(1-2\epsilon)^2}{9\beta\epsilon^2 z}, 0, 0, 0, \frac{(1-2\epsilon)^2}{9\beta^2\epsilon^2}, \frac{2(1-2\epsilon)^2}{9\beta\epsilon^2(z+1)}, \\
& \frac{(1-2\epsilon)^2}{9\beta^2\epsilon^2}, \frac{(1-2\epsilon)^2}{9\beta^2\epsilon^2}, \frac{2(1-2\epsilon)^2}{9\beta\epsilon^2 z(z+1)}, \frac{(1-2\epsilon)^2}{9\beta^2\epsilon^2} \Bigg) ,
\end{aligned} \tag{C.7}$$

and the non-zero elements of $\hat{T}_{\mathrm{can}}^{\mathrm{extra}}$ read

$$\left(\hat{T}_{\mathrm{can}}^{\mathrm{extra}} \right)_{\{5,1\}} = -\frac{z}{2} , \tag{C.8}$$

$$\left(\hat{T}_{\text{can}}^{\text{extra}}\right)_{\{5,5\}} = \frac{(2\epsilon-1)(z+1)\left(\beta^2(4\epsilon-1)(z-1)+(2\epsilon-1)(z+3)\right)}{12\beta^2\epsilon(4\epsilon-1)}, \tag{C.9}$$

$$\left(\hat{T}_{\text{can}}^{\text{extra}}\right)_{\{5,6\}} = -\frac{11(2\epsilon-1)(z+1)(3\epsilon z+\epsilon-z-1)}{36\beta^\epsilon(4\epsilon-1)}, \tag{C.10}$$

$$\left(\hat{T}_{\text{can}}^{\text{extra}}\right)_{\{5,7\}} = -\frac{(2\epsilon-1)\left(\epsilon\left(15z^2+18z+7\right)-5z^2-10z-7\right)}{18\beta^\epsilon(4\epsilon-1)}, \tag{C.11}$$

$$\left(\hat{T}_{\text{can}}^{\text{extra}}\right)_{\{6,1\}} = -\frac{(2\epsilon-1)z(z+1)}{2\beta^2(4\epsilon-3)}, \tag{C.12}$$

$$\begin{aligned}\left(\hat{T}_{\text{can}}^{\text{extra}}\right)_{\{6,5\}} = {} & \frac{(1-2\epsilon)^2(z+1)}{12\beta^4\epsilon(4\epsilon-3)(4\epsilon-1)}\Bigg[\beta^2\left(8\epsilon\left(z^2+z+1\right)-3(z+1)^2\right) \\ & -(2\epsilon-1)(z+1)^2\Bigg],\end{aligned} \tag{C.13}$$

$$\begin{aligned}\left(\hat{T}_{\text{can}}^{\text{extra}}\right)_{\{6,6\}} = {} & -\frac{11(1-2\epsilon)^2(z+1)}{36\beta^3\epsilon(4\epsilon-3)(4\epsilon-1)}\Bigg[\beta^2\left(2\epsilon\left(z^2+1\right)-(z+1)^2\right) \\ & +\epsilon(z+1)^2\Bigg],\end{aligned} \tag{C.14}$$

$$\begin{aligned}\left(\hat{T}_{\text{can}}^{\text{extra}}\right)_{\{6,7\}} = {} & -\frac{(1-2\epsilon)^2}{18\beta^3\epsilon(4\epsilon-3)(4\epsilon-1)}\Bigg[\epsilon(z+1)^2(5z+7) \\ & +\beta^2\left(2\epsilon\left(5z^3+3z^2+9z+7\right)-5z^3-15z^2-21z-7\right)\Bigg],\end{aligned} \tag{C.15}$$

$$\left(\hat{T}_{\text{can}}^{\text{extra}}\right)_{\{7,5\}} = \frac{(1-2\epsilon)^2(z+1)}{6\beta^2\epsilon(4\epsilon-1)}, \tag{C.16}$$

$$\left(\hat{T}_{\text{can}}^{\text{extra}}\right)_{\{7,6\}} = -\frac{11(1-2\epsilon)^2(z+1)}{36\beta^\epsilon(4\epsilon-1)}, \tag{C.17}$$

$$\left(\hat{T}_{\text{can}}^{\text{extra}}\right)_{\{7,7\}} = -\frac{(1-2\epsilon)^2(5z+7)}{18\beta^\epsilon(4\epsilon-1)}, \tag{C.18}$$

where $\left(\hat{T}_{\text{can}}^{\text{extra}}\right)_{\{i,j\}}$ denotes the entry in the i-th row and the j-th column of $\hat{T}_{\text{can}}^{\text{extra}}$.

To present the system of differential equations in Eq. (3.63), we write

$$\mathrm{d}\boldsymbol{J} = \epsilon\sum_{k=1}^{11}\hat{a}_k\,\mathrm{dln}\left(R_k\right), \tag{C.19}$$

where we defined the alphabet

$$\begin{gathered} R_1 = z, \quad R_2 = 1+z, \quad R_3 = \beta, \quad R_{4,5} = 1\pm\beta, \\ R_{6,7} = z+\frac{1\pm\beta}{2}, \quad R_{8,9} = z+\frac{1\pm\beta}{1\mp\beta}, \quad R_{10,11} = 1+z+\frac{1\pm\beta}{1\mp\beta}. \end{gathered} \tag{C.20}$$

The matrices $\hat{a}_k$ in Eq. (C.19) read

$$\hat{a}_1 = \begin{pmatrix} -2 & 0 & 0 & 0 & 0 & 0 & 0 & 0 & 0 & 0 & 0 & 0 & 0 \\ 0 & -2 & 0 & 0 & 0 & 0 & 0 & 0 & 0 & 0 & 0 & 0 & 0 \\ 0 & 0 & -2 & 0 & 0 & 0 & 0 & 0 & 0 & 0 & 0 & 0 & 0 \\ 0 & 0 & 0 & -2 & 0 & 0 & 0 & 0 & 0 & 0 & 0 & 0 & 0 \\ 0 & 0 & 0 & 0 & 0 & 0 & 0 & 0 & 0 & 0 & 0 & 0 & 0 \\ 0 & 0 & 0 & 0 & 0 & -7 & -\frac{70}{11} & 0 & 0 & 0 & 0 & 0 & 0 \\ 0 & 0 & 0 & 0 & 0 & \frac{11}{2} & 5 & 0 & 0 & 0 & 0 & 0 & 0 \\ 0 & 0 & 0 & 0 & 0 & 0 & 0 & 0 & 0 & 0 & 0 & 0 & 0 \\ 0 & \frac{3}{4} & 0 & 0 & 0 & \frac{11}{16} & \frac{5}{8} & 0 & 0 & 0 & 0 & 0 & 0 \\ 0 & 0 & 0 & 0 & \frac{3}{2} & 0 & 0 & 0 & 0 & -2 & 0 & 0 & 0 \\ 0 & 0 & 0 & 0 & \frac{3}{2} & 0 & 0 & 0 & 0 & 0 & -2 & 0 & 0 \\ 0 & 0 & 0 & 0 & 0 & 0 & 0 & 0 & 0 & 0 & 0 & -2 & 0 \\ 0 & 0 & 0 & 0 & -\frac{3}{2} & 0 & 0 & 0 & 0 & 0 & 0 & 0 & -2 \end{pmatrix}, \tag{C.21}$$

$$\hat{a}_2 = \begin{pmatrix} 0 & 0 & 0 & 0 & 0 & 0 & 0 & 0 & 0 & 0 & 0 & 0 & 0 \\ 0 & 0 & 0 & 0 & 0 & 0 & 0 & 0 & 0 & 0 & 0 & 0 & 0 \\ 0 & 0 & 0 & 0 & 0 & 0 & 0 & 0 & 0 & 0 & 0 & 0 & 0 \\ 0 & 0 & 0 & 0 & 0 & 0 & 0 & 0 & 0 & 0 & 0 & 0 & 0 \\ -3 & 0 & 0 & 0 & -2 & 0 & 0 & 0 & 0 & 0 & 0 & 0 & 0 \\ 0 & 0 & 0 & 0 & 0 & -2 & -\frac{24}{11} & 0 & 0 & 0 & 0 & 0 & 0 \\ 0 & 0 & 0 & 0 & 0 & 0 & 0 & 0 & 0 & 0 & 0 & 0 & 0 \\ 0 & 0 & 0 & 0 & 0 & 0 & 0 & 0 & 0 & 0 & 0 & 0 & 0 \\ 0 & 0 & 0 & 0 & 0 & 0 & 0 & 0 & -2 & 0 & 0 & 0 & 0 \\ 0 & 0 & 0 & 0 & 0 & 0 & 0 & 0 & 0 & 0 & 0 & 0 & 0 \\ 0 & 0 & 0 & 0 & 0 & 0 & 0 & 0 & 0 & 0 & 0 & 0 & 0 \\ 0 & 0 & 0 & 0 & 0 & 0 & 0 & 0 & 0 & 0 & 0 & -2 & 0 \\ 0 & 0 & 0 & 0 & 0 & 0 & 0 & 0 & 0 & 0 & 0 & 0 & 0 \end{pmatrix}, \tag{C.22}$$

$$\hat{a}_3 = \begin{pmatrix} 0&0&0&0&0&0&0&0&0&0&0&0&0\\ 0&2&0&0&0&0&0&0&0&0&0&0&0\\ 0&0&4&0&0&0&0&0&0&0&0&0&0\\ 0&0&0&2&0&0&0&0&0&0&0&0&0\\ 0&0&0&0&4&0&0&0&0&0&0&0&0\\ 0&0&0&0&0&2&0&0&0&0&0&0&0\\ 0&0&0&0&0&0&2&0&0&0&0&0&0\\ 0&0&0&0&0&0&0&4&0&0&0&0&0\\ 0&0&0&0&0&0&0&0&2&0&0&0&0\\ 0&0&0&0&0&0&0&0&0&4&0&0&0\\ 0&0&0&0&0&0&0&0&0&0&4&0&0\\ 0&0&0&0&0&0&0&0&0&0&0&2&0\\ 0&0&0&0&0&0&0&0&0&0&0&0&4 \end{pmatrix}, \tag{C.23}$$

$$\hat{a}_4 = \begin{pmatrix} 0&0&0&0&0&0&0&0&0&0&0&0&0\\ -\frac{3}{2}&-1&0&0&0&0&0&0&0&0&0&0&0\\ 0&-3&-2&0&0&0&0&0&0&0&0&0&0\\ \frac{9}{4}&0&-1&0&0&0&0&0&0&0&0&0&0\\ 0&0&0&0&-2&-\frac{11}{6}&-\frac{5}{3}&0&0&0&0&0&0\\ \frac{45}{11}&0&0&0&-\frac{42}{11}&-1&0&0&0&0&0&0&0\\ -\frac{9}{2}&0&0&0&3&0&-1&0&0&0&0&0&0\\ 0&-\frac{3}{2}&0&0&0&-\frac{11}{4}&-3&-2&0&0&0&0&0\\ \frac{9}{8}&0&0&0&\frac{3}{8}&0&0&-\frac{1}{2}&0&0&0&0&0\\ 0&-\frac{3}{2}&0&0&0&0&-\frac{1}{2}&0&0&-2&0&0&0\\ 0&0&0&0&\frac{3}{4}&-\frac{11}{8}&-\frac{5}{4}&0&0&0&-1&0&0\\ \frac{9}{8}&\frac{3}{8}&0&0&\frac{9}{16}&\frac{11}{32}&\frac{7}{16}&0&0&0&-\frac{1}{4}&0&0\\ 0&-\frac{3}{2}&0&0&0&0&\frac{1}{2}&0&0&0&0&0&-2 \end{pmatrix}, \tag{C.24}$$

$$\hat{a}_5 = \begin{pmatrix} 0 & 0 & 0 & 0 & 0 & 0 & 0 & 0 & 0 & 0 & 0 & 0 & 0 \\ \frac{3}{2} & -1 & 0 & 0 & 0 & 0 & 0 & 0 & 0 & 0 & 0 & 0 & 0 \\ 0 & 3 & -2 & 0 & 0 & 0 & 0 & 0 & 0 & 0 & 0 & 0 & 0 \\ -\frac{9}{4} & 0 & 1 & 0 & 0 & 0 & 0 & 0 & 0 & 0 & 0 & 0 & 0 \\ 0 & 0 & 0 & 0 & -2 & \frac{11}{6} & \frac{5}{3} & 0 & 0 & 0 & 0 & 0 & 0 \\ -\frac{45}{11} & 0 & 0 & 0 & \frac{42}{11} & -1 & 0 & 0 & 0 & 0 & 0 & 0 & 0 \\ \frac{9}{2} & 0 & 0 & 0 & -3 & 0 & -1 & 0 & 0 & 0 & 0 & 0 & 0 \\ 0 & \frac{3}{2} & 0 & 0 & 0 & \frac{11}{4} & 3 & -2 & 0 & 0 & 0 & 0 & 0 \\ -\frac{9}{8} & 0 & 0 & 0 & -\frac{3}{8} & 0 & 0 & \frac{1}{2} & 0 & 0 & 0 & 0 & 0 \\ 0 & \frac{3}{2} & 0 & 0 & 0 & 0 & \frac{1}{2} & 0 & 0 & -2 & 0 & 0 & 0 \\ 0 & 0 & 0 & 0 & \frac{3}{4} & \frac{11}{8} & \frac{5}{4} & 0 & 0 & 0 & -1 & 0 & 0 \\ -\frac{9}{8} & \frac{3}{8} & 0 & 0 & -\frac{9}{16} & \frac{11}{32} & \frac{7}{16} & 0 & 0 & 0 & \frac{1}{4} & 0 & 0 \\ 0 & \frac{3}{2} & 0 & 0 & 0 & 0 & -\frac{1}{2} & 0 & 0 & 0 & 0 & 0 & -2 \end{pmatrix}, \tag{C.25}$$

$$\hat{a}_6 = \begin{pmatrix} 0 & 0 & 0 & 0 & 0 & 0 & 0 & 0 & 0 & 0 & 0 & 0 & 0 \\ 0 & 0 & 0 & 0 & 0 & 0 & 0 & 0 & 0 & 0 & 0 & 0 & 0 \\ 0 & 0 & 0 & 0 & 0 & 0 & 0 & 0 & 0 & 0 & 0 & 0 & 0 \\ 0 & 0 & 0 & 0 & 0 & 0 & 0 & 0 & 0 & 0 & 0 & 0 & 0 \\ 0 & 0 & 0 & 0 & 0 & 0 & 0 & 0 & 0 & 0 & 0 & 0 & 0 \\ 0 & 0 & 0 & 0 & 0 & 0 & 0 & 0 & 0 & 0 & 0 & 0 & 0 \\ 0 & 0 & 0 & 0 & 0 & 0 & 0 & 0 & 0 & 0 & 0 & 0 & 0 \\ 0 & 0 & 0 & 0 & 0 & 0 & 0 & 0 & 0 & 0 & 0 & 0 & 0 \\ 0 & 0 & 0 & 0 & 0 & 0 & 0 & 0 & 0 & 0 & 0 & 0 & 0 \\ 0 & 0 & 0 & 0 & 0 & 0 & 0 & 0 & 0 & 0 & 0 & 0 & 0 \\ 0 & \frac{3}{2} & 0 & 0 & -\frac{3}{4} & \frac{11}{8} & \frac{7}{4} & 0 & 0 & 0 & -1 & 0 & 0 \\ 0 & -\frac{3}{8} & 0 & 0 & \frac{3}{16} & -\frac{11}{32} & -\frac{7}{16} & 0 & 0 & 0 & \frac{1}{4} & 0 & 0 \\ 0 & 0 & 0 & 0 & 0 & 0 & 0 & 0 & 0 & 0 & 0 & 0 & 0 \end{pmatrix}, \tag{C.26}$$

$$\hat{a}_7 = \begin{pmatrix} 0 & 0 & 0 & 0 & 0 & 0 & 0 & 0 & 0 & 0 & 0 & 0 & 0 \\ 0 & 0 & 0 & 0 & 0 & 0 & 0 & 0 & 0 & 0 & 0 & 0 & 0 \\ 0 & 0 & 0 & 0 & 0 & 0 & 0 & 0 & 0 & 0 & 0 & 0 & 0 \\ 0 & 0 & 0 & 0 & 0 & 0 & 0 & 0 & 0 & 0 & 0 & 0 & 0 \\ 0 & 0 & 0 & 0 & 0 & 0 & 0 & 0 & 0 & 0 & 0 & 0 & 0 \\ 0 & 0 & 0 & 0 & 0 & 0 & 0 & 0 & 0 & 0 & 0 & 0 & 0 \\ 0 & 0 & 0 & 0 & 0 & 0 & 0 & 0 & 0 & 0 & 0 & 0 & 0 \\ 0 & 0 & 0 & 0 & 0 & 0 & 0 & 0 & 0 & 0 & 0 & 0 & 0 \\ 0 & 0 & 0 & 0 & 0 & 0 & 0 & 0 & 0 & 0 & 0 & 0 & 0 \\ 0 & 0 & 0 & 0 & 0 & 0 & 0 & 0 & 0 & 0 & 0 & 0 & 0 \\ 0 & -\frac{3}{2} & 0 & 0 & -\frac{3}{4} & -\frac{11}{8} & -\frac{7}{4} & 0 & 0 & 0 & -1 & 0 & 0 \\ 0 & -\frac{3}{8} & 0 & 0 & -\frac{3}{16} & -\frac{11}{32} & -\frac{7}{16} & 0 & 0 & 0 & -\frac{1}{4} & 0 & 0 \\ 0 & 0 & 0 & 0 & 0 & 0 & 0 & 0 & 0 & 0 & 0 & 0 & 0 \end{pmatrix}, \tag{C.27}$$

$$\hat{a}_8 = \begin{pmatrix} 0 & 0 & 0 & 0 & 0 & 0 & 0 & 0 & 0 & 0 & 0 & 0 & 0 \\ 0 & 0 & 0 & 0 & 0 & 0 & 0 & 0 & 0 & 0 & 0 & 0 & 0 \\ 0 & 0 & 0 & 0 & 0 & 0 & 0 & 0 & 0 & 0 & 0 & 0 & 0 \\ 0 & 0 & 0 & 0 & 0 & 0 & 0 & 0 & 0 & 0 & 0 & 0 & 0 \\ \frac{3}{2} & 0 & 0 & 0 & -1 & 0 & \frac{1}{3} & 0 & 0 & 0 & 0 & 0 & 0 \\ \frac{54}{11} & 0 & 0 & 0 & -\frac{36}{11} & 0 & \frac{12}{11} & 0 & 0 & 0 & 0 & 0 & 0 \\ -\frac{9}{2} & 0 & 0 & 0 & 3 & 0 & -1 & 0 & 0 & 0 & 0 & 0 & 0 \\ 0 & 0 & 0 & 0 & 0 & 0 & 0 & 0 & 0 & 0 & 0 & 0 & 0 \\ 0 & 0 & 0 & 0 & 0 & 0 & 0 & 0 & 0 & 0 & 0 & 0 & 0 \\ 0 & 0 & 0 & 0 & 0 & 0 & 0 & 0 & 0 & 0 & 0 & 0 & 0 \\ 0 & 0 & 0 & 0 & 0 & 0 & 0 & 0 & 0 & 0 & 0 & 0 & 0 \\ 0 & 0 & 0 & 0 & 0 & 0 & 0 & 0 & 0 & 0 & 0 & 0 & 0 \\ 0 & 0 & 0 & 0 & 0 & 0 & 0 & 0 & 0 & 0 & 0 & 0 & 0 \end{pmatrix}, \tag{C.28}$$

$$\hat{a}_9 = \begin{pmatrix} 0 & 0 & 0 & 0 & 0 & 0 & 0 & 0 & 0 & 0 & 0 & 0 & 0 \\ 0 & 0 & 0 & 0 & 0 & 0 & 0 & 0 & 0 & 0 & 0 & 0 & 0 \\ 0 & 0 & 0 & 0 & 0 & 0 & 0 & 0 & 0 & 0 & 0 & 0 & 0 \\ 0 & 0 & 0 & 0 & 0 & 0 & 0 & 0 & 0 & 0 & 0 & 0 & 0 \\ \frac{3}{2} & 0 & 0 & 0 & -1 & 0 & -\frac{1}{3} & 0 & 0 & 0 & 0 & 0 & 0 \\ -\frac{54}{11} & 0 & 0 & 0 & \frac{36}{11} & 0 & \frac{12}{11} & 0 & 0 & 0 & 0 & 0 & 0 \\ \frac{9}{2} & 0 & 0 & 0 & -3 & 0 & -1 & 0 & 0 & 0 & 0 & 0 & 0 \\ 0 & 0 & 0 & 0 & 0 & 0 & 0 & 0 & 0 & 0 & 0 & 0 & 0 \\ 0 & 0 & 0 & 0 & 0 & 0 & 0 & 0 & 0 & 0 & 0 & 0 & 0 \\ 0 & 0 & 0 & 0 & 0 & 0 & 0 & 0 & 0 & 0 & 0 & 0 & 0 \\ 0 & 0 & 0 & 0 & 0 & 0 & 0 & 0 & 0 & 0 & 0 & 0 & 0 \\ 0 & 0 & 0 & 0 & 0 & 0 & 0 & 0 & 0 & 0 & 0 & 0 & 0 \\ 0 & 0 & 0 & 0 & 0 & 0 & 0 & 0 & 0 & 0 & 0 & 0 & 0 \end{pmatrix}, \tag{C.29}$$

$$\hat{a}_{10} = \begin{pmatrix} 0 & 0 & 0 & 0 & 0 & 0 & 0 & 0 & 0 & 0 & 0 & 0 & 0 \\ 0 & 0 & 0 & 0 & 0 & 0 & 0 & 0 & 0 & 0 & 0 & 0 & 0 \\ 0 & 0 & 0 & 0 & 0 & 0 & 0 & 0 & 0 & 0 & 0 & 0 & 0 \\ 0 & 0 & 0 & 0 & 0 & 0 & 0 & 0 & 0 & 0 & 0 & 0 & 0 \\ 0 & 0 & 0 & 0 & 0 & 0 & 0 & 0 & 0 & 0 & 0 & 0 & 0 \\ 0 & 0 & 0 & 0 & 0 & 0 & 0 & 0 & 0 & 0 & 0 & 0 & 0 \\ 0 & 0 & 0 & 0 & 0 & 0 & 0 & 0 & 0 & 0 & 0 & 0 & 0 \\ 0 & -\frac{3}{2} & 0 & 0 & -\frac{3}{4} & -\frac{11}{8} & -\frac{5}{4} & -1 & 0 & 0 & 0 & 0 & 0 \\ 0 & -\frac{3}{8} & 0 & 0 & -\frac{3}{16} & -\frac{11}{32} & -\frac{5}{16} & -\frac{1}{4} & 0 & 0 & 0 & 0 & 0 \\ 0 & 0 & 0 & 0 & 0 & 0 & 0 & 0 & 0 & 0 & 0 & 0 & 0 \\ 0 & 0 & 0 & 0 & 0 & 0 & 0 & 0 & 0 & 0 & 0 & 0 & 0 \\ 0 & 0 & 0 & 0 & 0 & 0 & 0 & 0 & 0 & 0 & 0 & 0 & 0 \\ 0 & 0 & 0 & 0 & 0 & 0 & 0 & 0 & 0 & 0 & 0 & 0 & 0 \end{pmatrix}, \tag{C.30}$$

$$\hat{a}_{11} = \begin{pmatrix} 0 & 0 & 0 & 0 & 0 & 0 & 0 & 0 & 0 & 0 & 0 & 0 & 0 \\ 0 & 0 & 0 & 0 & 0 & 0 & 0 & 0 & 0 & 0 & 0 & 0 & 0 \\ 0 & 0 & 0 & 0 & 0 & 0 & 0 & 0 & 0 & 0 & 0 & 0 & 0 \\ 0 & 0 & 0 & 0 & 0 & 0 & 0 & 0 & 0 & 0 & 0 & 0 & 0 \\ 0 & 0 & 0 & 0 & 0 & 0 & 0 & 0 & 0 & 0 & 0 & 0 & 0 \\ 0 & 0 & 0 & 0 & 0 & 0 & 0 & 0 & 0 & 0 & 0 & 0 & 0 \\ 0 & 0 & 0 & 0 & 0 & 0 & 0 & 0 & 0 & 0 & 0 & 0 & 0 \\ 0 & \frac{3}{2} & 0 & 0 & -\frac{3}{4} & \frac{11}{8} & \frac{5}{4} & -1 & 0 & 0 & 0 & 0 & 0 \\ 0 & -\frac{3}{8} & 0 & 0 & \frac{3}{16} & -\frac{11}{32} & -\frac{5}{16} & \frac{1}{4} & 0 & 0 & 0 & 0 & 0 \\ 0 & 0 & 0 & 0 & 0 & 0 & 0 & 0 & 0 & 0 & 0 & 0 & 0 \\ 0 & 0 & 0 & 0 & 0 & 0 & 0 & 0 & 0 & 0 & 0 & 0 & 0 \\ 0 & 0 & 0 & 0 & 0 & 0 & 0 & 0 & 0 & 0 & 0 & 0 & 0 \\ 0 & 0 & 0 & 0 & 0 & 0 & 0 & 0 & 0 & 0 & 0 & 0 & 0 \end{pmatrix} . \tag{C.31}$$

C.2.3 *Results*

Coefficients of $1/\epsilon$ poles of the functions $f_{ij}^{gg,q\bar{q}}(\beta,\epsilon)$ can be expressed though HPLs of β up to weight three. We employ the Duhr-Gangl-Rhodes algorithm [266] to write them in terms of independent classical polylogarithms. We abbreviate

$$x_\beta = \frac{1-\beta}{1+\beta}, \qquad y_\beta^\pm = \frac{1\pm\beta}{2}, \qquad z_\beta = 1+\beta^2, \tag{C.32}$$

and find

$$\begin{aligned} f_{AA}^{gg}(\beta,\epsilon) = & -\frac{1}{8\epsilon^3} + \frac{1}{\epsilon^2}\frac{1}{4\beta}\Big\{\ln(x_\beta)+\beta\Big\} + \frac{1}{\epsilon}\frac{1}{4\beta}\Big\{2\beta - 3\ln(x_\beta) - 8\beta\ln(2) \\ & - 2\Big[\mathrm{Li}_2(y_\beta^-) + \mathrm{Li}_2(\beta) - \mathrm{Li}_2(-\beta)\Big] + y_\beta^- \ln^2(x_\beta) \\ & - \ln^2(y_\beta^-) + \zeta_2\Big\} + \mathcal{O}(\epsilon^0) , \end{aligned} \tag{C.33}$$

$$\begin{aligned} f_{AB}^{gg}(\beta,\epsilon) = & \frac{1}{\epsilon^3}\frac{1}{8\beta}\Big\{3\beta + 2z_\beta\ln(x_\beta)\Big\} - \frac{1}{\epsilon^2}\frac{1}{24\beta^2}\Big\{32\beta^2 + \beta\left(31+13\beta^2\right)\ln(x_\beta) \\ & + 12z_\beta\beta\left[\mathrm{Li}_2(\beta) - \mathrm{Li}_2(-\beta)\right] + 3z_\beta^2\ln^2(x_\beta)\Big\} \\ & - \frac{1}{\epsilon}\frac{1}{72\beta^2}\Big\{104\beta^2 + 27z_\beta^2\zeta_3 - 120\beta^2\ln(2) \\ & + 36z_\beta^2\Big(\mathrm{Li}_3(x_\beta) - \mathrm{Li}_3(y_\beta^-) - \mathrm{Li}_3(y_\beta^+)\Big) + 72\beta z_\beta\left(\mathrm{Li}_3(\beta) - \mathrm{Li}_3(-\beta)\right) \\ & + 2\beta\left(62\beta^2 - 25\right)\ln(x_\beta) - 12\beta\left(4\beta^2+13\right)\left(\mathrm{Li}_2(\beta) - \mathrm{Li}_2(-\beta)\right) \end{aligned}$$

$$
\begin{aligned}
&+ 6\beta\left(\beta^2-2\right)\Big(\zeta_2 - 2\,\mathrm{Li}_2(y_\beta^-) - \ln^2(y_\beta^-)\Big) \\
&- 18 z_\beta^2 \ln(x_\beta)\left(\mathrm{Li}_2(\beta) - \mathrm{Li}_2(-\beta)\right) \\
&- 3\Big(24 + 2\beta + 9\beta^2 - \beta^3 + 12\beta^4\Big)\ln^2(x_\beta) \\
&- 132\beta z_\beta \ln(2)\ln(x_\beta) - 18\zeta_2 z_\beta^2\Big(3\ln(x_\beta) - 2\ln(y_\beta^-)\Big) \\
&+ 18 z_\beta^2 \ln(\beta)\ln^2(x_\beta) + 6 z_\beta\left(3 + 2\beta + 3\beta^2\right)\ln^3(x_\beta) \\
&+ 6 z_\beta^2\Big(3\ln(x_\beta)\ln^2(y_\beta^-) - 2\ln^3(y_\beta^-) - 6\ln^2(x_\beta)\ln(y_\beta^-)\Big)\Bigg\} \\
&+ \mathcal{O}(\epsilon^0)\,,
\end{aligned}
\tag{C.34}
$$

$$
f_{AA}^{q\bar{q}}(\beta,\epsilon) = -\frac{1}{4\epsilon^2} + \frac{1}{\epsilon}\frac{1}{4\beta}\Big\{6\beta - 4\beta\ln(2) + \ln(x_\beta)\Big\} + \mathcal{O}(\epsilon^0)\,,
\tag{C.35}
$$

$$
\begin{aligned}
f_{AB}^{q\bar{q}}(\beta,\epsilon) = {}& \frac{1}{\epsilon^2}\frac{1}{12\beta}\Big\{z_\beta\ln(x_\beta) - \beta\Big\} + \frac{1}{\epsilon}\frac{1}{72\beta}\Big\{34\beta - \left(37\beta^2 + 43\right)\ln(x_\beta) \\
&- 24 z_\beta\Big(\mathrm{Li}_2(y_\beta^-) + \mathrm{Li}_2(\beta) - \mathrm{Li}_2(-\beta)\Big) - 24\beta\ln(2) \\
&+ 6 z_\beta\Big(\ln^2(x_\beta) - 2\ln^2(y_\beta^-) + 4\ln(2)\ln(x_\beta) + 2\zeta_2\Big)\Big\} + \mathcal{O}(\epsilon^0)\,.
\end{aligned}
\tag{C.36}
$$

In the threshold limit, energies of emitting particles are comparable to their masses, i. e. $E \approx m \Leftrightarrow \beta \ll 1$. We perform a Taylor expansion in small β and find

$$
\begin{aligned}
f_{AA}^{gg}(\beta\approx 0,\epsilon) = {}& \beta^0\left[-\frac{1}{8\epsilon^3} - \frac{1}{4\epsilon^2} + \frac{1-2\ln(2)}{\epsilon} + 2\left(2\ln(2) - 1 - \frac{\pi^2}{6}\right)\right] \\
&+ \beta^2\left[-\frac{1}{6\epsilon^2} - \frac{4}{9\epsilon} + \left(\frac{1}{27} - \frac{8}{3}\ln(2)\right)\right] + \mathcal{O}\left(\beta^4\right)\,,
\end{aligned}
\tag{C.37}
$$

$$
\begin{aligned}
f_{AB}^{gg}(\beta\approx 0,\epsilon) = {}& \beta^0\left[-\frac{1}{8\epsilon^3} - \frac{1}{4\epsilon^2} + \frac{1-2\ln(2)}{\epsilon} + 2\left(2\ln(2) - 1 - \frac{\pi^2}{6}\right)\right] \\
&+ \beta^2\Bigg[-\frac{2}{3\epsilon^3} - \frac{1}{2\epsilon^2} + \frac{1}{\epsilon}\left(1 - \frac{44}{9}\ln(2)\right) \\
&+ \left(\frac{104}{27}\ln(2) - \frac{1}{3} - \frac{22}{27}\pi^2\right)\Bigg] + \mathcal{O}\left(\beta^4\right)\,,
\end{aligned}
\tag{C.38}
$$

$$
\begin{aligned}
f_{AA}^{q\bar{q}}(\beta\approx 0,\epsilon) = {}& \beta^0\left[-\frac{1}{4\epsilon^2} + \frac{1-\ln(2)}{\epsilon} + \left(4\ln(2) - \frac{3}{2} - \frac{\pi^2}{6}\right)\right] \\
&+ \beta^2\left[-\frac{1}{6\epsilon} + \left(\frac{13}{18} - \frac{4}{3}\ln(2)\right)\right] + \mathcal{O}\left(\beta^4\right)\,,
\end{aligned}
\tag{C.39}
$$

$$
\begin{aligned}
f_{AB}^{q\bar{q}}(\beta\approx 0,\epsilon) = {}& \beta^0\left[-\frac{1}{4\epsilon^2} + \frac{1-\ln(2)}{\epsilon} + \left(4\ln(2) - \frac{3}{2} - \frac{\pi^2}{6}\right)\right] \\
&+ \beta^2\Bigg[-\frac{2}{9\epsilon^2} + \frac{1}{\epsilon}\left(\frac{25}{54} - \frac{8}{9}\ln(2)\right) + \Bigg(\frac{23}{162} - \frac{4}{27}\pi^2
\end{aligned}
$$

$$+\frac{44}{27}\ln(2)\Big)\Big]+\mathcal{O}\Big(\beta^4\Big)\ . \tag{C.40}$$

As already noted in Sec. 3.2.2, the spatial parts of momenta p_A and p_B vanish in the threshold limit, $\beta \to 0$. Therefore, the leading terms in Eqs. (C.37)-(C.40) are equal for the case of two back-to-back emitters (AB) and the case of self-correlated emissions (AA), i. e.

$$f_{AA}^{gg,q\bar{q}}(\beta,\epsilon) = f_{AB}^{gg,q\bar{q}}(\beta,\epsilon) + \mathcal{O}(\beta^2)\ . \tag{C.41}$$

In the high-energy limit, energies of the emitting particles are much larger than their masses, i. e. $E \gg m \Leftrightarrow \beta \approx 1$. We perform an expansion in $1-\beta$ and find

$$\begin{aligned}
&f_{AA}^{gg}(\beta\approx 1,\epsilon) = \\
&(1-\beta)^0\Big[-\frac{1}{8\epsilon^3}+\frac{1-\ln(2)}{4\epsilon^2}+\frac{1}{2\epsilon}\Big(1-\frac{\pi^2}{6}-\frac{5}{2}\ln(2)-\frac{1}{2}\ln^2(2)\Big)\\
&+\Big(\frac{21}{2}\ln(2)-3-\frac{\pi^2}{6}\ln(2)-\frac{\pi^2}{24}-\frac{1}{6}\ln^3(2)-\frac{7}{4}\ln^2(2)-\frac{\zeta_3}{2}\Big)\Big]\\
&+\ln(1-\beta)\Big[\frac{1}{4\epsilon^2}+\frac{1}{\epsilon}\Big(\frac{1}{2}\ln(2)-\frac{3}{4}\Big)+\Big(\frac{\pi^2}{6}-\frac{1}{2}+3\ln(2)+\frac{1}{2}\ln^2(2)\Big)\Big]\\
&-\ln^2(1-\beta)\Big[\frac{1}{4\epsilon}+\Big(\frac{1}{2}\ln(2)-\frac{3}{4}\Big)\Big]+\frac{1}{6}\ln^3(1-\beta)+\mathcal{O}\Big((1-\beta)^1\Big)\ ,
\end{aligned} \tag{C.42}$$

$$\begin{aligned}
&f_{AB}^{gg}(\beta\approx 1,\epsilon) = \\
&(1-\beta)^0\Big[\frac{1}{\epsilon^3}\Big(\frac{3}{8}-\frac{1}{2}\ln(2)\Big)+\frac{1}{\epsilon^2}\Big(\frac{11}{6}\ln(2)-\frac{4}{3}-\frac{\pi^2}{4}-\frac{1}{2}\ln^2(2)\Big)\\
&+\frac{1}{\epsilon}\Big(\frac{13\pi^2}{18}-3\zeta_3-\frac{13}{9}-\frac{1}{3}\ln^3(2)-\frac{11}{6}\ln^2(2)+\frac{97}{36}\ln(2)-\frac{5\pi^2}{12}\ln(2)\Big)\\
&+\Big(6\,\mathrm{Li}_4(\tfrac{1}{2})+\frac{7\zeta_3}{3}+\frac{5\zeta_3}{2}\ln(2)+\frac{1787}{108}+\frac{179\pi^2}{108}-\frac{13\pi^4}{48}+\frac{1}{12}\ln^4(2)\\
&+\frac{11}{9}\ln^3(2)+\frac{881}{36}\ln^2(2)-\frac{2\pi^2}{3}\ln^2(2)-\frac{2059}{54}\ln(2)-\frac{13\pi^2}{18}\ln(2)\Big)\Big]\\
&+\ln(1-\beta)\Big[\frac{1}{2\epsilon^3}+\frac{1}{\epsilon^2}\Big(\ln(2)-\frac{11}{6}\Big)+\frac{1}{\epsilon}\Big(\ln^2(2)+\frac{5\pi^2}{12}-\frac{37}{36}\Big)\\
&+\Big(\frac{11\zeta_3}{4}+\frac{491}{27}-\frac{10\pi^2}{9}+\frac{2}{3}\ln^3(2)-\frac{163}{6}\ln(2)+\frac{5\pi^2}{6}\ln(2)\Big)\Big]\\
&+\ln^2(1-\beta)\Big[-\frac{1}{2\epsilon^2}-\frac{1}{\epsilon}\Big(\ln(2)-\frac{11}{6}\Big)-\Big(\ln^2(2)+\frac{5\pi^2}{12}-\frac{37}{36}\Big)\Big]\\
&+\ln^3(1-\beta)\Big[\frac{1}{3\epsilon}+\Big(\frac{2}{3}\ln(2)-\frac{11}{9}\Big)\Big]-\frac{1}{6}\ln^4(1-\beta)+\mathcal{O}\Big((1-\beta)^1\Big)\ ,
\end{aligned} \tag{C.43}$$

$$f^{q\bar{q}}_{AA}(\beta \approx 1, \epsilon) =$$
$$(1-\beta)^0\left[-\frac{1}{4\epsilon^2} + \frac{1}{\epsilon}\left(\frac{3}{2} - \frac{5}{4}\ln(2)\right) + \left(\frac{43}{4}\ln(2) - \frac{7}{4}\ln^2(2) - 6 - \frac{5\pi^2}{24}\right)\right]$$
$$+\ln(1-\beta)\left[\frac{1}{4\epsilon} + \left(3\ln(2) - \frac{11}{4}\right)\right] - \frac{1}{4}\ln^2(1-\beta) + \mathcal{O}\Big((1-\beta)^1\Big)\,, \qquad \text{(C.44)}$$

$$f^{q\bar{q}}_{AB}(\beta \approx 1, \epsilon) =$$
$$(1-\beta)^0\left[-\frac{1}{\epsilon^2}\left(\frac{1}{12} + \frac{1}{6}\ln(2)\right) + \frac{1}{\epsilon}\left(\frac{17}{36} - \frac{\pi^2}{9} - \frac{5}{6}\ln^2(2) + \frac{7}{9}\ln(2)\right)\right.$$
$$\left.+\left(\frac{77\pi^2}{108} - \frac{13\zeta_3}{6} - \frac{161}{54} - \frac{1}{9}\ln^3(2) + \frac{44}{9}\ln^2(2) + \frac{31}{27}\ln(2) - \frac{5\pi^2}{9}\ln(2)\right)\right]$$
$$+\ln(1-\beta)\left[\frac{1}{6\epsilon^2} + \frac{1}{\epsilon}\left(\ln(2) - \frac{10}{9}\right) + \left(\frac{139}{54} + \frac{2\pi^2}{9} + \ln^2(2) - \frac{17}{3}\ln(2)\right)\right]$$
$$-\ln^2(1-\beta)\left[\frac{1}{6\epsilon} + \left(\ln(2) - \frac{10}{9}\right)\right] + \frac{1}{9}\ln^3(1-\beta) + \mathcal{O}\Big((1-\beta)^1\Big)\,. \qquad \text{(C.45)}$$

We note that the results in Eqs. (C.42)-(C.45) are not regular in the $\beta \to 1$ limit; on the contrary, they contain logarithms of the form $\ln^n(1-\beta)\,, n = 0\ldots4$. These quasi-collinear divergences appear, since the masses of the hard emitters that screen actual collinear singularities, become negligible in the high-energy limit. They manifest themselves as poles in $1/\epsilon$ in the massless calculation [37].

C.3 Triple-collinear subtraction terms

In the following, we present additional formulas for the computation of genuine triple-collinear subtraction terms in Sec. 3.2.3. differential equations and computation of the required boundary constant is discussed in Sec. C.3.1 and Sec. C.3.2, respectively. We present some analytic results in Sec. C.3.3.

C.3.1 *Differential equations*

The transformation defined in Eq. (3.88) reads

$$\hat{T}_{\text{can}} = \frac{(1-2\epsilon)^2}{(1-6\epsilon)} \times \begin{pmatrix} \frac{(1-6\epsilon)\omega_4\omega_5}{(2\epsilon-1)^2} & 0 & 0 & 0 \\ 0 & \frac{2\omega_4+2\omega_5-1}{\epsilon} & \frac{-\omega_4-1}{\epsilon} & \frac{-\omega_5-1}{\epsilon} \\ 0 & \frac{2\omega_4-2\epsilon(4\omega_4-2\omega_5+1)}{\epsilon} & \frac{2\epsilon(2\omega_4-1)-\omega_4}{\epsilon} & -2(\omega_5+1) \\ 0 & \frac{2\epsilon(2\omega_4-4\omega_5-1)+2\omega_5}{\epsilon} & -2(\omega_4+1) & \frac{2\epsilon(2\omega_5-1)-\omega_5}{\epsilon} \end{pmatrix}. \tag{C.46}$$

The coefficient matrices in Eq. (3.90) are given by

$$\hat{m}_{\omega_4}^{(\omega_4)} = \begin{pmatrix} -40 & 0 & 0 & 0 \\ 1 & -12 & 16 & 0 \\ -3 & 36 & -48 & 0 \\ 2 & -24 & 32 & 0 \end{pmatrix}, \qquad \hat{m}_{\omega_4}^{(\omega_4-1)} = \begin{pmatrix} 0 & 0 & 0 & 0 \\ -2 & -8 & 0 & -16 \\ 1 & 4 & 0 & 8 \\ -4 & -16 & 0 & -32 \end{pmatrix},$$

$$\hat{m}_{\omega_4}^{(\omega_4+\omega_5)} = \begin{pmatrix} 0 & 0 & 0 & 0 \\ -2 & -24 & 16 & 16 \\ 1 & 12 & -8 & -8 \\ 1 & 12 & -8 & -8 \end{pmatrix}, \qquad \hat{m}_{\omega_4}^{(\omega_4+\omega_5-1)} = \begin{pmatrix} 0 & 0 & 0 & 0 \\ 3 & -60 & 0 & 0 \\ 1 & -20 & 0 & 0 \\ 1 & -20 & 0 & 0 \end{pmatrix}, \tag{C.47}$$

and

$$\hat{m}_{\omega_5}^{(\omega_5)} = \begin{pmatrix} -40 & 0 & 0 & 0 \\ 1 & -12 & 0 & 16 \\ 2 & -24 & 0 & 32 \\ -3 & 36 & 0 & -48 \end{pmatrix}, \qquad \hat{m}_{\omega_5}^{(\omega_5-1)} = \begin{pmatrix} 0 & 0 & 0 & 0 \\ -2 & -8 & -16 & 0 \\ -4 & -16 & -32 & 0 \\ 1 & 4 & 8 & 0 \end{pmatrix},$$

$$\hat{m}_{\omega_5}^{(\omega_4+\omega_5)} = \begin{pmatrix} 0 & 0 & 0 & 0 \\ -2 & -24 & 16 & 16 \\ 1 & 12 & -8 & -8 \\ 1 & 12 & -8 & -8 \end{pmatrix}, \qquad \hat{m}_{\omega_5}^{(\omega_4+\omega_5-1)} = \begin{pmatrix} 0 & 0 & 0 & 0 \\ 3 & -60 & 0 & 0 \\ 1 & -20 & 0 & 0 \\ 1 & -20 & 0 & 0 \end{pmatrix}. \tag{C.48}$$

C.3.2 *Boundary integral*

Fixing the constants of integration requires the computation of MI $\bar{I}_{0,0,0,1}$ in the limit $\omega_4 \sim \omega_5 \to 0$. To this end, we consider the integral

$$\mathcal{I}_{\text{b.c.}} = \int \frac{d\Omega_4^{(d-1)}\, d\Omega_5^{(d-1)}}{\left[\Omega^{(d-1)}\right]^2} \frac{1}{[\eta_{i4}+\eta_{i5}]}, \tag{C.49}$$

where $\eta_{ik} = (1 - \boldsymbol{e}_i \boldsymbol{e}_k)/2 \in [0,1]$. In this parameterization, the measure reads

$$\mathrm{d}\Omega_k^{(d-1)} = 2\left[4\eta_{ik}(1-\eta_{ik})\right]^{-\epsilon} \mathrm{d}\eta_{ik} \times \mathrm{d}\Omega^{(d-2)}\,, \quad k \in \{4,5\}\,. \tag{C.50}$$

We obtain

$$\begin{aligned}
&\mathcal{I}_{\text{b.c.}} \\
&= \left[2^{1-2\epsilon}\frac{\Omega^{(d-2)}}{\Omega^{(d-1)}}\right]^2 \int_0^1 \mathrm{d}\eta_{i4} \int_0^1 \mathrm{d}\eta_{i5} \frac{\left[\eta_{i4}(1-\eta_{i4})\right]^{-\epsilon}\left[\eta_{i5}(1-\eta_{i5})\right]^{-\epsilon}}{\left[\eta_{i4}+\eta_{i5}\right]} \\
&= \frac{\Gamma\left(2-2\epsilon\right)}{\Gamma^2\left(1-\epsilon\right)} \int_0^1 \mathrm{d}\eta_{i4}\, \eta_{i4}^{-1-\epsilon}(1-\eta_{i4})^{-\epsilon}\, {}_2F_1\left[\{1,1-\epsilon\},\{2(1-\epsilon)\};\frac{-1}{\eta_{i4}}\right]\,.
\end{aligned} \tag{C.51}$$

We apply the linear transformation shown in Eq. (A.8) to the hypergeometric function and find

$$\begin{aligned}
\mathcal{I}_{\text{b.c.}} = {}& \frac{\Gamma^2\left(2-2\epsilon\right)\Gamma\left(1+\epsilon\right)}{\epsilon\,\Gamma^3\left(1-\epsilon\right)} \int_0^1 \mathrm{d}\eta_{i4}\, \eta_{i4}^{-2\epsilon}(1-\eta_{i4})^{-\epsilon}(1+\eta_{i4})^{-\epsilon} \\
& - \frac{\Gamma^2\left(2-2\epsilon\right)}{\epsilon\,\Gamma\left(1-2\epsilon\right)\Gamma^2\left(1-\epsilon\right)} \int_0^1 \mathrm{d}\eta_{i4}\, \left[\eta_{i4}(1-\eta_{i4})\right]^{-\epsilon} \\
& \qquad \times {}_2F_1\left[\{1,2\epsilon\},\{1+\epsilon\};-\eta_{i4}\right]\,.
\end{aligned} \tag{C.52}$$

Using Eq. (A.11), the remaining integral over η_{i4} evaluates to

$$\begin{aligned}
\mathcal{I}_{\text{b.c.}} = \frac{(1-2\epsilon)}{\epsilon}\Bigg\{ & \frac{4^{-\epsilon}(1-2\epsilon)}{(1-4\epsilon)} \frac{\Gamma^4\left(1-2\epsilon\right)\Gamma\left(1+\epsilon\right)}{\Gamma\left(1-4\epsilon\right)\Gamma^3\left(1-\epsilon\right)} \\
& - {}_3F_2\left[\{1,1-\epsilon,2\epsilon\},\{2(1-\epsilon),1+\epsilon\};-1\right]\Bigg\}\,.
\end{aligned} \tag{C.53}$$

We note that the ϵ-expansion of $\mathcal{I}_{\text{b.c.}}$ can be obtained using `HypExp` [127, 128].

C.3.3 *Results for triple-collinear subtraction terms*

In the following, we present some explicit results for triple-collinear subtraction terms.

Initial state radiation

We begin by illustrating results relevant for NNLO QCD computations in case of initial-state radiation for two partonic configurations, $q \to q^* + gg$ and $g \to q^* + qg$. Then, we present the result for the splitting $q \to q^* + g\gamma$, which arises in QCD-EW corrections to W boson production and was obtained in Ref. [9].

$q \to q^* + gg$ Since the case $f_{4,5} = gg$ exhibits a double-soft singularity, we employ the energy-ordered phase-space parametrization. We decompose the quantities in Eq. (2.116) into color factors

$$R_{\delta,+,\mathrm{reg}} = C_F^2 R^{\mathrm{A}}_{\delta,+,\mathrm{reg}} + C_F C_A\, R^{\mathrm{NA}}_{\delta,+,\mathrm{reg}}\,, \tag{C.54}$$

we obtain

$$\begin{aligned}
R^{\mathrm{A}}_{\delta} &= \frac{1}{\epsilon}\left(\frac{\pi^2}{3}\ln(2)\right) - \frac{7\pi^2}{6}\ln^2(2) + 8\zeta_3\ln(2),\\
R^{\mathrm{N}A}_{\delta} &= \frac{1}{\epsilon}\left(-\frac{1571}{216} + \frac{11\pi^2}{36} + \frac{3}{8}\zeta_3 + \frac{\pi^2}{3}\ln(2) + \frac{11}{2}\ln^2(2) + \left(-\frac{32}{9} + \frac{\pi^2}{6} - \frac{11\ln(2)}{3}\right)\ln(\,E_{\mathrm{max}}/E_1)\right)\\
&- \frac{1}{12}\ln^4(2) - \frac{176}{9}\ln^3(2) - \left(\frac{79}{9} + \frac{11\pi^2}{12}\right)\ln^2(2) + \frac{513\zeta_3 + 913 + 165\pi^2}{108}\ln(2)\\
&+ \left(\frac{64}{9} - \frac{\pi^2}{3} + \frac{22\ln(2)}{3}\right)\ln^2(\,E_{\mathrm{max}}/E_1)\\
&+ \left(\frac{11\zeta_3}{2} + \frac{383}{54} - \frac{22\pi^2}{9} - 11\ln^2(2) + \frac{\ln(2)}{3} - \frac{2}{3}\pi^2\ln(2)\right)\ln(\,E_{\mathrm{max}}/E_1)\,,\\
R^{A}_{+} &= -\frac{4\pi^2}{3}\ln(2),\\
R^{\mathrm{N}A}_{+} &= \frac{1}{\epsilon}\left(\frac{11}{3}\ln(2) - \frac{\pi^2}{6} + \frac{32}{9}\right) - 11\ln^2(2) - \frac{1+2\pi^2}{3}\ln(2) - 7\zeta_3 + \frac{11\pi^2}{9} + 22.
\end{aligned} \tag{C.55}$$

The results for regular parts are more complex. For the abelian part, we find

$$\begin{aligned}
R^{\mathrm{A}}_{\mathrm{reg}} &= \frac{1}{\epsilon}\left(-\frac{z+1}{2}\ln(2)\ln(z) + (1-z)\ln(2) + \frac{(z^2+3)}{4(z-1)}\ln^2(z) - \ln(z)z + \frac{3(z-1)}{2}\right)\\
&+ \frac{z^2\left(-36\zeta_3 + 33 + 4\pi^2\right) - 2\left(33+2\pi^2\right)z - 60\zeta_3 + 33}{6(z-1)} + \frac{7(z-1)}{2}\ln^2(2)\\
&+ \left(-6z + \pi^2(z+1) + 6\right)\ln(2) + \frac{\left(3(z-1)z - \pi^2\left(3z^2+5\right)\right)}{3(z-1)}\ln(z)\\
&+ \frac{z}{2}\ln^2(z) + \frac{(9z^2+19)}{12(1-z)}\ln^3(z) + \frac{7(z+1)}{4}\ln^2(2)\ln(z) + \frac{(z^2+7)}{2(1-z)}\ln(2)\ln^2(z)\\
&+ (3z-1)\ln(2)\ln(z) + 6(1-z)\ln(1-z) - 4(1-z)\ln(1-z)\ln(2)\\
&+ \left(-2(z+1)\ln(2) - \frac{2\left(z^2+1\right)}{z-1}\ln(z) - 4z\right)\mathrm{Li}_2(z) + \left(\frac{2\left(3z^2+5\right)}{z-1}\right)\mathrm{Li}_3(z),
\end{aligned} \tag{C.56}$$

and for the non-abelian part we find

$$R^{\mathrm{NA}}_{\mathrm{reg}} = \frac{1}{\epsilon}\left(\frac{\left(6\pi^2-61\right)z^2 - 15z + 76}{36(z-1)} - \frac{11(z+1)}{6}\ln(2) + \frac{(11z^2+2)}{12(z-1)}\ln(z)\right.$$

$$+\frac{(z^2+1)}{2(1-z)}\ln(1-z)\ln(z)+\left(\frac{1+z^2}{2(1-z)}\right)\mathrm{Li}_2(z)\Bigg)$$
$$+\frac{3\left(z^2(48\zeta_3-119)-46z-36\zeta_3+165\right)+\pi^2\left(-50z^2+12z+12\right)}{36(z-1)}$$
$$+\frac{\left(\left(61-6\pi^2\right)z^2+15z-76\right)}{9(z-1)}\ln(1-z)+\frac{\left(49z^2+57z-20\right)}{36(z-1)}\ln(z)$$
$$+\frac{2\left(z^2+1\right)}{z-1}\ln^2(1-z)\ln(z)+\frac{(z-1)}{2}\ln(1-z)\ln(z)+\frac{\left(11z^2+2\right)}{8(1-z)}\ln^2(z) \quad \text{(C.57)}$$
$$+\frac{2\left(z^2+1\right)}{z-1}\ln(1-z)\ln(z)\ln(2)+\frac{22(z+1)}{3}\ln(1-z)\ln(2)+\frac{\left(z^2+1\right)}{4(z-1)}\ln(1-z)\ln^2(z)$$
$$+\frac{11(z+1)}{2}\ln^2(2)+\frac{\left(11z^2+2\right)}{3(1-z)}\ln(2)\ln(z)+\frac{\left(-7z^2+6z+4\pi^2+1\right)}{6(1-z)}\ln(2)$$
$$+\left(\frac{2\left(z^2+1\right)}{z-1}\ln(1-z)+\frac{2\left(z^2+1\right)}{z-1}\ln(2)+\frac{\left(z^2+1\right)}{2(z-1)}\ln(z)+\frac{25z^2-6z+7}{6(z-1)}\right)\mathrm{Li}_2(z)$$
$$+\left(\frac{2\left(z^2+1\right)}{z-1}\right)\mathrm{Li}_3(1-z)+\left(\frac{\left(z^2+1\right)}{2(1-z)}\right)\mathrm{Li}_3(z)\,.$$

$g \to q^* + qg$ As a second example, we present the integrated triple-collinear subtraction term that describes the splitting $g \to q^* + qg$. Due to the absence of a double-soft singularity, we do not have to order energies. We decompose the quantity $\widetilde{R}_{\mathrm{reg}}(z)$ in Eq. (2.123) into color factors

$$\widetilde{R}_{\mathrm{reg}}(z) = C_F^2\,\widetilde{R}^{\mathrm{A}}_{\mathrm{reg}}(z) + C_F C_A\,\widetilde{R}^{\mathrm{NA}}_{\mathrm{reg}}(z)\,, \quad \text{(C.58)}$$

and find

$$\tilde{R}^{\mathrm{A}}_{\mathrm{reg}} = \frac{1}{\epsilon}\Bigg(\frac{8\pi^2z^2-8\pi^2z-15z+4\pi^2-3}{12}+3\left(2z^2-2z+1\right)\ln(1-z)\ln(2)$$
$$+\left(-2z^2+2z-1\right)\ln(1-z)\ln(z)+\frac{1-2z}{2}\ln(z)\ln(2)+\frac{-9z^2+11z-5}{2}\ln(2)$$
$$+\frac{4z^2-6z+3}{4}\ln^2(z)-\frac{3}{4}\ln(z)-\left(2z^2-2z+1\right)\mathrm{Li}_2(z)$$
$$-3(1-2z+2z^2)\ln(2)\ln(E_{\max}/E_1)\Bigg)$$
$$+\frac{-3\pi^2z^2+12z\zeta_3+3\pi^2z-24z-6\zeta_3-\pi^2}{3}-9\left(2z^2-2z+1\right)\ln^2(1-z)\ln(2)$$
$$+4\left(2z^2-2z+1\right)\ln^2(1-z)\ln(z)-\frac{19\left(2z^2-2z+1\right)}{2}\ln(1-z)\ln^2(2)$$
$$+4\left(2z^2-2z+1\right)\ln(1-z)\ln(2)\ln(2)+\left(18z^2-22z+7\right)\ln(1-z)\ln(2) \quad \text{(C.59)}$$

$$
\begin{aligned}
&+\frac{(2z^2-2z+1)}{2}\ln(1-z)\ln^2(z)+\ln(1-z)\ln(z)+\frac{7(2z-1)}{4}\ln(z)\ln^2(2)\\
&+\frac{3-4\pi^2z^2+4\pi^2z+15z-2\pi^2}{3}\ln(1-z)+\frac{57z^2-71z+32}{4}\ln^2(2)\\
&+\frac{-8z^2+14z-7}{2}\ln^2(z)\ln(2)+2(z+2)\ln(z)\ln(2)\\
&+\frac{-4\pi^2z^2-117z^2+8\pi^2z+150z-4\pi^2-27}{6}\ln(2)+\frac{-28z^2+38z-19}{12}\ln^3(z)\\
&+\frac{(8z+9)}{8}\ln^2(z)+\frac{-32\pi^2z^2+40\pi^2z-21z-20\pi^2+9}{12}\ln(z)\\
&+\Big(\ln(2)\left(8z^2-12z+6\right)+\left(-2z^2+2z-1\right)\left(\ln(z)-4\ln(1-z)\right)-2\Big)\mathrm{Li}_2(z)\\
&+\Big(8z^2-8z+4\Big)\mathrm{Li}_3(1-z)+\Big(14z^2-18z+9\Big)\mathrm{Li}_3(z)\\
&+3(1-2z+2z^2)\ln(2)\ln^2(E_{\max}/E_1)\\
&+\Big(\frac{19(1-2z+2z^2)}{2}\ln^2(2)+6(1-2z+2z^2)\ln(1-z)\ln(2)+3\ln(2)\\
&-\frac{2\pi^2(1-2z+2z^2)}{3}\Big)\ln(E_{\max}/E_1)\,, \qquad \text{(C.60)}
\end{aligned}
$$

and

$$
\begin{aligned}
\tilde{R}^{\mathrm{NA}}_{\mathrm{reg}} =\ & \frac{1}{\epsilon}\Bigg(\frac{-6\pi^2z^3-67z^3+3\pi^2z^2+81z^2-3\pi^2z-27z+13}{9z}\\
&+\left(2z^2-2z+1\right)\ln(1-z)\ln(2)+\left(2z^2-2z+1\right)\ln(1-z)\ln(z)\\
&-\left(2z^2+2z+1\right)\ln(1+z)\ln(z)+(4z+1)\ln(z)\ln(2)+\frac{4-31z^3+24z^2+3z}{6z}\ln(2)\\
&+\frac{6z+1}{2}\ln^2(z)+\frac{12z+1}{2}\ln(z)-\Big(2z^2+2z+1\Big)\mathrm{Li}_2(-z)+\Big(2z^2-2z+1\Big)\mathrm{Li}_2(z)\\
&-(1-2z+2z^2)\ln(2)\ln(E_{\max}/E_1)\Bigg)\\
&+\Big(\left(8z^2+8z+4\right)\left(\ln(1-z)+\ln(2)\right)+\left(2z^2-6z+1\right)\ln(z)\Big)\mathrm{Li}_2(-z)\\
&+\Big(\left(-8z^2+8z-4\right)\ln(1-z)-8(z-3)z\ln(2)-4z\ln(z)\Big)\mathrm{Li}_2(z) \qquad \text{(C.61)}\\
&+\frac{44z^3+48z^2+15z+8}{3z}\mathrm{Li}_2(-z)+\frac{-22z^3+96z^2-3z+20}{3z}\mathrm{Li}_2(z)\\
&-\Big(18z^2-2z+9\Big)\mathrm{Li}_3(1-z)+\Big(10z^2+26z+5\Big)\mathrm{Li}_3(-z)
\end{aligned}
$$

$$
\begin{aligned}
&+ \Big(4z^2+4z+2\Big)\left(3\mathrm{Li}_3\left(\frac{z}{1+z}\right)+\mathrm{Li}_3(1-z^2)\right)+\Big(32z+4\Big)\mathrm{Li}_3(z)\\
&+(1-2z+2z^2)\ln(2)\ln^2(E_{\max}/E_1)\\
&+\left(\frac{7(1-2z+2z^2)}{2}\ln(2)+2(1-2z+2z^2)\ln(1-z)+1\right)\ln(2)\ln(E_{\max}/E_1)\,.
\end{aligned}
$$

Final state radiation

We illustrate results in case of initial-state radiation for two partonic configurations, $q^* \to ggq$ and $q^* \to \bar{q}q'\bar{q}'$. To present results, we write

$$
\mathcal{I}_{TC}^{qf_4f_5} = [\alpha_s]^2 E^{-4\epsilon} R^{qf_4f_5}\,, \tag{C.62}
$$

and obtain[1]

$$
\begin{aligned}
R^{qgg} = C_A C_F \Bigg\{ &\frac{1}{\epsilon}\left[-\frac{1015}{108}+\frac{19\zeta_3}{8}+\frac{\pi^2}{8}+\frac{11}{2}\ln^2(2)-\frac{11}{4}\ln(2)+\frac{1}{3}\pi^2\ln(2)\right]\\
&+\Bigg[-\frac{2281}{48}-2\mathrm{Li}_4(1/2)+\frac{25\zeta_3}{24}-\frac{13}{4}\zeta_3\ln(2)-\frac{119\pi^2}{144}+\frac{173\pi^4}{480}-\frac{\ln^4(2)}{12}\\
&\quad-\frac{176}{9}\ln^3(2)-\frac{19}{36}\ln^2(2)-\frac{11}{12}\pi^2\ln^2(2)-\frac{1247}{108}\ln(2)+\frac{161}{36}\pi^2\ln(2)\Bigg]\Bigg\}
\end{aligned}
\tag{C.63}
$$

$$
\begin{aligned}
&+C_F^2\Bigg\{\frac{1}{\epsilon}\left[\frac{31}{16}-2\zeta_3+\frac{9}{8}\ln(2)+\frac{1}{3}\pi^2\ln(2)\right]+\Bigg[\frac{715}{32}+16\zeta_3\ln(2)-\frac{7\pi^4}{30}\\
&\quad-\frac{63}{16}\ln^2(2)-\frac{7}{6}\pi^2\ln^2(2)+\frac{17}{8}\ln(2)+\pi^2\ln(2)\Bigg]\Bigg\},
\end{aligned}
$$

$$
\begin{aligned}
R^{q\bar{q}'q'} = C_F T_R \Bigg\{&\frac{1}{\epsilon}\left[\frac{329}{108}-2\ln^2(2)+\ln(2)\right]+\Bigg[\frac{2773}{216}+\frac{19\zeta_3}{6}\\
&+\frac{35\pi^2}{72}+\frac{64}{9}\ln^3(2)+\frac{32}{9}\ln^2(2)+\frac{43}{27}\ln(2)-\frac{13}{9}\pi^2\ln(2)\Bigg]\Bigg\}\,,
\end{aligned}
\tag{C.64}
$$

$$
\begin{aligned}
R^{q\bar{q}q,\mathrm{id}} = C_F\left(C_F-\frac{1}{2}C_A\right)\Bigg\{&\frac{1}{\epsilon}\left[-\frac{13}{4}-2\zeta_3+\frac{\pi^2}{2}\right]\\
&+\left[-\frac{335}{8}+39\zeta_3+8\zeta_3\ln(2)+\frac{5\pi^2}{3}-\frac{14\pi^4}{45}+13\ln(2)-2\pi^2\ln(2)\right]\Bigg\}\,.
\end{aligned}
\tag{C.65}
$$

1 Following Ref. [123], we split $P_{\bar{q}_1q_2q_3} = P_{\bar{q}'_1q'_2q_3} + P^{\mathrm{id}}_{\bar{q}_1q_2q_3}$, which allows the description of final states with both identical and different quark flavors.

D MIXED CORRECTIONS TO VECTOR BOSON PRODUCTION

In this Appendix, we show results in connection to Part II of this thesis. We describe the computation of two-loop master integrals with two internal masses that are required to describe QCD-EW corrections to the on-shell W-boson form factor in Appendix D.1. Furthermore, we present helicity amplitudes required for double-real corrections to W-boson production at $\mathcal{O}(\alpha_s\alpha)$ in Appendix D.2. We collect some additional formulas in Sec. D.3.

D.1 COMPUTATION OF MASTER INTEGRALS FOR THE TWO-LOOP QCD-EW FORM FACTOR

We begin with the discussion of two-loop $\mathcal{O}(\alpha_s\alpha)$ corrections to the $q\bar{q}' \to W^+$ form factor. The computation requires the evaluation of two-loop diagrams with up to two massive propagators, for example

$$\mathcal{A}^{VV}_{q\bar{q}\to W} \supset$$

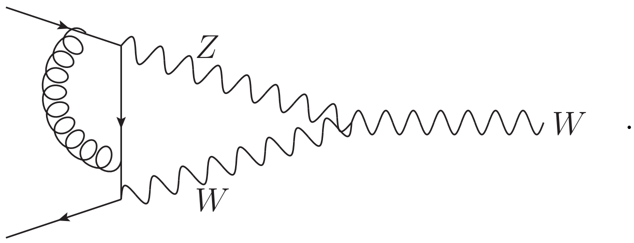

(D.1)

While all necessary master integrals have been computed in the equal-mass limit $M_Z = M_W$ [267–269], the on-shell form factor for *different* values of M_W and M_Z is not available in the literature.[1]

In the following, we will describe the computation of additional master integrals with two different internal masses, which are required in the unequal mass case. Since we are interested in the on-shell form factor, the center-of-mass energy squared $s = (p_1+p_2)^2$ equals to $s = M_W^2$ so that these integrals are functions of M_Z and M_W only. All contributions to the form factor with two internal masses can be expressed through one planar integral topology,

$$\mathcal{T}^{\text{EWZ}}_{\vec{a}} = \int \mathrm{d}^d k_1\, \mathrm{d}^d k_2 \prod_{n=1}^{7} D_n^{-a_n}\,, \tag{D.2}$$

1 We note that in Ref. [270], the form factor was presented as an expansion in $\sin^2\theta_W$.

where we have defined inverse propagators

$$\begin{gathered} D_1 = k_1^2\,, \quad D_2 = k_2^2 - M_W^2\,, \quad D_3 = (k_1-k_2)^2\,, \quad D_4 = (k_1-p_1)^2\,, \\ D_5 = (k_2-p_1)^2\,, \quad D_6 = (k_2-p_{12})^2\,, \quad D_7 = (k_2-p_{12})^2 - M_Z^2\,. \end{gathered} \tag{D.3}$$

We use the computer program `Reduze2` [144] to express all integrals with two internal masses that contribute to the form factor through ten master integrals $\boldsymbol{I}(M_Z, M_W, \epsilon)$,

$$\begin{aligned} &I_1 = \mathcal{T}^{\text{EWZ}}_{\{1,1,1,0,0,0,1\}}\,, I_2 = \mathcal{T}^{\text{EWZ}}_{\{0,1,1,1,0,0,1\}}\,, I_3 = \mathcal{T}^{\text{EWZ}}_{\{0,2,1,1,0,0,1\}}\,, I_4 = \mathcal{T}^{\text{EWZ}}_{\{1,1,0,0,0,1,1\}}\,, \\ &I_5 = \mathcal{T}^{\text{EWZ}}_{\{0,1,1,0,0,1,1\}}\,, I_6 = \mathcal{T}^{\text{EWZ}}_{\{1,1,1,1,0,0,1\}}\,, I_7 = \mathcal{T}^{\text{EWZ}}_{\{1,1,1,0,1,0,1\}}\,, I_8 = \mathcal{T}^{\text{EWZ}}_{\{1,1,1,0,0,1,1\}}\,, \\ &I_9 = \mathcal{T}^{\text{EWZ}}_{\{0,1,1,1,0,1,1\}}\,, I_{10} = \mathcal{T}^{\text{EWZ}}_{\{0,1,1,0,1,1,1\}}\,. \end{aligned} \tag{D.4}$$

With the help of `Reduze2`, we derive a closed system of differential equations for the vector of master integrals $\boldsymbol{I}$ by differentiating w. r. t. M_Z and M_W and expressing the result through $\boldsymbol{I}$ again. We then introduce a dimensionless Landau variable y

$$\frac{M_Z^2}{M_W^2} = \frac{(1+y)^2}{y}\,, \tag{D.5}$$

and write the DEQ in the following form

$$\frac{\partial}{\partial y}\boldsymbol{I} = \hat{M}_{\text{ih}}(y,\epsilon)\,\boldsymbol{I} + \hat{M}_{\text{ih}}(y,\epsilon)\,\boldsymbol{f}\,. \tag{D.6}$$

Integrals $\boldsymbol{f}$ in Eq. (D.6) are known and can be found in Refs. [267–269]. Result in those references describe off-shell contributions with one internal mass and are expressed through HPLs with arguments $x_{Z,W} = -q^2/M_{Z,W}^2$, where $q = p_1 + p_2$. To accommodate our on-shell constraint, we require $\boldsymbol{f}$ as a function of y, in the limit $q^2 \to M_W^2$; in this limit we find

$$x_W \to -1\,, \quad x_Z \to -\frac{y}{(1+y)^2}\,. \tag{D.7}$$

It is beneficial to rewrite the results of Refs. [267–269] through GPLs with argument y. To accomplish this, we use a combination of `PolyLogTools` [171] and a private `Mathematica` implementation of the "super-shuffle" procedure, which we explain in Appendix A.5.

We are now in position to compute $\boldsymbol{I}$ as a function of y by solving the DEQ in Eq. (D.6). To simplify this task, we use `Libra` [168] to construct a transformation

$$\boldsymbol{I} = \hat{T}_{\text{can}}(y,\epsilon)\boldsymbol{J}\,, \tag{D.8}$$

into a new "canonical-like" basis. In the new basis $\boldsymbol{J}$, the DEQ reads

$$\frac{\partial}{\partial y}\boldsymbol{J} = \epsilon\hat{B}_{\text{h}}(y)\,\boldsymbol{J} + \hat{B}_{\text{ih}}(y,\epsilon)\,\boldsymbol{f}\,, \tag{D.9}$$

where

$$\epsilon \hat{B}_{\text{h}} = \epsilon \sum_{a \in \{0, \pm 1\}} \frac{\hat{b}_a}{y-a} = \hat{T}_{\text{can}}^{-1} \left[\hat{M}_{\text{ih}} - \frac{\partial}{\partial y} \right] \hat{T}_{\text{can}} \,, \tag{D.10}$$

and

$$\hat{B}_{\text{ih}}(y,\epsilon) = \hat{T}_{\text{can}}^{-1} \hat{M}_{\text{ih}}(y,\epsilon) \,. \tag{D.11}$$

We note that the inhomogeneous term $\hat{B}_{\text{ih}}(y,\epsilon)\, \boldsymbol{f}$ has poles starting at $1/\epsilon^2$. We expand up to the required order in ϵ and write[2]

$$\hat{B}_{\text{ih}}(y,\epsilon)\, \boldsymbol{f} = \sum_{n=-2}^{2} \epsilon^n \left[\hat{B}_{\text{ih}}(y,\epsilon)\, \boldsymbol{f} \right]^{(n)} \,, \tag{D.12}$$

$$\boldsymbol{J} = \sum_{n=-2}^{2} \epsilon^n \boldsymbol{J}^{(n)} \,. \tag{D.13}$$

Thanks to the ϵ-factorized from, the DEQ in Eq. (D.9) decouples order-by order in ϵ. The solution reads[3]

$$\boldsymbol{J}^{(n)}(y) = \int^y \mathrm{d}t \left\{ \sum_{a \in \{0,\pm 1\}} \frac{\hat{b}_a}{t-a} \boldsymbol{J}^{(n-1)}(t) + \left[\hat{B}_{\text{ih}}(t,\epsilon)\, \boldsymbol{f}(t) \right]^{(n)} \right\} + \boldsymbol{C}^{(n)} \,, \tag{D.14}$$

where $n \geq -2$ and $\boldsymbol{C}^{(n)}$ are constants of integration. We express the integrals in Eq. (D.14) through GPLs of y up to weight four, where letters are drawn from the alphabet

$$\mathcal{A}_y = \{0 \,,\, \pm 1 \,,\, \pm \mathrm{i} \,,\, e^{\pm \mathrm{i}\pi/3} \,,\, e^{\pm 2\mathrm{i}\pi/3} \} \,. \tag{D.15}$$

We fix the constants $\boldsymbol{C}^{(n)}$ in the equal-mass limit

$$M_Z = M_W \quad \Leftrightarrow \quad y = e^{2\mathrm{i}\pi/3} \,, \tag{D.16}$$

using the results of Refs. [267–269]. We have verified the correctness of our results by comparing them to numerical results obtained with `pySecDec` [271–279]. We note that the complete computation of the renormalized two-loop on-shell form factor can be found in Ref. [9].

2 For the finite part of the two-loop form factor, we require integrals $\boldsymbol{J}$ up to ϵ^2, which corresponds to weight four.

3 In this recursive formula, we set $\boldsymbol{J}^{(-3)} = 0$.

D.2 DOUBLE-REAL MATRIX ELEMENTS FOR W-BOSON PRODUCTION

In this Section, we present the amplitudes that are required to describe double-real $\mathcal{O}(\alpha_s\alpha)$ corrections to on-shell W^+-boson production in spinor-helicity formalism. All matrix elements can be obtained from crossing the following two amplitudes

$$\mathcal{A}_{\bar{u}\bar{q}qd} \;:\; 0 \to \bar{u}(p_1)\, \bar{q}(p_2)\, q(p_3)\, d(p_4)\; W^+(\to \nu(p_5)\, \bar{\ell}(p_6))\,, \tag{D.17}$$

$$\mathcal{A}_{\bar{u}d\gamma g} \;:\; 0 \to \bar{u}(p_1)\, d(p_2)\, \gamma(p_3)\, g(p_4)\; W^+(\to \nu(p_5)\, \bar{\ell}(p_6))\,. \tag{D.18}$$

In Eqs. (D.17)-(D.18), all momenta are outgoing such that $-p_{1234} = p_W = p_{56}$. In what follows, we define conventions for Feynman rules and spinor-helicity notations in Appendix D.2.1. We then provide expressions for the four-quark and the two-quark amplitude in Appendix D.2.2 and Appendix D.2.3, respectively.[4]

D.2.1 *Conventions*

Feynman rules

We use the Feynman rules given in Appendix A of Ref. [253]. There, the couplings that enter electroweak fermion-boson and three-boson couplings are defined as

$$\begin{aligned} c^-_{A,f} &= -Q_f\,, & c^+_{A,f} &= -Q_f\,, \\ c^-_{Z,f} &= \frac{I_3 - \sin^2\theta_W Q_f}{\sin\theta_W \cos\theta_W}\,, & c^+_{Z,f} &= -\frac{\sin\theta_W}{\cos\theta_W} Q_f\,, \\ c^-_W &= \frac{1}{\sin\theta_W\sqrt{2}}\,, & c^+_W &= 0\,, \end{aligned} \tag{D.19}$$

and

$$c_{AWW} = 1\,, \quad c_{ZWW} = -\frac{\cos\theta_W}{\sin\theta_W}\,, \tag{D.20}$$

respectively.

Spinor-helicity formalism

We describe amplitudes in spinor-helicity formalism following the conventions of Ref. [281]. In particular, we denote four-spinors by

$$\overline{U}_L(p) = \langle p|\,, \qquad \overline{U}_R(p) = [p|\,, \tag{D.21}$$

$$U_L(p) = |p]\,, \qquad U_R(p) = |p\rangle\,, \tag{D.22}$$

4 We note the gluon-photon amplitude $\mathcal{A}_{ud\gamma g}$ in Eq. (D.18) was also computed in Ref. [280].

where $\overline{U}_L(p)$ and $\overline{U}_R(p)$ denote left-and right-handed, outgoing fermions. $U_R(p)$ and $U_L(p)$ denote left- and right-handed outgoing antifermions. Polarization vectors for outgoing vector-like particles are defined to be transverse to a reference momentum r. They read

$$\varepsilon_+^{*,\mu}(k) = \frac{1}{\sqrt{2}} \frac{\langle r|\,\gamma^\mu\,|k]}{\langle rk\rangle} \qquad \varepsilon_-^{*,\mu}(k) = -\frac{1}{\sqrt{2}} \frac{[r|\,\gamma^\mu\,|k\rangle}{[rk]}\,, \tag{D.23}$$

and satisfy

$$\varepsilon_\pm^{*,\mu} \cdot \varepsilon_{\pm,\mu} = -1\,, \quad \varepsilon_\pm^{*,\mu} \cdot p_\mu = \varepsilon_\pm^{*,\mu} \cdot r_\mu = 0\,. \tag{D.24}$$

D.2.2 *Four-quark amplitudes*

In the following, we obtain mixed $\mathcal{O}(\alpha_s\alpha)$ corrections that involve four quarks. In particular, we consider strong and electroweak corrections to the amplitude $\mathcal{A}_{u\bar{q}qd}$ in Eq. (D.17) for the case $q = u$.[5] We use the fact that the amplitude $\mathcal{A}_{\bar{u}\bar{u}ud}$ is symmetric in $p_1 \leftrightarrow p_2$ and write

$$\mathcal{A}^{\alpha_s}_{\bar{u}\bar{u}ud} = \mathcal{P}_W \sum_{t\in\{\mathrm{I},\mathrm{II}\}} \mathcal{A}^t_\mu(1_{\bar{u}}, 2_{\bar{u}}, 3_u, 4_d, g)\,\langle 5|\,\gamma^\mu\,|6]\, + 1 \longleftrightarrow 2\,, \tag{D.25}$$

$$\begin{aligned}\mathcal{A}^{\alpha,V_0}_{\bar{u}\bar{u}ud} = \mathcal{P}_W &\left[\sum_{t\in\{\mathrm{I},\mathrm{II},\mathrm{IV}\}} \mathcal{A}^t_\mu(1_{\bar{u}}, 2_{\bar{u}}, 3_u, 4_d, V_0) + \mathcal{A}^{\mathrm{III}}_\mu(1_{\bar{u}}, 2_{\bar{u}}, 3_u, 4_d, W)\right] \langle 5|\,\gamma^\mu\,|6] \\ &+ 1 \longleftrightarrow 2\,,\end{aligned} \tag{D.26}$$

where $V_0 = \gamma, Z$ and

$$\mathcal{P}_W = \frac{\mathrm{i}ec_W^-}{\left[s_{56} - M_W^2\right]^2}\,. \tag{D.27}$$

5 The case $q = d$ can be obtained along the same lines.

The four diagrams that contribute to Eqs. (D.25)-(D.26) are

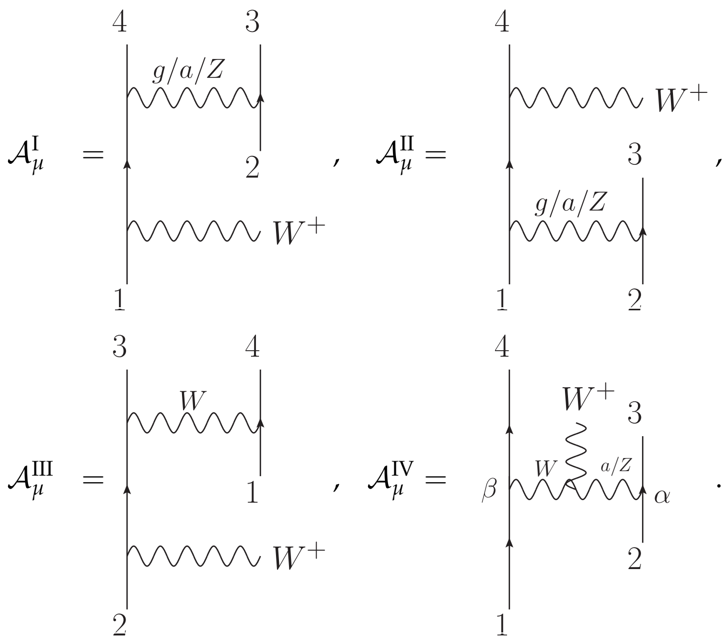

(D.28)

To compute mixed corrections at $\mathcal{O}(\alpha_s\alpha)$, we have to take the interference between strong and electroweak corrections given in Eq. (D.25) and Eq. (D.26), respectively; we write

$$\left|\mathcal{A}_{\bar u\bar u u d}\right|^2\Big|_{\mathcal{O}(\alpha_s\alpha)} = \sum_{\text{helicities}} 2\,\mathrm{Re}\left\{\mathcal{A}^{\alpha_s}_{\bar u\bar u u d}\times\left[\mathcal{A}^{\alpha,\gamma}_{\bar u\bar u u d}+\mathcal{A}^{\alpha,Z}_{\bar u\bar u u d}\right]^\dagger\right\}. \tag{D.29}$$

However, products of strong and electroweak amplitudes that contain the *same* assignment for momenta $p_{1,2}$ produce two disjunct quark traces. Hence, they are proportional to $\mathrm{Tr}(T^a)=0$ and vanish. The remaining products, which contain a *different* assignment for momenta $p_{1,2}$, have one continuous quark line. Hence, we only have to consider all-minus helicity configurations. We find

$$\begin{aligned}\left|\mathcal{A}_{\bar u\bar u u d}\right|^2\Big|_{\mathcal{O}(\alpha_s\alpha)} &= \frac{\left[g_s\, e^3 c_W^{-}\right]^2 C_F}{\left[s_{56}-M_W^2\right]^2}\times 2\,\mathrm{Re}\Bigg\{\left[\sum_{t\in\{\mathrm{I,II}\}}\mathcal{A}^t(1^-_{\bar u},2^-_{\bar u},3^-_u,4^-_d,g)\right]\\ &\times\left[\mathcal{A}^{\mathrm{III}}(2^-_{\bar u},1^-_{\bar u},3^-_u,4^-_d,W)+\sum_{t\in\{\mathrm{I,II,IV}\}}\;\sum_{V_0\in\{\gamma,Z\}}\left(\mathcal{A}^t(2^-_{\bar u},1^-_{\bar u},3^-_u,4^-_d,V_0)\right)\right]^\dagger\Bigg\} \\ &+1\longleftrightarrow 2\,,\end{aligned} \tag{D.30}$$

where $\mathcal{A}^{\text{I...IV}} = \mathcal{A}_\mu^{\text{I...IV}} \langle 5|\,\gamma^\mu\,|6]$ denotes the product of the diagrams in Eq. (D.28) with the W^+-decay amplitude. Explicitly, they read[6]

$$\begin{aligned}
\mathcal{A}^{\text{I}} &= \mathcal{N}^{\text{I}} \langle 43\rangle\, [2|\,\widehat{234}\,|5\rangle\, [61]\ , \\
\mathcal{A}^{\text{II}} &= \mathcal{N}^{\text{II}} \langle 45\rangle\, [6|\,\widehat{123}\,|3\rangle\, [21]\ , \\
\mathcal{A}^{\text{III}} &= \mathcal{N}^{\text{III}} \langle 34\rangle\, [1|\,\widehat{134}\,|5\rangle\, [62]\ , \\
\mathcal{A}^{\text{IV}} &= \mathcal{N}^{\text{IV}} \Big[\langle 34\rangle\, [12]\, \langle 5|\,\widehat{23}\,|6] + \langle 45\rangle\, [61]\, \langle 3|\,\widehat{14}\,|2] - \langle 35\rangle\, [62]\, \langle 4|\,\widehat{23}\,|1] \Big]\ ,
\end{aligned} \tag{D.31}$$

where we have defined[7]

$$\mathcal{N}^{\text{I}} = \frac{-4\left[c^-_{V,u}\right]^2}{(s_{23}-M_V^2)s_{234}}\ , \quad \mathcal{N}^{\text{II}} = \frac{4\left[c^-_{V,u}\right]^2}{(s_{23}-M_V^2)s_{123}}\ , \tag{D.32}$$

$$\mathcal{N}^{\text{III}} = \frac{-4\left[c^-_{W}\right]^2}{(s_{14}-M_W^2)s_{134}}\ , \quad \mathcal{N}^{\text{IV}} = \frac{-4c_{VWW}\,c^-_{V,u}}{(s_{14}-M_W^2)(s_{23}-M_V^2)}\ . \tag{D.33}$$

D.2.3 *Two-quark plus photon plus gluon amplitudes*

In the following, we consider the amplitude $\mathcal{A}_{ud\gamma g}$ in Eq. (D.18). We write the corresponding matrix element squared as a sum over helicities,

$$\left|\mathcal{A}_{\bar{u}d\gamma g}\right|^2\Big|_{\mathcal{O}(\alpha_s\alpha)} = \sum_{h_\gamma=+,-}\ \sum_{h_g=+,-} \left|\mathcal{A}(1^-_{\bar{u}}, 2^-_d, 3^{h_\gamma}_\gamma, 4^{h_g}_g)\right|^2\ , \tag{D.34}$$

where

$$\begin{aligned}
&\mathcal{A}(1^-_{\bar{u}}, 2^-_d, 3_\gamma, 4_g) \\
&= \frac{ie^3 g_s (T^a)_{ij}}{\left[s_{56}-M_W^2\right]^2}\left[Q_u\mathcal{A}^{\text{I}}_\mu + Q_d\mathcal{A}^{\text{II}}_\mu + \frac{Q_W}{s_{124}-M_W^2}\mathcal{A}^{\text{III}}_\mu\right] \langle 5|\,\gamma^\mu\,|6]\ ,
\end{aligned} \tag{D.35}$$

with $Q_W = Q_u - Q_d$. We note that terms with indices I...III in Eq. (D.35) collect diagrams where the photon is emitted from the up quark, the down quark and the W boson, respectively.

6 We omit arguments "$1^-2^-3^-4^-$".
7 For contributions with a gluon, $c^-_{g,f} \equiv 1$.

Diagrammatically, we have

$\mathcal{A}_\mu^{\mathrm{I}} =$

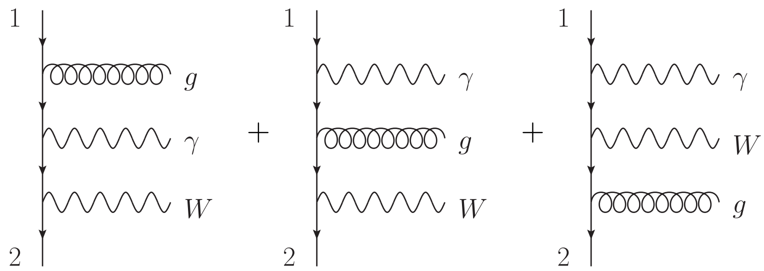

,

$\mathcal{A}_\mu^{\mathrm{II}} =$

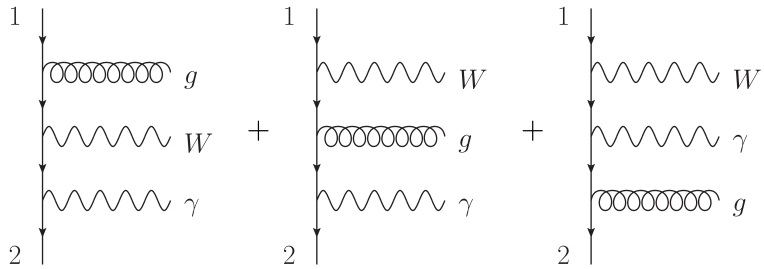

, (D.36)

$\mathcal{A}_\mu^{\mathrm{III}} =$

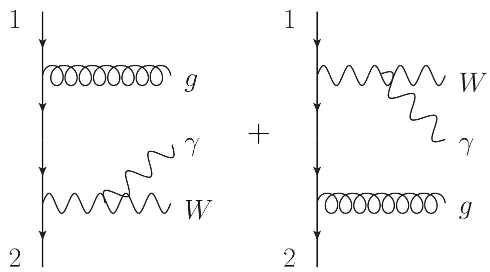

.

We obtain

$$\mathcal{A}(1_{\bar{u}}^-, 2_d^-, 3_\gamma^+, 4_g^+) = \frac{4\,\langle 25\rangle^2\,[56]}{\langle 24\rangle\,\langle 14\rangle\,\langle 23\rangle}\left[Q_u\frac{\langle 12\rangle}{\langle 13\rangle} + Q_W\frac{\langle 2|\,\widehat{14}\,|3]}{s_{124}-M_W^2}\right], \tag{D.37}$$

$$\begin{aligned}
&\mathcal{A}(1_{\bar{u}}^-, 2_d^-, 3_\gamma^+, 4_g^-) = \\
&-4\Bigg\{\frac{Q_u}{[14]\,\langle 13\rangle}\left(-\frac{\langle 25\rangle\,[6|\,\widehat{25}\,|4\rangle\,[13]}{s_{134}} + \frac{[1|\,\widehat{24}\,|5\rangle\,[6|\,\widehat{13}\,|2\rangle}{[42]\,\langle 23\rangle}\right) \\
&\quad - Q_d\frac{\langle 24\rangle\,[3|\,\widehat{16}\,|5\rangle\,[61]}{\langle 23\rangle\,[42]\,s_{234}} - \frac{Q_W}{s_{124}-M_W^2}\Bigg(\frac{\langle 24\rangle\,[31]\,\langle 53\rangle\,[36]}{[42]\,\langle 23\rangle} \\
&\quad + \frac{[1|\,\widehat{36}\,|5\rangle\,[61]\,\langle 2|\,\widehat{14}\,|3]}{[14]\,[42]\,\langle 23\rangle} + \frac{\langle 25\rangle\,[63]\,[1|\,\widehat{24}\,|3\rangle\,[31]}{[14]\,[42]\,\langle 23\rangle}\Bigg)\Bigg\},
\end{aligned} \tag{D.38}$$

$$\begin{aligned}
&\mathcal{A}(1_{\bar{u}}^-, 2_d^-, 3_\gamma^-, 4_g^+) = \\
&-4\Bigg\{-Q_u \times \frac{[14]\,\langle 25\rangle\,[6|\,\widehat{25}\,|3\rangle}{[13]\,\langle 14\rangle\,s_{134}}
\end{aligned}$$

$$
\begin{aligned}
&+ Q_d \times \left(\frac{[1|\widehat{46}|5\rangle\,[6|\widehat{35}|2\rangle}{\langle 14\rangle\,[13]\,\langle 24\rangle\,[32]} + \frac{\langle 23\rangle\,[4|\widehat{23}|5\rangle\,[61]}{s_{234}\,\langle 24\rangle\,[32]} \right) \\
&+ \frac{Q_W}{s_{124} - M_W^2} \times \left(\frac{\langle 23\rangle\,[14]\,\langle 53\rangle\,[36]}{\langle 14\rangle\,[13]} - \frac{\langle 25\rangle\,[6|\widehat{14}|2\rangle\,[1|\widehat{24}|3\rangle}{\langle 24\rangle\,\langle 14\rangle\,[13]} \right. \\
&\quad \left. + \frac{\langle 35\rangle\,[61]\,\langle 23\rangle\,[3|\widehat{14}|2\rangle}{\langle 24\rangle\,\langle 14\rangle\,[13]} \right) \Bigg\} ,
\end{aligned} \tag{D.39}
$$

$$
\mathcal{A}(1^-_{\bar{u}}, 2^-_{d}, 3^-_{\gamma}, 4^-_{g}) = \frac{4\,[16]^2\,\langle 56\rangle}{[13]\,[14]\,[42]} \left[Q_d \frac{[12]}{[32]} - Q_W \frac{\langle 3|\widehat{24}|1]}{s_{124} - M_W^2} \right] . \tag{D.40}
$$

D.3 ADDITIONAL DEFINITIONS

In this Section, we collect some formulas that we use in the fully-differential description of W-boson production in Sec. 4.2.

D.3.1 *Integrated subtraction term for a soft photon*

The integrated subtraction term that describes the emission of a soft photon in the gluon-initiated process $g_1 \bar{d}_2 \to W^+ + \bar{u}_4 \gamma_5$ reads [9]

$$
\begin{aligned}
J_\gamma(2,4,W) &= \frac{Q_2^2 + Q_4^2}{\epsilon^2} + \frac{Q_W}{\epsilon} \left[Q_W + 2Q_4 \ln\left(\frac{\kappa_{4W}}{\sqrt{1-\beta^2}} \right) \right. \\
&\quad \left. + 2Q_2 \ln\left(\frac{\kappa_{2W}}{\sqrt{1-\beta^2}} \right) \right] + \frac{2Q_2 Q_4}{\epsilon} \ln(\eta_{42}) \\
&\quad - Q_W^2 \left[\frac{1}{\beta} \ln\left(\frac{1-\beta}{1+\beta} \right) - \frac{1}{2} \ln^2\left(\frac{1-\beta}{1+\beta} \right) \right] \\
&\quad - 2Q_W \sum_{i\in\{2,4\}} Q_i \ln\left(\frac{\kappa_{iW}}{1-\beta} \right) \ln\left(\frac{\kappa_{iW}}{1+\beta} \right) \\
&\quad - 2Q_W \sum_{i\in\{2,4\}} Q_i \left[\mathrm{Li}_2\left(1 - \frac{\kappa_{iW}}{1-\beta} \right) + \mathrm{Li}_2\left(1 - \frac{\kappa_{iW}}{1+\beta} \right) \right] \\
&\quad - 2Q_2 Q_4 \left(\mathrm{Li}_2(1-\eta_{42}) + \frac{1}{2} \ln^2(\eta_{42}) \right) + \mathcal{O}(\epsilon) .
\end{aligned} \tag{D.41}
$$

D.3.2 *Additional splitting functions for W-boson production*

We use the function $P_{qq}^{\mathrm{NLO}}(z,L)$, defined in Eq. (4.29), to express integrands of soft-regulated collinear subtraction terms for initial-state splittings $q \to \gamma q^*$ and $q \to g q^*$. We use Eq. (B.8) to achieve an explicit cancellation of the $1/\epsilon$-poles, expand in ϵ and obtain

$$
\begin{aligned}
&P_{qq}^{\mathrm{NLO}}(z,L) = \\
&-2L\,\delta(1-z) + 2\,\mathcal{D}_0(z) - (1+z) \\
&+\Big(2L^2\delta(1-z) - 4\,\mathcal{D}_1(z) + 2(1+z)\ln(1-z) - (1-z)\Big)\epsilon \\
&-\Big(\frac{4}{3}L^3\delta(1-z) - 4\,\mathcal{D}_2(z) - 2(1-z)\ln(1-z) + 2(1+z)\ln^2(1-z)\Big)\epsilon^2 \\
&+\Big(\frac{2}{3}L^4\delta(1-z) - \frac{8}{3}\,\mathcal{D}_3(z) - 2(1-z)\ln^2(1-z) + \frac{4}{3}(1+z)\ln^3(1-z)\Big)\epsilon^3 \\
&+\mathcal{O}\Big(\epsilon^4\Big)\,.
\end{aligned}
\tag{D.42}
$$

The function $P_{qg}^{\mathrm{NLO}}(z,L)$ was used in Sec. 4.2.2 to write the integrand of soft-regulated collinear subtraction terms for initial-state splittings $g \to q q^*$ and $\gamma \to q q^*$; it reads

$$
P_{qg}^{\mathrm{NLO}}(z) = \frac{(1-z)^{-2\epsilon}}{(1-\epsilon)}\left[(1-z)^2 + z^2 - \epsilon\right]\,. \tag{D.43}
$$

Function $P_{qg}^{\mathrm{NLO}}(z)$ in Eq. (D.43) is integrable over $z \in [0,1]$, hence its expansion in ϵ is straightforward.

BIBLIOGRAPHY

[1] Fabrizio Caola, Kirill Melnikov, and Raoul Röntsch. "Nested soft-collinear subtractions in NNLO QCD computations." In: *Eur. Phys. J. C* 77.4 (2017), p. 248. DOI: 10.1140/epjc/s10052-017-4774-0. arXiv: 1702.01352 [hep-ph].

[2] Fabrizio Caola, Kirill Melnikov, and Raoul Röntsch. "Analytic results for color-singlet production at NNLO QCD with the nested soft-collinear subtraction scheme." In: *Eur. Phys. J. C* 79.5 (2019), p. 386. DOI: 10.1140/epjc/s10052-019-6880-7. arXiv: 1902.02081 [hep-ph].

[3] Fabrizio Caola, Kirill Melnikov, and Raoul Röntsch. "Analytic results for decays of color singlets to gg and $q\bar{q}$ final states at NNLO QCD with the nested soft-collinear subtraction scheme." In: *Eur. Phys. J. C* 79.12 (2019), p. 1013. DOI: 10.1140/epjc/s10052-019-7505-x. arXiv: 1907.05398 [hep-ph].

[4] Konstantin Asteriadis, Fabrizio Caola, Kirill Melnikov, and Raoul Röntsch. "Analytic results for deep-inelastic scattering at NNLO QCD with the nested soft-collinear subtraction scheme." In: *Eur. Phys. J. C* 80.1 (2020), p. 8. DOI: 10.1140/epjc/s10052-019-7567-9. arXiv: 1910.13761 [hep-ph].

[5] Maximilian Delto and Kirill Melnikov. "Integrated triple-collinear counter-terms for the nested soft-collinear subtraction scheme." In: *JHEP* 05 (2019), p. 148. DOI: 10.1007/JHEP05(2019)148. arXiv: 1901.05213 [hep-ph].

[6] Wojciech Bizoń and Maximilian Delto. "Analytic double-soft integrated subtraction terms for two massive emitters in a back-to-back kinematics." In: *JHEP* 07 (2020), p. 011. DOI: 10.1007/JHEP07(2020)011. arXiv: 2004.01663 [hep-ph].

[7] Maximilian Delto, Matthieu Jaquier, Kirill Melnikov, and Raoul Röntsch. "Mixed QCD$\otimes$QED corrections to on-shell Z boson production at the LHC." In: *JHEP* 01 (2020), p. 043. DOI: 10.1007/JHEP01(2020)043. arXiv: 1909.08428 [hep-ph].

[8] Federico Buccioni, Fabrizio Caola, Maximilian Delto, Matthieu Jaquier, Kirill Melnikov, and Raoul Röntsch. "Mixed QCD-electroweak corrections to on-shell Z production at the LHC." In: *Phys. Lett. B* 811 (2020), p. 135969. DOI: 10.1016/j.physletb.2020.135969. arXiv: 2005.10221 [hep-ph].

[9] Arnd Behring, Federico Buccioni, Fabrizio Caola, Maximilian Delto, Matthieu Jaquier, Kirill Melnikov, and Raoul Röntsch. "Mixed QCD-electroweak corrections to W-boson production in hadron collisions." In: *Phys. Rev. D* 103.1 (2021), p. 013008. DOI: 10.1103/PhysRevD.103.013008. arXiv: 2009.10386 [hep-ph].

[10] Arnd Behring, Federico Buccioni, Fabrizio Caola, Maximilian Delto, Matthieu Jaquier, Kirill Melnikov, and Raoul Röntsch. "Estimating the impact of mixed QCD-electroweak corrections on the W-mass determination at the LHC." In: *Phys. Rev. D* 103.11 (2021), p. 113002. arXiv: 2103.02671 [hep-ph].

[11] Georges Aad et al. "Observation of a new particle in the search for the Standard Model Higgs boson with the ATLAS detector at the LHC." In: *Phys. Lett. B* 716 (2012), pp. 1–29. DOI: 10.1016/j.physletb.2012.08.020. arXiv: 1207.7214 [hep-ex].

[12] Serguei Chatrchyan et al. "Observation of a New Boson at a Mass of 125 GeV with the CMS Experiment at the LHC." In: *Phys. Lett. B* 716 (2012), pp. 30–61. DOI: 10.1016/j.physletb.2012.08.021. arXiv: 1207.7235 [hep-ex].

[13] R.P. Feynman and Murray Gell-Mann. "Theory of Fermi interaction." In: *Phys. Rev.* 109 (1958). Ed. by L.M. Brown, pp. 193–198. DOI: 10.1103/PhysRev.109.193.

[14] S.L. Glashow. "Partial Symmetries of Weak Interactions." In: *Nucl. Phys.* 22 (1961), pp. 579–588. DOI: 10.1016/0029-5582(61)90469-2.

[15] Murray Gell-Mann. "Symmetries of baryons and mesons." In: *Phys. Rev.* 125 (1962), pp. 1067–1084. DOI: 10.1103/PhysRev.125.1067.

[16] Jeffrey Goldstone, Abdus Salam, and Steven Weinberg. "Broken Symmetries." In: *Phys. Rev.* 127 (1962), pp. 965–970. DOI: 10.1103/PhysRev.127.965.

[17] Peter W. Higgs. "Broken symmetries, massless particles and gauge fields." In: *Phys. Lett.* 12 (1964), pp. 132–133. DOI: 10.1016/0031-9163(64)91136-9.

[18] F. Englert and R. Brout. "Broken Symmetry and the Mass of Gauge Vector Mesons." In: *Phys. Rev. Lett.* 13 (1964). Ed. by J.C. Taylor, pp. 321–323. DOI: 10.1103/PhysRevLett.13.321.

[19] Peter W. Higgs. "Broken Symmetries and the Masses of Gauge Bosons." In: *Phys. Rev. Lett.* 13 (1964). Ed. by J.C. Taylor, pp. 508–509. DOI: 10.1103/PhysRevLett.13.508.

[20] G.S. Guralnik, C.R. Hagen, and T.W.B. Kibble. "Global Conservation Laws and Massless Particles." In: *Phys. Rev. Lett.* 13 (1964). Ed. by J.C. Taylor, pp. 585–587. DOI: 10.1103/PhysRevLett.13.585.

[21] Peter W. Higgs. "Spontaneous Symmetry Breakdown without Massless Bosons." In: *Phys. Rev.* 145 (1966), pp. 1156–1163. DOI: 10.1103/PhysRev.145.1156.

[22] Steven Weinberg. "A Model of Leptons." In: *Phys. Rev. Lett.* 19 (1967), pp. 1264–1266. DOI: 10.1103/PhysRevLett.19.1264.

[23] Abdus Salam. "Weak and Electromagnetic Interactions." In: *Conf. Proc. C* 680519 (1968), pp. 367–377. DOI: 10.1142/9789812795915_0034.

[24] H. Fritzsch, Murray Gell-Mann, and H. Leutwyler. "Advantages of the Color Octet Gluon Picture." In: *Phys. Lett. B* 47 (1973), pp. 365–368. DOI: 10.1016/0370-2693(73)90625-4.

[25] Morad Aaboud et al. "Measurement of the W-boson mass in pp collisions at $\sqrt{s} = 7$ TeV with the ATLAS detector." In: *Eur. Phys. J. C* 78.2 (2018). [Erratum: Eur.Phys.J.C 78, 898 (2018)], p. 110. DOI: 10.1140/epjc/s10052-017-5475-4. arXiv: 1701.07240 [hep-ex].

[26] S. Schael et al. "Electroweak Measurements in Electron-Positron Collisions at W-Boson-Pair Energies at LEP." In: *Phys. Rept.* 532 (2013), pp. 119–244. DOI: 10.1016/j.physrep.2013.07.004. arXiv: 1302.3415 [hep-ex].

[27] Timo Antero Aaltonen et al. "Combination of CDF and D0 W-Boson Mass Measurements." In: *Phys. Rev. D* 88.5 (2013), p. 052018. DOI: 10.1103/PhysRevD.88.052018. arXiv: 1307.7627 [hep-ex].

[28] "Prospects for the measurement of the W-boson mass at the HL- and HE-LHC." In: (2018).

[29] M. Baak, J. Cúth, J. Haller, A. Hoecker, R. Kogler, K. Mönig, M. Schott, and J. Stelzer. "The global electroweak fit at NNLO and prospects for the LHC and ILC." In: *Eur. Phys. J. C* 74 (2014), p. 3046. DOI: 10.1140/epjc/s10052-014-3046-5. arXiv: 1407.3792 [hep-ph].

[30] Jorge de Blas, Marco Ciuchini, Enrico Franco, Satoshi Mishima, Maurizio Pierini, Laura Reina, and Luca Silvestrini. "Electroweak precision observables and Higgs-boson signal strengths in the Standard Model and beyond: present and future." In: *JHEP* 12 (2016), p. 135. DOI: 10.1007/JHEP12(2016)135. arXiv: 1608.01509 [hep-ph].

[31] John C. Collins, Davison E. Soper, and George F. Sterman. "Factorization for Short Distance Hadron - Hadron Scattering." In: *Nucl. Phys. B* 261 (1985), pp. 104–142. DOI: 10.1016/0550-3213(85)90565-6.

[32] John C. Collins, Davison E. Soper, and George F. Sterman. "Factorization of Hard Processes in QCD." In: *Adv. Ser. Direct. High Energy Phys.* 5 (1989), pp. 1–91. DOI: 10.1142/9789814503266_0001. arXiv: hep-ph/0409313.

[33] F. Bloch and A. Nordsieck. "Note on the Radiation Field of the electron." In: *Phys. Rev.* 52 (1937), pp. 54–59. DOI: 10.1103/PhysRev.52.54.

[34] T. Kinoshita. "Mass singularities of Feynman amplitudes." In: *J. Math. Phys.* 3 (1962), pp. 650–677. DOI: 10.1063/1.1724268.

[35] T. D. Lee and M. Nauenberg. "Degenerate Systems and Mass Singularities." In: *Phys. Rev.* 133 (1964). Ed. by G. Feinberg, B1549–B1562. DOI: 10.1103/PhysRev.133.B1549.

[36] Maximilian Delto. "The double-soft integral." unpublished. M.Sc. Thesis. 2018.

[37] Fabrizio Caola, Maximilian Delto, Hjalte Frellesvig, and Kirill Melnikov. "The double-soft integral for an arbitrary angle between hard radiators." In: *Eur. Phys. J. C* 78.8 (2018), p. 687. DOI: 10.1140/epjc/s10052-018-6180-7. arXiv: 1807.05835 [hep-ph].

[38] Daniel de Florian, Manuel Der, and Ignacio Fabre. "QCD⊕QED NNLO corrections to Drell Yan production." In: *Phys. Rev. D* 98.9 (2018), p. 094008. DOI: 10.1103/PhysRevD.98.094008. arXiv: 1805.12214 [hep-ph].

[39] Charalampos Anastasiou and Kirill Melnikov. "Higgs boson production at hadron colliders in NNLO QCD." In: *Nucl. Phys. B* 646 (2002), pp. 220–256. DOI: 10.1016/S0550-3213(02)00837-4. arXiv: hep-ph/0207004.

[40] Gerard 't Hooft and M. J. G. Veltman. "Regularization and Renormalization of Gauge Fields." In: *Nucl. Phys. B* 44 (1972), pp. 189–213. DOI: 10.1016/0550-3213(72)90279-9.

[41] C. G. Bollini and J. J. Giambiagi. "Dimensional Renormalization: The Number of Dimensions as a Regularizing Parameter." In: *Nuovo Cim. B* 12 (1972), pp. 20–26. DOI: 10.1007/BF02895558.

[42] G. M. Cicuta and E. Montaldi. "Analytic renormalization via continuous space dimension." In: *Lett. Nuovo Cim.* 4 (1972), pp. 329–332. DOI: 10.1007/BF02756527.

[43] W. T. Giele and E. W. Nigel Glover. "Higher order corrections to jet cross-sections in e+ e- annihilation." In: *Phys. Rev. D* 46 (1992), pp. 1980–2010. DOI: 10.1103/PhysRevD.46.1980.

[44] Zoltan Kunszt, Adrian Signer, and Zoltan Trocsanyi. "Singular terms of helicity amplitudes at one loop in QCD and the soft limit of the cross-sections of multi-parton processes." In: *Nucl. Phys. B* 420 (1994), pp. 550–564. DOI: 10.1016/0550-3213(94)90077-9. arXiv: hep-ph/9401294.

[45] Stefano Catani. "The Singular behavior of QCD amplitudes at two loop order." In: *Phys. Lett. B* 427 (1998), pp. 161–171. DOI: 10.1016/S0370-2693(98)00332-3. arXiv: hep-ph/9802439.

[46] Thomas Becher and Matthias Neubert. "Infrared singularities of scattering amplitudes in perturbative QCD." In: *Phys. Rev. Lett.* 102 (2009). [Erratum: Phys.Rev.Lett. 111, 199905 (2013)], p. 162001. DOI: 10.1103/PhysRevLett.102.162001. arXiv: 0901.0722 [hep-ph].

[47] K. Fabricius, I. Schmitt, G. Kramer, and G. Schierholz. "Higher Order Perturbative QCD Calculation of Jet Cross-Sections in e+ e- Annihilation." In: *Z. Phys. C* 11 (1981), p. 315. DOI: 10.1007/BF01578281.

[48] R. Keith Ellis, D. A. Ross, and A. E. Terrano. "The Perturbative Calculation of Jet Structure in e+ e- Annihilation." In: *Nucl. Phys. B* 178 (1981), pp. 421–456. DOI: 10.1016/0550-3213(81)90165-6.

[49] John M. Campbell, R. Keith Ellis, and Ciaran Williams. "Direct Photon Production at Next-to–Next-to-Leading Order." In: *Phys. Rev. Lett.* 118.22 (2017). [Erratum: Phys.Rev.Lett. 124, 259901 (2020)], p. 222001. DOI: 10.1103/PhysRevLett.118.222001. arXiv: 1612.04333 [hep-ph].

[50] S. Alekhin, A. Kardos, S. Moch, and Z. Trócsányi. "Precision studies for Drell-Yan processes at NNLO." In: (Apr. 2021). arXiv: 2104.02400 [hep-ph].

[51] S. Frixione, Z. Kunszt, and A. Signer. "Three jet cross-sections to next-to-leading order." In: *Nucl. Phys. B* 467 (1996), pp. 399–442. DOI: 10.1016/0550-3213(96)00110-1. arXiv: hep-ph/9512328.

[52] S. Frixione. "A General approach to jet cross-sections in QCD." In: *Nucl. Phys. B* 507 (1997), pp. 295–314. DOI: 10.1016/S0550-3213(97)00574-9. arXiv: hep-ph/9706545.

[53] S. Catani and M. H. Seymour. "A General algorithm for calculating jet cross-sections in NLO QCD." In: *Nucl. Phys. B* 485 (1997). [Erratum: Nucl.Phys.B 510, 503–504 (1998)], pp. 291–419. DOI: 10.1016/S0550-3213(96)00589-5. arXiv: hep-ph/9605323.

[54] Stefano Catani, Stefan Dittmaier, Michael H. Seymour, and Zoltan Trocsanyi. "The Dipole formalism for next-to-leading order QCD calculations with massive partons." In: *Nucl. Phys. B* 627 (2002), pp. 189–265. DOI: 10.1016/S0550-3213(02)00098-6. arXiv: hep-ph/0201036.

[55] Zoltan Nagy and Davison E. Soper. "General subtraction method for numerical calculation of one loop QCD matrix elements." In: *JHEP* 09 (2003), p. 055. DOI: 10.1088/1126-6708/2003/09/055. arXiv: hep-ph/0308127.

[56] Zoltan Nagy and Davison E. Soper. "Parton showers with quantum interference." In: *JHEP* 09 (2007), p. 114. DOI: 10.1088/1126-6708/2007/09/114. arXiv: 0706.0017 [hep-ph].

[57] C. H. Chung, M. Kramer, and T. Robens. "An alternative subtraction scheme for next-to-leading order QCD calculations." In: *JHEP* 06 (2011), p. 144. DOI: 10.1007/JHEP06(2011)144. arXiv: 1012.4948 [hep-ph].

[58] Cheng-Han Chung and Tania Robens. "Nagy-Soper subtraction scheme for multi-parton final states." In: *Phys. Rev. D* 87 (2013), p. 074032. DOI: 10.1103/PhysRevD.87.074032. arXiv: 1209.1569 [hep-ph].

[59] G. Bevilacqua, M. Czakon, M. Kubocz, and M. Worek. "Complete Nagy-Soper subtraction for next-to-leading order calculations in QCD." In: *JHEP* 10 (2013), p. 204. DOI: 10.1007/JHEP10(2013)204. arXiv: 1308.5605 [hep-ph].

[60] Giovanni Ossola, Costas G. Papadopoulos, and Roberto Pittau. "Reducing full one-loop amplitudes to scalar integrals at the integrand level." In: *Nucl. Phys. B* 763 (2007), pp. 147–169. DOI: 10.1016/j.nuclphysb.2006.11.012. arXiv: hep-ph/0609007.

[61] R. Keith Ellis, W. T. Giele, and Z. Kunszt. "A Numerical Unitarity Formalism for Evaluating One-Loop Amplitudes." In: *JHEP* 03 (2008), p. 003. DOI: 10.1088/1126-6708/2008/03/003. arXiv: 0708.2398 [hep-ph].

[62] Walter T. Giele, Zoltan Kunszt, and Kirill Melnikov. "Full one-loop amplitudes from tree amplitudes." In: *JHEP* 04 (2008), p. 049. DOI: 10.1088/1126-6708/2008/04/049. arXiv: 0801.2237 [hep-ph].

[63] Tanju Gleisberg and Frank Krauss. "Automating dipole subtraction for QCD NLO calculations." In: *Eur. Phys. J. C* 53 (2008), pp. 501–523. DOI: 10.1140/epjc/s10052-007-0495-0. arXiv: 0709.2881 [hep-ph].

[64] Rikkert Frederix, Thomas Gehrmann, and Nicolas Greiner. "Automation of the Dipole Subtraction Method in MadGraph/MadEvent." In: *JHEP* 09 (2008), p. 122. DOI: 10.1088/1126-6708/2008/09/122. arXiv: 0808.2128 [hep-ph].

[65] Rikkert Frederix, Stefano Frixione, Fabio Maltoni, and Tim Stelzer. "Automation of next-to-leading order computations in QCD: The FKS subtraction." In: *JHEP* 10 (2009), p. 003. DOI: 10.1088/1126-6708/2009/10/003. arXiv: 0908.4272 [hep-ph].

[66] K. Hasegawa, S. Moch, and P. Uwer. "AutoDipole: Automated generation of dipole subtraction terms." In: *Comput. Phys. Commun.* 181 (2010), pp. 1802–1817. DOI: 10.1016/j.cpc.2010.06.044. arXiv: 0911.4371 [hep-ph].

[67] Simone Alioli, Paolo Nason, Carlo Oleari, and Emanuele Re. "A general framework for implementing NLO calculations in shower Monte Carlo programs: the POWHEG BOX." In: *JHEP* 06 (2010), p. 043. DOI: 10.1007/JHEP06(2010)043. arXiv: 1002.2581 [hep-ph].

[68] Johannes Bellm et al. "Herwig 7.0/Herwig++ 3.0 release note." In: *Eur. Phys. J. C* 76.4 (2016), p. 196. DOI: 10.1140/epjc/s10052-016-4018-8. arXiv: 1512.01178 [hep-ph].

[69] Stefano Catani and Massimiliano Grazzini. "An NNLO subtraction formalism in hadron collisions and its application to Higgs boson production at the LHC." In: *Phys. Rev. Lett.* 98 (2007), p. 222002. DOI: 10.1103/PhysRevLett.98.222002. arXiv: hep-ph/0703012.

[70] Roberto Bonciani, Stefano Catani, Massimiliano Grazzini, Hayk Sargsyan, and Alessandro Torre. "The q_T subtraction method for top quark production at hadron colliders." In: *Eur. Phys. J. C* 75.12 (2015), p. 581. DOI: 10.1140/epjc/s10052-015-3793-y. arXiv: 1508.03585 [hep-ph].

[71] Massimiliano Grazzini, Stefan Kallweit, and Marius Wiesemann. "Fully differential NNLO computations with MATRIX." In: *Eur. Phys. J. C* 78.7 (2018), p. 537. DOI: 10.1140/epjc/s10052-018-5771-7. arXiv: 1711.06631 [hep-ph].

[72] Stefano Catani, Simone Devoto, Massimiliano Grazzini, Stefan Kallweit, Javier Mazzitelli, and Hayk Sargsyan. "Top-quark pair hadroproduction at next-to-next-to-leading order in QCD." In: *Phys. Rev. D* 99.5 (2019), p. 051501. DOI: 10.1103/PhysRevD.99.051501. arXiv: 1901.04005 [hep-ph].

[73] Stefano Catani, Simone Devoto, Massimiliano Grazzini, Stefan Kallweit, and Javier Mazzitelli. "Top-quark pair production at the LHC: Fully differential QCD predictions at NNLO." In: *JHEP* 07 (2019), p. 100. DOI: 10.1007/JHEP07(2019)100. arXiv: 1906.06535 [hep-ph].

[74] Stefan Kallweit, Vasily Sotnikov, and Marius Wiesemann. "Triphoton production at hadron colliders in NNLO QCD." In: *Phys. Lett. B* 812 (2021), p. 136013. DOI: 10.1016/j.physletb.2020.136013. arXiv: 2010.04681 [hep-ph].

[75] Stefano Catani, Simone Devoto, Massimiliano Grazzini, Stefan Kallweit, and Javier Mazzitelli. "Bottom-quark production at hadron colliders: fully differential predictions in NNLO QCD." In: *JHEP* 03 (2021), p. 029. DOI: 10.1007/JHEP03(2021)029. arXiv: 2010.11906 [hep-ph].

[76] Stefano Catani, Ignacio Fabre, Massimiliano Grazzini, and Stefan Kallweit. "$t\bar{t}H$ production at NNLO: the flavour off-diagonal channels." In: (Feb. 2021). arXiv: 2102.03256 [hep-ph].

[77] Radja Boughezal, Christfried Focke, Xiaohui Liu, and Frank Petriello. "W-boson production in association with a jet at next-to-next-to-leading order in perturbative QCD." In: *Phys. Rev. Lett.* 115.6 (2015), p. 062002. DOI: 10.1103/PhysRevLett.115.062002. arXiv: 1504.02131 [hep-ph].

[78] Radja Boughezal, Christfried Focke, Walter Giele, Xiaohui Liu, and Frank Petriello. "Higgs boson production in association with a jet at NNLO using jettiness subtraction." In: *Phys. Lett. B* 748 (2015), pp. 5–8. DOI: 10.1016/j.physletb.2015.06.055. arXiv: 1505.03893 [hep-ph].

[79] Jonathan Gaunt, Maximilian Stahlhofen, Frank J. Tackmann, and Jonathan R. Walsh. "N-jettiness Subtractions for NNLO QCD Calculations." In: *JHEP* 09 (2015), p. 058. DOI: 10.1007/JHEP09(2015)058. arXiv: 1505.04794 [hep-ph].

[80] Radja Boughezal, John M. Campbell, R. Keith Ellis, Christfried Focke, Walter Giele, Xiaohui Liu, Frank Petriello, and Ciaran Williams. "Color singlet production at NNLO in MCFM." In: *Eur. Phys. J. C* 77.1 (2017), p. 7. DOI: 10.1140/epjc/s10052-016-4558-y. arXiv: 1605.08011 [hep-ph].

[81] A. Gehrmann-De Ridder, T. Gehrmann, and E. W. Nigel Glover. "Antenna subtraction at NNLO." In: *JHEP* 09 (2005), p. 056. DOI: 10.1088/1126-6708/2005/09/056. arXiv: hep-ph/0505111.

[82] A. Gehrmann-De Ridder, T. Gehrmann, and E. W. Nigel Glover. "Gluon-gluon antenna functions from Higgs boson decay." In: *Phys. Lett. B* 612 (2005), pp. 49–60. DOI: 10.1016/j.physletb.2005.03.003. arXiv: hep-ph/0502110.

[83] A. Gehrmann-De Ridder, T. Gehrmann, and E. W. Nigel Glover. "Quark-gluon antenna functions from neutralino decay." In: *Phys. Lett. B* 612 (2005), pp. 36–48. DOI: 10.1016/j.physletb.2005.02.039. arXiv: hep-ph/0501291.

[84] A. Daleo, T. Gehrmann, and D. Maitre. "Antenna subtraction with hadronic initial states." In: *JHEP* 04 (2007), p. 016. DOI: 10.1088/1126-6708/2007/04/016. arXiv: hep-ph/0612257.

[85] A. Gehrmann-De Ridder, T. Gehrmann, E. W. N. Glover, and G. Heinrich. "Second-order QCD corrections to the thrust distribution." In: *Phys. Rev. Lett.* 99 (2007), p. 132002. DOI: 10.1103/PhysRevLett.99.132002. arXiv: 0707.1285 [hep-ph].

[86] Alejandro Daleo, Aude Gehrmann-De Ridder, Thomas Gehrmann, and Gionata Luisoni. "Antenna subtraction at NNLO with hadronic initial states: initial-final configurations." In: *JHEP* 01 (2010), p. 118. DOI: 10.1007/JHEP01(2010)118. arXiv: 0912.0374 [hep-ph].

[87] Thomas Gehrmann and Pier Francesco Monni. "Antenna subtraction at NNLO with hadronic initial states: real-virtual initial-initial configurations." In: *JHEP* 12 (2011), p. 049. DOI: 10.1007/JHEP12(2011)049. arXiv: 1107.4037 [hep-ph].

[88] Radja Boughezal, Aude Gehrmann-De Ridder, and Mathias Ritzmann. "Antenna subtraction at NNLO with hadronic initial states: double real radiation for initial-initial configurations with two quark flavours." In: *JHEP* 02 (2011), p. 098. DOI: 10.1007/JHEP02(2011)098. arXiv: 1011.6631 [hep-ph].

[89] Aude Gehrmann-De Ridder, Thomas Gehrmann, and Mathias Ritzmann. "Antenna subtraction at NNLO with hadronic initial states: double real initial-initial configurations." In: *JHEP* 10 (2012), p. 047. DOI: 10.1007/JHEP10(2012)047. arXiv: 1207.5779 [hep-ph].

[90] James Currie, E. W. N. Glover, and Steven Wells. "Infrared Structure at NNLO Using Antenna Subtraction." In: *JHEP* 04 (2013), p. 066. DOI: 10.1007/JHEP04(2013)066. arXiv: 1301.4693 [hep-ph].

[91] James Currie, Thomas Gehrmann, and Jan Niehues. "Precise QCD predictions for the production of dijet final states in deep inelastic scattering." In: *Phys. Rev. Lett.* 117.4 (2016), p. 042001. DOI: 10.1103/PhysRevLett.117.042001. arXiv: 1606.03991 [hep-ph].

[92] James Currie, Aude Gehrmann-De Ridder, Thomas Gehrmann, E. W. N. Glover, Alexander Huss, and Joao Pires. "Precise predictions for dijet production at the LHC." In: *Phys. Rev. Lett.* 119.15 (2017), p. 152001. DOI: 10.1103/PhysRevLett.119.152001. arXiv: 1705.10271 [hep-ph].

[93] James Currie, Aude Gehrmann-De Ridder, Thomas Gehrmann, E. W. Nigel Glover, Alexander Huss, and João Pires. "Infrared sensitivity of single jet inclusive production at hadron colliders." In: *JHEP* 10 (2018), p. 155. DOI: 10.1007/JHEP10(2018)155. arXiv: 1807.03692 [hep-ph].

[94] Franz Herzog. "Geometric IR subtraction for final state real radiation." In: *JHEP* 08 (2018), p. 006. DOI: 10.1007/JHEP08(2018)006. arXiv: 1804.07949 [hep-ph].

[95] M. Czakon. "A novel subtraction scheme for double-real radiation at NNLO." In: *Phys. Lett. B* 693 (2010), pp. 259–268. DOI: 10.1016/j.physletb.2010.08.036. arXiv: 1005.0274 [hep-ph].

[96] M. Czakon. "Double-real radiation in hadronic top quark pair production as a proof of a certain concept." In: *Nucl. Phys. B* 849 (2011), pp. 250–295. DOI: 10.1016/j.nuclphysb.2011.03.020. arXiv: 1101.0642 [hep-ph].

[97] Michał Czakon, Paul Fiedler, and Alexander Mitov. "Total Top-Quark Pair-Production Cross Section at Hadron Colliders Through $O(\alpha_S^4)$." In: *Phys. Rev. Lett.* 110 (2013), p. 252004. DOI: 10.1103/PhysRevLett.110.252004. arXiv: 1303.6254 [hep-ph].

[98] M. Czakon and D. Heymes. "Four-dimensional formulation of the sector-improved residue subtraction scheme." In: *Nucl. Phys. B* 890 (2014), pp. 152–227. DOI: 10.1016/j.nuclphysb.2014.11.006. arXiv: 1408.2500 [hep-ph].

[99] Michał Czakon, Andreas van Hameren, Alexander Mitov, and Rene Poncelet. "Single-jet inclusive rates with exact color at $\mathcal{O}(\alpha_s^4)$." In: *JHEP* 10 (2019), p. 262. DOI: 10.1007/JHEP10(2019)262. arXiv: 1907.12911 [hep-ph].

[100] Herschel A. Chawdhry, Micha L. Czakon, Alexander Mitov, and Rene Poncelet. "NNLO QCD corrections to three-photon production at the LHC." In: *JHEP* 02 (2020), p. 057. DOI: 10.1007/JHEP02(2020)057. arXiv: 1911.00479 [hep-ph].

[101] L. Magnea, E. Maina, G. Pelliccioli, C. Signorile-Signorile, P. Torrielli, and S. Uccirati. "Local analytic sector subtraction at NNLO." In: *JHEP* 12 (2018). [Erratum: JHEP 06, 013 (2019)], p. 107. DOI: 10.1007/JHEP12(2018)107. arXiv: 1806.09570 [hep-ph].

[102] Lorenzo Magnea, Ezio Maina, Giovanni Pelliccioli, Chiara Signorile-Signorile, Paolo Torrielli, and Sandro Uccirati. "Factorisation and Subtraction beyond NLO." In: *JHEP* 12 (2018), p. 062. DOI: 10.1007/JHEP12(2018)062. arXiv: 1809.05444 [hep-ph].

[103] Lorenzo Magnea, Giovanni Pelliccioli, Chiara Signorile-Signorile, Paolo Torrielli, and Sandro Uccirati. "Analytic integration of soft and collinear radiation in factorised QCD cross sections at NNLO." In: *JHEP* 02 (2021), p. 037. DOI: 10.1007/JHEP02(2021)037. arXiv: 2010.14493 [hep-ph].

[104] Gabor Somogyi, Zoltan Trocsanyi, and Vittorio Del Duca. “Matching of singly- and doubly-unresolved limits of tree-level QCD squared matrix elements.” In: *JHEP* 06 (2005), p. 024. DOI: 10.1088/1126-6708/2005/06/024. arXiv: hep-ph/0502226.

[105] Gabor Somogyi and Zoltan Trocsanyi. “A New subtraction scheme for computing QCD jet cross sections at next-to-leading order accuracy.” In: (Sept. 2006). arXiv: hep-ph/0609041.

[106] Gabor Somogyi, Zoltan Trocsanyi, and Vittorio Del Duca. “A Subtraction scheme for computing QCD jet cross sections at NNLO: Regularization of doubly-real emissions.” In: *JHEP* 01 (2007), p. 070. DOI: 10.1088/1126-6708/2007/01/070. arXiv: hep-ph/0609042.

[107] Gabor Somogyi and Zoltan Trocsanyi. “A Subtraction scheme for computing QCD jet cross sections at NNLO: Regularization of real-virtual emission.” In: *JHEP* 01 (2007), p. 052. DOI: 10.1088/1126-6708/2007/01/052. arXiv: hep-ph/0609043.

[108] Gabor Somogyi and Zoltan Trocsanyi. “A Subtraction scheme for computing QCD jet cross sections at NNLO: Integrating the subtraction terms. I.” In: *JHEP* 08 (2008), p. 042. DOI: 10.1088/1126-6708/2008/08/042. arXiv: 0807.0509 [hep-ph].

[109] Ugo Aglietti, Vittorio Del Duca, Claude Duhr, Gabor Somogyi, and Zoltan Trocsanyi. “Analytic integration of real-virtual counterterms in NNLO jet cross sections. I.” In: *JHEP* 09 (2008), p. 107. DOI: 10.1088/1126-6708/2008/09/107. arXiv: 0807.0514 [hep-ph].

[110] Gabor Somogyi. “Subtraction with hadronic initial states at NLO: An NNLO-compatible scheme.” In: *JHEP* 05 (2009), p. 016. DOI: 10.1088/1126-6708/2009/05/016. arXiv: 0903.1218 [hep-ph].

[111] Paolo Bolzoni, Sven-Olaf Moch, Gabor Somogyi, and Zoltan Trocsanyi. “Analytic integration of real-virtual counterterms in NNLO jet cross sections. II.” In: *JHEP* 08 (2009), p. 079. DOI: 10.1088/1126-6708/2009/08/079. arXiv: 0905.4390 [hep-ph].

[112] Paolo Bolzoni, Gabor Somogyi, and Zoltan Trocsanyi. “A subtraction scheme for computing QCD jet cross sections at NNLO: integrating the iterated singly-unresolved subtraction terms.” In: *JHEP* 01 (2011), p. 059. DOI: 10.1007/JHEP01(2011)059. arXiv: 1011.1909 [hep-ph].

[113] Vittorio Del Duca, Gabor Somogyi, and Zoltan Trocsanyi. “Integration of collinear-type doubly unresolved counterterms in NNLO jet cross sections.” In: *JHEP* 06 (2013), p. 079. DOI: 10.1007/JHEP06(2013)079. arXiv: 1301.3504 [hep-ph].

[114] Gabor Somogyi. “A subtraction scheme for computing QCD jet cross sections at NNLO: integrating the doubly unresolved subtraction terms.” In: *JHEP* 04 (2013), p. 010. DOI: 10.1007/JHEP04(2013)010. arXiv: 1301.3919 [hep-ph].

[115] Vittorio Del Duca, Claude Duhr, Adam Kardos, Gábor Somogyi, Zoltán Szőr, Zoltán Trócsányi, and Zoltán Tulipánt. "Jet production in the CoLoRFulNNLO method: event shapes in electron-positron collisions." In: *Phys. Rev. D* 94.7 (2016), p. 074019. DOI: 10.1103/PhysRevD.94.074019. arXiv: 1606.03453 [hep-ph].

[116] Tao Han, G. Valencia, and S. Willenbrock. "Structure function approach to vector boson scattering in p p collisions." In: *Phys. Rev. Lett.* 69 (1992), pp. 3274–3277. DOI: 10.1103/PhysRevLett.69.3274. arXiv: hep-ph/9206246.

[117] Mathias Brucherseifer, Fabrizio Caola, and Kirill Melnikov. "On the NNLO QCD corrections to single-top production at the LHC." In: *Phys. Lett. B* 736 (2014), pp. 58–63. DOI: 10.1016/j.physletb.2014.06.075. arXiv: 1404.7116 [hep-ph].

[118] Matteo Cacciari, Frédéric A. Dreyer, Alexander Karlberg, Gavin P. Salam, and Giulia Zanderighi. "Fully Differential Vector-Boson-Fusion Higgs Production at Next-to-Next-to-Leading Order." In: *Phys. Rev. Lett.* 115.8 (2015). [Erratum: Phys.Rev.Lett. 120, 139901 (2018)], p. 082002. DOI: 10.1103/PhysRevLett.115.082002. arXiv: 1506.02660 [hep-ph].

[119] X. Chen, X. Chen, T. Gehrmann, E. W. N. Glover, A. Huss, B. Mistlberger, and A. Pelloni. "Fully Differential Higgs Boson Production to Third Order in QCD." In: (Feb. 2021). arXiv: 2102.07607 [hep-ph].

[120] Gudrun Heinrich. "Collider Physics at the Precision Frontier." In: (Sept. 2020). arXiv: 2009.00516 [hep-ph].

[121] R. Keith Ellis, W. James Stirling, and B. R. Webber. *QCD and collider physics*. Vol. 8. Cambridge University Press, Feb. 2011. ISBN: 978-0-511-82328-2, 978-0-521-54589-1.

[122] John M. Campbell and E. W. Nigel Glover. "Double unresolved approximations to multiparton scattering amplitudes." In: *Nucl. Phys. B* 527 (1998), pp. 264–288. DOI: 10.1016/S0550-3213(98)00295-8. arXiv: hep-ph/9710255.

[123] Stefano Catani and Massimiliano Grazzini. "Infrared factorization of tree level QCD amplitudes at the next-to-next-to-leading order and beyond." In: *Nucl. Phys. B* 570 (2000), pp. 287–325. DOI: 10.1016/S0550-3213(99)00778-6. arXiv: hep-ph/9908523.

[124] Konstantin Asteriadis. "Application of the nested soft-collinear subtraction scheme to the description of deep inelastic scattering." to be published. PhD thesis. 2020.

[125] R. Keith Ellis, Howard Georgi, Marie Machacek, H. David Politzer, and Graham G. Ross. "Perturbation Theory and the Parton Model in QCD." In: *Nucl. Phys. B* 152 (1979), pp. 285–329. DOI: 10.1016/0550-3213(79)90105-6.

[126] Fabrizio Caola, Gionata Luisoni, Kirill Melnikov, and Raoul Röntsch. "NNLO QCD corrections to associated WH production and $H \to b\bar{b}$ decay." In: *Phys. Rev. D* 97.7 (2018), p. 074022. DOI: 10.1103/PhysRevD.97.074022. arXiv: 1712.06954 [hep-ph].

[127] T. Huber and Daniel Maitre. "HypExp: A Mathematica package for expanding hypergeometric functions around integer-valued parameters." In: *Comput. Phys. Commun.* 175 (2006), pp. 122–144. DOI: 10.1016/j.cpc.2006.01.007. arXiv: hep-ph/0507094.

[128] Tobias Huber and Daniel Maitre. "HypExp 2, Expanding Hypergeometric Functions about Half-Integer Parameters." In: *Comput. Phys. Commun.* 178 (2008), pp. 755–776. DOI: 10.1016/j.cpc.2007.12.008. arXiv: 0708.2443 [hep-ph].

[129] Gabor Somogyi. "Angular integrals in d dimensions." In: *J. Math. Phys.* 52 (2011), p. 083501. DOI: 10.1063/1.3615515. arXiv: 1101.3557 [hep-ph].

[130] K. G. Chetyrkin and F. V. Tkachov. "Integration by Parts: The Algorithm to Calculate beta Functions in 4 Loops." In: *Nucl. Phys. B* 192 (1981), pp. 159–204. DOI: 10.1016/0550-3213(81)90199-1.

[131] F. V. Tkachov. "A Theorem on Analytical Calculability of Four Loop Renormalization Group Functions." In: *Phys. Lett. B* 100 (1981), pp. 65–68. DOI: 10.1016/0370-2693(81)90288-4.

[132] A. V. Kotikov. "Differential equations method: New technique for massive Feynman diagrams calculation." In: *Phys. Lett. B* 254 (1991), pp. 158–164. DOI: 10.1016/0370-2693(91)90413-K.

[133] A. V. Kotikov. "Differential equations method: The Calculation of vertex type Feynman diagrams." In: *Phys. Lett. B* 259 (1991), pp. 314–322. DOI: 10.1016/0370-2693(91)90834-D.

[134] A. V. Kotikov. "Differential equation method: The Calculation of N point Feynman diagrams." In: *Phys. Lett. B* 267 (1991). [Erratum: Phys.Lett.B 295, 409–409 (1992)], pp. 123–127. DOI: 10.1016/0370-2693(91)90536-Y.

[135] Ettore Remiddi. "Differential equations for Feynman graph amplitudes." In: *Nuovo Cim. A* 110 (1997), pp. 1435–1452. arXiv: hep-th/9711188.

[136] T. Gehrmann and E. Remiddi. "Differential equations for two loop four point functions." In: *Nucl. Phys. B* 580 (2000), pp. 485–518. DOI: 10.1016/S0550-3213(00)00223-6. arXiv: hep-ph/9912329.

[137] R. E. Cutkosky. "Singularities and discontinuities of Feynman amplitudes." In: *J. Math. Phys.* 1 (1960), pp. 429–433. DOI: 10.1063/1.1703676.

[138] R. N. Lee. "Group structure of the integration-by-part identities and its application to the reduction of multiloop integrals." In: *JHEP* 07 (2008), p. 031. DOI: 10.1088/1126-6708/2008/07/031. arXiv: 0804.3008 [hep-ph].

[139] S. Laporta. "High precision calculation of multiloop Feynman integrals by difference equations." In: *Int. J. Mod. Phys. A* 15 (2000), pp. 5087–5159. DOI: 10.1016/S0217-751X(00)00215-7. arXiv: hep-ph/0102033.

[140] Charalampos Anastasiou and Achilleas Lazopoulos. "Automatic integral reduction for higher order perturbative calculations." In: *JHEP* 07 (2004), p. 046. DOI: 10.1088/1126-6708/2004/07/046. arXiv: hep-ph/0404258.

[141] A. V. Smirnov. "Algorithm FIRE – Feynman Integral REduction." In: *JHEP* 10 (2008), p. 107. DOI: 10.1088/1126-6708/2008/10/107. arXiv: 0807.3243 [hep-ph].

[142] A. V. Smirnov and F. S. Chuharev. "FIRE6: Feynman Integral REduction with Modular Arithmetic." In: *Comput. Phys. Commun.* 247 (2020), p. 106877. DOI: 10.1016/j.cpc.2019.106877. arXiv: 1901.07808 [hep-ph].

[143] C. Studerus. "Reduze-Feynman Integral Reduction in C++." In: *Comput. Phys. Commun.* 181 (2010), pp. 1293–1300. DOI: 10.1016/j.cpc.2010.03.012. arXiv: 0912.2546 [physics.comp-ph].

[144] A. von Manteuffel and C. Studerus. "Reduze 2 - Distributed Feynman Integral Reduction." In: (Jan. 2012). arXiv: 1201.4330 [hep-ph].

[145] Philipp Maierhöfer, Johann Usovitsch, and Peter Uwer. "Kira—A Feynman integral reduction program." In: *Comput. Phys. Commun.* 230 (2018), pp. 99–112. DOI: 10.1016/j.cpc.2018.04.012. arXiv: 1705.05610 [hep-ph].

[146] Jonas Klappert, Fabian Lange, Philipp Maierhöfer, and Johann Usovitsch. "Integral Reduction with Kira 2.0 and Finite Field Methods." In: (Aug. 2020). arXiv: 2008.06494 [hep-ph].

[147] A. V. Smirnov and A. V. Petukhov. "The Number of Master Integrals is Finite." In: *Lett. Math. Phys.* 97 (2011), pp. 37–44. DOI: 10.1007/s11005-010-0450-0. arXiv: 1004.4199 [hep-th].

[148] R. N. Lee. "Presenting LiteRed: a tool for the Loop InTEgrals REDuction." In: (Dec. 2012). arXiv: 1212.2685 [hep-ph].

[149] Roman N. Lee. "LiteRed 1.4: a powerful tool for reduction of multiloop integrals." In: *J. Phys. Conf. Ser.* 523 (2014). Ed. by Jianxiong Wang, p. 012059. DOI: 10.1088/1742-6596/523/1/012059. arXiv: 1310.1145 [hep-ph].

[150] A. V. Smirnov. "An Algorithm to construct Grobner bases for solving integration by parts relations." In: *JHEP* 04 (2006), p. 026. DOI: 10.1088/1126-6708/2006/04/026. arXiv: hep-ph/0602078.

[151] Johannes M. Henn. "Multiloop integrals in dimensional regularization made simple." In: *Phys. Rev. Lett.* 110 (2013), p. 251601. DOI: 10.1103/PhysRevLett.110.251601. arXiv: 1304.1806 [hep-th].

[152] Kuo-Tsai Chen. "Iterated path integrals." In: *Bull. Am. Math. Soc.* 83 (1977), pp. 831–879. DOI: 10.1090/S0002-9904-1977-14320-6.

[153] Marco Besier, Pascal Wasser, and Stefan Weinzierl. "RationalizeRoots: Software Package for the Rationalization of Square Roots." In: *Comput. Phys. Commun.* 253 (2020), p. 107197. DOI: 10.1016/j.cpc.2020.107197. arXiv: 1910.13251 [cs.MS].

[154] Alexander B. Goncharov. “Multiple polylogarithms, cyclotomy and modular complexes.” In: *Math. Res. Lett.* 5 (1998), pp. 497–516. DOI: 10.4310/MRL.1998.v5.n4.a7. arXiv: 1105.2076 [math.AG].

[155] A. B. Goncharov. “Polylogarithms in Arithmetic and Geometry.” In: *Proceeding of the International Congress of Mathematicians* (1994), pp. 374–387.

[156] Matthias Heller, Andreas von Manteuffel, Robert M. Schabinger, and Hubert Spiesberger. “Mixed EW-QCD two-loop amplitudes for $q\bar{q} \to \ell^+\ell^-$ and γ_5 scheme independence of multi-loop corrections.” In: (Dec. 2020). arXiv: 2012.05918 [hep-ph].

[157] Francis Brown and Claude Duhr. “A double integral of dlog forms which is not polylogarithmic.” In: June 2020. arXiv: 2006.09413 [hep-th].

[158] Johannes Henn, Bernhard Mistlberger, Vladimir A. Smirnov, and Pascal Wasser. “Constructing d-log integrands and computing master integrals for three-loop four-particle scattering.” In: *JHEP* 04 (2020), p. 167. DOI: 10.1007/JHEP04(2020)167. arXiv: 2002.09492 [hep-ph].

[159] Kasper J. Larsen and Robbert Rietkerk. “MultivariateResidues - a Mathematica package for computing multivariate residues.” In: *PoS* RADCOR2017 (2017). Ed. by Andre Hoang and Carsten Schneider, p. 021. DOI: 10.22323/1.290.0021. arXiv: 1712.07050 [hep-th].

[160] Thomas Gehrmann, Andreas von Manteuffel, Lorenzo Tancredi, and Erich Weihs. “The two-loop master integrals for $q\bar{q} \to VV$.” In: *JHEP* 06 (2014), p. 032. DOI: 10.1007/JHEP06(2014)032. arXiv: 1404.4853 [hep-ph].

[161] Mario Argeri, Stefano Di Vita, Pierpaolo Mastrolia, Edoardo Mirabella, Johannes Schlenk, Ulrich Schubert, and Lorenzo Tancredi. “Magnus and Dyson Series for Master Integrals.” In: *JHEP* 03 (2014), p. 082. DOI: 10.1007/JHEP03(2014)082. arXiv: 1401.2979 [hep-ph].

[162] Maik Höschele, Jens Hoff, and Takahiro Ueda. “Adequate bases of phase space master integrals for $gg \to h$ at NNLO and beyond.” In: *JHEP* 09 (2014), p. 116. DOI: 10.1007/JHEP09(2014)116. arXiv: 1407.4049 [hep-ph].

[163] Christoph Dlapa, Johannes Henn, and Kai Yan. “Deriving canonical differential equations for Feynman integrals from a single uniform weight integral.” In: *JHEP* 05 (2020), p. 025. DOI: 10.1007/JHEP05(2020)025. arXiv: 2002.02340 [hep-ph].

[164] Roman N. Lee. “Reducing differential equations for multiloop master integrals.” In: *JHEP* 04 (2015), p. 108. DOI: 10.1007/JHEP04(2015)108. arXiv: 1411.0911 [hep-ph].

[165] Roman N. Lee and Andrei A. Pomeransky. “Normalized Fuchsian form on Riemann sphere and differential equations for multiloop integrals.” In: (July 2017). arXiv: 1707.07856 [hep-th].

[166] Mario Prausa. "epsilon: A tool to find a canonical basis of master integrals." In: *Comput. Phys. Commun.* 219 (2017), pp. 361–376. DOI: 10.1016/j.cpc.2017.05.026. arXiv: 1701.00725 [hep-ph].

[167] Oleksandr Gituliar and Vitaly Magerya. "Fuchsia: a tool for reducing differential equations for Feynman master integrals to epsilon form." In: *Comput. Phys. Commun.* 219 (2017), pp. 329–338. DOI: 10.1016/j.cpc.2017.05.004. arXiv: 1701.04269 [hep-ph].

[168] Roman N. Lee. "Libra: a package for transformation of differential systems for multiloop integrals." In: (Dec. 2020). arXiv: 2012.00279 [hep-ph].

[169] Christoph Meyer. "Transforming differential equations of multi-loop Feynman integrals into canonical form." In: *JHEP* 04 (2017), p. 006. DOI: 10.1007/JHEP04(2017)006. arXiv: 1611.01087 [hep-ph].

[170] Christoph Meyer. "Algorithmic transformation of multi-loop master integrals to a canonical basis with CANONICA." In: *Comput. Phys. Commun.* 222 (2018), pp. 295–312. DOI: 10.1016/j.cpc.2017.09.014. arXiv: 1705.06252 [hep-ph].

[171] Claude Duhr and Falko Dulat. "PolyLogTools — polylogs for the masses." In: *JHEP* 08 (2019), p. 135. DOI: 10.1007/JHEP08(2019)135. arXiv: 1904.07279 [hep-th].

[172] Hjalte Frellesvig. "Generalized Polylogarithms in Maple." In: (June 2018). arXiv: 1806.02883 [hep-th].

[173] Arnd Behring and Wojciech Bizoń. "Higgs decay into massive b-quarks at NNLO QCD in the nested soft-collinear subtraction scheme." In: *JHEP* 01 (2020), p. 189. DOI: 10.1007/JHEP01(2020)189. arXiv: 1911.11524 [hep-ph].

[174] M. Czakon. "Automatized analytic continuation of Mellin-Barnes integrals." In: *Comput. Phys. Commun.* 175 (2006), pp. 559–571. DOI: 10.1016/j.cpc.2006.07.002. arXiv: hep-ph/0511200.

[175] Christian W. Bauer, Alexander Frink, and Richard Kreckel. "Introduction to the GiNaC framework for symbolic computation within the C++ programming language." In: *J. Symb. Comput.* 33 (2002), pp. 1–12. DOI: 10.1006/jsco.2001.0494. arXiv: cs/0004015.

[176] Jens Vollinga and Stefan Weinzierl. "Numerical evaluation of multiple polylogarithms." In: *Comput. Phys. Commun.* 167 (2005), p. 177. DOI: 10.1016/j.cpc.2004.12.009. arXiv: hep-ph/0410259.

[177] Helaman R. P. Ferguson and David H. Bailey. "A Polynomial Time, Numerically Stable Integer Relation Algorithm." In: *RNR Technical Report RNR-91-032* (1992).

[178] David H. Bailey and David J. Broadhurst. "Parallel integer relation detection: Techniques and applications." In: *Math. Comput.* 70 (2001), pp. 1719–1736. DOI: 10.1090/S0025-5718-00-01278-3. arXiv: math/9905048.

[179] F. J. Hasert et al. “Observation of Neutrino Like Interactions Without Muon Or Electron in the Gargamelle Neutrino Experiment.” In: *Phys. Lett. B* 46 (1973), pp. 138–140. DOI: 10.1016/0370-2693(73)90499-1.

[180] G. Arnison et al. “Experimental Observation of Isolated Large Transverse Energy Electrons with Associated Missing Energy at $\sqrt{s} = 540$ GeV.” In: *Phys. Lett. B* 122 (1983), pp. 103–116. DOI: 10.1016/0370-2693(83)91177-2.

[181] M. Banner et al. “Observation of Single Isolated Electrons of High Transverse Momentum in Events with Missing Transverse Energy at the CERN anti-p p Collider.” In: *Phys. Lett. B* 122 (1983), pp. 476–485. DOI: 10.1016/0370-2693(83)91605-2.

[182] G. Arnison et al. “Experimental Observation of Lepton Pairs of Invariant Mass Around 95-GeV/c**2 at the CERN SPS Collider.” In: *Phys. Lett. B* 126 (1983), pp. 398–410. DOI: 10.1016/0370-2693(83)90188-0.

[183] P. Bagnaia et al. “Evidence for $Z^0 \to e^+e^-$ at the CERN $\bar{p}p$ Collider.” In: *Phys. Lett. B* 129 (1983), pp. 130–140. DOI: 10.1016/0370-2693(83)90744-X.

[184] S. D. Drell and Tung-Mow Yan. “Massive Lepton Pair Production in Hadron-Hadron Collisions at High-Energies.” In: *Phys. Rev. Lett.* 25 (1970). [Erratum: Phys.Rev.Lett. 25, 902 (1970)], pp. 316–320. DOI: 10.1103/PhysRevLett.25.316.

[185] Georges Aad et al. “Measurement of the Z/γ^* boson transverse momentum distribution in pp collisions at $\sqrt{s}$ = 7 TeV with the ATLAS detector.” In: *JHEP* 09 (2014), p. 145. DOI: 10.1007/JHEP09(2014)145. arXiv: 1406.3660 [hep-ex].

[186] Vardan Khachatryan et al. “Measurement of the differential cross section and charge asymmetry for inclusive pp $\to$ W$^\pm + X$ production at $\sqrt{s} = 8$ TeV.” In: *Eur. Phys. J. C* 76.8 (2016), p. 469. DOI: 10.1140/epjc/s10052-016-4293-4. arXiv: 1603.01803 [hep-ex].

[187] M. Aaboud et al. “Measurement of the Drell-Yan triple-differential cross section in pp collisions at $\sqrt{s} = 8$ TeV.” In: *JHEP* 12 (2017), p. 059. DOI: 10.1007/JHEP12(2017)059. arXiv: 1710.05167 [hep-ex].

[188] Georges Aad et al. “Measurement of the cross-section and charge asymmetry of W bosons produced in proton–proton collisions at $\sqrt{s} = 8$ TeV with the ATLAS detector.” In: *Eur. Phys. J. C* 79.9 (2019), p. 760. DOI: 10.1140/epjc/s10052-019-7199-0. arXiv: 1904.05631 [hep-ex].

[189] Albert M Sirunyan et al. “Measurements of the W boson rapidity, helicity, double-differential cross sections, and charge asymmetry in pp collisions at $\sqrt{s}$ = 13 TeV.” In: *Phys. Rev. D* 102.9 (2020), p. 092012. DOI: 10.1103/PhysRevD.102.092012. arXiv: 2008.04174 [hep-ex].

[190] M. Dittmar, F. Pauss, and D. Zurcher. "Towards a precise parton luminosity determination at the CERN LHC." In: *Phys. Rev. D* 56 (1997), pp. 7284–7290. DOI: 10.1103/PhysRevD.56.7284. arXiv: hep-ex/9705004.

[191] Valery A. Khoze, Alan D. Martin, R. Orava, and M. G. Ryskin. "Luminosity monitors at the LHC." In: *Eur. Phys. J. C* 19 (2001), pp. 313–322. DOI: 10.1007/s100520100616. arXiv: hep-ph/0010163.

[192] Walter T. Giele and Stephane A. Keller. "Hard Scattering Based Luminosity Measurement at Hadron Colliders." In: (Apr. 2001). arXiv: hep-ph/0104053.

[193] S. Haywood et al. "Electroweak physics." In: *CERN Workshop on Standard Model Physics (and more) at the LHC (Final Plenary Meeting)*. Oct. 1999. arXiv: hep-ph/0003275.

[194] Albert M. Sirunyan et al. "Measurement of the weak mixing angle using the forward-backward asymmetry of Drell-Yan events in pp collisions at 8 TeV." In: *Eur. Phys. J. C* 78.9 (2018), p. 701. DOI: 10.1140/epjc/s10052-018-6148-7. arXiv: 1806.00863 [hep-ex].

[195] L. A. Harland-Lang, A. D. Martin, P. Motylinski, and R. S. Thorne. "Parton distributions in the LHC era: MMHT 2014 PDFs." In: *Eur. Phys. J. C* 75.5 (2015), p. 204. DOI: 10.1140/epjc/s10052-015-3397-6. arXiv: 1412.3989 [hep-ph].

[196] Richard D. Ball et al. "Parton distributions from high-precision collider data." In: *Eur. Phys. J. C* 77.10 (2017), p. 663. DOI: 10.1140/epjc/s10052-017-5199-5. arXiv: 1706.00428 [hep-ph].

[197] Sergey Alekhin, Johannes Bluemlein, Sven-Olaf Moch, and Rengaile Placakyte. "The new ABMP16 PDF." In: *PoS* DIS2016 (2016), p. 016. DOI: 10.22323/1.265.0016. arXiv: 1609.03327 [hep-ph].

[198] Tie-Jiun Hou et al. "Progress in the CTEQ-TEA NNLO global QCD analysis." In: (Aug. 2019). arXiv: 1908.11394 [hep-ph].

[199] Marco Farina, Giuliano Panico, Duccio Pappadopulo, Joshua T. Ruderman, Riccardo Torre, and Andrea Wulzer. "Energy helps accuracy: electroweak precision tests at hadron colliders." In: *Phys. Lett. B* 772 (2017), pp. 210–215. DOI: 10.1016/j.physletb.2017.06.043. arXiv: 1609.08157 [hep-ph].

[200] J. Smith, W. L. van Neerven, and J. A. M. Vermaseren. "The Transverse Mass and Width of the *W* Boson." In: *Phys. Rev. Lett.* 50 (1983), p. 1738. DOI: 10.1103/PhysRevLett.50.1738.

[201] G. Bozzi, J. Rojo, and A. Vicini. "The Impact of PDF uncertainties on the measurement of the W boson mass at the Tevatron and the LHC." In: *Phys. Rev. D* 83 (2011), p. 113008. DOI: 10.1103/PhysRevD.83.113008. arXiv: 1104.2056 [hep-ph].

[202] Giuseppe Bozzi, Luca Citelli, and Alessandro Vicini. "Parton density function uncertainties on the W boson mass measurement from the lepton transverse momentum distribution." In: *Phys. Rev. D* 91.11 (2015), p. 113005. DOI: 10.1103/PhysRevD.91.113005. arXiv: 1501.05587 [hep-ph].

[203] Emanuele Bagnaschi and Alessandro Vicini. "Parton Density Uncertainties and the Determination of Electroweak Parameters at Hadron Colliders." In: *Phys. Rev. Lett.* 126.4 (2021), p. 041801. DOI: 10.1103/PhysRevLett.126.041801. arXiv: 1910.04726 [hep-ph].

[204] Stephen Farry, Olli Lupton, Martina Pili, and Mika Vesterinen. "Understanding and constraining the PDF uncertainties in a W boson mass measurement with forward muons at the LHC." In: *Eur. Phys. J. C* 79.6 (2019), p. 497. DOI: 10.1140/epjc/s10052-019-6997-8. arXiv: 1902.04323 [hep-ex].

[205] Stefan Berge, Pavel M. Nadolsky, and Fredrick I. Olness. "Heavy-flavor effects in soft gluon resummation for electroweak boson production at hadron colliders." In: *Phys. Rev. D* 73 (2006), p. 013002. DOI: 10.1103/PhysRevD.73.013002. arXiv: hep-ph/0509023.

[206] Piotr Pietrulewicz, Daniel Samitz, Anne Spiering, and Frank J. Tackmann. "Factorization and Resummation for Massive Quark Effects in Exclusive Drell-Yan." In: *JHEP* 08 (2017), p. 114. DOI: 10.1007/JHEP08(2017)114. arXiv: 1703.09702 [hep-ph].

[207] Guido Altarelli, R. Keith Ellis, and G. Martinelli. "Large Perturbative Corrections to the Drell-Yan Process in QCD." In: *Nucl. Phys. B* 157 (1979), pp. 461–497. DOI: 10.1016/0550-3213(79)90116-0.

[208] R. Hamberg, W. L. van Neerven, and T. Matsuura. "A complete calculation of the order $\alpha - s^2$ correction to the Drell-Yan K factor." In: *Nucl. Phys. B* 359 (1991). [Erratum: Nucl.Phys.B 644, 403–404 (2002)], pp. 343–405. DOI: 10.1016/0550-3213(91)90064-5.

[209] W. L. van Neerven and E. B. Zijlstra. "The $O(\alpha_s^2)$ corrected Drell-Yan K factor in the DIS and MS scheme." In: *Nucl. Phys. B* 382 (1992). [Erratum: Nucl.Phys.B 680, 513–514 (2004)], pp. 11–62. DOI: 10.1016/0550-3213(92)90078-P.

[210] Robert V. Harlander and William B. Kilgore. "Next-to-next-to-leading order Higgs production at hadron colliders." In: *Phys. Rev. Lett.* 88 (2002), p. 201801. DOI: 10.1103/PhysRevLett.88.201801. arXiv: hep-ph/0201206.

[211] Claude Duhr, Falko Dulat, and Bernhard Mistlberger. "Drell-Yan Cross Section to Third Order in the Strong Coupling Constant." In: *Phys. Rev. Lett.* 125.17 (2020), p. 172001. DOI: 10.1103/PhysRevLett.125.172001. arXiv: 2001.07717 [hep-ph].

[212] Claude Duhr, Falko Dulat, and Bernhard Mistlberger. "Charged current Drell-Yan production at N^{3}LO." In: *JHEP* 11 (2020), p. 143. DOI: 10.1007/JHEP11(2020)143. arXiv: 2007.13313 [hep-ph].

[213] Taushif Ahmed, Maguni Mahakhud, Narayan Rana, and V. Ravindran. "Drell-Yan Production at Threshold to Third Order in QCD." In: *Phys. Rev. Lett.* 113.11 (2014), p. 112002. DOI: 10.1103/PhysRevLett.113.112002. arXiv: 1404.0366 [hep-ph].

[214] Stefano Catani, Leandro Cieri, Daniel de Florian, Giancarlo Ferrera, and Massimiliano Grazzini. "Threshold resummation at N^3LL accuracy and soft-virtual cross sections at N^3LO." In: *Nucl. Phys. B* 888 (2014), pp. 75–91. DOI: 10.1016/j.nuclphysb.2014.09.012. arXiv: 1405.4827 [hep-ph].

[215] Kirill Melnikov and Frank Petriello. "The W boson production cross section at the LHC through $O(\alpha_s^2)$." In: *Phys. Rev. Lett.* 96 (2006), p. 231803. DOI: 10.1103/PhysRevLett.96.231803. arXiv: hep-ph/0603182.

[216] Kirill Melnikov and Frank Petriello. "Electroweak gauge boson production at hadron colliders through $O(\alpha_s^2)$." In: *Phys. Rev. D* 74 (2006), p. 114017. DOI: 10.1103/PhysRevD.74.114017. arXiv: hep-ph/0609070.

[217] Stefano Catani, Leandro Cieri, Giancarlo Ferrera, Daniel de Florian, and Massimiliano Grazzini. "Vector boson production at hadron colliders: a fully exclusive QCD calculation at NNLO." In: *Phys. Rev. Lett.* 103 (2009), p. 082001. DOI: 10.1103/PhysRevLett.103.082001. arXiv: 0903.2120 [hep-ph].

[218] Stefano Catani, Giancarlo Ferrera, and Massimiliano Grazzini. "W Boson Production at Hadron Colliders: The Lepton Charge Asymmetry in NNLO QCD." In: *JHEP* 05 (2010), p. 006. DOI: 10.1007/JHEP05(2010)006. arXiv: 1002.3115 [hep-ph].

[219] Ryan Gavin, Ye Li, Frank Petriello, and Seth Quackenbush. "FEWZ 2.0: A code for hadronic Z production at next-to-next-to-leading order." In: *Comput. Phys. Commun.* 182 (2011), pp. 2388–2403. DOI: 10.1016/j.cpc.2011.06.008. arXiv: 1011.3540 [hep-ph].

[220] Ryan Gavin, Ye Li, Frank Petriello, and Seth Quackenbush. "W Physics at the LHC with FEWZ 2.1." In: *Comput. Phys. Commun.* 184 (2013), pp. 208–214. DOI: 10.1016/j.cpc.2012.09.005. arXiv: 1201.5896 [hep-ph].

[221] Stefano Camarda et al. "DYTurbo: Fast predictions for Drell-Yan processes." In: *Eur. Phys. J. C* 80.3 (2020). [Erratum: Eur.Phys.J.C 80, 440 (2020)], p. 251. DOI: 10.1140/epjc/s10052-020-7757-5. arXiv: 1910.07049 [hep-ph].

[222] Stefan Dittmaier and Michael Krämer. "Electroweak radiative corrections to W boson production at hadron colliders." In: *Phys. Rev. D* 65 (2002), p. 073007. DOI: 10.1103/PhysRevD.65.073007. arXiv: hep-ph/0109062.

[223] U. Baur, O. Brein, W. Hollik, C. Schappacher, and D. Wackeroth. "Electroweak radiative corrections to neutral current Drell-Yan processes at hadron colliders." In: *Phys. Rev. D* 65 (2002), p. 033007. DOI: 10.1103/PhysRevD.65.033007. arXiv: hep-ph/0108274.

[224] U. Baur and D. Wackeroth. “Electroweak radiative corrections to $p\bar{p} \to W^{\pm} \to \ell^{\pm}\nu$ beyond the pole approximation.” In: *Phys. Rev. D* 70 (2004), p. 073015. DOI: 10.1103/PhysRevD.70.073015. arXiv: hep-ph/0405191.

[225] A. Arbuzov, D. Bardin, S. Bondarenko, P. Christova, L. Kalinovskaya, G. Nanava, and R. Sadykov. “One-loop corrections to the Drell-Yan process in SANC. I. The Charged current case.” In: *Eur. Phys. J. C* 46 (2006). [Erratum: Eur.Phys.J.C 50, 505 (2007)], pp. 407–412. DOI: 10.1140/epjc/s2006-02505-y. arXiv: hep-ph/0506110.

[226] V. A. Zykunov. “Weak radiative corrections to Drell-Yan process for large invariant mass of di-lepton pair.” In: *Phys. Rev. D* 75 (2007), p. 073019. DOI: 10.1103/PhysRevD.75.073019. arXiv: hep-ph/0509315.

[227] V. A. Zykunov. “Radiative corrections to the Drell-Yan process at large dilepton invariant masses.” In: *Phys. Atom. Nucl.* 69 (2006), p. 1522. DOI: 10.1134/S1063778806090109.

[228] C. M. Carloni Calame, G. Montagna, O. Nicrosini, and A. Vicini. “Precision electroweak calculation of the charged current Drell-Yan process.” In: *JHEP* 12 (2006), p. 016. DOI: 10.1088/1126-6708/2006/12/016. arXiv: hep-ph/0609170.

[229] C. M. Carloni Calame, G. Montagna, O. Nicrosini, and A. Vicini. “Precision electroweak calculation of the production of a high transverse-momentum lepton pair at hadron colliders.” In: *JHEP* 10 (2007), p. 109. DOI: 10.1088/1126-6708/2007/10/109. arXiv: 0710.1722 [hep-ph].

[230] A. Arbuzov, D. Bardin, S. Bondarenko, P. Christova, L. Kalinovskaya, G. Nanava, and R. Sadykov. “One-loop corrections to the Drell–Yan process in SANC. (II). The Neutral current case.” In: *Eur. Phys. J. C* 54 (2008), pp. 451–460. DOI: 10.1140/epjc/s10052-008-0531-8. arXiv: 0711.0625 [hep-ph].

[231] Stefan Dittmaier and Max Huber. “Radiative corrections to the neutral-current Drell-Yan process in the Standard Model and its minimal supersymmetric extension.” In: *JHEP* 01 (2010), p. 060. DOI: 10.1007/JHEP01(2010)060. arXiv: 0911.2329 [hep-ph].

[232] Matthias Heller, Andreas von Manteuffel, and Robert M. Schabinger. “Multiple polylogarithms with algebraic arguments and the two-loop EW-QCD Drell-Yan master integrals.” In: *Phys. Rev. D* 102.1 (2020), p. 016025. DOI: 10.1103/PhysRevD.102.016025. arXiv: 1907.00491 [hep-th].

[233] Roberto Bonciani, Luca Buonocore, Massimiliano Grazzini, Stefan Kallweit, Narayan Rana, Francesco Tramontano, and Alessandro Vicini. “Mixed strong−electroweak corrections to the Drell−Yan process.” In: (June 2021). arXiv: 2106.11953 [hep-ph].

[234] Ye Li and Frank Petriello. “Combining QCD and electroweak corrections to dilepton production in FEWZ.” In: *Phys. Rev. D* 86 (2012), p. 094034. DOI: 10.1103/PhysRevD.86.094034. arXiv: 1208.5967 [hep-ph].

[235] Luca Barze, Guido Montagna, Paolo Nason, Oreste Nicrosini, Fulvio Piccinini, and Alessandro Vicini. “Neutral current Drell-Yan with combined QCD and electroweak corrections in the POWHEG BOX.” In: *Eur. Phys. J. C* 73.6 (2013), p. 2474. DOI: 10.1140/epjc/s10052-013-2474-y. arXiv: 1302.4606 [hep-ph].

[236] Leandro Cieri, Daniel de Florian, Manuel Der, and Javier Mazzitelli. “Mixed QCD⊗QED corrections to exclusive Drell Yan production using the q_T -subtraction method.” In: *JHEP* 09 (2020), p. 155. DOI: 10.1007/JHEP09(2020)155. arXiv: 2005.01315 [hep-ph].

[237] Stefan Dittmaier, Timo Schmidt, and Jan Schwarz. “Mixed NNLO QCD×electroweak corrections of $\mathcal{O}(N_f \alpha_s \alpha)$ to single-W/Z production at the LHC.” In: *JHEP* 12 (2020), p. 201. DOI: 10.1007/JHEP12(2020)201. arXiv: 2009.02229 [hep-ph].

[238] Luca Buonocore, Massimiliano Grazzini, Stefan Kallweit, Chiara Savoini, and Francesco Tramontano. “Mixed QCD-EW corrections to $\boldsymbol{pp \to \ell \nu_\ell + X}$ at the LHC.” In: (Feb. 2021). arXiv: 2102.12539 [hep-ph].

[239] Victor S. Fadin, Valery A. Khoze, and Alan D. Martin. “How suppressed are the radiative interference effects in heavy instable particle production?” In: *Phys. Lett. B* 320 (1994), pp. 141–144. DOI: 10.1016/0370-2693(94)90837-0. arXiv: hep-ph/9309234.

[240] Stefan Dittmaier, Alexander Huss, and Christian Schwinn. “Mixed QCD-electroweak $\mathcal{O}(\alpha_s \alpha)$ corrections to Drell-Yan processes in the resonance region: pole approximation and non-factorizable corrections.” In: *Nucl. Phys. B* 885 (2014), pp. 318–372. DOI: 10.1016/j.nuclphysb.2014.05.027. arXiv: 1403.3216 [hep-ph].

[241] Stefan Dittmaier, Alexander Huss, and Christian Schwinn. “Dominant mixed QCD-electroweak O($\alpha_s \alpha$) corrections to Drell–Yan processes in the resonance region.” In: *Nucl. Phys. B* 904 (2016), pp. 216–252. DOI: 10.1016/j.nuclphysb.2016.01.006. arXiv: 1511.08016 [hep-ph].

[242] Roberto Bonciani, Federico Buccioni, Roberto Mondini, and Alessandro Vicini. “Double-real corrections at $\mathcal{O}(\alpha \alpha_s)$ to single gauge boson production.” In: *Eur. Phys. J. C* 77.3 (2017), p. 187. DOI: 10.1140/epjc/s10052-017-4728-6. arXiv: 1611.00645 [hep-ph].

[243] Roberto Bonciani, Federico Buccioni, Narayan Rana, Ilario Triscari, and Alessandro Vicini. “NNLO QCD×EW corrections to Z production in the $q\bar{q}$ channel.” In: *Phys. Rev. D* 101.3 (2020), p. 031301. DOI: 10.1103/PhysRevD.101.031301. arXiv: 1911.06200 [hep-ph].

[244] Roberto Bonciani, Federico Buccioni, Narayan Rana, and Alessandro Vicini. “Next-to-Next-to-Leading Order Mixed QCD-Electroweak Corrections to on-Shell Z Production.” In: *Phys. Rev. Lett.* 125.23 (2020), p. 232004. DOI: 10.1103/PhysRevLett.125.232004. arXiv: 2007.06518 [hep-ph].

[245] A. Kotikov, Johann H. Kuhn, and O. Veretin. "Two-Loop Formfactors in Theories with Mass Gap and Z-Boson Production." In: *Nucl. Phys. B* 788 (2008), pp. 47–62. DOI: 10.1016/j.nuclphysb.2007.07.018. arXiv: hep-ph/0703013.

[246] A. Djouadi and P. Gambino. "Electroweak gauge bosons selfenergies: Complete QCD corrections." In: *Phys. Rev. D* 49 (1994). [Erratum: Phys.Rev.D 53, 4111 (1996)], pp. 3499–3511. DOI: 10.1103/PhysRevD.49.3499. arXiv: hep-ph/9309298.

[247] Fabio Cascioli, Philipp Maierhofer, and Stefano Pozzorini. "Scattering Amplitudes with Open Loops." In: *Phys. Rev. Lett.* 108 (2012), p. 111601. DOI: 10.1103/PhysRevLett.108.111601. arXiv: 1111.5206 [hep-ph].

[248] Stefan Kallweit, Jonas M. Lindert, Philipp Maierhöfer, Stefano Pozzorini, and Marek Schönherr. "NLO electroweak automation and precise predictions for W+multijet production at the LHC." In: *JHEP* 04 (2015), p. 012. DOI: 10.1007/JHEP04(2015)012. arXiv: 1412.5157 [hep-ph].

[249] Ansgar Denner, Stefan Dittmaier, and Lars Hofer. "Collier: a fortran-based Complex One-Loop LIbrary in Extended Regularizations." In: *Comput. Phys. Commun.* 212 (2017), pp. 220–238. DOI: 10.1016/j.cpc.2016.10.013. arXiv: 1604.06792 [hep-ph].

[250] Federico Buccioni, Stefano Pozzorini, and Max Zoller. "On-the-fly reduction of open loops." In: *Eur. Phys. J. C* 78.1 (2018), p. 70. DOI: 10.1140/epjc/s10052-018-5562-1. arXiv: 1710.11452 [hep-ph].

[251] Federico Buccioni, Jean-Nicolas Lang, Jonas M. Lindert, Philipp Maierhöfer, Stefano Pozzorini, Hantian Zhang, and Max F. Zoller. "OpenLoops 2." In: *Eur. Phys. J. C* 79.10 (2019), p. 866. DOI: 10.1140/epjc/s10052-019-7306-2. arXiv: 1907.13071 [hep-ph].

[252] J. Alwall, R. Frederix, S. Frixione, V. Hirschi, F. Maltoni, O. Mattelaer, H. S. Shao, T. Stelzer, P. Torrielli, and M. Zaro. "The automated computation of tree-level and next-to-leading order differential cross sections, and their matching to parton shower simulations." In: *JHEP* 07 (2014), p. 079. DOI: 10.1007/JHEP07(2014)079. arXiv: 1405.0301 [hep-ph].

[253] Ansgar Denner and Stefan Dittmaier. "Electroweak Radiative Corrections for Collider Physics." In: *Phys. Rept.* 864 (2020), pp. 1–163. DOI: 10.1016/j.physrep.2020.04.001. arXiv: 1912.06823 [hep-ph].

[254] Valerio Bertone, Stefano Carrazza, Nathan P. Hartland, and Juan Rojo. "Illuminating the photon content of the proton within a global PDF analysis." In: *SciPost Phys.* 5.1 (2018), p. 008. DOI: 10.21468/SciPostPhys.5.1.008. arXiv: 1712.07053 [hep-ph].

[255] Aneesh V. Manohar, Paolo Nason, Gavin P. Salam, and Giulia Zanderighi. "The Photon Content of the Proton." In: *JHEP* 12 (2017), p. 046. DOI: 10.1007/JHEP12(2017)046. arXiv: 1708.01256 [hep-ph].

[256] Aneesh Manohar, Paolo Nason, Gavin P. Salam, and Giulia Zanderighi. "How bright is the proton? A precise determination of the photon parton distribution function." In: *Phys. Rev. Lett.* 117.24 (2016), p. 242002. DOI: 10.1103/PhysRevLett.117.242002. arXiv: 1607.04266 [hep-ph].

[257] S. Alioli et al. "Precision studies of observables in $pp \to W \to l\nu_l$ and $pp \to \gamma, Z \to l^+l^-$ processes at the LHC." In: *Eur. Phys. J. C* 77.5 (2017), p. 280. DOI: 10.1140/epjc/s10052-017-4832-7. arXiv: 1606.02330 [hep-ph].

[258] John C. Collins and Davison E. Soper. "Angular Distribution of Dileptons in High-Energy Hadron Collisions." In: *Phys. Rev. D* 16 (1977), p. 2219. DOI: 10.1103/PhysRevD.16.2219.

[259] U. Baur, S. Keller, and W. K. Sakumoto. "QED radiative corrections to Z boson production and the forward backward asymmetry at hadron colliders." In: *Phys. Rev. D* 57 (1998), pp. 199–215. DOI: 10.1103/PhysRevD.57.199. arXiv: hep-ph/9707301.

[260] Giovanni Balossini, Guido Montagna, Carlo Michel Carloni Calame, Mauro Moretti, Oreste Nicrosini, Fulvio Piccinini, Michele Treccani, and Alessandro Vicini. "Combination of electroweak and QCD corrections to single W production at the Fermilab Tevatron and the CERN LHC." In: *JHEP* 01 (2010), p. 013. DOI: 10.1007/JHEP01(2010)013. arXiv: 0907.0276 [hep-ph].

[261] Carlo Michel Carloni Calame, Mauro Chiesa, Homero Martinez, Guido Montagna, Oreste Nicrosini, Fulvio Piccinini, and Alessandro Vicini. "Precision Measurement of the W-Boson Mass: Theoretical Contributions and Uncertainties." In: *Phys. Rev. D* 96.9 (2017), p. 093005. DOI: 10.1103/PhysRevD.96.093005. arXiv: 1612.02841 [hep-ph].

[262] W. T. Giele and S. Keller. "Determination of W boson properties at hadron colliders." In: *Phys. Rev. D* 57 (1998), pp. 4433–4440. DOI: 10.1103/PhysRevD.57.4433. arXiv: hep-ph/9704419.

[263] Milton Abramowitz and Irene Stegun. *Handbook of Mathematical Functions, With Formulas, Graphs, and Mathematical Tables*. Dover Publications, Incorporated, 1974. ISBN: 0486612724.

[264] E. Remiddi and J. A. M. Vermaseren. "Harmonic polylogarithms." In: *Int. J. Mod. Phys. A* 15 (2000), pp. 725–754. DOI: 10.1142/S0217751X00000367. arXiv: hep-ph/9905237.

[265] L. Naterop, A. Signer, and Y. Ulrich. "handyG —Rapid numerical evaluation of generalised polylogarithms in Fortran." In: *Comput. Phys. Commun.* 253 (2020), p. 107165. DOI: 10.1016/j.cpc.2020.107165. arXiv: 1909.01656 [hep-ph].

[266] Claude Duhr, Herbert Gangl, and John R. Rhodes. "From polygons and symbols to polylogarithmic functions." In: *JHEP* 10 (2012), p. 075. DOI: 10.1007/JHEP10(2012)075. arXiv: 1110.0458 [math-ph].

[267] U. Aglietti and R. Bonciani. "Master integrals with one massive propagator for the two loop electroweak form-factor." In: *Nucl. Phys. B* 668 (2003), pp. 3–76. DOI: 10.1016/j.nuclphysb.2003.07.004. arXiv: hep-ph/0304028.

[268] U. Aglietti and R. Bonciani. "Master integrals with 2 and 3 massive propagators for the 2 loop electroweak form-factor - planar case." In: *Nucl. Phys. B* 698 (2004), pp. 277–318. DOI: 10.1016/j.nuclphysb.2004.07.018. arXiv: hep-ph/0401193.

[269] Roberto Bonciani, Stefano Di Vita, Pierpaolo Mastrolia, and Ulrich Schubert. "Two-Loop Master Integrals for the mixed EW-QCD virtual corrections to Drell-Yan scattering." In: *JHEP* 09 (2016), p. 091. DOI: 10.1007/JHEP09(2016)091. arXiv: 1604.08581 [hep-ph].

[270] Roberto Bonciani. "Two-loop mixed QCD-EW virtual corrections to the Drell-Yan production of Z and W bosons." In: *PoS* EPS-HEP2011 (2011), p. 365. DOI: 10.22323/1.134.0365.

[271] J. A. M. Vermaseren. "New features of FORM." In: (Oct. 2000). arXiv: math-ph/0010025.

[272] J. Kuipers, T. Ueda, J. A. M. Vermaseren, and J. Vollinga. "FORM version 4.0." In: *Comput. Phys. Commun.* 184 (2013), pp. 1453–1467. DOI: 10.1016/j.cpc.2012.12.028. arXiv: 1203.6543 [cs.SC].

[273] J. Kuipers, T. Ueda, and J. A. M. Vermaseren. "Code Optimization in FORM." In: *Comput. Phys. Commun.* 189 (2015), pp. 1–19. DOI: 10.1016/j.cpc.2014.08.008. arXiv: 1310.7007 [cs.SC].

[274] Ben Ruijl, Takahiro Ueda, and Jos Vermaseren. "FORM version 4.2." In: (July 2017). arXiv: 1707.06453 [hep-ph].

[275] T. Hahn. "CUBA: A Library for multidimensional numerical integration." In: *Comput. Phys. Commun.* 168 (2005), pp. 78–95. DOI: 10.1016/j.cpc.2005.01.010. arXiv: hep-ph/0404043.

[276] T. Hahn. "Concurrent Cuba." In: *J. Phys. Conf. Ser.* 608.1 (2015). Ed. by L. Fiala, M. Lokajicek, and N. Tumova, p. 012066. DOI: 10.1088/1742-6596/608/1/012066. arXiv: 1408.6373 [physics.comp-ph].

[277] S. Borowka, G. Heinrich, S. Jahn, S. P. Jones, M. Kerner, J. Schlenk, and T. Zirke. "pySecDec: a toolbox for the numerical evaluation of multi-scale integrals." In: *Comput. Phys. Commun.* 222 (2018), pp. 313–326. DOI: 10.1016/j.cpc.2017.09.015. arXiv: 1703.09692 [hep-ph].

[278] S. Borowka, G. Heinrich, S. Jahn, S. P. Jones, M. Kerner, and J. Schlenk. "A GPU compatible quasi-Monte Carlo integrator interfaced to pySecDec." In: *Comput. Phys. Commun.* 240 (2019), pp. 120–137. DOI: 10.1016/j.cpc.2019.02.015. arXiv: 1811.11720 [physics.comp-ph].

[279] M. Galassi, J. Davies, J. Theiler, B. Gough, G. Jungman, P. Alken, M. Booth, and F. Rossi. *GNU Scientific Library Reference Manual*. Ed. by B. Gough. Third. Network Theory Ltd., 2009.

[280] Raphael Krüger. "Streuamplituden für die W-Erzeugung aus zwei Quarks unter Abstrahlungvon Photon und Gluon." unpublished. B.Sc. Thesis. 2020.

[281] Michael E. Peskin. "Simplifying Multi-Jet QCD Computation." In: *13th Mexican School of Particles and Fields*. Jan. 2011. arXiv: 1101.2414 [hep-ph].

[282] D. Binosi and L. Theussl. "JaxoDraw: A Graphical user interface for drawing Feynman diagrams." In: *Comput. Phys. Commun.* 161 (2004), pp. 76–86. DOI: 10.1016/j.cpc.2004.05.001. arXiv: hep-ph/0309015.

DANKSAGUNG

Zuvorderst möchte mich an dieser Stelle bei Prof. Kirill Melnikov für die durchgehend intensive Betreuung mit vielen interessanten Diskussionen und Ratschlägen bedanken, die diese Arbeit überhaupt erst ermöglicht hat.

Außerdem möchte ich mich bei meinem Korreferenten Prof. Matthias Steinhauser für viele wertvolle Anregungen und Kommentare bedanken.

Mein Dank gilt allen, mit denen ich das Glück hatte, zusammen arbeiten zu dürfen. Sowohl Daniel Baranowski, Arnd Behring, Wojciech Bizon und Matthieu Jaquier aus der Arbeitsgruppe, als auch Federico Buccioni, Fabrizio Caola und Raoul Röntsch. Außerdem gilt mein Dank den Computeradmins des Instituts, sowie Martina Schorn.

Herzlich möchte ich mich bei Konstantin Asteriadis, Daniel Baranowski, Marco Bonetti, Christian Broennum-Hansen, Florian Herren, Kirill Kudashkin und Matthias Linster für die gute Zeit in Büro 12/15, Kino- und Koch- und Tischtennisabende, Laufrunden durch den Hardwald und den Oberwald, (virtuelle) Stammtische und generell drei tolle Jahre am Institut bedanken.

Zu guter Letzt gilt mein Dank meinen Eltern und meinem Bruder, für die kontinuierliche Ermutigung und den Rückhalt. Danke Sophie, für all deine Unterstützung während dem Schreiben dieser Arbeit und dass du mich jeden Tag aufs Neue zum Lächeln bringst.

COLOPHON

All Feynman diagrams in this document were drawn using Jaxodraw [282].

This document was typeset using the typographical look-and-feel classicthesis developed by André Miede and Ivo Pletikosić. The style was inspired by Robert Bringhurst's seminal book on typography "*The Elements of Typographic Style*". classicthesis is available for both LaTeX and LyX:

https://bitbucket.org/amiede/classicthesis/

Happy users of classicthesis usually send a real postcard to the author, a collection of postcards received so far is featured here:

http://postcards.miede.de/

Thank you very much for your feedback and contribution.

Final Version as of July 18, 2022 (classicthesis v4.6).